FIFTH INTERNATIONAL CONFERENCE ON STABILITY
OF
SHIPS AND OCEAN VEHICLES

NOVEMBER 7-11, 1994

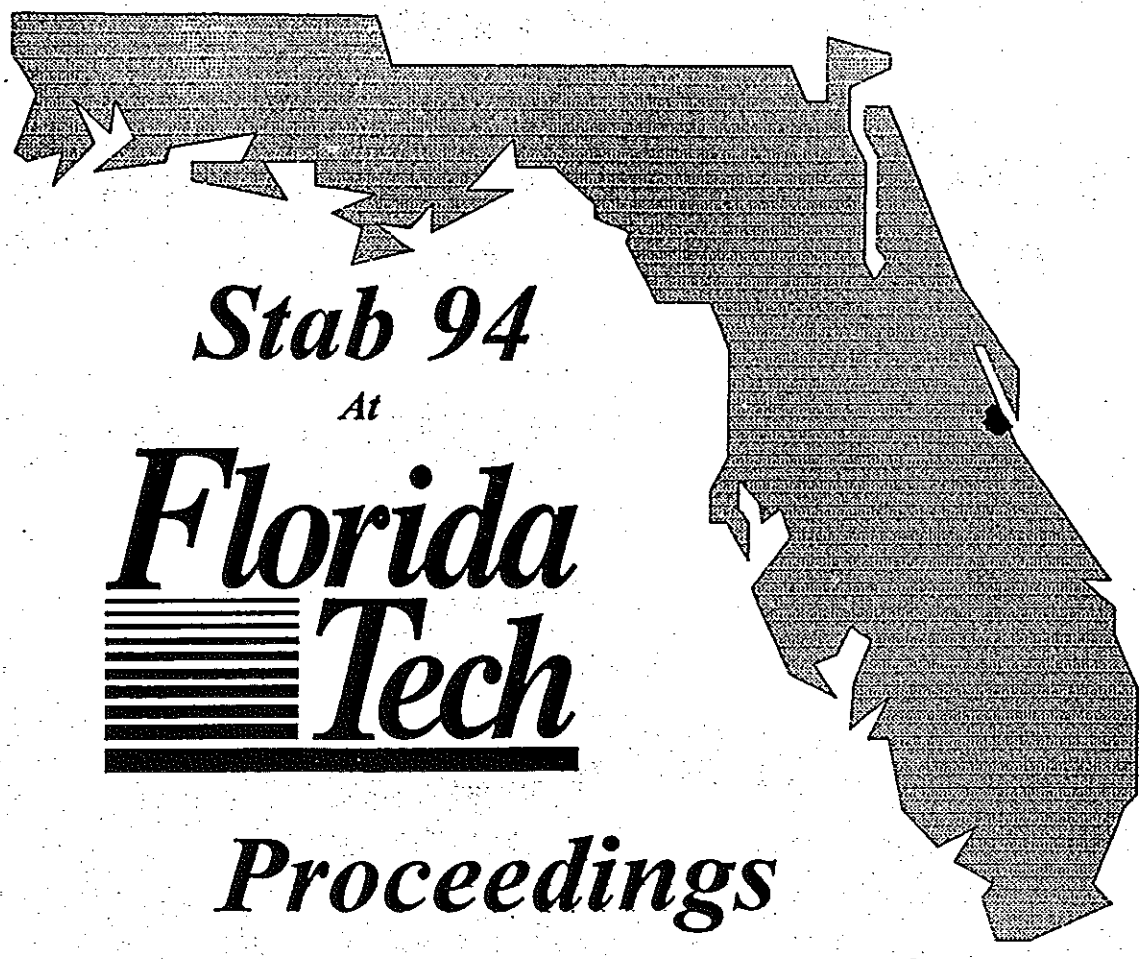

Stab 94

At

Florida Tech

Proceedings

Volume 1

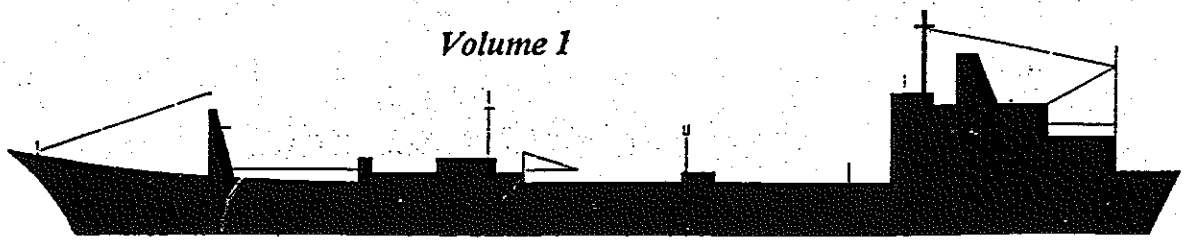

150 W. UNIVERSITY BLVD.
MELBOURNE, FL 32901-6988

FLORIDA INSTITUTE OF TECHNOLOGY

LYNN E. WEAVER, Ph.D. - PRESIDENT

COLLEGE OF ENGINEERING
ROBERT L. SULLIVAN, Ph.D. - DEAN

DIVISION OF MARINE AND ENVIRONMENTAL SYSTEMS
GEORGE A. MAUL, Ph.D. - DIRECTOR

OCEAN ENGINEERING PROGRAM
ANDREW ZBOROWSKI, Ph.D. - CHAIRMAN

WILLIAM R. DALLY, Ph.D.

GRAEME RAE, Ph.D.

GEOFFREY W. J. SWAIN, Ph.D.

LEE HARRIS - ASSOCIATE PROFESSOR

W. A. CLEARY, JR. - ADJUNCT PROFESSOR

PURPOSE OF STAB 94

STAB 94 had been offered to promote a full exchange of ideas and methodologies regarding STABILITY OF SHIPS AND OCEAN VEHICLES and to provide an opportunity to professional naval architects, capsize prevention researcher, regulatory agencies, inspection and certifying authorities, ship owners, consultants and ship operators to present, discuss and listen to improvements in capsize prevention for all types and sizes of ships.

SPONSORS
The Society of Naval Architects and Marine Engineers
The Royal Institution of Naval Architects

STAB 94

TABLE OF CONTENTS

VOLUME NO. 1	Monday 7 November Papers Sessions - 1, 2, 3, 4
VOLUME NO. 2	Tuesday 8 November Papers Sessions - 5, 6, 7, 8
VOLUME NO. 3	Wednesday 9 November Papers Sessions - 9, 10, 11, 12
VOLUME NO. 4	Thursday 10 November Papers Sessions - 13, 14, 15, 16
VOLUME NO. 5	Friday 11 November Papers Sessions - 17, 18, 19
SUPPLEMENT TO NO. 5	Executive Summaries of workshops 1 through 7 by workshop moderator (To be mailed to all registrants after conference completion.)

MONDAY 7 NOVEMBER

GLEASON AUDITORIUM

0845-0900 OPENING SESSION

PAPERS SESSION 1

Moderator: H. HORMANN
Germanischer Lloyd, Chairman IMO-SLF

0900-0925
IMO Activities in respect of the
Development of International Requirements on Intact and
Damage Stability of Ships
Authors: F. Plaza A. Petrov

0930-0955
A Study of the Dynamic Stability of a RoRo Ship in Waves
Authors: J. Hua O. Rutgersson

1000-1025
Dangerous Encounter Wave Conditions for Ships Navigating
in Following and Quartering Seas
Author: Y. Takaishi

A. M. BREAK

PAPERS SESSION 2

Moderator: Prof. P. BOGDANOV
Bulgarian Ship Hydrodynamic Center

1035-1100
NonLinearities in SemiSubmersible Roll Behavior Under First
and Second Order Wave Excitation
Authors: G. Spyrou D. Vassalos

1105-1130
Ship Stability in Following Waves:
A Theoretical and Experimental Investigation
Authors: L. Crudu R. Nabergoj,
G. Trincas D. Obreja

1135-1200
The Development of an ISO Stability Standard for Small Craft
Author: A. Blyth

LUNCH - DELEGATES LOUNGE

PAPERS SESSION 3

Moderator: H. VERMEER
Netherlands Shipping Directorate

1330-1355
Intact Ship Survivability in Extreme Waves:
New Criteria from a Research and Navy Perspective
Authors: J.O. deKat R. Brouwer
K. McTaggart W. L. Thomas

1400-1425
Wind Heeling Loads on a Naval Frigate
Authors: K. McTaggart M. Savage

1430-1455
Complete Six Degrees of Freedom Nonlinear Ship Rolling
Author: J. Falzarano

P. M. BREAK

PAPERS SESSION 4

Moderator: PROF. R. BHATTACHARYYA
U.S. Naval Academy

1515-1540
Experimental Evidence of Strong NonLinear Effects
in the Rolling Motion of a Destroyer in Beam Seas
Authors A Francescutto, G Contento R. Penna

1545-1610
Dynamic Stability of a SWATH Research Vessel
in Following Seas
Author: A. D. Papanikolaou

1615-1640
Roll Motions of High Speed Slender Vessels
Authors: Y. Ikeda, T. Katayama

CENTRAL BAPTIST AUDITORIUM

WORKSHOP / PANEL

Moderator: Prof. L Kobylinski
Ship Research Institute
Gdansk, Poland

PROBABILITY IN STABILITY

P. M. BREAK

PROBABILITY IN STABILITY

(continued)

and

(concluded)

IMO ACTIVITIES IN RESPECT OF THE DEVELOPMENT OF INTERNATIONAL REQUIREMENTS ON INTACT AND DAMAGE STABILITY OF SHIPS

F. Plaza and A. Petrov

International Maritime Organization

ABSTRACT

This paper provides a brief description of the work the International Maritime Organization has undertaken in respect of developing international requirements and recommendations on intact and damage stability for various types of ships during the period from 1990 to 1994. This paper also includes a brief account of the current work on the subject within the Sub-Committee on Stability and Load Lines and on Fishing Vessels Safety which is the IMO's body responsible for the work of the Organization in this area.

1 PREAMBLE

The International Maritime Organization (until 22 May 1982 the Organization was called the Inter-Governmental Maritime Consultative Organization (IMCO)) was established by the United Nations Conference held in Geneva in 1948. In 1958 the Organization came into being as the only United Nations specialized agency solely concerned with maritime affairs.

The establishment of IMO was initiated by the recognition of fact that, because of the international nature of the shipping industry, it is only through concerted efforts of States, co-ordinated on an international level, that action to enhance safety at sea would be more effective, and that a permanent body which would co-ordinate and promote further measures on a more continuing basis would serve well the cause of maritime safety.

The main objective of IMO is to facilitate co-operation among governments in technical matters affecting shipping in order to achieve the highest practicable standards of maritime safety and navigation. Since 1967, the Organization has given special emphasis to issues of pollution prevention of sea from ships and to legal matters associated with its technical work. Since its inception the membership of the Organization has risen to 149.

The main organs of the Organization are the Assembly, which is the supreme body of IMO and meets once every two years, a Council, which exercises the functions of the Assembly in running the affairs of the Organization, and Committees, namely, the Maritime Safety Committee, the Marine Environment Protection Committee, the Legal Committee, the Committee on Technical Co-operation and the Facilitation Committee.

The Maritime Safety Committee carries out the technical work of the Organization relating to the safety at sea and performs its functions with the assistance of its sub-committees which deal with ship design and equipment; stability, load lines and fishing vessels safety; fire protection; life-saving, search and rescue; radiocommunications; safety of navigation; carriage of dangerous goods; containers and cargoes; bulk chemicals; and standards of training and watchkeeping.

To achieve its objectives IMO has adopted some 30 conventions and protocols as well as hundreds of codes, guidelines, recommendations, etc. In case of the conventions and protocols this work has been done by a committee or sub-committee and a draft instrument prepared is submitted to a conference to which delegations from all States within the United Nations are invited. The conference adopts the final text which is submitted to Governments for ratification. As to codes, guidelines, standards, recommendations, etc., these documents as prepared by the sub-committees and after approval by the Committee are adopted by the Assembly. Compliance with the requirements of a convention is mandatory by ships flying the flag of a State which is a party to the convention, while codes, guidelines, standards, recommendations are not so binding on Governments. However, in most cases they are implemented by Governments through incorporation into national legislation.

To deal with matters related to the intact and damage stability of ships and ocean vehicles, the Maritime Safety Committee established a specialized sub-committee, at present, the Sub-Committee on Stability and Load Lines and on Fishing Vessels Safety (SLF Sub-Committee), which developed so far a great deal of intact stability requirements and standards of damage stability for various types of ships which are included in various conventions, codes, guidelines, etc. adopted by the Organization.

The developments within IMO on matters related to intact and damage stability of ships until 1990 were described in papers presented at the respective International Conferences on Stability of Ships and Ocean Vehicles. This paper summarizes the outcome of the work undertaken by the SLF Sub-Committee since 1990 and provides general description of provisions relating to intact and damage stability. For the specific requirements contained in IMO instruments, documents listed in the REFERENCES section should be consulted.

2 INTACT STABILITY REQUIREMENTS

2.1 Intact Stability Code

The Code on Intact Stability for All Types of Ships Covered by IMO Instruments (Intact Stability Code) [1] was developed in recognition of the need for the establishing of an internationally agreed code on intact stability of ships which would summarize the work carried out by the Organization on the subject so far, and for this reason the Code incorporates provisions of the IMO instruments (conventions, codes, recommendations, guidelines) relating to intact stability. The Code was adopted in November 1993 by the Assembly of the Organization by resolution A.749(18).

The Code includes intact stability criteria for the following types of ships and other marine vehicles of 24 metres in length and upwards:

- cargo ships including ships carrying timber deck cargoes and grain in bulk
- passenger ships
- fishing vessels
- special purpose ships
- offshore supply vessels
- mobile offshore drilling units
- pontoons
- dynamically supported craft
- containerships.

The Code contains chapters on:

- general provisions against capsizing and information for the master;
- design criteria applicable to all ships, which specify general intact stability criteria, severe wind and rolling criterion, effect of free surface of liquids in tanks, assessment of compliance with stability criteria, standard loading conditions and calculation of stability curves;

- special criteria for certain types of ships;
- icing considerations;
- consideration for watertight integrity;
- determination of lightship displacement and centres of gravity,

and two annexes on detailed guidance for the conduct of an inclining test and on recommendations for skippers of fishing vessels on ensuring a vessel's endurance in conditions of ice formation.

2.2 Open-top containerships

Open-top containerships is a new concept of containerships which are specially designed so that one or more of the cargo holds need not be fitted with hatch covers. With such arrangements containers are handled in a considerably short period of time which makes operation of such ships more cost-effective. However, as the hatches are open such ships are exposed to shipping of water due to ship's motion at sea, rainfall, etc. and dependent on the effectiveness of drainage systems installed to remove the water collected in the cargo holds of the ship.

It is important that such ships are assigned an adequate minimum freeboard which should be determined by seekeeping characteristics and stability. For this reason model tests and calculations should be carried out to provide the Administration with measured data for the maximum hourly rate of ingress of green water likely to be shipped into each cargo hold and evaluation of the adequacy of the discharge rates from cargo hold freeing ports.

The stability of open-top containerships, as specified in the Interim Guidelines for Open-Top Containerships [2], in all conditions of loading should meet the provisions of the Intact Stability Code [1], that is those of resolution A.167(ES.IV) [3]. Additionally, instead of the mentioned criteria, the Code allows the application of an equivalent stability criteria which are based on the concept of the hull form factor which takes into account individual characteristics of the hull forms.

There are certain conditions indicated in the Interim Guidelines to be observed which require that where cargo hold freeing ports are fitted, they should be considered closed for the purpose of determining the flooding angle, provided that the reliable and effective control of closing of these freeing ports is satisfactory to the Administration.

It is also specified that with all open holds completely filled with water (permeability of 0.70 for container holds) to the level of the top of the hatch side or hatch coaming or, in the case of a ship fitted with cargo hold freeing ports, to the level of those ports, the stability of the fully laden ship in the intact condition should meet the survival criteria for cargo ships contained in part B-1 of chapter II-1 of the 1974 SOLAS Convention [4].

2.3 High speed craft

In recognition of the growth in sizes and types of high speed craft now existing and in the light of the latest developments of new designs and experience gained with their operation, the International Code of Safety for High Speed Craft [5] was developed which was derived from the previous Code of Safety for Dynamically Supported Craft adopted by the Organization in 1977 [6]. The Code defines the high speed craft as a craft capable of maximum speed equal to or exceeding value of $3.7\ \nabla^{0.1667}$, where ∇ is a displacement corresponding to the design waterline, and covers such passenger and cargo high speed craft as air-cushion vehicles, hydrofoil boats, surface effect ships, multihulls etc. The Code specifies intact stability requirements of the high speed craft for various modes of operation i.e. displacement, non-displacement

and transient modes.

According to the provisions of the Code, the hydrofoils, in the displacement mode, should have sufficient stability under all permitted cases of loading and specifically maintain a heel angle of less than 10° subject to the greater of the heeling moments indicated in the Code. Multihull craft should have sufficient stability when rolling in a seaway to successfully withstand the effect of either passenger crowding or high speed turning. Other high speed craft should meet, in all permitted conditions of loading, provisions of the recommendation on severe wind and rolling criterion (weather criterion) specified in resolution A.562(14) [7] and stability criteria of resolution A.167 (ES.IV) [3] except that the maximum righting lever should occur at an angle of heel not less than 15° and the area under the righting lever curve (GZ curve) should not be less than 0.07 m.rad up to θ=15° when the maximum righting lever occurs at θ=15° and 0.055 m.rad up to θ=30° when the maximum righting lever occurs at θ=30° or above. Where the maximum righting lever occurs at angles of between θ=15° and θ=30° , the corresponding area under righting lever curve should be A = 0.055 + 0.001(30° - θmax) (m.rad), where θmax is the angle of heel at which the righting lever curve reaches its maximum.

For craft in the non-displacement mode intact stability provisions of the Code are provided in general terms, except that for passenger craft it is required that the total heel angle in still water due to the effect of passenger movements and due to beam wind pressure should not exceed 10° , and in all loading conditions, the outward heel due to turning should not exceed 8° and the total heel due to beam wind pressure and due to turning should not exceed 12° outward.

The method of calculating stability in the transient mode is not specified in the Code and only general recommendations are given to the effect that the time to pass from the displacement mode to the non-displacement mode and vice versa should be minimized unless it is demonstrated that no substantial reduction of stability occurs during this transition.

3 SUBDIVISION AND DAMAGE STABILITY REQUIREMENTS

3.1 Cargo ships

In May 1990, a set of amendments to the International Convention for the Safety of Life at Sea, 1974 was adopted by IMO which constitutes a new part B-1 of chapter II-1 of the Convention entitled "Subdivision and damage stability of cargo ships" [8]. These amendments entered into force on 1 February 1992 and apply to cargo ships, including ro-ro ships, over 100 metres in length but exclude those ships which are shown to comply with subdivision and damage stability regulations in other IMO instruments. The new requirements are based on probabilistic concept similar to that applied in resolution A.265(VIII) [9] for passenger ships, which takes the probability of survival after collision as a measure of ship's safety in the damaged condition. This probability of survival is called as "the attained subdivision index A" and is determined by the formula for entire probability as the sum of the products for each compartment or group of compartments of the probability that a space is flooded multiplied by the probability that the ship will not capsize or sink with the considered space flooded. Although the requirements are based on the probabilistic approach, several deterministic elements are introduced to make the concept practicable.

It is considered that the subdivision of a ship is sufficient if the attained subdivision index A is not less than the required subdivision index R which determines the degree of subdivision with which the ship should be provided,

determined by the formula $R = (0.002 + 0.0009\ Ls)^{1/3}$, where Ls is a subdivision length of the ship.

Following the adoption of the requirements for cargo ships over 100 metres in length, the Organization undertook the development of requirements for cargo ships less than 100 metres in length. The work resulted in the preparation by the SLF Sub-Committee of draft amendments to part B-1 of chapter II-1 of the 1974 SOLAS Convention which are still subject to approval by the Maritime Safety Committee. The amendments introduce a formula for calculation, in case of cargo ships over 80 metres in length but less than 100 metres, of the required subdivision index R as follows:
$R = 1-[1/(1+Ls/100\ .\ R_o/1-R_o)]$, where R_o is the value R calculated in accordance with resolution MSC.19(58) [8].

Following the recent experience gained from the application of the regulations on subdivision and damage stability for cargo ships referred to in part B-1 of chapter II-1 of the 1974 SOLAS Convention, in order to ensure a uniform application of the regulations, the Maritime Safety Committee approved a set of interpretations of those regulations [10] concerning the permeability values for cargo spaces in case of a ship fitted with significant quantities of cargo insulation, the application of linear interpolation only to the GM values, a need for fitting a position indicator display at the bridge control position for certain types of watertight doors and ramps which are fitted to subdivide large cargo spaces and are not required to be remotely controlled.

In the course of its work, the SLF Sub-Committee, in considering a definition of the term "modification of a major character" for the purpose of application of the provisions of chapter II-1 of the 1974 SOLAS Convention on subdivision and damage stability, decided that it should be sufficient to relate the modification, which the ship will undergo, to the effect on the level of subdivision of the ship. Subsequently, the interpretation of alterations and modifications of a major character [11] was adopted which defines that where an existing cargo ship is subject to any modification which affects the level of subdivision of that ship, it should be demonstrated that the A/R ratio calculated for the ship after such modification is not less than the A/R ratio calculated for the ship before the modification. However, in those cases where the ship's A/R ratio before modification is equal to or greater than unity, it is only necessary to demonstrate that the ship after such modification has an 'A' value which is not less than 'R' calculated for the modified ship.

3.2 Passenger ships

Subdivision and damage stability requirements for passenger ships are contained in the International Convention for the Safety of Life at Sea, 1974 as amended [4]. The subdivision and damage stability provisions of the 1974 SOLAS Convention, being deterministic, specify the number of adjacent compartments the flooding of which the ship has to withstand. These requirements also establish stability criteria of the ship in damaged condition. It should be noted that instead of the requirements of the Convention, the Regulations on Subdivision and Stability of Passenger Ships as an Equivalent to Part B of Chapter II of the 1960 SOLAS Convention (resolution A.265 (VIII)) [9], which are based on the probabilistic concept, may be used, if applied in their entirety.

Following a number of serious casualties pertaining to passenger ships, IMO adopted amendments to regulation 8 "Stability of passenger ships in damaged condition" of chapter II-1 of the 1974 SOLAS Convention [12] which entered into force on 29 April 1990 and is called "the SOLAS 90

standard". The amendments considerably changed stability requirements relating to the minimum range of the positive residual righting lever curve, the area under the righting lever curve, the residual righting lever, and introduced new requirements for intermediate stages of flooding and the maximum permissible angle of heel after flooding but before the equalization.

The SLF Sub-Committee, at its thirty-eighth session (March 1994), in considering that the criteria in regulation 8 of chapter II-1 are adequate to prevent the rapid capsize of a ship in moderate seas and bearing in mind that the measure of the dynamic capability of a damaged ship to resist heeling is the area under the residual stability curve, which is a function of both the range and the residual righting lever, agreed that some reduction in the range of positive residual righting lever curve may be accepted if accompanied with appropriate increase in the area under residual righting lever curve. The Sub-Committee developed a draft amendment to regulation II-1/8 of the 1974 SOLAS Convention to this effect for further approval by the Maritime Safety Committee.

In the aftermath of loss of ro-ro passenger ships incurring heavy loss of life, the Organization adopted measures to improve the damage stability of existing ro-ro passenger ships by adopting further amendments to regulation 8 of chapter II-1 of the 1974 SOLAS Convention [13]. A slightly modified SOLAS 90 standard has been phased in for such ships built before 29 April 1990 during an 11-year period beginning on 1 October 1994. The phased-in period depends upon the value of A/Amax determined in accordance with the calculation procedure to assess the survivability characteristics of existing ro-ro passenger ships [14] which was adopted by the Maritime Safety Committee to ensure that the upgrading procedure will proceed in a logical and orderly manner. A ratio, A/Amax, is used to establish a ranking order for the upgrading process. Those ships with value of A/Amax less than 70% will have to comply with the requirements of amendments by 1 October 1994, ships having A/Amax of 90% or more but less than 95% by 1 October 2005 while ships with A/Amax of 95% and over need not be upgraded.

There was a need for consistent guidance on application of certain provisions of the above amendments and the calculation procedure used for the purpose of ships' upgrading. Consequently, a set of interpretations [15] of the provisions of both the amendments and calculation procedure were developed, concerning residual righting lever curve; potential downflooding openings, permeabilities to be used in the A/Amax calculation, assumed damage penetration in way of sponsons; calculation of the A/Amax ratio; acceptance of A/Amax calculations by the Administration. In accordance with these interpretations the survivability of a ship may be upgraded step by step, in accordance with the scale outlined in the amendments adopted by resolution MSC.26(60)[13].

3.3 Open-top containerships

The Interim Guidelines for Open-Top Containerships [2] require that open-top containerships should comply with the subdivision and damage stability criteria of part B-1 of chapter II-1 of the 1974 SOLAS Convention. The coamings of open-top holds should be considered as downflooding areas.

3.4 High speed craft

The International Code of Safety for High Speed Craft [5], which covers passenger and cargo high speed craft, following provisions for assumed damages indicated in the Code, specifies conditions for sufficient buoyancy and positive stability after craft's damage and

requires that residual stability of craft, other than multihull craft, should meet the requirements of regulation 8 of chapter II-1 of the 1974 SOLAS Convention. In case of multihull craft, the method of application of criteria to the residual stability curve is similar to that for intact stability except that the craft in the final condition after damage should be considered to have an adequate standard of residual stability provided that the required area confined by the righting lever curve, the line of heeling lever due to combined action of wind and passenger crowding and the line corresponding to angle of downflooding or angle of roll, whichever is the less, should not be less than 0.028 m.rad. There is no requirement regarding the angle at which the maximum GZ value should occur. The conditions for sufficient buoyancy and positive stability following damage for passenger and cargo high speed craft differ in respect of the distance of the final waterline below the level of any opening through which further flooding could take place, being 300 mm for passenger craft and 150 mm for cargo craft, and in respect of the angle of inclination of the craft from the horizontal which should not normally exceed 10° for passenger craft and 15° for cargo craft, in any direction. However, where this is clearly impractical, angles of inclination up to 15° for passenger ships and up to 20° for cargo craft, immediately after damage but reducing to 10° within 15 minutes for passenger craft and to 15° within 15 minutes for cargo craft may be permitted provided that efficient non-slip deck surfaces and suitable holding points are provided.

It should be underlined that by way of recently adopted amendments to the 1974 SOLAS Convention which introduced a new chapter X "Safety Measures for High Speed Craft"[16], the provisions of the Code will become mandatory to high speed craft constructed on or after 1 January 1996.

3.5 Ships engaged in the carriage of irradiated nuclear fuel

Noting the increase in maritime transport of irradiated nuclear fuel, plutonium and high-level radioactive wastes and recognizing that the International Maritime Dangerous Goods Code, which generally implements the International Atomic Energy Agency Regulations for the Safe Transport of Radioactive Material, contains no specific requirements for the design and equipment of ships engaged in the carriage of irradiated nuclear fuel, plutonium and high-level radioactive wastes, the Organization developed the Code for the Safe Carriage of Irradiated Nuclear Fuel, Plutonium and High-Level Radioactive Wastes in Flasks on Board Ships [17]. The Code requires that all ships regardless of size should comply with requirements of the 1974 SOLAS Convention and, in addition, with the requirements of the Code regarding damage stability, fire protection, temperature control of cargo spaces, structural considerations, etc. For the purpose of the Code, ships carrying radioactive materials, depending on the total radioactive quantity which may be carried on board, have been assigned class INF 1, class INF 2 and class INF 3. In case of ship's class INF 1, damage stability of passenger and cargo ships carrying radioactive substances should be to the satisfaction of the Administration concerned. For passenger ships of class INF 2, damage stability criteria of part B of chapter II-1 of the 1974 SOLAS Convention as amended by resolution MSC.12(56) [12] or resolution A.265(VIII) [9] should apply. Cargo ships of class INF 2, should comply with requirements of part B-1 of chapter II-1 of the 1974 SOLAS Convention. Radioactive materials to be transported on ship's class INF 3 are not allowed to be carried on passenger ships. For cargo ships of class INF 3, survival capability and location of cargo

spaces provisions for type 1 ships specified in chapter 2 of the International Code for the Construction and Equipment of Ships Carrying Dangerous Chemicals in Bulk (IBC Code) [18] or, regardless of ship length, requirements in part B-1 of chapter II-1 of the 1974 SOLAS Convention (resolution MSC.19(58)) [8] with subdivision index R_{INF} calculated by formula $R_{INF} = R + 0.2(1-R)$ should apply.

4 CURRENT WORK ON INTACT AND DAMAGE STABILITY CRITERIA

4.1 Intact stability

4.1.1 Revision of the Intact Stability Code

Throughout the development of the Code it was recognized that in view of a wide variety of types and sizes of ships and their operating and environmental conditions, problems of safety against accidents related to stability have generally not yet been solved. In particular, the safety of a ship in a seaway involves complex hydrodynamic phenomena which up to now have not been adequately investigated and understood. It was recognized that development of stability criteria based on hydrodynamic aspects and stability analysis of a ship in a seaway, poses, at present, complex problems which require further research. Criteria included in the Code are based on the best "state of art" concept taking into account sound designs and engineering principles and experience gained from operating such ships. However, as technology for modern ships is rapidly evolving, the Code needs to be re-evaluated and revised as necessary.

In line with this approach and following the instruction by the Assembly to amend the Code as necessary in the light of further studies and experience gained from the implementation of the provisions contained in the Code, further work towards the revision of the Code is scheduled to be undertaken by the SLF Sub-Committee. It was agreed that the following issues should be considered in the context of the work on the improvement of the Code:

- guidance to the master for avoiding dangerous situations in following and quartering seas;

- guidelines for performing operational inclining test;

- procedures for determining the acceptable weight movement during inclining test;

- evaluation of wind forces used in the severe wind and rolling criterion for small ships;

- development of criteria for tugs and tow boats;

- improvement of the intact stability requirements for ships carrying grain , etc.

4.1.2 Ship's stability in following and quartering seas

The stability of a ship in following and quartering seas has been under consideration of the SLF Sub-Committee for a number of years and a draft guidance has been prepared for further consideration at the future sessions of the Sub-Committee with a view to its finalization.

4.1.3 Intact stability of double hull tankers

In view of entry into force of new regulation 13F of Annex I to MARPOL 73/78 [19] regarding prevention of oil pollution in the event of collision or stranding which requires introduction of double hull for tankers, concern was expressed that new double hull tankers, being built without longitudinal bulkheads and having cargo tanks extending their full beam, would need to be subject to operational restrictions in order to maintain adequate intact and reserve stability during cargo/ballast operations.

It was noted that the intact stability characteristics of

double hull tankers and other tanker designs under regulation 13F of Annex I to the MARPOL 73/78, which have significant slack space during loading/unloading/ballasting/ tank cleaning procedure, may require special consideration. The SLF Sub-Committee, at its thirty-eighth session, (March 1994) noted that design solutions which achieve positive intact stability under all operating conditions without reliance upon operational restrictions relating to stability should be encouraged, but did not recommend mandatory design criteria for intact stability. Although proposals were made for amending the MARPOL 73/78 and for modifications to the Intact Stability Code, the decision was made to continue consideration of the proposed amendments to both IMO instruments at the subsequent sessions of the Sub-Committee.

4.1.4 Safety of passenger submersible craft

In the context of the development of the draft guidelines on safety of passenger submersible craft, the SLF Sub-Committee was assigned the task to consider buoyancy and stability matters of passenger submersible craft which are expected to be finalized in 1996.

4.2 Damage stability

4.2.1 Harmonization of damage stability provisions in IMO instruments

The main work on damage stability matters the SLF Sub-Committee has planned to undertake, is the harmonization of damage stability provisions in IMO instruments based on probabilistic method. At its meeting in March 1994, the Sub-Committee considered, in general, overall strategy and philosophy for the work on the harmonization and agreed to initially proceed with harmonization of the cargo and passenger ships damage stability regulations, bearing in mind the future inclusion of other ship types. In this respect the SLF Sub-Committee decided to consider at its next sessions such issues as damage statistics, probability factors, draughts for evaluation, permeabilities, survivability factor(s), subdivision for minor damage, required index (R), definitions, watertight integrity, classification of openings, immersion lines etc. It is envisaged that the work would result in the development of a new chapter II-1, parts A, B and B-1 of the 1974 SOLAS Convention relating to subdivision and damage stability of ships.

In this context it has been recognized that the task to introduce harmonized probabilistic subdivision and damage stability provisions in all related IMO instruments would result in major amendments to the SOLAS, Load Line, and MARPOL Conventions as well as Codes.

REFERENCES

[1] Code on Intact Stability for All Types of Ships Covered by IMO Instruments (resolution A.749(18))

[2] Interim Guidelines for Open-Top Containerships (MSC/Circ.608)

[3] Recommendation on Intact Stability for Passenger and Cargo Ships Under 100 Metres in Length (resolution A.167(ES.IV))

[4] International Convention for the Safety of Life at Sea, 1974, as amended

[5] International Code of Safety for High Speed Craft (resolution MSC.36(63))

[6] Code of Safety for Dynamically Supported Craft (resolution A.373(X))

[7] Recommendation on a Severe Wind and Rolling Criterion (Weather Criterion) for the Intact Stability of

Passenger and Cargo Ships of 24 Metres in Length and Over (resolution A.562(14))

[8] Amendments to chapter II-1 of the 1974 SOLAS Convention (resolution MSC.19(58))

[9] Regulations on Subdivision and Stability of Passenger Ships as an Equivalent to Part B of Chapter II of the International Convention for the Safety of Life at Sea, 1960 (resolution A.265(VIII))

[10] Interpretations of regulations of part B-1 of SOLAS chapter II-1 (MSC/Circ.651)

[11] Interpretation of alterations and modifications of a major character (MSC/Circ.650)

[12] Amendments to regulation II-1/8 of the 1974 SOLAS Convention (resolution MSC.12(56))

[13] Amendments to chapter II-1 of the International Convention for the Safety of Life at Sea, 1974 (Existing ro-ro passenger ships) (resolution MSC.26(60))

[14] Calculation Procedure to Assess the Survivability Characteristics of Existing Ro-Ro Passenger Ships When Using a Simplified Method Based Upon Resolution A.265 (VIII) (MSC/Circ.574)

[15] Interpretations of provisions of resolution MSC.26(60) and MSC/Circ.574 (MSC/Circ.649)

[16] Amendments to the International Convention for the Safety of Life at Sea, 1974 adopted by resolution 1 of the Conference of Contracting Governments to the 1974 SOLAS Convention on 24 May 1994

[17] Code for the Safe Carriage of Irradiated Nuclear Fuel, Plutonium and High-Level Radioactive Wastes in Flasks on Board Ships (resolution A.748(18))

[18] International Code for the Construction and Equipment of Ships Carrying Dangerous Chemicals in Bulk (IBC Code) (resolution MSC.4(48))

[19] International Convention for the Prevention of Pollution from Ships, 1973, as modified by the Protocol of 1978 relating thereto (MARPOL 73/78)

FERNANDO PLAZA, a Spanish national, graduated in naval architecture and marine engineering from the Superior Technical School at Madrid University. He then entered Lloyds Register of Shipping as a Ship Surveyor and after some years he joined the International Maritime Organization (IMO) in 1975. He is, at present, Head of the Sub-Division for Technology and TC Implementation and Senior Deputy Director of the Maritime Safety Division of IMO.

ALEXANDER A. PETROV is a Technical Officer of the Maritime Safety Division of IMO and is the Secretary of the Sub-Committee on Stability and Load Lines and on Fishing Vessels Safety. In 1969, he graduated in naval architecture from the St. Petersburg Marine Technical University and started work as a naval architect at a shipyard in St. Petersburg. Before joining IMO in 1992, he held a position as a Senior Surveyor with the Russian Federation Register of Shipping.

A Study of the Dynamic Stability of a RoRo-Ship in Waves

by Jianbo Hua and Olle Rutgersson
Div. of Naval Architecture, KTH, Royal Institute of Technology Stockholm, Sweden

Abstract

A study is carried out for investigation of the dynamic stability problems of a RoRo-ship in regular and irregular waves by means of time-domain simulation. The result presented in this paper has shown that the ship can be subjected to the parametrically excited roll motion not only in regular but also in irregular waves. It is concluded from the calculation of the simultaneous effect of vertical, horizontal acceleration and roll motion on the load shifting onboard that special attention should be paid to the danger of the simultaneous effect in the design of the cargo lashing system onboard and by the onboard crew.

The importance of the interaction between the roll, heave and pitch motion in the dynamic stability problem is emphasised and the further research effort should be made to identify the parameters describing the interaction.

Finally, it is discussed about the survivability of a RoRo-ship after a severe cargo shifting, with thought to the capsizing scenario of the RoRo-ship accidents due to severe weather and sea condition.

.c.1. General
;

1.1 Dynamic stability problems of a RoRo-ship in waves

Intact dynamic stability problems of a ship in waves are more or less connected with large roll motion. Depending on the phase relationship between the roll motion and the roll moments acting on the ship, the roll motion can appear in different manners. The simplest case is the roll motion in resonance with wave excitation. In addition, a ship can be subjected to such as parametrically excited roll motion, roll motion due to pure loss of stability in waves, coupled course instability and roll motion as a consequence of the stability reduction in waves. Furthermore, the simultaneous effect of vertical, horizontal acceleration and roll motion on the load shifting onboard should be considered as a dynamic stability problem when RoRo-ship type is concerned. The lashing system on a RoRo-ship is usually scanted for a limited roll angle of about 30 degrees, while the simultaneous effect is more dangerous than only the maximal roll angle.

Large B/T ratio, high mass centre usually above the still water line, fine hull form and relatively high speed is the main configuration of a RoRo-ship. The cargo decks in a RoRo-ship are often open in the transversal direction. Due to this

configuration, the following aspects which are important in the ship dynamics of view, should be considered in comparison with conventional ships:

* That the RoRo-ship have low natural roll frequency between 0.3 to 0.45 rad/sec, while conventional ships having natural roll frequency usually greater than 0.5 rad/sec.
That means that occurrence of encounter frequency twice the natural roll frequency is more probable to the RoRoship in the waves which can induce considerable parametric excitation;

* That considerable magnitude of GM-variation in waves relatively to the initial mean GM could be expected due to the large B/T ratio in combination with fine hull form;

* That the roll motion is strongly coupled to sway, heave, pitch and yaw motion due to the high mass centre and fine hull form.

* That longer encounter periods in following waves in combination with severer loss of the transverse stability is crucial for the course instability in waves;

* That a poosible load shifting onboard can cause large heel angle due to the transversely open decks, which in turn leads to severe consequences. The worst case can be a total loss of the ship.

In Europe, numberous capsizing accidents of RoRo-ships have been reported during the last fifteen years. Among those RoRoships there are ZENOBIA, HERALD OF FREE ENTERPRISE, VINCA GORTHON and JAN HEWELIUSZ. ZENOBIA capsized in 1980 as a consequence of load shifting onboard caused by an uncontrollable manoeuvre motion. About four months before the capsize ZENOBIA was also subject to load shifting due to the large ship motions at a severe sea. HERALD OF FREE ENTERPRISE capsized outside the breakwater of Zeebrugge on her route to Dover 6th March 1987. Over 180 human lives were lost. The basic reason for the capsize was that the ferry was trimmed by bow and had the bow doors left open so that water got ingress to the car deck as the ship's speed increased. VINCA GORTHON was a RoRo-ship for paper-product transport from Sweden to European Continent, and she sank in 1988 due to the load shifting caused by the simultaneous effect of vertical and horizontal acceleration, and roll motion at a moderate sea. At the last year JAN HEWELIUSZ capsized under a severe storm over the Baltic Sea. 55 lives were lost in the accident. That is one of the heaviest human losses due to ship capsizing during 1993.

The consequence of a RoRo-ship loss is usually considerable. The price of a RoRo-ship is in average higher than other kind ships in same size for cargo transport and the transported goods are high-valued, which means that a RoRo-ship casualty could lead to a large economical losses for the partners involved in the goods transport. The casualty of a ferry of RoRo-type can be a catastrophe for

the passengers onboard. The capsizes of HERALD OF FREE ENTERPRISE and JAN HEWELIUSZ are the cases with heavy losses of human life.

The RoRo-ship is a relatively new type ship, and so the technical aspect into the accident mechanisms becomes always an important object for discussion. No ageing problem has been observed to those capsized RoRo-ships, which often occurs to other kinds of ships. In fact, the dynamic behaviour is often a governing factor to the most of the capsize accidents of RoRoship.

1.2 A review of research works

Parametrically excited roll motion of a ship was observed by Froude more than one hundred years ago. The interest arose
early in the beginning of the fifties to study this kind problem. Kerwin investigated in 1959 the GM-variation of a ship model in longitudinal waves and its effect on the roll motion. The result from the numerical calculation showed a fair agreement with the model measurement. Paulling and Rosenberg studied in 1959 the problem by assuming that the variation of roll restoring moment of a ship is a result of forced heave motion of the ship in still water.

A lot numbers of study of ship dynamic stability in waves can be found in the literature. In the following, however, the review will be focused on the studies which are more or less associated with the RoRo-ships or of interest to the object studied in this paper.

Nayfeh et. al carried out in 1973 an analysis of a mathematical model which takes into account the non-linear coupling of the pitch and roll modes of ship motions in regular longitudinal waves. By means of the method of multiple scales the cases were studied where ratio between the natural pitch and roll frequencies are two or one, i.e. the roll motion is parametrically excited by the pitch motion. The saturation phenomenon as a consequence of the interaction between pitch and roll motions was observed. This phenomenon occurs when the wave amplitude is sufficiently large. The kinematic energy delivered by the waves what exciting the pitch motion of the ship is partly transferred to the roll motion so that the roll amplitude grows gradually while the pitch amplitude remains constant.

Wright and Marshfield proposed in 1980 a simple roll equation in their study of ship roll response and capsize behaviour in beam seas. The non-linear wave excitation is taken into account by introducing a relative roll angle between the roll angle and the wave slope as the variable instead of roll angle in the roll equation. Addition to the simple roll equation are proposed which allow heave, pitch and sway to be included and also parametric excitation.

Lindemann and Skomedal investigated in 1982 the behaviour of a RoRo-ship with respect to the parametrically excited roll motion using a time-domain simulation method. They assumed that the magnitude of the parametric excitation is proportional to the relative motion between wave surface and ship amidships.

A quasi-static equilibrium calculation of the GM-variation of a RoRo-ship passed by a longitudinal wave was done by Sjšholm and Kjellberg 1985. The result shows that the wave pattern constitutes the dominant part of the quasi-hydrostatic effect on the GM-variation. In comparison, the heave or pitch motion gives less contribution to the GM-variation

A systematic investigation was carried out by Huss 1988 into the influence of hull form of modern RoRo-ships in waves on the GM-variation. He took the effect of the wave-induced heave and pitch motions into account. The conclusion was that the modern hull forms are more sensitive to the GM-variation in waves than the conventional hull forms.

A theoretical study on the capsize of the ferry 'Herald of Free Enterprise' was carried out by Hua in 1988. The result from time-domain simulation of a simplified mathematical model has shown that the capsize was a consequence of the dynamic interaction between heeling and turning motion.

Hua made in 1988 also an analysis of the dynamic behaviour of
RoRo-ship 'ZENOBIA' in connection with the ship loss the 2nd June 1980. The result has shown that a fine hull form with large B/T ratio: in combination with high vertical position of the mass centre has an influence on Zenobia's manoeuvre properties and seaworthiness.

Kan et al. made both experimental and theoretical study of dynamic instability of ships in quartering waves under the later 80's and early 90's. Large number model tests have been carried out and several capsizing modes have been observed, including the bifurcation phenomenon.

Time-domain simulation method was used by Hua in 1990 to study the parametrically excited roll motion of a RoRo-ship in longitudinal waves. The influence of parameters such as ship speed, KG-value, wave amplitude etc. on this kind of roll motion has been investigated.

1.3 The work presented in this paper

The assumption to the mathematical model used in this study will be described briefly. The dynamic problems are investigated for a RoRo-ship in oblique waves , for which the problem of parametrically excited roll motion in following waves was observed in model scale.

The GZ- and GM-varaitions of the ship in regular waves are calculated based on the assumption of quasi-static equilibrium, and expressed as Fourier Series with aspect to time and encounter frequency. The zero- and first order GZ- and GM-variations are presented as a function of wave length.

The GZ- and GM-varaition calculated based on the assumption of quasi-staic equilibrium are the characteristic parameters for the stability reduction of the ship in

following waves, and also important for the course-instability in waves. The GM-variation is also used as an important parameter for the analysis of the results from the time-domain simulation of the parametrically excited roll motion of the ship in waves.

The parametrically excited roll motion are calculated in time domain for the ship in regular and irregular waves. Different combinations of ship speed, wave direction and wave length are used as input data in order to study the effect of service condition on the roll motion behaviour.

The simultaneous effect of vertical, horizontal acceleration and roll motion on the load shifting onboard is calculated.

Finally, it is discussed about the survivability of a RoRo-ship after a severe cargo shifting, with thought to the capsizing scenario of the RoRo-ship accidents due to severe weather and sea condition.

.c.2. Basic Assumptions and Calculation Methods of the Study;

The mathematical model for the actual study is implemented in the general computer program SMS developed at The Royal Institute of Technology, division of Naval Architecture. All details can be found in /6/.

The ship is assumed as a rigid body. So the ship motions follow the Newton's second law ;

$$[M]\cdot\left\{\ddot{\eta}\right\}=\{F\} \qquad (2.1)$$

where $\ddot{\eta}$ is the vector for the six degrees of motion freedoms defined in Figure.2.1, [M] represents the mass properties of the ship and is defined as the following:

$$\begin{aligned} &M(i,i)=m \qquad for\, i=1,2,3\\ &M(4,4)=m\cdot r_4^2\\ &M(5,5)=m\cdot r_5^2\\ &M(6,6)=m\cdot r_6^2\\ &M(i,j)=0 \qquad for\, i\neq j \end{aligned} \qquad (2.2)$$

(2.2)

There above, r4, r5 and r6 are the radii of mass moment of inertia of roll, pitch and yaw motion respectively.

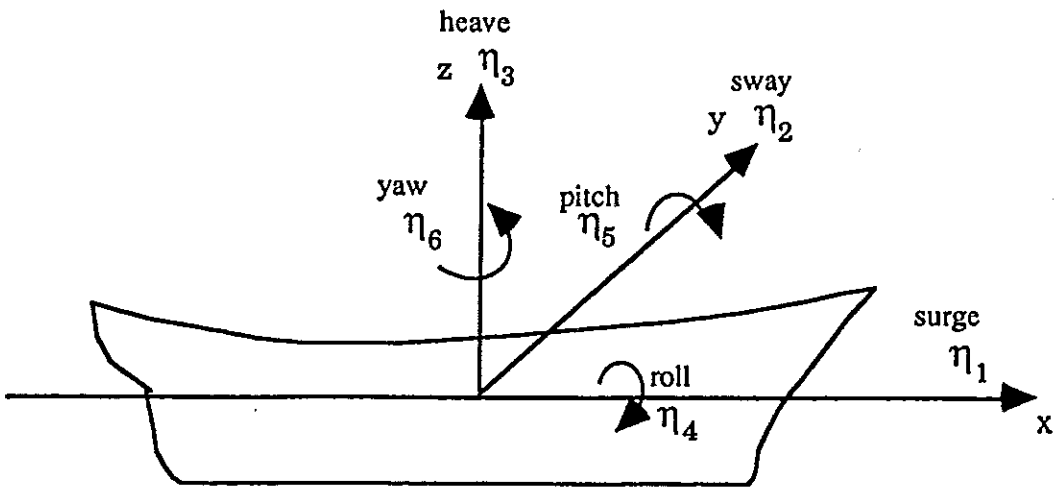

Fig.2.1 Ship body-fixed co-ordinate system and the definition of the six degrees of motion freedom, η_i i=1,2...6.

{F} in (2.1) is the force vector. The forces acting on the hull in general consist of control forces from propeller and ruder, environmental forces from wind and waves and reaction forces due to the ship motions. In this study only deep water is considered.

When the problem of parametrically excited roll motion in concerned, only the forces due to wave excitation and reaction forces due to the wave-induced ship motions are taken into account. The other forces are assumed to be neutralised by each other. In an another word, the ship speed and relative course of the ship to wave direction keep constant during the timedomain simulation for a same service condition. The wave excitation forces consist of Froude-Kryloff forces and diffraction forces, and the reaction forces of restoring forces and radiation forces.

When calculating the radiation and diffraction forces, the extraordinary strip theory /13/ is applied and only the submerged hull body at mean draught in still water is considered. The two-dimensional frequency-dependent added masses and damping coefficients are calculated by using the two-dimensional boundary element method so called 'close-fit method', developed by Frank 1967 with the assumptions of small motion magnitude and linearilized free surface condition.

The Froude-Kryloff forces and restoring forces are calculated by integrating the quasi-hydrostatic pressure distributed over the momentary submerged hull under the wave surface, which is corrected for the Smith-effect due to the incident wave potential.

The hydrodynamic memory effect due to the roll motion and consequently its effect expressed as roll damping is almost negligible at the frequencies lower than 0.5 rad/s, see Figure 2.2. The radii of the added moment of inertia for roll motion is generally about 15% of the ship beam. In comparison, the radii of the mass moment of inertia is 30%. That means that the added moment of inertia is about 20% of the sum of the added and mass moments of inertia. At the roll resonance, the hydrodynamic roll moment is only about 20% of the hydrostatic restoring moment.

In /5/ the parametrically excited roll motion of the actual RoRo-ship in longitudinal waves was studied and the added masses and damping coefficients calculated with consideration to the momentary submerged hull body under the wave surface. However, the hydrodynamic component of the parametric excitation is insignificant in comparison the quasi-hydrostatic excitation caused by the incident wave potential and the waveinduced heave and pitch motion. The fact is that the hydrodynamic component is strongly dependent upon the submerged hull form, while the quasi-hydrostatic one is more dependent upon the hull form near the still wave line and therefore sensitive to the wave profile passing through the hull. That is why only the quasi-hydrostatic component of the parametric excitation is taken into account in this study.

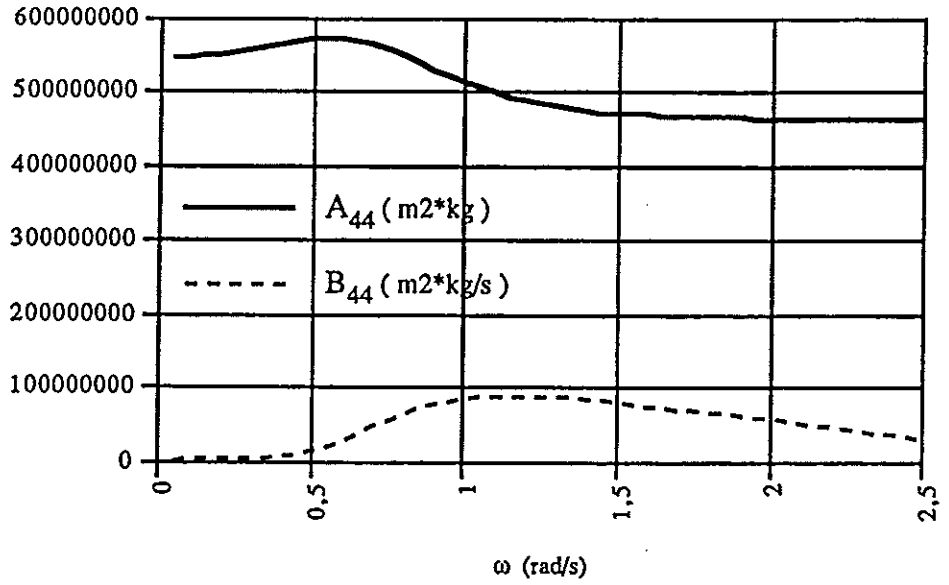

Figure.2.2 Added moment of inertia and hydrodynamic damping coefficient of roll motion.

Equation (2.1) can be rewritten so that the hydromechanic reactions due to the ship motions can be expressed in terms of added masses [A], damping coefficients [B] and hydro-restoring coefficient [C] in the left side of the motion equations and the right side is for the wave excitation forces, see (2.3).

$$([M]+[A])\cdot\left\{\ddot{\eta}\right\}+[B]\cdot\left\{\dot{\eta}\right\}+[C]\cdot\left\{\eta\right\}=\{F\} \qquad (\ 2.3\ )$$

The roll damping can be expressed as a percentage of the magnitude of the critical roll damping if the roll damping of a ship has a linear character. In this study 10% of the critical roll damping is generally used if not noted. However, it is simplified because the roll damping is usually non-linear.

.c.3. The Studied RoRo-ship;

The main particulars of the studied RoRo-ship are shown in Tab.3.1 and follow the statistic average ones in the same size of the RoRo-ships recorded in DET NORSKE VERITAS ÇRegister of ShipsÈ, see the diagrams illustrated in /2/. The hull form is also commonly for a RoRo-ship, see Fig.3.1 and its GZ-curve in still water is shown in Fig.3.2.

Tab.3.1 The Ship«s Main Particulars

Lpp	180 m	B	27.3 m
T	9.1 m	Cb	0.65
KG	11.2 m	GM0	0.81

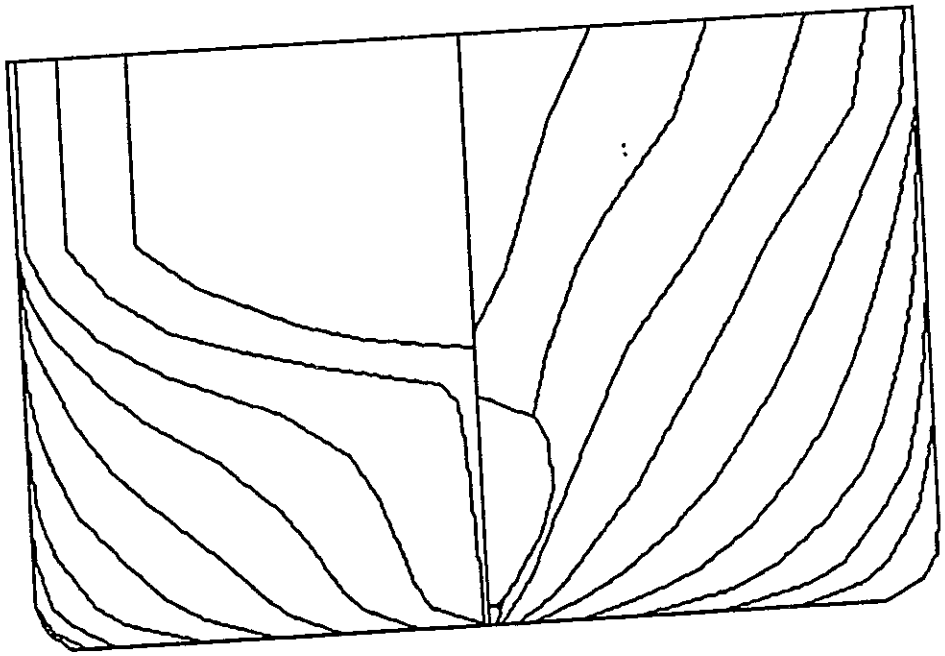

Fig.3.0.1 The hull form

The ship motions in waves in model scale has been investigated by Söderberg in 1985 at SSPA. The parametrically excited roll motion was observed for the ship model in following sea. Fig.3.3 shows roll -, heave -, and pitch motions, wave height, rudder angle and speed variation as function of time. The roll frequency is about half the encounter frequency, which is typical to the parametrically excited roll motion.The roll angle grows up to 15 - 18 degrees within 7 -8 encounter periods.

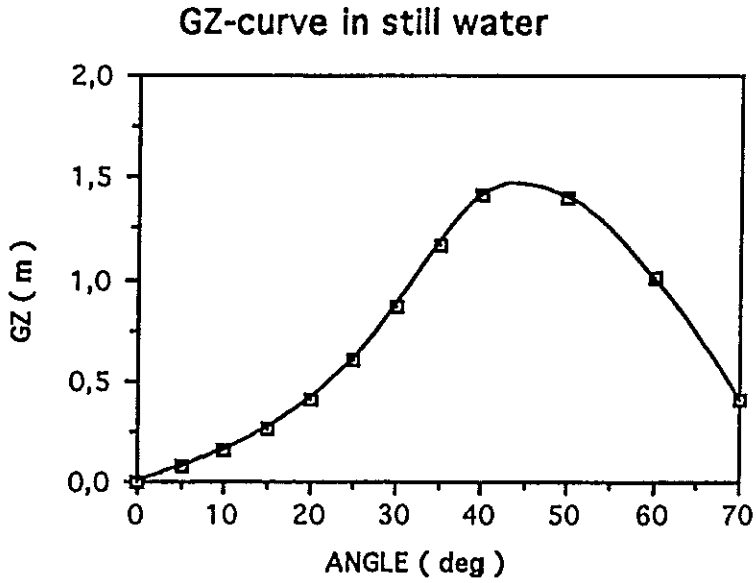

Fig. 3.2 GZ-curve in still water

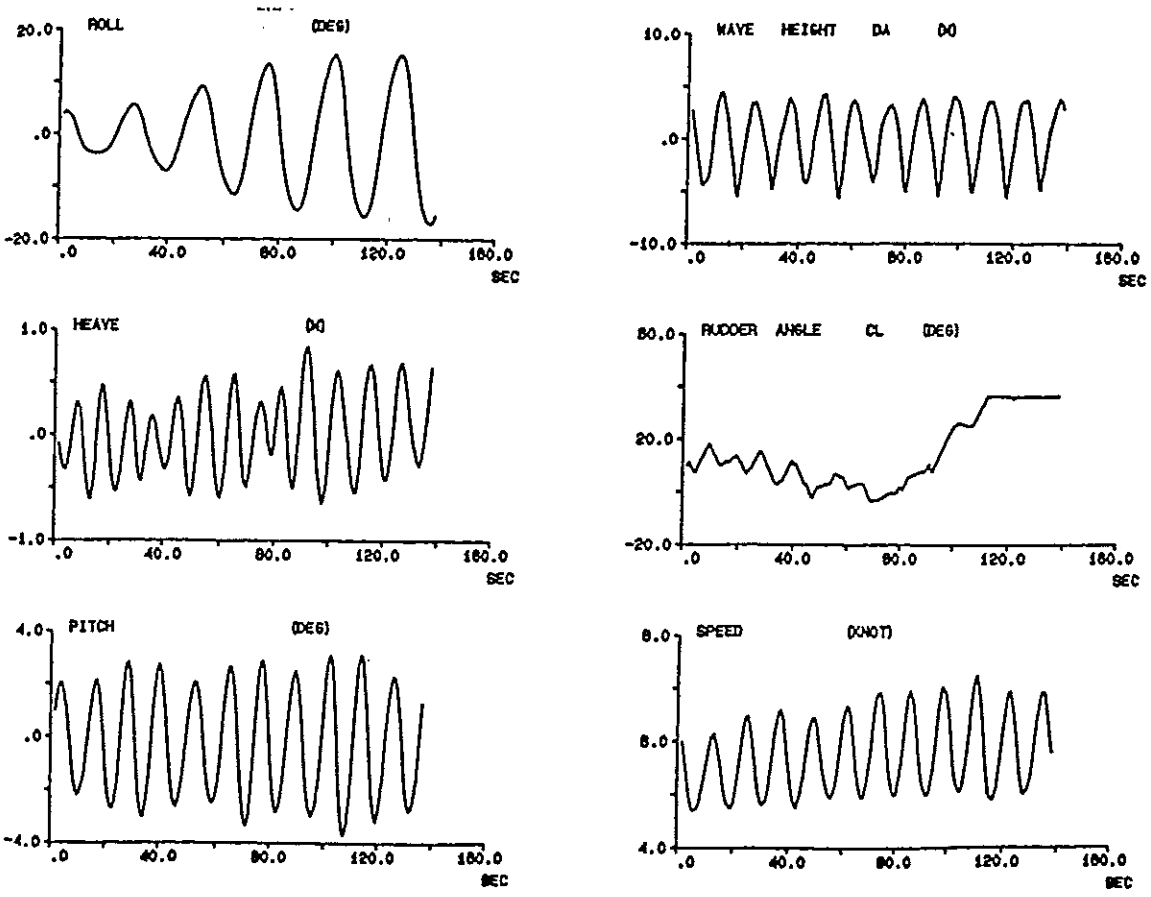

Fig.3.3 Ship motions in a following sea observed in model scale.

.c.4. Quasi-Static Equilibrium Calculation of GZ-variation in Waves;

The GZ-curve of a ship is an important parameter to the roll motion, particularly in the context of dynamic stability. As known, the IMO's intact stability criterion is totally based on the calculation of the GZ-curve in still water. However, the GZ-curve of the ship in waves changes with time and the configuration of the GZ-variation is governed by both the wave profile passing through the hull, and the wave-induced ship motions. So the wave amplitude, wave length and the relative course angle together with ship speed are the governing parameters of the GZ-variation in regular waves.

The assumption of quasi-static equilibrium, i.e. that the displacement of the ship submerged by the quasi-wave surface is equal to that in still water and that the trim moment is zero, is used for the following calculation of the GM- and GZvariations of the RoRo-ship in following waves without forward speed.

As mensioned early, the calculated GZ- and GM-varaitions are the characteristic parameters for the stability reduction of the ship in following waves, and also important for the courseinstability in waves.

When the parametrically excited roll motion is concerned; the GZ-variation can be expressed as followed:

$$GZ(\phi,t) = GZ_0(\phi) + \sum_{n=1}^{N}\left[GZ_n^c(\phi)\cdot\cos(n\cdot\omega_e\cdot t) + GZ_n^s(\phi)\cdot\sin(n\cdot\omega_e\cdot t)\right] \qquad (4.1)$$

The curves $GZ_n^c(\phi)$ and $GZ_n^s(\phi)$ are determined by means of Fourier-analysis of $GZ(\phi,t)$. It was shown in /4/ that it is an appropriate approach to study the problem.

As well, the initial GM-variation in a regular wave can be expressed:

(4.2)

In Fig.4.1, the GZ-variation is shown for the actual ship in a regular wave of wave length 156.0 meters (wave period 10 seconds). The wave amplitude is 3 meters. The higher order
and for n>=2 are insignificant in comparison with
the zero and first order GZ-variation.

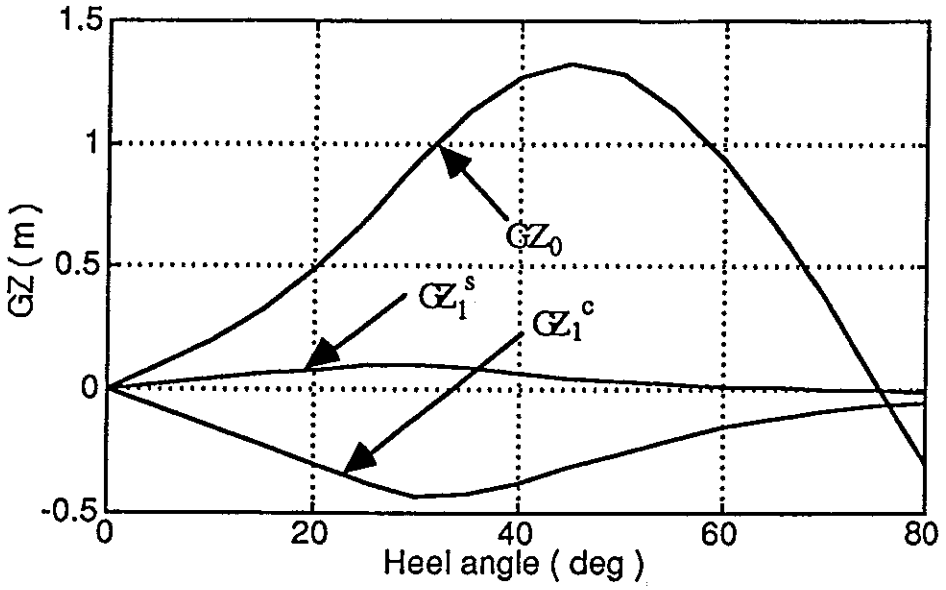

Fig.4.1 The zero, first order GZ-curves in a regular wave with 3 meters amplitude and 156.0 meters wave length.

As seen in Fig.4.1, the Mathius Equation (5.1) represents the GZ-variation only in the initial stage of the roll motion. When the roll angle becomes larger than about 30 degrees, the GZ-variation is overestimated in the Mathius Equation, because the curves $GZ_1^c(\phi)$ and $GZ_1^s(\phi)$ decrease with increasing roll angle.

Fig.4.2 shows the zero order GZ-curves in three regular waves with the same wave length of 156.0 meters and wave amplitudes 1, 3 and 5 meters respectively. The zero order GZ-curves can be compared with the GZ curve in still water, see Fig.3.2. The one in the wave with 5 meters amplitude is obviously considerably different from that in still water.

Fig.4.3 shows that the zero-order initial GM for wave amplitudes 1, 3 and 5 meters decreases asymptotically to the value in still water as the wave length increases to 4 times the ship length.

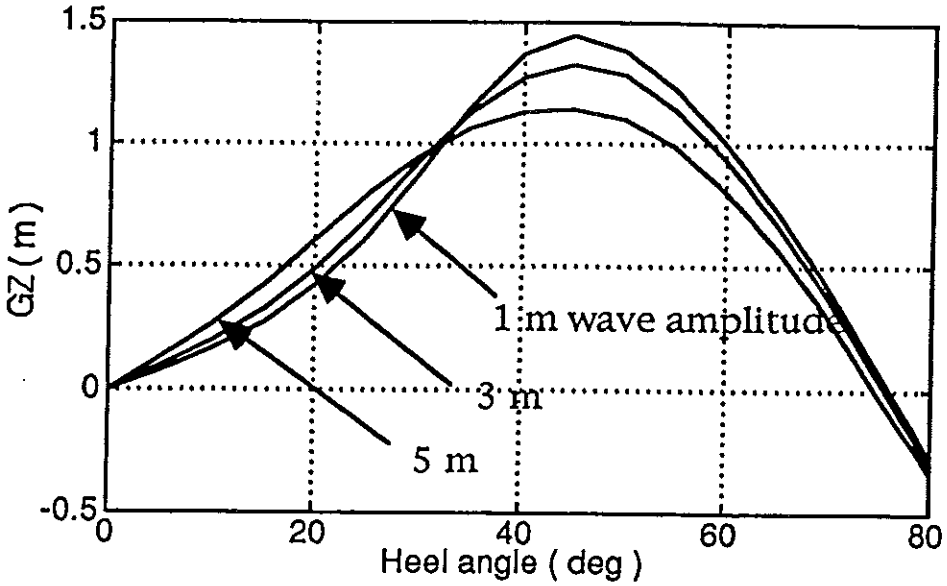

Fig.4.2 The zero order GZ-curves in three regular waves with a same wave length of 156.0 meters.

The first order initial GM-variation as a function of wave length is demonstrated in Fig.4.4 for wave amplitudes 1, 3 and 5 meters. As seen, the first order GM-variations have their maximums at the wave length about 80% of the ship length. Comparing Fig.4.4 with Fig.4.3, the maximal zero GM and the maximal first order GM-variation appear at the same wave length.

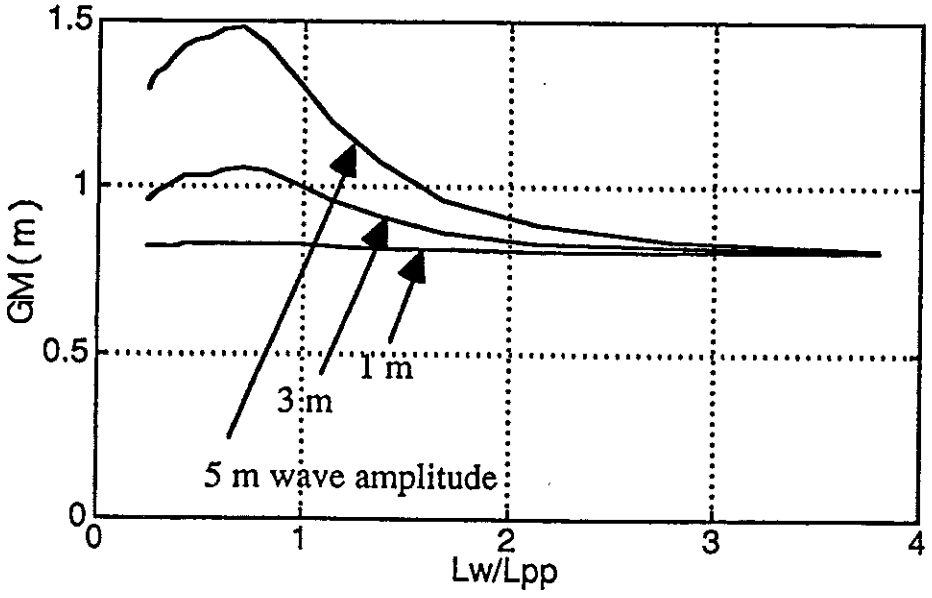

Fig.4.3 The zero order GM in waves as function of wave length. The wave amplitudes are 1, 3 and 5 meters.

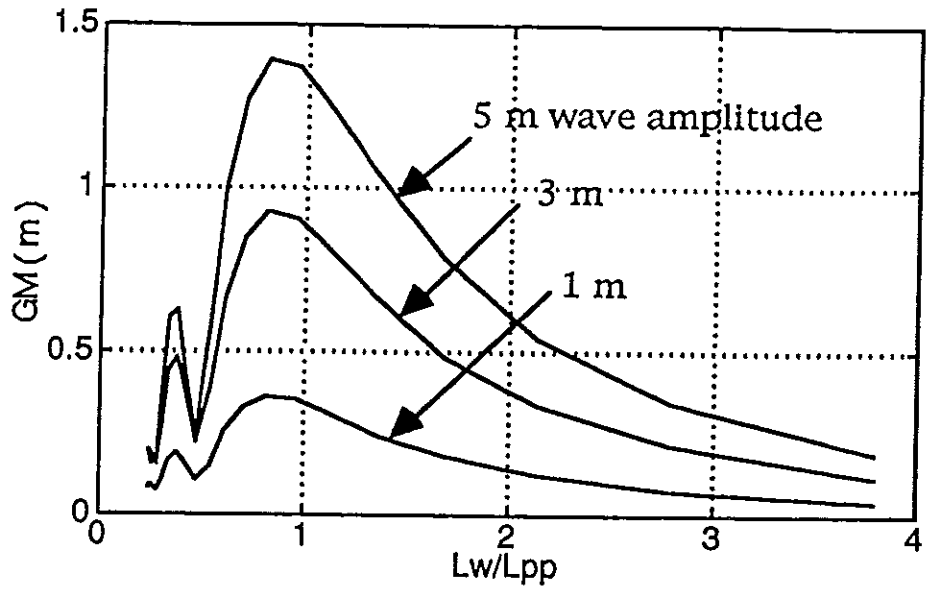

Fig.4.4 The first order GM-variation as function of wave length for wave amplitudes 1, 3 and 5 meters.

.c.5. Parametrically Excited Roll Motion in Oblique Regular Waves;

Parametrically excited roll motion of a ship in waves is a resonance phenomena, which occurs when the uprighting moment arm GZ varies about a mean value with a frequency in a specific ratio, such as 2, 1, 1/2, 1/3,.1/4....., to the natural roll frequency of the ship. The characteristics of this problem is usually described mathematically by means of the Mathius Equation:

$$\ddot{\phi}+2\cdot\rho\cdot\omega_0\cdot\dot{\phi}+\omega_0^2\cdot\left(1+h\cdot\cos(\omega_e\cdot t)\right)\cdot\phi=0 \qquad (5.1)$$

The solution to the Mathius Equation shows that the most dangerous case occurs when the specific ratio is equal to 2, which demands lowest h-parameter to result in unstable roll motion. Fig.5.1 shows the borderline between stable and unstable zoons as function of h and w0/we for different roll damping coefficients.

h in the above equation is a characteristic value for the parametric excitation, and ρ the linear damping coefficient expressed as percentage of the critical roll damping.

Both the frequency and magnitude of the GZ-variation are functions of ship speed, wave length, ship course in relation to the wave direction, hull form, vertical position of the mass centre, wave amplitude and finally ship motion responses in waves. Exactly, the frequency of the GZ-variation means here the encounter frequency.

The following calculation will be concentrated upon the most dangerous case, i.e. the encounter frequency keeps constant equal to 0.6 rad/s while the natural roll frequency of the ship in still water is 0.3 rad/s. For a same encounter frequency, the relationships between wave frequency, relative course and ship speed follows the equation:

$$\omega-\frac{\omega^2}{g}\cdot U\cdot\cos(\beta)=\omega_e=constant \qquad (5.2)$$

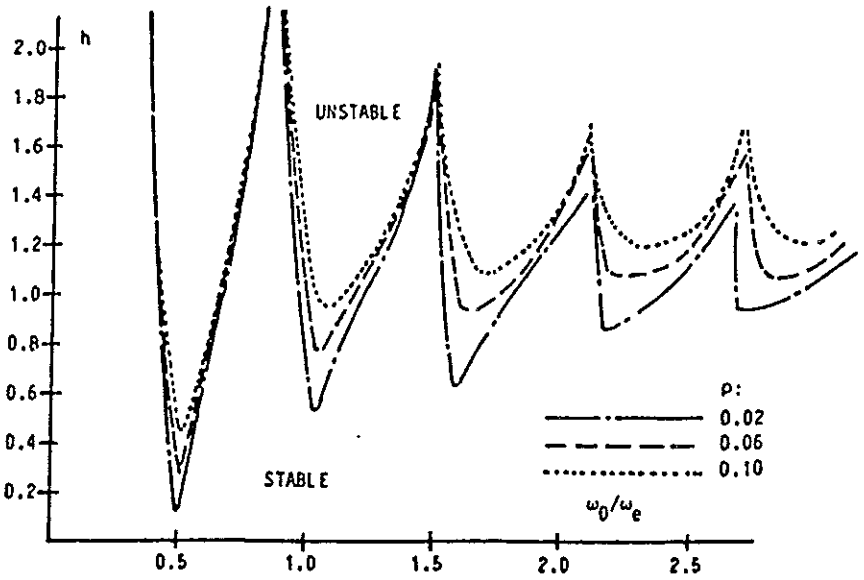

Fig.5.1 The borderline between stable and unstable zoons as function of h and w0/we for different roll damping coefficients,made by Huss by means of numerical simulation of the equation (5.1).

A initial heel angle of three degrees was onset at the beginning of a time-domain simulation to initialise the parametrically excited roll motion.

The calculation is carried out with the ship speed U, relative course β, wave amplitude, ratio of the wave length to ship length, h-parameter and zero order GM as the characteristic parameters for every case of the parametrically excited roll motion of the ship in oblique regular waves. The h-parameter is defined as the following:

$$h = \frac{GM_1}{GM_0} \qquad (5.3)$$

where GM_0 and GM_1 are defined in (4.2).

Fig.5.2 shows the calculation of the parametrically excited roll motion in following and heading waves in five conditions. The values of the characteristic parameters for the five conditions are found in Tab.5.1.

Tab.5.1 Characteristic parameters for the result in Fig.5.2 (ω_e=0.6 rad/s for all the cases)

Case No.	Speed (knot)	β (deg.)	Wave am. (m)	λ_w/L_{pp}	h-value	GM_0 (m)
A.1	5	0	3	0.626	0.648	1.087
A.2	0	0	3	0.95	0.861	1.046
A.3	6	180	3	1.281	0.728	0.961
A.4	10	180	3	1.487	0.626	0.926
A.5	14	180	3	1.674	0.544	0.902

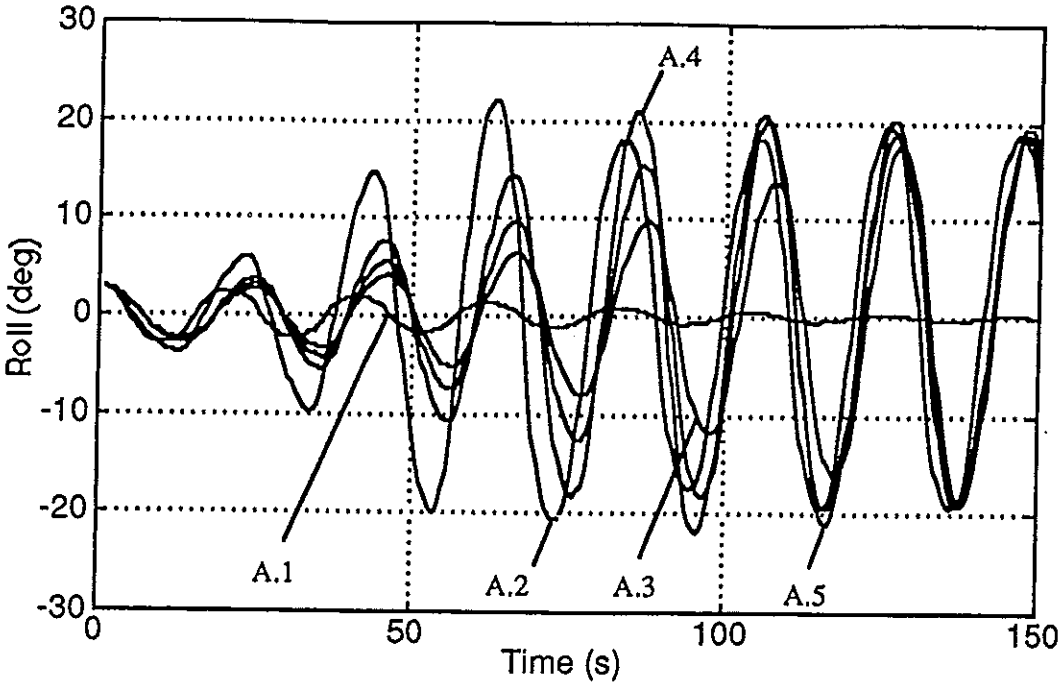

Fig.5.2 Parametrically excited roll motion in following and heading waves. The values of the characteristic parameters for the five conditions can be found in Tab.5.1.

Fig.5.3 shows the calculation of the parametrically excited roll motion in oblique waves for five conditions. The values of the characteristic parameters for the five conditions can be found in Tab.5.2.

Tab.5.2 Characteristic parameters for the result in Fig. 5.3 (ω_e=0.6 rad/s for all the cases)

Case No.	Speed (knot)	β (deg.)	Wave am. (m)	L_W/L_{pp}	h-value	GM_0 (m)
B.1	0	0	3	0.95	0.861	1.046
B.2	0	30	3	0.95	0.772	1.004
B.3	0	45	3	0.95	0.606	0.955
B.4	0	60	3	0.95	0.311	0.910
B.5	0	90	3	0.95	0.107	0.880

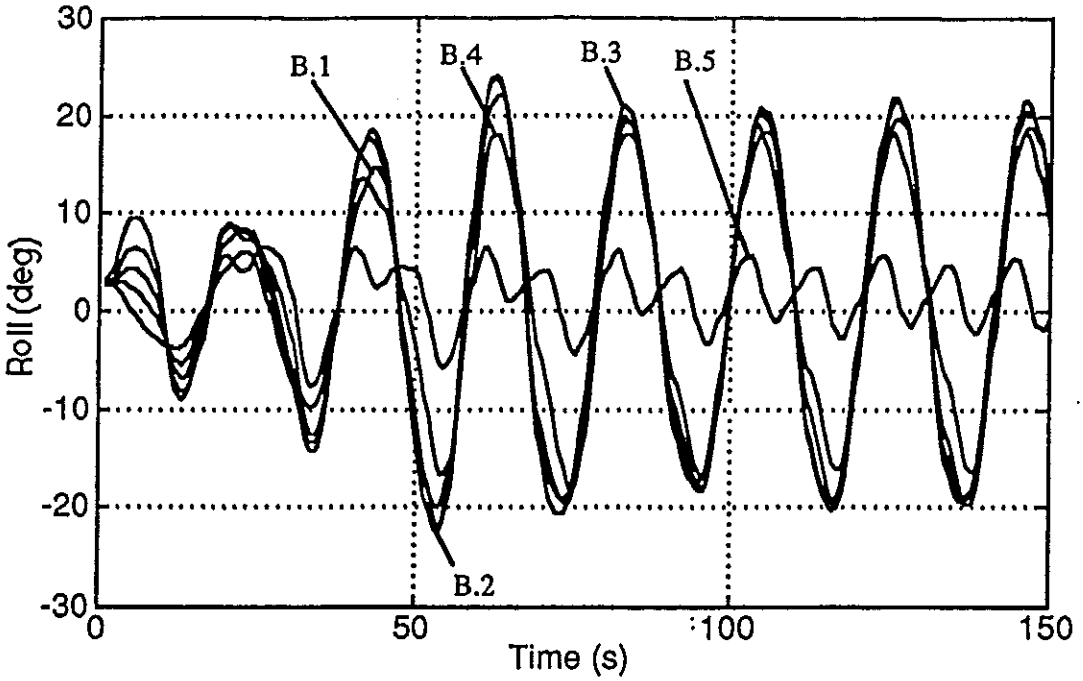

Fig.5.3 Parametrically excited roll motion in oblique waves.
The values of the characteristic parameters for the five cases can be found in Tab.5.2.

Fig.5.4 shows the time histories of parametrically excited roll motion in oblique waves for five conditions. The values of the characteristic parameters for the five conditions can be found
in Tab.5.3. The special in Fig.5.4 is that the ratio of the projected wave length along the ship to ship length keeps constant equal to 0.95. The projected wave length along the ship is defined as:

$$L_e = \frac{L_{pp}}{\cos\beta}$$

Tab.5.3 Characteristic parameters for the results in Fig.5.4 (ω_e=0.6 rad/s and L_e/L_{pp}=0.95 for all the cases)

Case No.	Speed (knot)	β (deg.)	Wave am. (m)	L_w/L_{pp}	h-value	GM_0 (m)
C.1	0	0	3	0.95	0.861	1.046
C.2	0.147	15	3	0.92	0.852	1.056
C.3	0.627	30	3	0.82	0.815	1.072
C.4	1.590	45	3	0.67	0.601	1.060
C.5	3.480	60	3	0.475	0.073	0.986

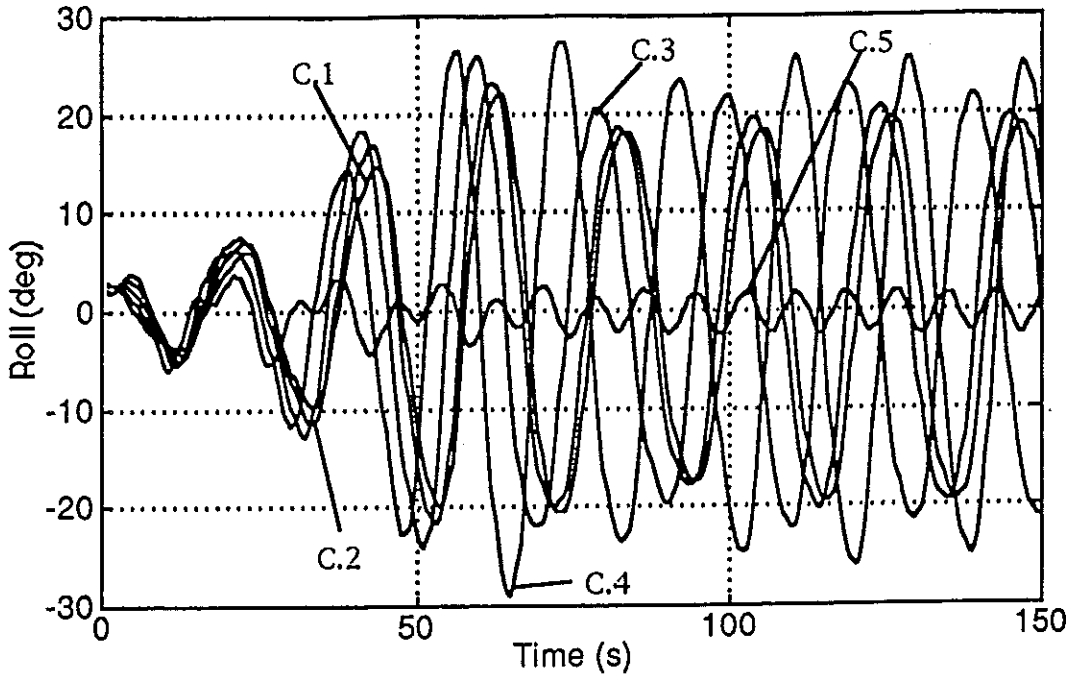

Fig.5.4 Parametrically excited roll motion in oblique waves.
The values of the characteristic parameters for the five conditions can be found in Tab.5.3.

A time history of parametrically excited roll motion can be divided into two stages, firstly the transient and secondarily stationary stage. From the results in Fig.5.2 - Fig.5.4, it can be found that the maximal roll angle in the transient stage due to the initial effect can be greater than the maximal one in
the stationary stage.

Although different values to the characteristic parameters, particularly the h-parameter, the maximal roll angle of the parametrically excited roll motion in the stationary stage seems very closed each other in Fig.5.2 except the curve A.1. That is about the same in Fig.5.3 and Fig.5.4. The reason may be a strong coupling between the roll, heave and pitch motion, which counteracts an increase of the roll amplitude. A similar phenomenon was also found in the study carried out early by one of the authors, see /5/.

It should be reminded that the unstable roll motion to the equation(5.1) means that the roll amplitude becomes infinitely with the time. However, that is not the case in the presented result.

In general, a h-parameter defined as in (5.3) can result in parametrically excited roll motion if it is greater than the critical h-value about 0.43 in the borderline in Fig.5.1. But
there is still an exception. The h-parameter is only 0.311 in the case B.4 where the parametrically excited roll motion still occurs.

No parametrically excited roll motion takes place in the case A.1 although the h-parameter in that case is greater than that in A.5 where this kind roll motion is observed. The results of both the case A.1 and B.4 are the consequence of the strong coupling between the roll, heave and pitch motion, which also has the effect upon the GZ-variation in the waves.

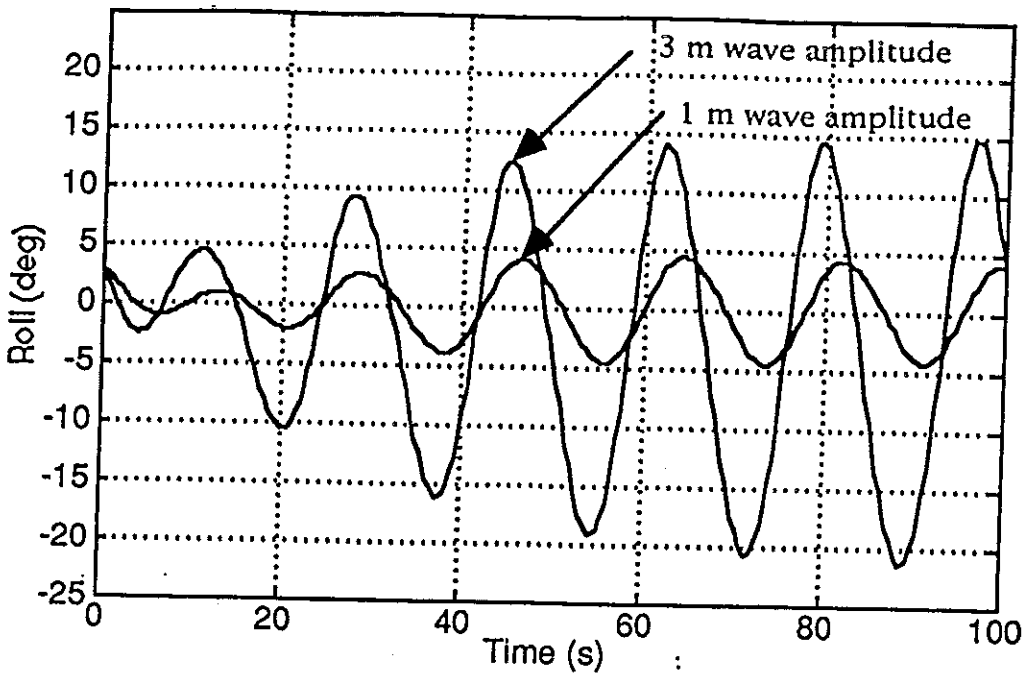

Fig.5.5 The roll motions of the ship in two regular quartering wave with β=30 degrees. The encouter frequency $\omega_e \approx \omega_n$. The wave amplitudes are 1 and 3

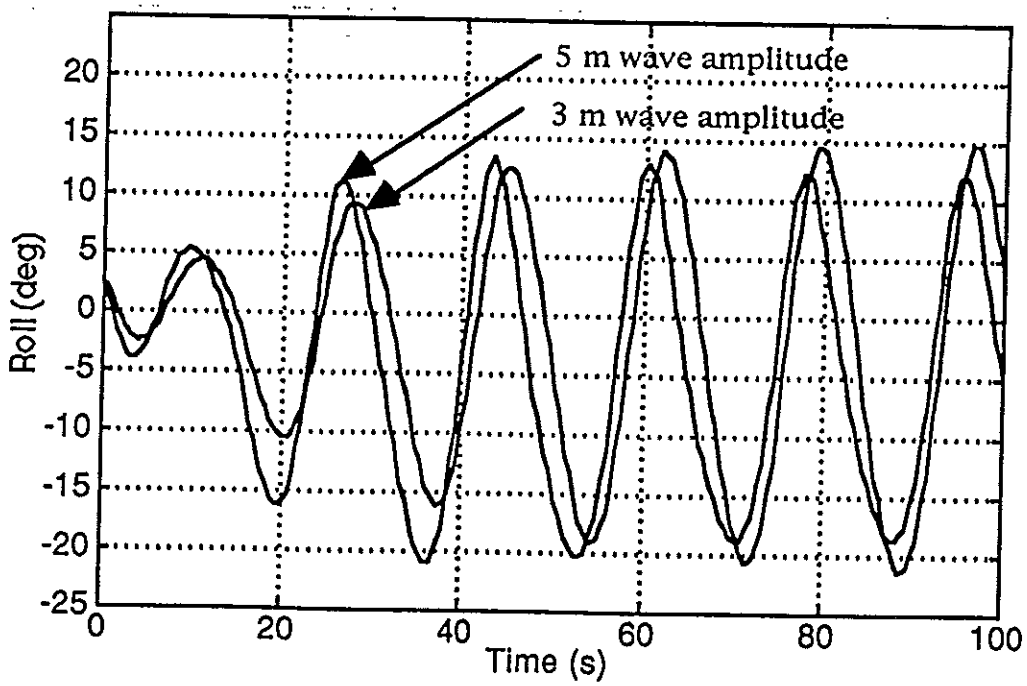

Fig.5.6 Same as for Fig.5.5, but the wave amplitudes are 3 and 5 meters.

Fig.5.5 shows the roll motions of the ship in two quartering waves of wave ampliudes 1 and 3 meters. The ship speed is 15 knots, the relative course b 30 degrees and the wave length 156 meters, which result in an encounter frequency of 0.317 rad/s, very near the natural roll frequency. As seen, the roll motion is symmetric with a roll amplitude miner than 5 degrees around the time-axe in the wave of 1 m amplitude, while it is asymmentric in the wave of 3 m amplitude and the minimal roll angle is miner than -20 degrees. Simply, the ship is subjected to both the direct and paramtric roll moment in the later case.

The roll motion is also calculated for the ship in a quartering wave of 5 m wave amplitude, and the other input parameters are the same as the previsous calculation. The comparison is shown in Fig.5.6 with the roll motion in the wave of 3 m wave amplitude. The remarkable is that the maximal roll angle is miner for the 5 m wave amplitude than for the 3 m. The calculation result has shown that the interaction between the roll, heave and pitch counteracts strongly the increase of the roll amplitude in the case of 5 m wave amplitude. Both the heave and picth motion in that case become asymmetric about the equilibrium position in still water.

.c.6. Parametrically Excited Roll Motion in Irregular Waves;

P-M spectrum with signficant wave height , zero-close mean period as independent parameters is used for the description of a long crested irregular wave in this study.

It is well known that the wave profile of an irregular wave has infinite variances both in time and space. To make a statitisc analysis of the parametrically excited roll motion in an irregular wave, it demands a time-domain simulation with different combinations of the random wave phases, corresponding to the real time of at least 3 hours. That requires considerable computer capacity. However, it is essential to achelv the knowledge about the relationship between the wave spectrum characteristics and the main ship particulars, which can result in the parametrically excited roll motion. That is the aim of this study.

In the calculation of parametrically excited roll motion in irregular waves, a roll moment, which in still water induces a heel angle of three degrees is assumed acting on the ship. The roll moment can be caused due to wind load on the superstructure and/or unsymmetrical cargo distribution.

Tab.6.1 Input parameters to the parametrically excited roll motion in irregular oblique waves

Fig. No.	$H_{1/3}$ (m)	T (s)	Speed (kniot)	Course (deg)
Fig.3.3.1	10	11	10	180
Fig.3.3.2	10	10	10	150
Fig.3.3.3	10	10	10	210
Fig.3.3.4	10	10	10	135
Fig.3.3.5	10	10	5	0

Tab.6.1 shows the input parameters to the parametrically excited roll motion in irregular waves demonstrated in Fig.6.1- Fig.6.5.

As shown in the presented result in Fig.6.1-Fig.6.5, the prametrically excited roll motion can occur in irregular long crested waves. The bow waves seems to be more probable to induce this kind motion with considerable roll angle.

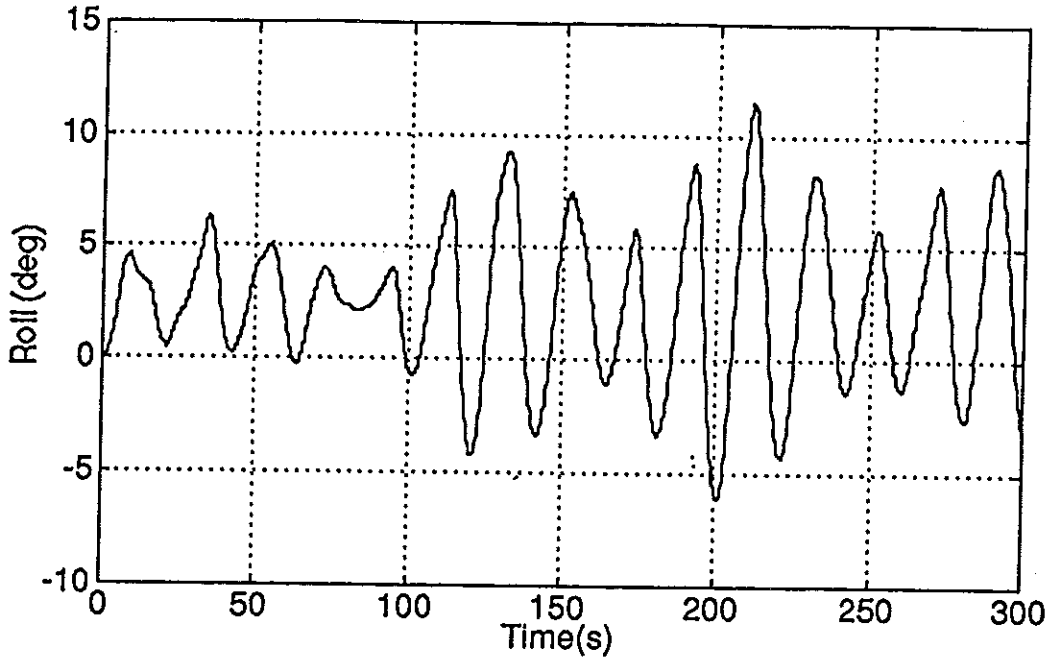

Fig.6.1 The parametrically excited roll motion in a heading wave.The input parameters can be found in Tab.6.1.

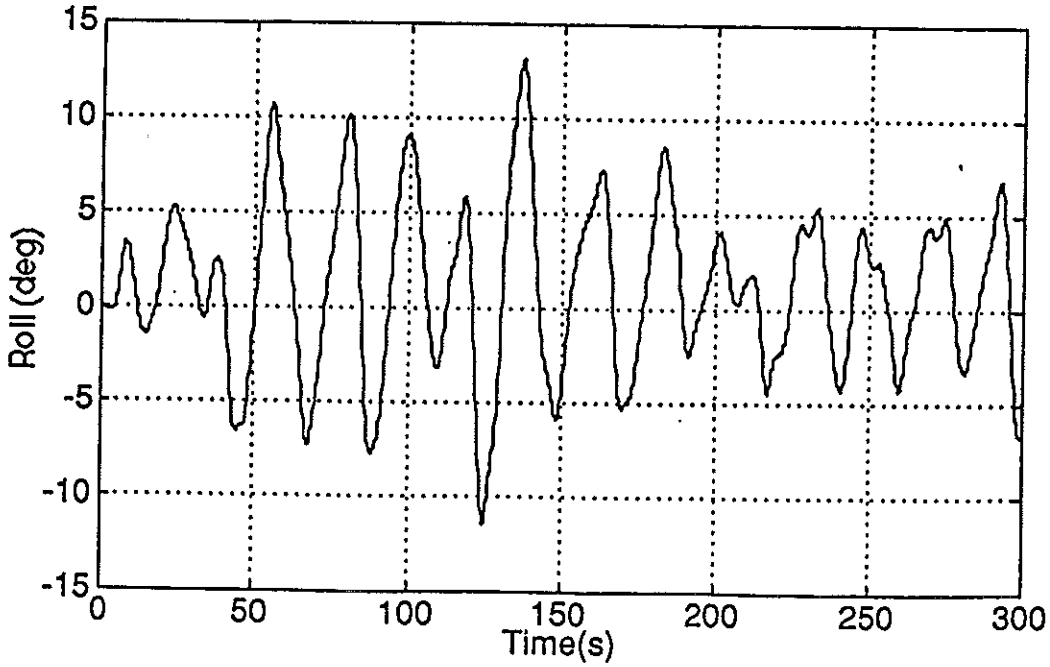

Fig.6.2 Parametrically excited roll motion in a bow wave.The input parameters can be found in Tab.6.1.

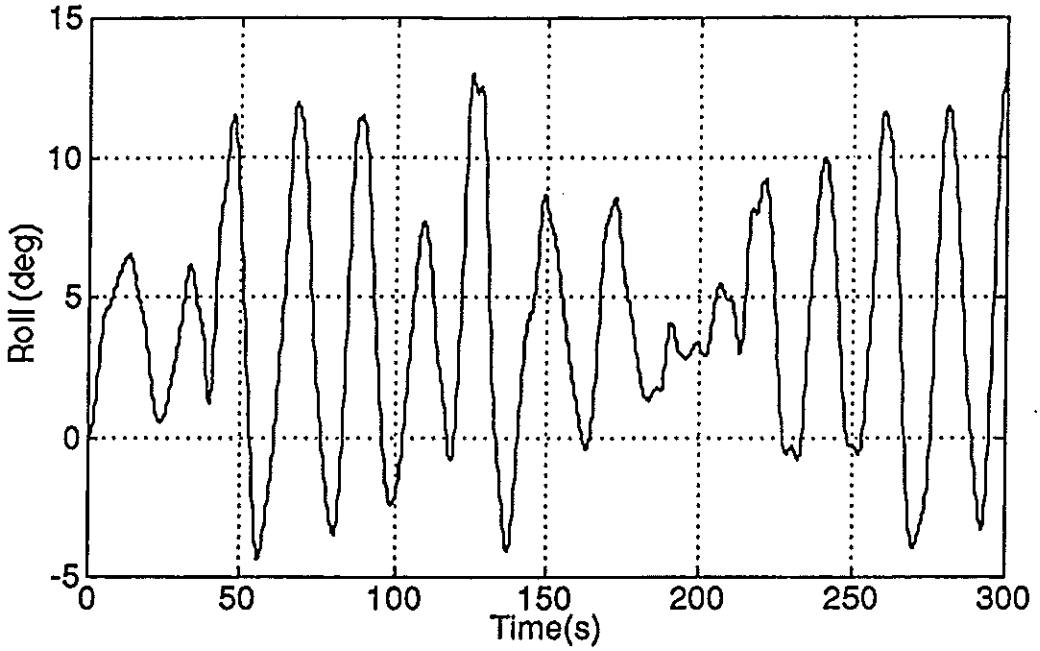

Fig.6.3 Parametrically excited roll motion in a bow wave.The input parameters can be found in Tab.6.1.

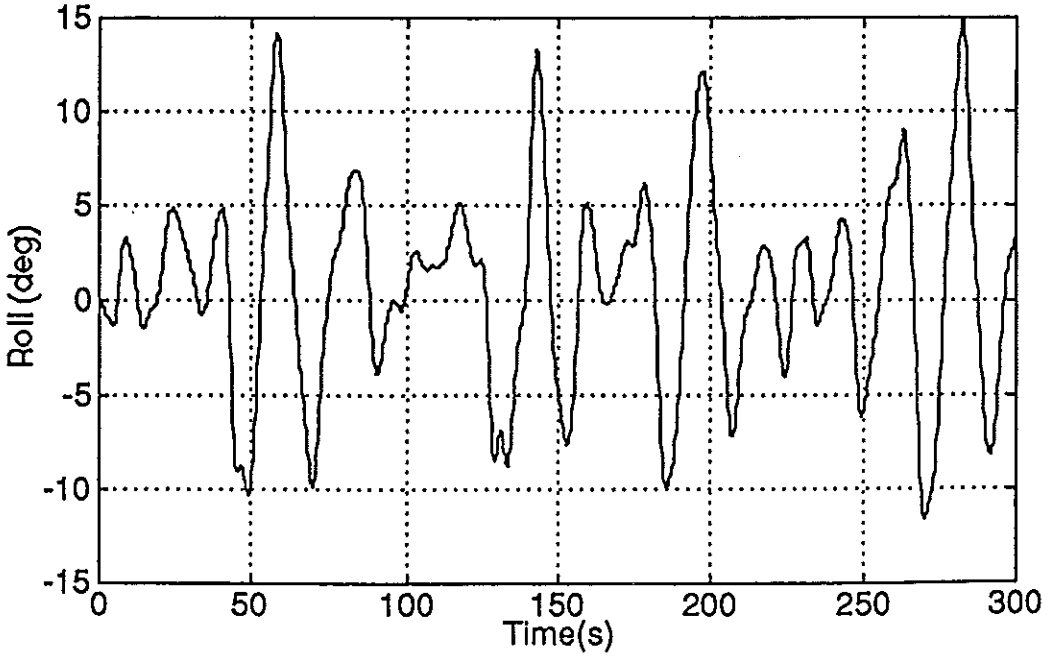

Fig.6.4 Parametrically excited roll motion in a bow wave. The input parameters can be found in Tab.6.1.

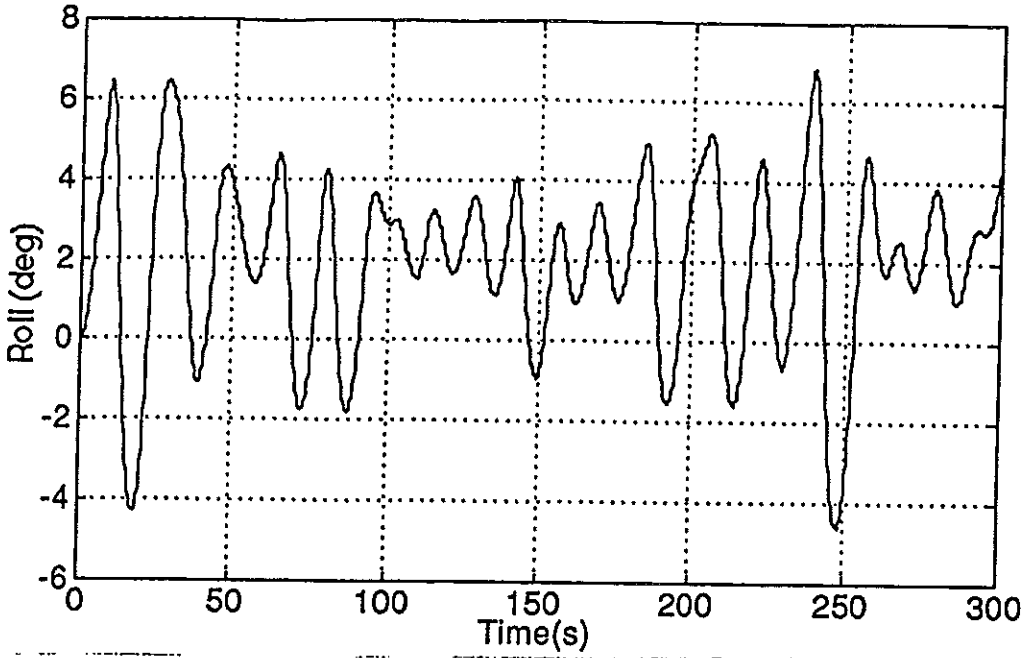

Fig.6.5 Parametrically excited roll motion in a following wave. The input parameters can be found in Tab.6.1.

.c.7. Load Shifting Due to the Simultaneous Effect of Vertical, Horizontal Acceleration and Roll Motion;

Usually, load shifting onboard appears in the form of tipping or gliding if the cargo is undeformable. The maginitudes of tangitial and normal force, F and N respectively are the governing parameter to the initialisation of load shifting, see definition of N and F i Fig.7.1. Gliding can occur only when the tangential force exceeds the sum of lashing and friction force. The friction force is equal to the friction coefficient time the normal force. The condition to tipping is that a tipping moment refering to the support point for the cargo exceeds the lashing moment and cargo weight effect.

However, a cargo onboard exposes to roll motion, vertical and horizontal acceleration simultaneously due to the ship motions in waves. As a consequence, not only gravidation force but also force of inertia act on the cargo. Therefore the eqvivalent roll angle defined according (7.1) should be used a parameter to jedge the risk of load shifting onboard. The eqvivalent roll angle has the same effect on a cargo onboard as it lies on a heeled plane with an angle of the same magnituide.

Definition of the eqvivalent roll angle:

$$\alpha = \arctan\left(\frac{F}{N}\right) \qquad (\ 7.1\ )$$

where;

$$F = m \cdot \left(a_v \cdot \sin\phi + a_h \cdot \cos\phi - z \cdot \ddot{\phi} + g \cdot \sin\phi\right)$$

$$N = m \cdot \left(a_v \cdot \cos\phi - a_h \cdot \sin\phi + y \cdot \ddot{\phi} + g \cdot \cos\phi\right)$$

m is cargo mass and f roll angle. y and z is the horizontal and vertical distance from the roll axe.

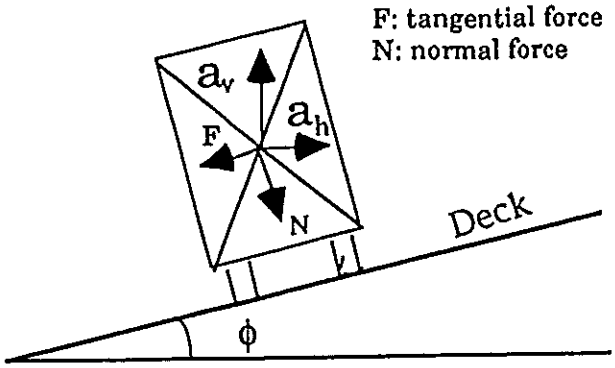

Fig.7.1 The forces on a cargo onboard due to the simultaneous effect of vertical, horisontal acceleration and roll motion.

It is shown in the previously chapter that the actual ship in bow waves can occur to the parametrically excited roll motion. Due to the low value of the natural roll frequence, the roll motion in direct resonance with wave excitation is impossible to happen to the actual ship in bow waves. In practice, bow or heading waves are prefered by experenced seaman for a ship in at a severe sea. That is why it is interesting to investigate the simultaneous effect in connection with the parametrically excited roll motion.

Fig.7.2 shows the time histories of the roll and eqvivalent roll motion of the ship in an irregular bow wave of 10 m significant wave height and 10 seconds mean period. The ship speed is 10 knots in bow wave with a relative course angle 135 degrees to the wave direction. The eqvivalent roll motion is calculated at the centre line through KG with a longitudinal distance 70 meters from the mass centre.

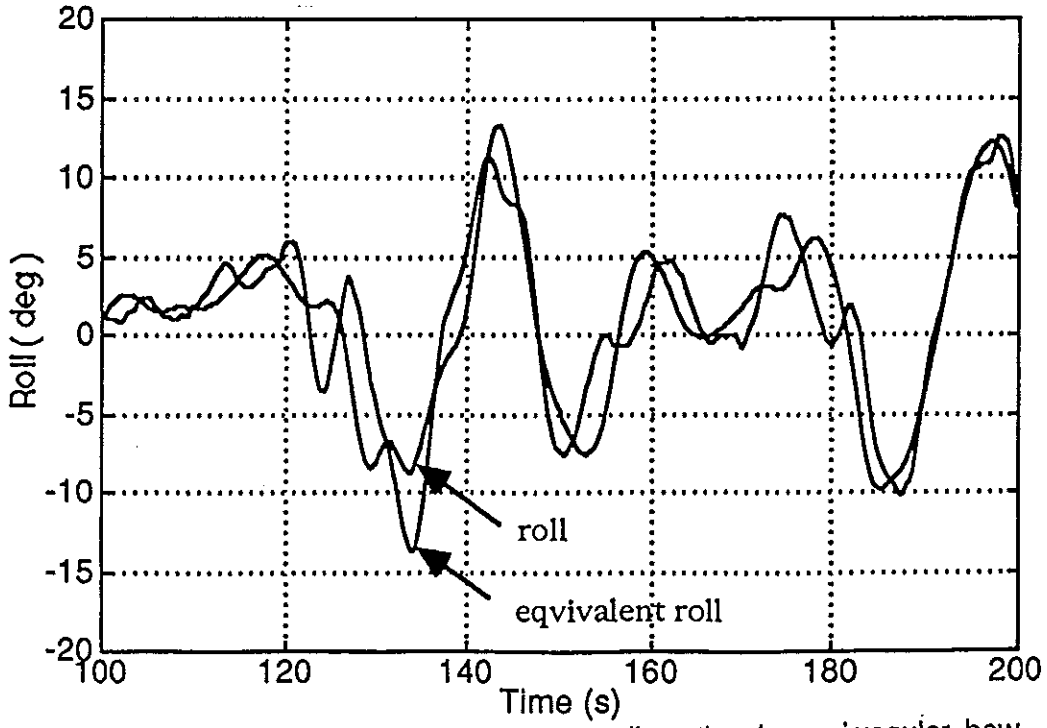

Fig.7.2 Time histories of the roll and eqvivalent roll motion in an irregular bow waves. H10T10.K135U10.S1

Fig.7.3 shows the time histories of the eqvivalent roll motions at three points longitudinally along the centre line through the mass centre in the wave condition as same as for Fig.7.2. Fig.7.4 shows the eqvivalent roll motions at three points along the vertical line through the mass centre.

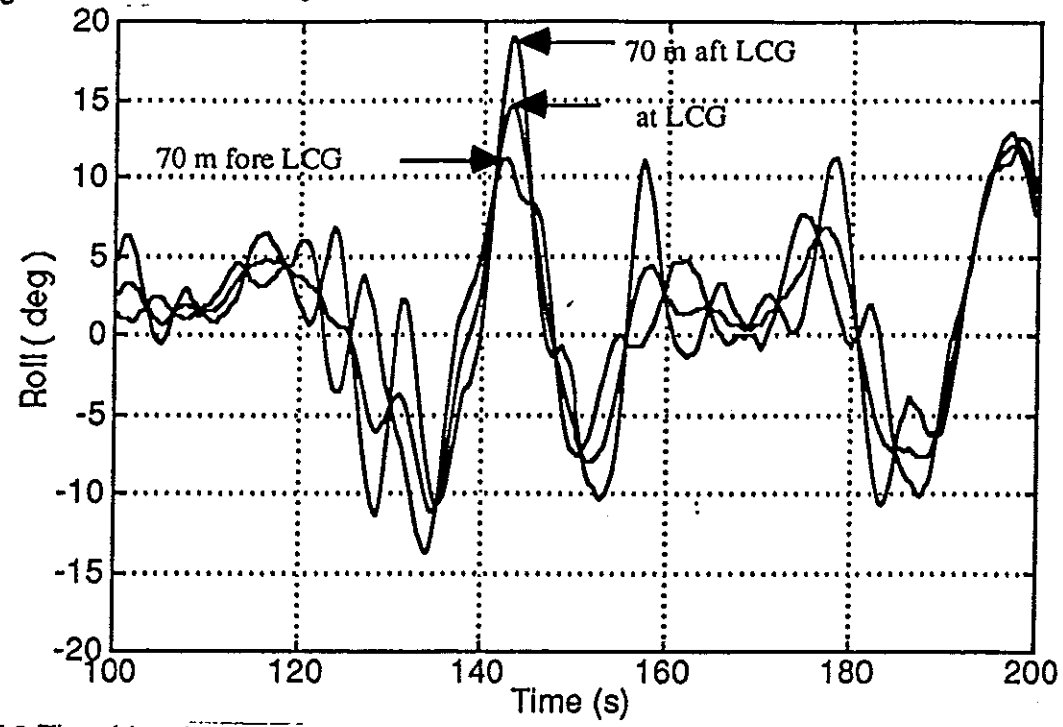

Fig.7.3 Time histories of the eqvivalent roll motion at three points onboard in the same wave condition as for Fig.7.2

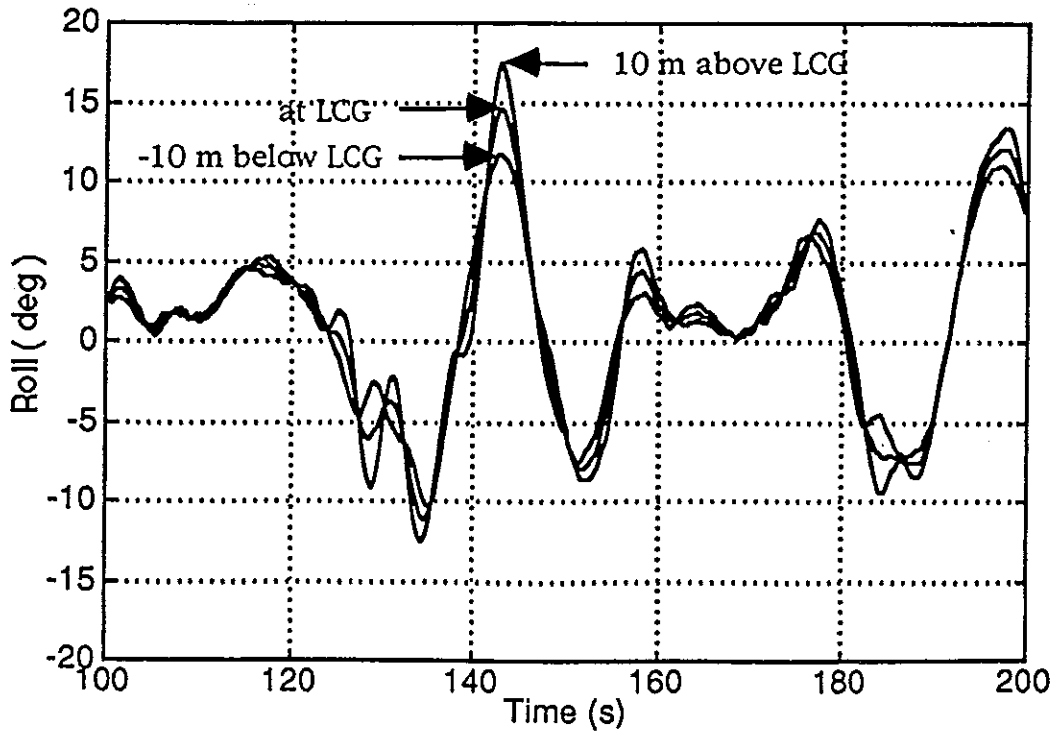

Fig.7.4 Time histories of the eqvivalent roll motion at three points onboard in the same wave condition as for Fig.7.2

Obviously, the simultanous effect is completely dependent upon
the phase-relations between the roll, vertical and horizontal acceleration. That means that the statistic distribution of eqvivalent roll angles are different at different points onboard. The maximal eqvivalent roll angle is about 18 degrees in the Fig.7.2 - Fig.7.4 and the mamximal roll angle is miner than 15 dgrees in the same time interval. The calculation has shown that a eqvivalent roll angle greater than 20 degrees can be obtained at the point 10 m above and 70 aft the mass centre.

It should be pointed out that the presented calculation is aimed to demonstrate the significance of the simultaneous effect of vertical, horizontal acceleration and roll motion on the cargo shifting onboard. The calculated result is not sufficiently to make a statistic analysis of the maximal eqvivalent roll angle and the presented result is not unusual.

.c.8. Conclusion Remarks and Discussions;

From the presented result, the conclusion can be drawn that the parametrically excited roll motion can happed to the actual RoRo-ship in both regular and irregular waves when the ratio of
encounter frequence to the natural roll frequence has the value around one or two and the magnitude of the GZ-variation is sufficiently large. However, the magnitude of roll motion is limited under 30 degrees in the cases presented and no instable roll motion has been observed.

A linear roll damping of 10% of the critical roll damping is used in this study, which is over-estimated to a RoRo-ship in roll motion of small and moderate magnitude. In fact, the roll damping is strongly non-linear. Therefore, it can be expected that the parametrically excited roll motion of the actual ship will be more severe if a more realistic roll damping is used.

The studied ship is an average RoRo-ship with aspect to its main particulars. Its B/T-ratio is 3. There are many RoRo-ships with larger B/T ratio up to 4. It can be shown that larger B/Tration can result in larger magnitude of GZ-variation in waves. Those ships can be subjected to more severe parametrically excited roll motions.

The calculation has shown that the interaction between the roll, heave and pitch motion in both regular and irregular waves seems to be important to the parametrically excited roll motion. Further effort should be made to find the parameters for description of the interaction. Those parameters will be useful for comparison of the dynamic properties of different hull forms. And it will be essential for establishing the rational stability criteria.

When the parametrically excited roll motion occurs in bow waves, it will be dangerous with consideration to the risk of load shifting onboard, because the simultaneous effect of vertical, horizontal acceleration and roll motion, defined as equivalent roll angle can become considerably greater than the only roll angle so that the cargo lashing system onboard is not sufficiently to resist the cargo shifting. One factor to the large magnitude of vertical and horizontal acceleration in bow waves is the higher encounter frequence than in following wave, particularly when the ship speed is high.

The technical invetigations into capsizing of RoRo-ships have shown that the load shifting onboard is an important source to the most losses of the RoRo-ships. The simultaneous effect of vertical, horizontal acceleration and roll motion should therefore be paid special attention. It is essential that the cargo lashing system of a RoRo-ship should be designed with consideration to this problem instead of the maximal roll angle expected under the service life.

Several capsizing accidents of RoRo-ships in waves have shown that a capsizing scenario usually consists of two stages. In the initial stage cargo shifting occurs onboard due to the large roll amplitude or the simultaneous effect of vertical, horizontal acceleration and roll motion, and consequently the ship gets a new equilibrium position at a large heel angle and losses the control capability. During the second stage, the ship continues to be subjected to wave-induced roll motion around the new equilibrium position several hours or even more untill the ship capsizes becomes completed meanwhile the cargo shifting occurs steadily in larger or smaller amount.

It has happened that some ships survived and got back to its uppright position after a severe cargo shifting onboard even though the hours of roll motion in waves at a severe heeled condition. The question arises why some ships survived and the others does not after the cargo shifting. It may be so that
some ships may have better survivability than the others. If it is true, it will be interesting to investigate how to identify a ship's survivability.

Time domain simulation is a useful tool for study of the complexity of the dynamic stability problems of ships in waves. However, due to its time-consuming, it is hardly belived to be able to draw general conclusions in the probability term to the ship stability problems by means of the kind time-domain simulation used in this dtudy. Futher effort should be devoted to develop simplified and adquate equations fšr description of the dynaimc stability problems. Thereby, it would be possible to establish rational stability criteria for those problems by means of the probability theory.

The result presented in this paper is a theoretical study. Rutgersson and Ottosson in /20/ studied the broaching phenomenon of a high speed craft in waves by means of the combination of model test and computer-simulation. It is believed that the dynamic stability problems of RoRo-ships in waves should be studied in the same manner if the research result will be useful in practice.

.c.9. Nomenclature

B	ship breath
C_B	block coefficient
g	gravitation acceleration
GM	metacentric height
$\bar{H}_{1/3}$	significant wave height
KG	the mass centre above the keel
L_{pp}	length between the perpendiculars
LCG	lonitudinal position of the mass center
m	ship mass
r_4	radii of mass inertia moment of roll
r_5	radii of mass inertia moment of pitch
r_6	radii of mass inertia moment of yaw
$S(\omega)$	wave energy spectrum
T	ship mean draught
$\bar{T}_2$	zero-crossed mean wave period
β	the relative course angle of a ship in relation to the wave propagation direction
λ	wave length
φ	roll angle
ω	wave frequency
ω_0	natural roll frequency
ω_e	encounter wave frequency

.c.10. References;

/1/ Frank W., 1967
"Oscillating of Cylinders in or below the Free Surface of Deep Fluids"
NSRDC Report 2375, Oct. 1967.

/2/ Guidelines of Det Norske Veritas, 1980
"Design and Calssification of Roll on/Roll off Ships"

/3/ Hua J., 1988
"A Theoretical Study on the Capsize of the Ferry HERALD OF FREE ENTERPRISE".
The Royal Institute of Technology,
Department of Naval Architecture,1988, TRITA-SKP 1062.

/4/ Hua J., 1990
"Egenskaper hos RoRo/passagerarfartyget ZENOBIA
- en studie med anledning av fartygets fšrlisning den 2 juni 1980". in Swedish
The Royal Institute of Technology,
Department of Naval Architecture,1990, TRITA-SKP 1063.

/5/ Hua J., 1992
" A Study of the Parametrically Excited Roll Motion of a RoRo-Ship in Following and Heading Waves "
Int Shipbuild. Progr., 39, no.420 (1992) pp.345-366

/6/ Hua J. and Palmquist M., 1994
"A Description of SMS"
The Royal Institute of Technology,
Division of Naval Architecture,1994

/7/ Huss M., 1988
"The Stability of Ships in Waves; a comparative study of modern hull forms with large B/T ratio".
The Royal Institute of Technology,
Division of Naval Architecture,TRITA-SKP 1060, 1988.

/8/ Kan M., Saruta T. and Taguchi H., 1990
"Capsizing of a Ship in Quartering Waves"
(Part 5. Comparative Model Experiments on Machanism of Capsizing)
J.S.N.A. Japan Vol. 171, June 1993

/9/ Kervin J.E., 1959
"Notes on Rolling in Longitudinal Waves"
Intern. Shipbuilding Progress, Vol.2 No. 16, 1959.

/10/ Lindemann and Skomedal N. G., 1982
"Parametric Excitation of Roll Motion and its Influence on Stability "
Second International conference on Stability of ships and Ocean Vechicles,Tokyo, Oct. 1982

/11/ Paulling J.R. and Rosenberg R.M., 1959
"On Unstable Ship Motion Resulting from Nonlinear Coupling"
Journal of Ship Research, Vol.3 No.1, 1959.

/12/ Rutgersson O. and Ottosson O., 1987
" Model Tests and Computer Simulations --- An Effective Combination for Investigation of Broaching Phenomena " SNAME Transactions, Vol.95, 1987, pp. 263-281

/13/ Salvsen N., Tuck E.O. and Faltinsen O., 1970
" Ship Motions and Sea Loads "
Trans. Vol.78, SNAME, 1970

/14/ Sjšholm U. and Kjellberg A., 1985
"RoRo Ship Hull form:Stability and Seakeeping Properties" The Naval Architect, Jan. 1985.

/15/ Sšderberg P., 1985
"Ro-Ro/Containerfartyg och fŠrjor - rullning " In Swedish Transportforskningsdelegation, SSPA Report 3534-1,1985

/16/ Wright J.H. and Marshfield W.B., 1980
"Ship Roll Response and Capsize Behaviour in Beam Seas"
RINA 1980, Vol.122

FIFTH INTERNATIONAL CONFERENCE ON STABILITY OF SHIPS
AND OCEAN VEHICLES Florida Institute of Technology

Dangerous Encounter Wave Conditions for Ships Navigating in Following and Quartering Seas

Yoshifumi TAKAISHI
Nihon University

ABSTRACT

Many casualty records as well as model test results on capsizing of ships in wave have shown a specific danger for ships navigating under heavy following or quartering sea conditions. The author recognizes this danger being based on a special feature of encounter waves in following sea which is different from beam sea or bow sea conditions.

When ship speed is almost the same as the group velocity of dominant wave in following or quartering seas, the ship will be attacked by highest waves successively under a certain probability. This phenomena is particularly dangerous, because such repeated attack of high waves will induce various bad effects on ship safety such as stability loss on wave crests, unstable or synchronous rolling motions, shipping water on deck, and so on.

This dangerous encounter wave group phenomena can be explained by analyzing the feature of encounter wave spectrum which is transformed from wave spectrum of the sea state concerned. A dominant part of wave energy of the sea concentrates in a narrow band of encounter wave frequency so that the ship encounters to waves likely as regular waves having a single encounter period.

By introducing the new concept of wave energy concentration ratio, the author has determined the degree of danger to encounter to successive high waves. The model test results of two container ships have shown that the capsize probability is proportional to the wave energy concentration ratio. By using this results, the author proposes a diagram to judge the dangerous condition in relation with ship speed, encounter angle and wave period.

1.INTRODUCTION

The author had pointed out the dangerous encounter wave group phenomena and proposed a diagram to judge the conditions to meet this phenomena as the function of ship speed, encounter angle and wave period.[1] The model test result[2] shows that the most capsized cases occurred in the vicinity of this condition. Some actual ship disasters are also considered to have occurred under the similar situation. However, the diagram gives only one definite point as the dangerous conditions, while the model test results show the spreading of conditions under which the models have capsized. The author has tried to explain this spreading of the dangerous conditions by introducing concept of wave energy concentration ratio which is derived from the shape of the energy spectrum of encounter waves.[3] This value becomes largest when a ship runs with the same velocity as the group velocity of dominant wave and decreases gradually as the ship speed is increased or decreased.

The model test results have been re-examined on a diagram which indicates the wave energy concentration ratio as the function of non-dimensional navigation conditions in following and quartering seas. As the result, it has been clarified that the capsized rate of the model experiments is proportional to the wave energy concentration ratio. This is attributed to the special feature of encounter wave conditions that the ship encounters to a group of large waves successively and serious wave actions are executed to the ship repeatedly.

Therefore, the diagram proposed by the author can indicate a dangerous zone to encounter to large wave group.

2.DEFINITION OF WAVE ENERGY CONCENTRATION RATIO

The ship responses in waves are governed by the encountering waves. The encounter waves show different features according to the direction of waves relative to ship's course and ship's speed relative to wave period. Such difference of encounter waves appears in the wave elevation record at the ship as well as the energy spectrum of encounter wave elevations. The energy spectrum of

encounter waves is derived by a transformation of the wave spectrum at a fixed point of the sea. The encounter wave spectrum shows a special form for following and quartering seas which is quite different from those of head, bow or beam sea conditions. This special form of encounter wave spectrum is related to the special danger for ships navigating in following and quartering seas.

In this chapter, the procedures of transformation of wave energy spectrum will be explained. The so-called Pierson-Moskowitz wave spectrum is assumed as the typical ocean wave spectrum, as shown in Figure 1. The spectrum is represented by Equation (1),

$$S_W'(\omega') = \frac{2\pi S_W(\omega)}{T_0 H_{1/3}^2} = 0.11\omega'^{-5}\exp\left\{-0.44\omega'^{-4}\right\} \tag{1}$$

where $\omega_0 = 2\pi/T_0$, T_0 mean wave period, $H_{1/3}$ significant wave height, $\omega' = \omega/\omega_0$, and $S_W'(\omega')$ is a non-dimensional formula of wave spectrum, $S_W(\omega)$.

The transformation of wave spectrum, equation (1), into the encounter wave spectrum, $S_W'(\omega_e)$, is performed by Equation (2), i.e.

$$S_W'(\omega_e') = S_W'(\omega') \big/ \left|1-\alpha'\omega'\right| \tag{2}$$

and $S_W'(\omega_e')$ is represented versus the encounter wave frequency, ω_e', which is calculated by Equation (3).

$$\omega_e' = \omega'(1-\alpha'\omega'/2) \tag{3}$$

In the equation (2) and (3), a non-dimensional parameter, α', is used, which represents the ship speed/wave period ratio, i.e.

$$\alpha' = \frac{4\pi V \cos x}{g T_0} \tag{4}$$

At the encounter frequency, ω_{ee}', corresponding to the wave period, $\omega_e' = 2\omega_{ee}'$, where the denominator of Equation (2) equals zero, the encounter wave spectrum becomes infinity. If ω_e' is the representative wave frequency, or in other words, if it lays within the frequency range where the wave energy is large, then the encounter wave spectrum, $S_W'(\omega_e')$, will have a very narrow and high peak, as shown in Figure 1. It means that the encounter waves become like as regular waves with encounter frequency ω_{ee}'. The wave heights of these rather regular encounter waves can take various values from the highest value to the lowest value in the same sea state.

To illustrate this phenomena, the wave elevations measured by a wave probe at rest and with the advance speed equal to the group

velocity of wave in following sea condition are shown in Figure 2 and 3. The encounter wave elevation shown in Figure 2 (b) looks like as regular wave having a very large wave height which may exceed the heighest wave measured at rest. By the other measurements similar patterns as regular waves could be obtained, as shown in Figure 3, which have the same encounter period but different height.

It has been verified by the model experiments that encountering to such high wave group is the primary factor to lead a ship to capsize. Namely, a successive attack of very high waves causes various bad phenomenon as loss of stability on the wave crest, synchronous rolling motion, parametric resonance of rolling, shipping water on deck, etc..

The severity of such phenomena will be supposed to be proportional to the groupiness of encountering high waves. Then, the wave energy concentration ratio has been applied to represent the groupiness.

3. WAVE ENERGY CONCENTRATION RATIO

The wave energy concentration ratio is defined by the ratio of wave energy included within a definite small range of encounter frequency, $\omega_{ec}'\sim\omega_{ec}'-\delta\omega_e'$, against the total energy of wave, i.e. by β as shown in Figure 1 and Equation (5).

$$\beta = \frac{\sigma_e^2}{\sigma^2} = \frac{\int_{\omega_u'}^{\omega_l'} S_{ii}'(\omega')d\omega'}{\int_0^{\infty} S_{ii}'(\omega')d\omega'} \qquad (5)$$

where

$$\frac{\omega_u'}{\omega_l'} = \frac{1 \pm \sqrt{2\alpha'\delta\omega_l'}}{\alpha'} .$$

The value of β has been calculated under the assumption that $\delta\omega_e' = \omega_{ec}'/10$, and the result is shown in Figure 4 versus the non-dimensional parameter α', as Equation (4).

It is clear that β becomes largest at $\alpha'=1.1$ with a rather flat peak. It means that the dangerous condition has a some spreading around the maximum value of β. For application of this result to following and quartering seas, a diagram is drawn as Figure 5 to show the effect of heading angle of ship to wave

direction, χ, as well as the parameter $\alpha=4\pi V/(gT)$. In the diagram, the other parameter, V(knots)/T(sec), is shown instead of α for convenience of practical use. Now, let us call this figure as "V/T Diagram".

4. COMPARISON WITH MODEL EXPERIMENT RESULTS

A systematic capsizing experiment has been carried out by Kan et al.[2] by using two container ship models with special emphasis on capsizing in following and quartering seas. The ship forms of these container ships are shown in Figure 6, with the test conditions. The wave spectrum used in the experiments is shown in Figure 7.

The rate of capsized cases versus total runs is summarized in Figure 8 for ship-F and in Figure 9 for ship-G, with variation of ship speed and GM value as well as encounter angle.[2] These experimental results are compared with the wave energy concentration ratio which has been calculated by using the wave spectrum as shown in Figure 7. Figure 10 and 11 show the plotting of the experimental results on the V/T diagram, and the capsizing rates are compared with the wave energy concentration ratio. In plotting the experimental conditions on the V/T diagram, the measured mean speed of the models in wave is taken as the value of V.

According to these figures, a close correlation between β and the capsized rate can be clearly recognized. Then, it has been deduced that when β is higher than 0.6 capsizing danger becomes significant.

5. PROPOSAL OF DANGEROUS ZONE ON V/T DIAGRAM

Kan et al. have indicated that the capsizing modes in the model experiments are due to pure loss of stability, period bi-furcation and broaching, as shown in Figure 12.[2] The author would like to attribute these capsizing modes to the special feature of encounter waves attacked the models when they run with the dominant wave group. Under such situation, ships will receive excitation of heeling by large waves which may lead ships to synchronous rolling or non-

linear parametric rolling motions. Shipping water on deck can occur, too.

To prevent this dangerous situation for ships navigating in following and quartering seas, the V/T diagram will be very useful, on which the dangerous zone is shown as Figure 13. The master of a ship can see whether his ship is in or out of the dangerous zone which have possibility to encounter to successive large waves when he plots V/T value of his ship on the diagram, so that an appropriate handling will become possible to keep safety.

6. CONSIDERATION ON SOME IMPORTANT FACTORS

6.1 Encounter Period to Wave

The encounter period to waves is also an important parameter for estimating rolling motion of ship. To prevent the synchronous rolling, the master should also aware of the encounter period not to coincide to the natural period of rolling. The encounter period can easily derived by the V/T diagram, because the reverse of encounter period to wave period ratio, T/Te, is proportional to V/T. Namely, the encounter wave frequency is represented by equation (6) as the function of wave frequency and ship velocity,

$$\omega_e = \omega - \omega^2 V \cos\chi / g \tag{6}$$

and the encounter wave frequency is transformed to the encounter wave period by equation (7).

$$\frac{2\pi}{T_e} = \frac{2\pi}{T} - \frac{4\pi^2}{g}\frac{V\cos\chi}{T^2} \tag{7}$$

Then, T/Te is derived as equation (8), or equation (9) as the function of V/T, i.e.

$$\frac{T}{T_e} = 1 - \frac{2\pi}{g}\left(\frac{V\cos\chi}{T}\right) = 1 - \alpha'/2 \tag{8}$$

or

$$T/T_e = 1 - 0.33(V\cos\chi/T) \tag{9}$$

where V in knot and T in sec..

This relationship is represented on the V/T diagram, Figure 13. It is recognized that the encounter wave period is about twice of the observed wave period. This fact may give an useful information

for seamen to aware of dangerous zone.

6.2 Wave Length to Ship Length Ratio

The wave length to ship length ratio, λ/L, is an important parameter influencing on the ship motions. Wave with λ/L smaller than 0.5 or larger than 3 would excite rather little ship motions.

The relationship between λ/L and V/T is represented by Equation (10) with the parameter of Froude number, $Fn = V/\sqrt{gL}$, and wave length, $\lambda = 1.56 \cdot T^2$.

$$V/T = 7.6 Fn \sqrt{\lambda/L} \tag{10}$$

By using this relationship, it has become clear that λ/L is among 0.5 and 3.0 for the Froude number of 0.2 to 0.3 which may be the range of normal navigation speed for conventional vessels. It means that the wave length in the dangerous zone has values which effects significantly on the ship motions.

7. ON THE METHOD OF CAPSIZING MODEL EXPERIMENTS IN FOLLOWING AND QUARTERING SEAS

The author would like to emphasize that the capsizing model experiments should be conducted under the conditions including the dangerous zone of the V/T diagram, if the normal navigation condition is expected to lay within this zone. In addition, the experiments should be so conducted to encounter to the largest wave group which is considered as the most dangerous condition in following and quartering seas. The author understand that the capsizing model experiments at HSVA have been conducted under such conditions as above-mentioned, refer Blume et al.[4]

The records of actual ship disaster show also that many cases of capsizing events happened under the conditions within the dangerous zone. Therefore, the V/T diagram would be useful to analyze the actual ship disaster in following and quartering seas.

8. CONCLUSION

The idea of dangerous zone on V/T diagram has been proposed to represent danger to encounter to very large wave group when a ship is navigating in following and quartering seas. This idea has been derived from the concept of wave energy concentration ratio which could be calculated by using encounter wave spectrum. The range of dangerous zone, i.e the critical value of β, has been determined by using results of capsizing experiments of two container ship models. It has been concluded that the range of β greater than 0.6 is considered as the dangerous zone for capsizing or the other phenomenon relevant to ship stability in waves.

It is recommended that the model experiments in following or quartering waves should be conducted to include the severest conditions laying in the dangerous zone on the V/T diagram proposed by the author.

The diagram will be useful for ship masters to prevent dangerous situations in following and quartering seas.

ACKNOWLEDGEMENT

The author would like to acknowledge Dr. M. Kan for offering the comprehensive experimental results of two container ship models which were tested at the Ship Dynamics Division of Ship Research Institute, Ministry of Transport, Japan, and his comments on application of author's concept. The author also thanks to Mr. T. Saruta for offering the details of model velocity measured in the experiments in waves which were very helpful data to plot the results on the V/T diagram.

The author thanks to the members of RR 24 Research Committee of the Shipbuilding Research Association of Japan, the chairman of which is Prof. M. Fujino of The University of Tokyo, for their discussions on the application of V/T diagram to the operation guidance for masters of ships.

REFERENCES

1) Takaishi, Y.; Consideration on the Dangerous Situations Leading to Capsize of Ships in Waves, Proceedings of 2nd International Conference on Stability of Ships and Ocean Vehicles, Tokyo, (1982), pp.161-169

2) Kan, M., Saruta, T. and Taguchi, H.; Capsizing of a Ship in Quartering Seas, -Part 5. Comparative Model Experiments on Mechanism of Capsizing-, Journal of the Society of Naval Architects of Japan, Vol.173, (1993), pp.133-145

3) Takaishi, Y.; A Consideration on Dangerous Encounter Wave Group Phenomena in Quartering Seas, Journal of Japan Institute of Navigation, Vol.86, (1992), pp.161-167

4) Blume, P. and Hattendorf, H.G.; Ergebnisse von systematischen Modellversuchen zur Kentersicherheit, Jahrgang der Schiffbautechnischen Gesellschaft, Nr.78, (1984), pp.219-241

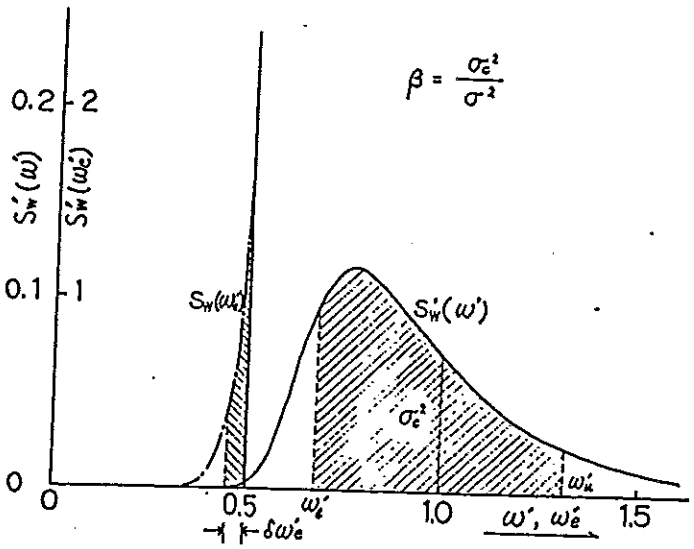

Figure 1 Pierson-Moskowitz's wave energy spectrum and its transformation into encounter wave spectrum

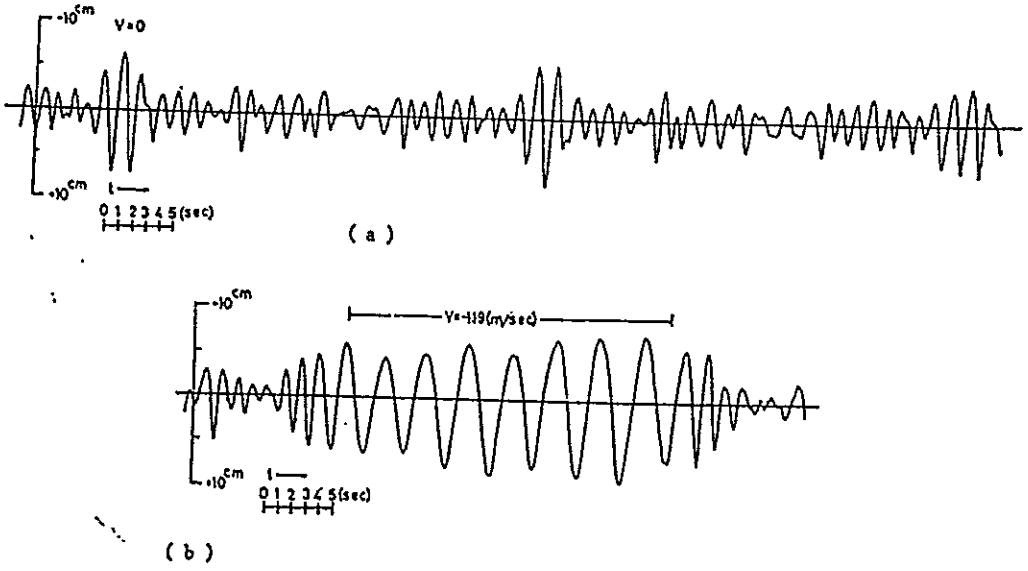

Figure 2 Wave elevation measured by wave probe at rest and with advance speed V_s in a following wave condition

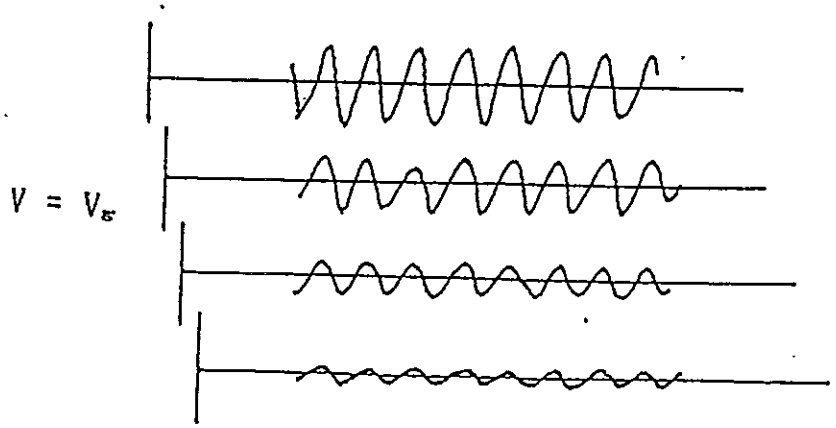

Figure 3 Various patterns of encounter wave elevation when advance speed is V_s

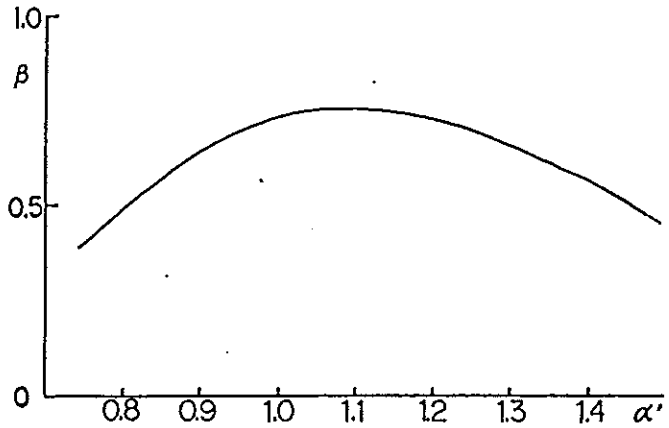

Figure 4 Wave energy concentration ratio β versus ship speed/wave period parameter α'

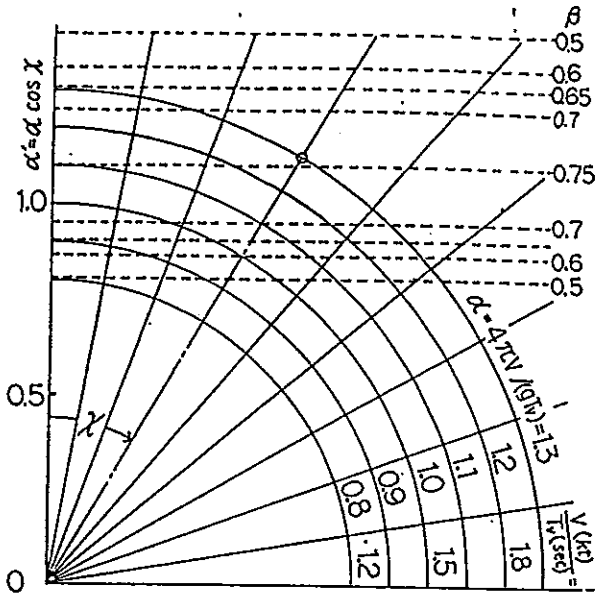

Figure 5 V/T diagram

MODEL F

Item	Ship	Model
Length Lpp(m)	135.0	3.50
Breadth B (m)	23.0	0.596
Depth D (m)	11.5	0.298
Draft dm(m)	8.37	0.217
Block Coeffi. C_b	0.589	0.589
Disp. Vol. ∇ (m³)	15307	0.267

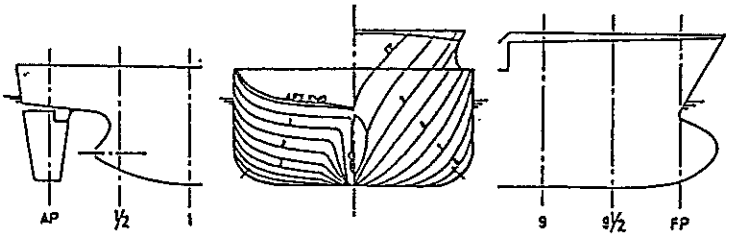

MODEL G

Item	Ship	Model
Length Lpp(m)	135.0	3.50
Breadth B (m)	24.3	0.630
Depth D (m)	11.5	0.298
Draft dm(m)	8.37	0.217
Block Coeffi. C_b	0.570	0.570
Disp. Vol. ∇ (m³)	15652	0.273

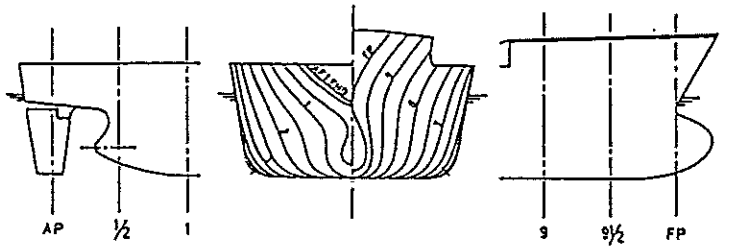

Figure 6 Container ship models used in capsizing experiments, Kan et al.[2)]

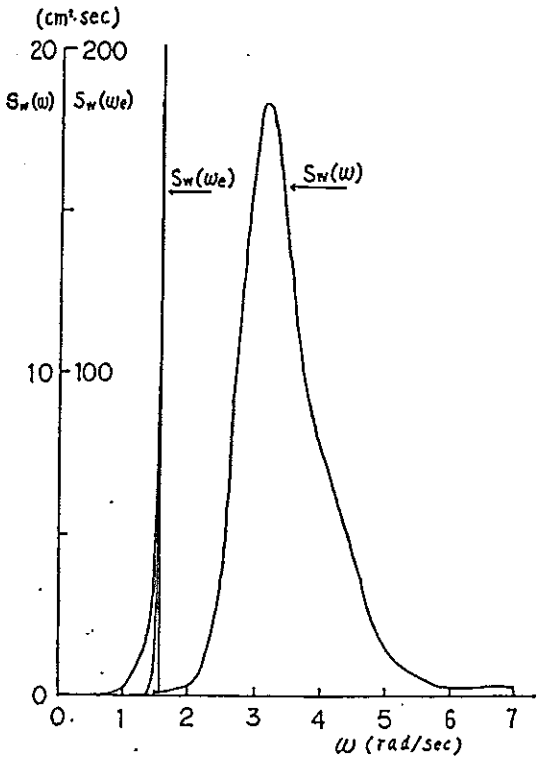

Figure 7 Wave energy spectrum used in the capsizing experiment

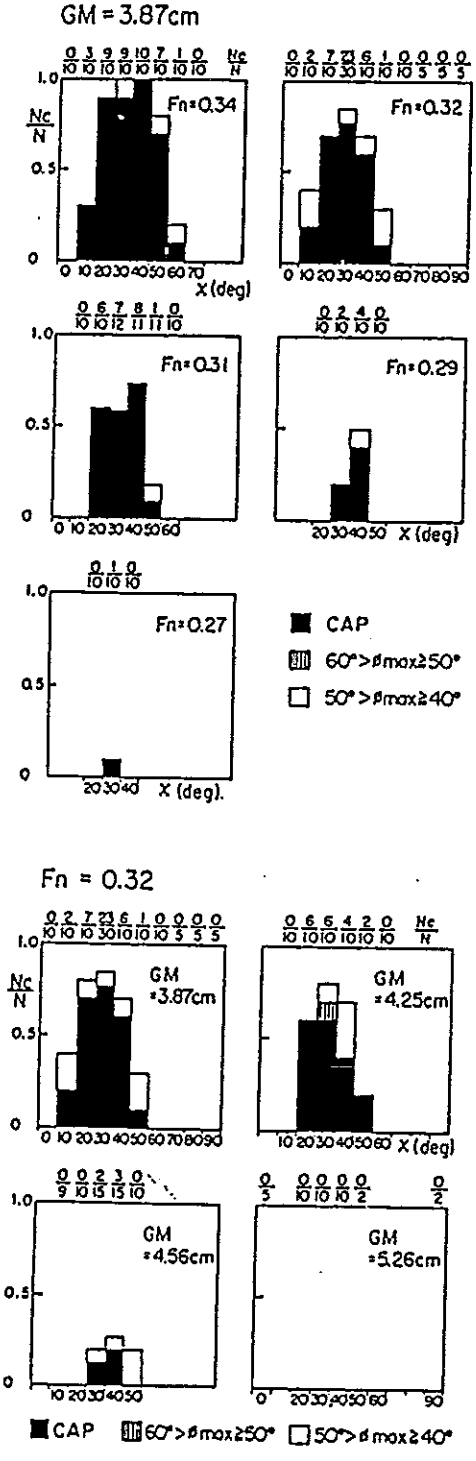

Figure 8 Capsizing rate for ship F, Kan et al.[2)]

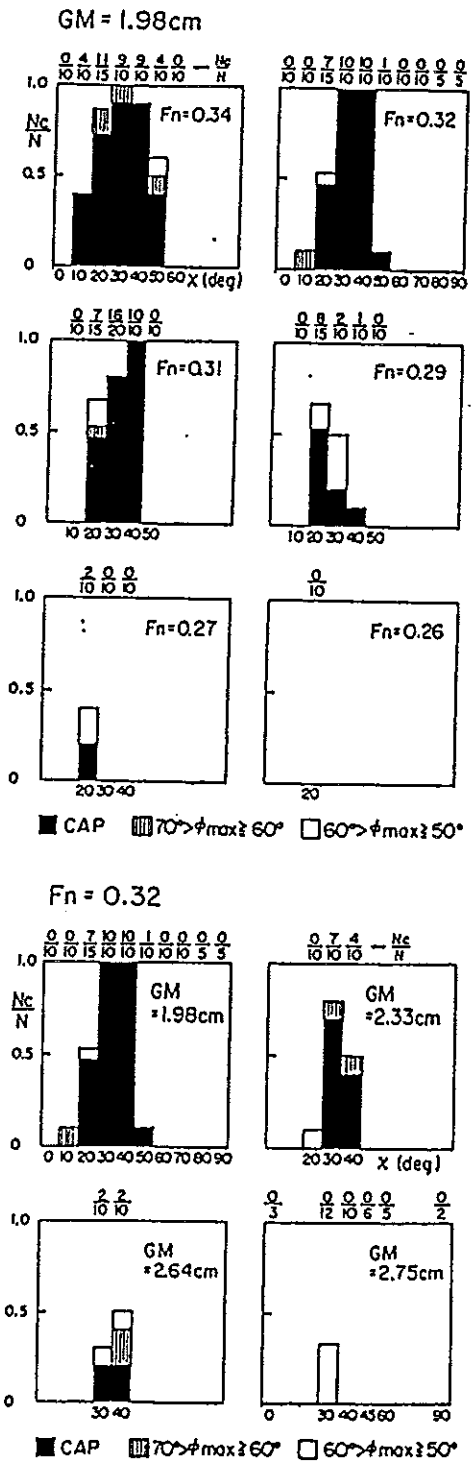

Figure 9 Capsizing rate for ship G, Kan, et al.[2)]

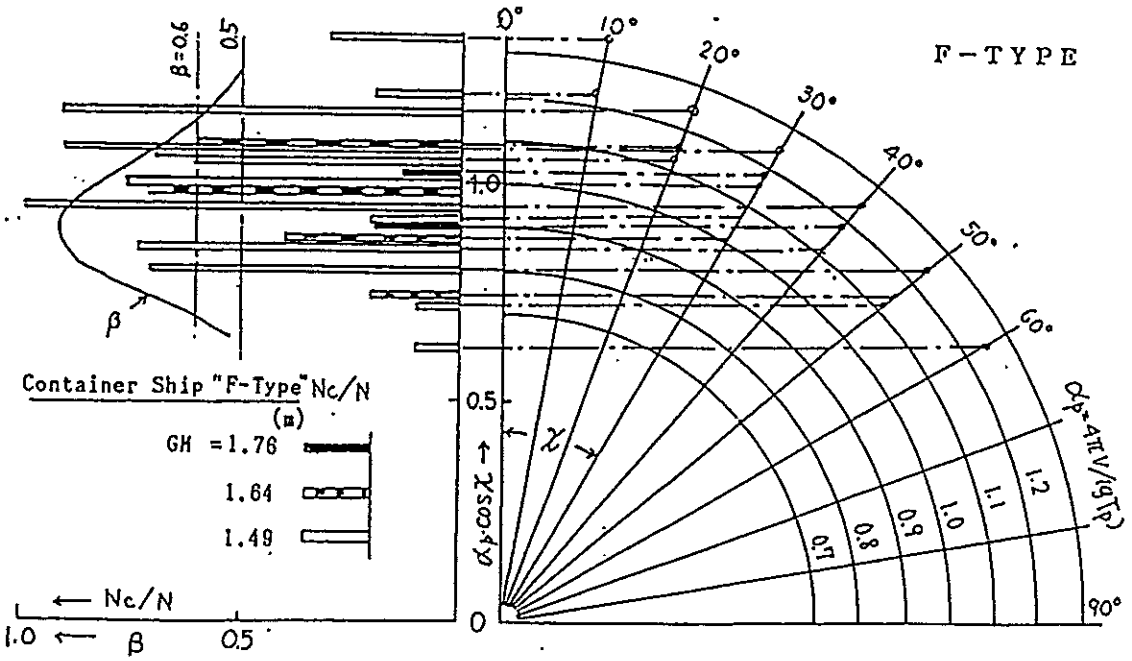

Figure 10 Plotting of capsizing rates on V/T diagram for ship F

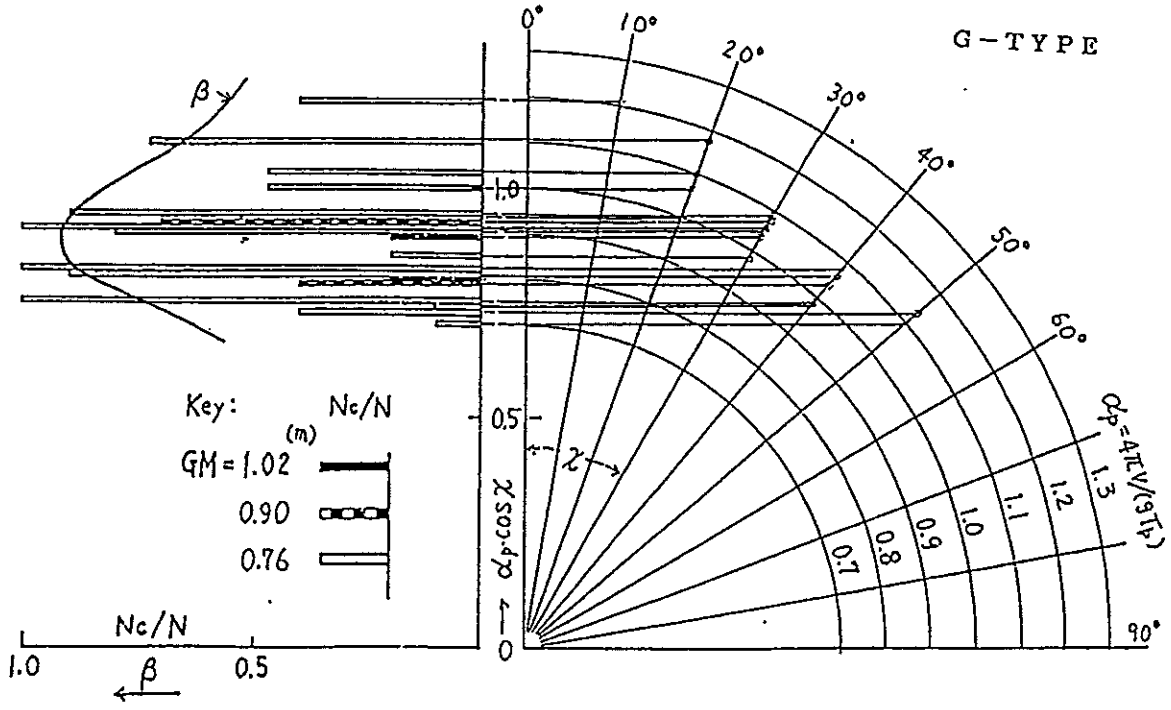

Figure 11 Plotting of capsizing rates on V/T diagram for ship G

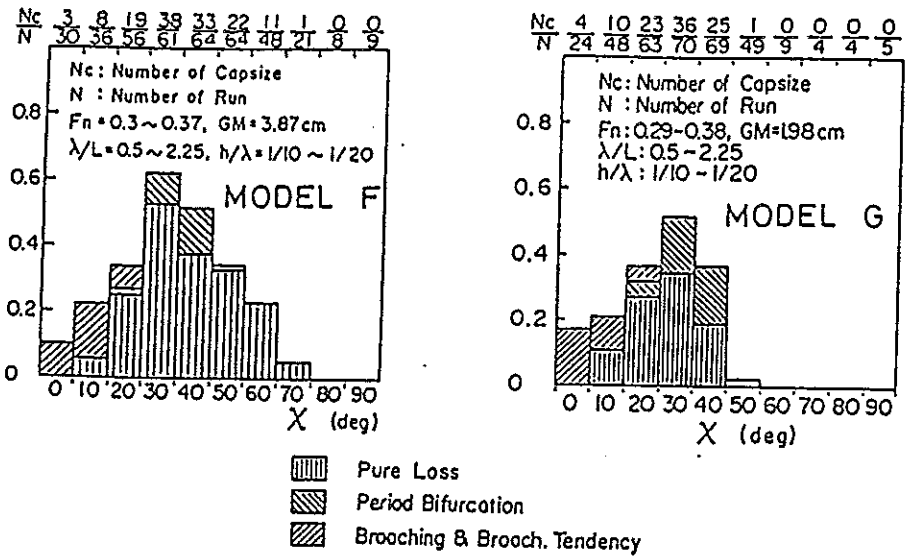

Figure 12 Classification of capsizing modes of the experiment for ship F and G in regular waves, Kan et al.[2)]

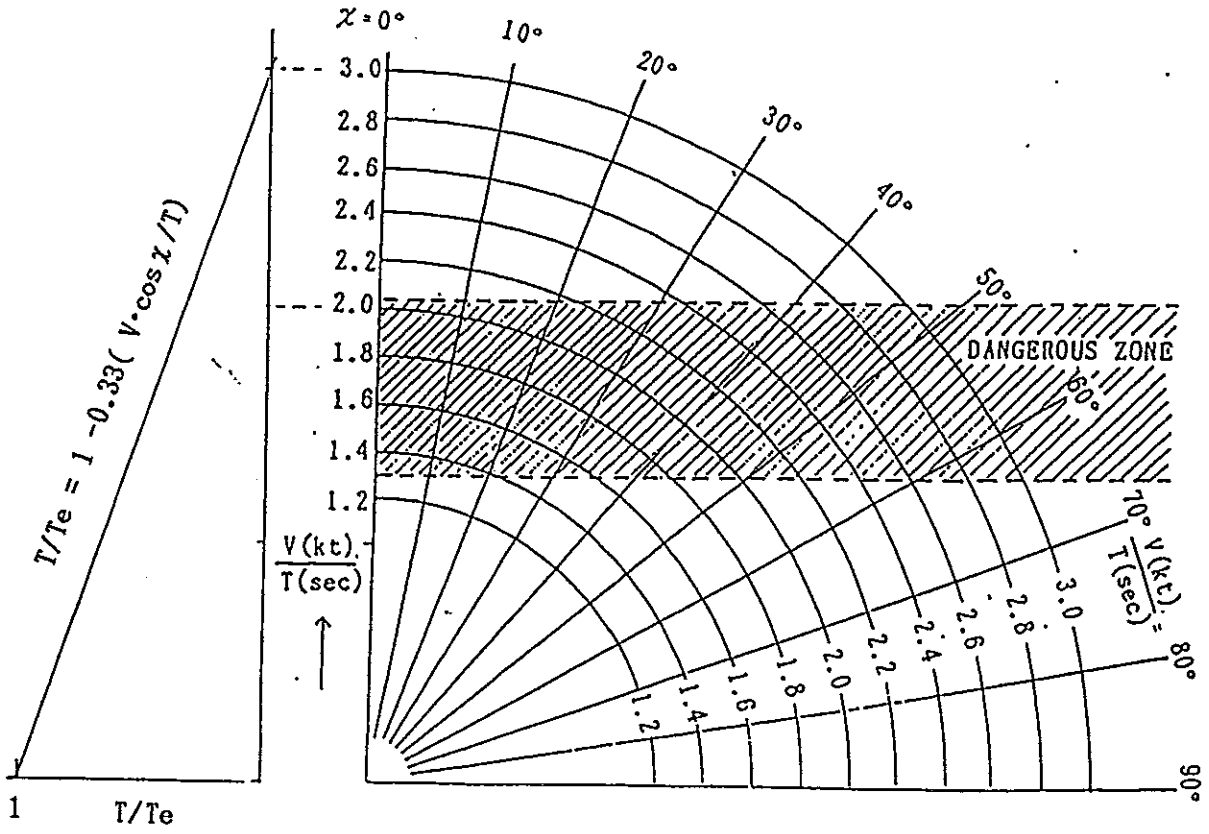

Figure 13 Dangerous zone to encounter to large wave group represented on V/T diagram

List of Figures and Tables

Figure 1 Pierson-Moskowitz's wave energy spectrum and its transformation into encounter wave spectrum

Figure 2 Wave elevation measured by wave probe at rest and with advance speed V_g in a following wave condition

Figure 3 Various patterns of encounter wave elevation when advance speed is V_g

Figure 4 Wave energy concentration ratio, β, versus ship speed/wave period parameter, α'

Figure 5 V/T diagram

Figure 6 Container ship models used in capsizing experiments, Kan et al.[2]

Figure 7 Wave energy spectrum used in the capsizing experiment

Figure 8 Capsizing rate for ship F, Kan et al.[2]

Figure 9 Capsizing rate for ship G, Kan et al.[2]

Figure 10 Plotting of capsizing rates on V/T diagram for ship F

Figure 11 Plotting of capsizing rates on V/T diagram for ship G

Figure 12 Classification of capsizing modes of the experiment for ships F and G, Kan et al.[2] (in regular waves)

Figure 13 Dangerous zone to encounter to large wave group represented on V/T diagram

NON-LINEARITIES IN SEMISUBMERSIBLE ROLL BEHAVIOUR UNDER FIRST AND SECOND-ORDER WAVE EXCITATION

by

K. Spyrou* and D. Vassalos**
*Currently at National Research Institute of Fisheries Engineering, Japan
**Dept of Ship and Marine Technology, University of Strathclyde, UK

ABSTRACT

This paper presents some findings from the last phase of a research programme on the influence of non-linear wave effects on the dynamic behaviour and stability of semisubmersibles. More specifically, the paper explores some non-linearities in the semisubmersible roll response, aiming to highlight their significance in affecting stability assessment. To enhance understanding of some of the qualitative aspects in the non-linear behaviour of semisubmersibles, an investigation is presented using a GVA 4000 semisubmersible, where conventional time domain simulation is combined with phase-plane analysis, highlighting the geometrical character of semisubmersible behaviour. Based on the derived results conclusions are drawn on the effectiveness of the existing procedures in assessing semisubmersible stability.

1. INTRODUCTION

Research efforts in the mid-eighties in the USA culminated in the formulation of *dynamic-response-based stability criteria* for semisubmersibles. These were subsequently adopted by IMO as an alternative standard for intact and as amendments to MODU Code for damage stability, [1]. This was indeed an outstanding achievement not least because the door is now open and an internationally accepted format established for the incorporation of dynamic responses directly in assessing semisubmersible stability . In fact, one of the recommendations of this research was to continually re-examine and improve motion predictions by drawing upon contemporary analytical and computational techniques. One notable improvement identified by the research team was the inclusion of non-linear wave effects in assessing the dynamic response of semisubmersibles.

At approximately the same time, another team in the UK were striving towards the same end results by adopting a procedure based on the calculation and weighing of the instantaneous time-varying excitation and restoring energies, the so called *Energy Balance Approach* (EBA), [2]. The researchers at UK were less successful in the international scale with much valuable results and knowledge "left out to dry" to use a direct quote from [1]. The EBA postulates that the balance between the energies gained and lost by the vessel over a critical half-cycle, or in other words the maximum roll angle attained, provides a realistic measure of stability. A critical half-cycle in turn was defined, following a detailed parametric investigation, as a function of initial conditions, vessel particulars and representative environmental parameters.

In retrospect, the lack of a rigorous definition of the ultimate half-roll did not help in this approach gaining a wider acceptance. Similar to the criteria formulated in the USA, non-linear wave effects were also omitted here.

Attempting among other things to fill the gaps discussed above, a research project was undertaken at the University of Strathclyde aiming to evaluate the influence of non-linear wave effects on the dynamic response and stability of semisubmersibles, [3], [4]. Some interesting results related to this research are presented and discussed in the

following. In particular, the paper investigates the qualitative (phase plane plots) and quantitative (time domain simulation) behaviour of a GVA 4000 semisubmersible subjected to fist and second-order waves in both the upright and tilted conditions.

2. BRIEF BACKGROUND

The wave-frequency induced motions of semisubmersibles are seldom significant for two main reasons: their natural frequencies are well below the wave frequencies with appreciable energy, and wave excitation is minimised by carefully distributing the buoyant members comprising the underwater volume.

Motion anomalies have however been reported in the literature, including steady tilt in regular waves as a result of second order steady forces, [5], subharmonic resonance in roll due to non-linear restoring and near-resonant response due to random wind and wave excitation, [6]. Moreover, model tests, [7], and full-scale measurements, [8], have conclusively shown that a significant component of the semisubmersible motions at sea occurs at frequencies near their own natural frequencies. Such motions can only be the result of a non-linear mechanism.

The low-frequency response of semisubmersibles, however, is customarily ignored in the design of these vessels, where only linear responses are taken into consideration. To improve upon this practice, the research at the University of Strathclyde focused in identifying and quantifying the influence of non-linear wave effects on the response of semisubmersibles with a view to incorporating these in assessing their dynamic behaviour and stability in realistic operating conditions.

3. APPROACH ADOPTED

3.1 General

The investigation is essentially a time-domain simulation study of the roll motion of a GVA 4000 semisubmersible subjected to monochromatic and bi-chromatic wave excitation. The layout of the rig is shown in Figure 1, first and second order moments for a 1/60th scale model in regular beam waves in Figures 2 and 3 and hydrodynamic coefficients in Figures 4 and 5.

In accordance with the EBA approach, stability is assessed on the basis of the maximum roll angle attained. Attention is focused on the following aspects:

- comparison between transient and steady state responses
- effect of non-linearities in the restoring curve
- dynamic behaviour under extreme excitation
- geometrical character of the semisubmersible roll behaviour

The semisubmersoble was considered at two conditions: intact upright and listed at 14° static heel.

3.2 Mathematical Formulation

A standard non-linear single-degree-of freedom roll motion equation was adopted in the following form:

$$I_v\ddot{\phi} + C(\dot{\phi}) + R(\phi) = W(t) \qquad (1)$$

where, ϕ : roll angle
$C(\dot{\phi})$: roll damping moment function
$R(\phi)$: roll restoring moment function
$W(t)$: wave excitation moment ($= W'(t) + W''(t)$), with
$W'(t)$: first-order wave excitation
$W''(t)$: second-order wave excitation

For a bi-chromatic wave with frequencies ω_1 and ω_2 and difference frequency ω_-, $W'(t)$ and $W''(t)$ can be expressed as follows:

$$W'(t) = \xi_1\{D'_{c_1}\cos(\omega_1 t + \delta_1) + D'_{s_1}\sin(\omega_1 t + \delta_1)\} + \xi_2\{D'_{c_2}\cos(\omega_2 t + \delta_2) + D'_{s_2}\sin(\omega_2 t + \delta_2)\} \quad (2)$$

$$W''(t) = \xi_1\xi_2\{D''_c\cos(\omega_- t + \delta_-) + D''_s\sin(\omega_- t + \delta_-)\} \quad (3)$$

where, ξ_1, ξ_2 : wave heights
$D'_{c_1}, D'_{c_2}, D'_{s_1}, D'_{s_2}$: first-order response amplitude operators
D''_c, D''_s : second-order response amplitude operators
$\delta_1, \delta_2, \delta_-$: phase angles

The mean drift force is not included in (3) above. Equation (1) was integrated numerically using a fourth order Runge-Kutta technique over a wide range of wave frequencies. The frequencies of the selected bi-chromatic waves are defined by fixing ω_1 at 0.7124 rad/sec whilst allowing ω_2 to vary from 0.47 to 0.9498 rad/sec, producing a difference frequency range that encompasses the roll natural frequency of the semisubmersible.

4. RESULTS AND DISCUSSION

4.1 Transient Vs Steady State Response

A selection of the computed roll realisations is presented in Figures 6 to 10. A clearly noticeable feature from these records is the considerably larger magnitude of the transient response exhibited by the vessel in comparison to the steady state response. Following the initial impact by the waves, the system attains a heel angle (primarily due to first order contribution), tending subsequently to follow a roll motion at its own natural period with the dynamic response at wave-period excitation superimposed. A comparison between the maximum transient and steady state responses is shown in Figure 11.

Based on these results, the EBA approach of judging stability based on the maximum roll angle attained during a critical half-cycle appears to be justified whereas the approach adopted in the *dynamic-response-based stability criteria* appears to have substantially under predicted the dynamic response taken into account in these criteria. After all, in practice, the semisubmersible motion is essentially a sequence of transient responses to waves of varying frequency and amplitude.

4.2 Effect of Extreme Level of Damping

For each combination of wave frequencies, the behaviour of the semisubmersible is examined at two extreme levels of damping, namely, zero and damping ratio of 0.7. The corresponding roll realisations are shown in Figures 6b to 10b and 6a to 10a, respectively. The maximum response amplitudes obtained were used as upper and lower bounds of the semisubmersible response, for the design KG, and are presented in Figure 12.

4.3 Effect of Non-Linearities in the Restoring Curve

As discussed earlier, near resonant excitation from second-order forces is a real possibility. In this case, if linear restoring is considered, the motion appears to be building up as is normally expected as shown in Figure 13. However, when the exact restoring is used, the vessel responds in a qualitatively different manner, the largest roll occurring at the initial stage with little variation in the motion amplitude with time, Figure 14.

4.4 Dynamic Behaviour Under Extreme Excitation

In this section the effect of increasing the wave height on the vessel roll response is discussed, with emphasis being placed on the observed non-linear behaviour. Under moderate second-order excitation, no significant motion is observed. Under extreme excitation, however, roll angles up to 30° are attained, Figures 15 and 16. Moreover, at ω_{-}=0.2216 rad/sec whilst undergoing insignificant motion again at moderate excitation, a supercritical bifurcation to double period subharmonic response occurs this time under extreme excitation, Figures 17 and 18. The same phenomenon has been reported in [9].

Finally, at a very low frequency of excitation, the response looses its symmetrical character of moderate excitation and becomes strongly asymmetrical under extreme excitation. This is indicated in Figures 19 to 22.

4.5 Geometrical Character of Semisubmersible Roll Behaviour

The qualitative character of some of the phenomena described in the foregoing can be more graphically illustrated through the geometry of motion by using phase-plane diagrams. The effect of damping, for example, can be seen in Figure 23, the effect of excitation level in Figures 15b to 22b and the double period bifurcation in Figure 18.

5. CONCLUDING REMARKS

On the basis of the results presented above, the following comments can be made:

- Special attention must be paid to the transient response in assessing the stability of a semisubmersible. In this respect, the *dynamic-response-based criteria* recently adopted at IMO, underestimate the dynamic response considerably. This is adequately taken into account in the *Energy Balance Approach.*

- Due primarily to the non-linearities in the roll restoring curve, severe second-order wave excitation may result in subharmonic or strongly asymmetrical responses. These aspects are not addressed by present day dynamic stability criteria.

- Second-order wave excitation can induce extreme near-resonant roll response, bounded essentially only by the level of damping present in the system. In this, respect accurate prediction of damping is essential.

6. ACKNOWLEDGMENTS

The support of the Science and Engineering Research Council (presently, Engineering and Physical Sciences Research Council) in undertaking this research is gratefully acknowledged.

7. REFERENCES

[1] **Shark, G. et al,** "Dynamic-Response-Based Intact and Residual Damage Stability Criteria for Semisubmersible Units", Trans. SNAME, vol. 97, 1989.

[2] **Vassalos, D. and Kuo, C.,** "Advances in the Stability Assessment of Semisubmersibles", STAB '90, Naples, 1990.

[3] **Spyrou, K.,** "Non-Linear Wave Effects on the Assessment of Semisubmersible Stability", Report GR/E/63261, Marine Technology Centre, University of Strathclyde, May 1991.

[4] **Pizer, D.,** "The Influence of Second-Order Wave Effects on the Roll and Pitch Motions of Semisubmersibles", PhD Thesis, Department of Ship and Marine Technology, University of Strathclyde, 1993.

[5] **Martin, J. and Kuo, C.,** "Calculations for the Steady Tilt of Semisubmersibles in Regular Waves", Trans. RINA, vol. 121, 1979.

[6] **Paulling, J.R.,** "Stability of Offshore Platforms in a Dynamic Environment", 28th Annual Joint Meeting, California Section of SNAME, 1985.

[7] **Lundgren, J. and Berg, A.,** "Wave-Induced Motions in a Four-Column Semisubmersible Obtained From Model Tests", OTC Proceedings, vol. 1, 1982.

[8] **MacLeod, I.K. and Vassalos, D.,** "Full-Scale Measurements of a Modified AKER-H3 Semisubmersible", Project MASS Report, Marine Technology Centre, University of Strathclyde, February 1986.

[9] **Huang, X.G.,** "On the Motion Response of a Damaged Semisubmersible Platform in Waves", OMAE, Tokyo 1986

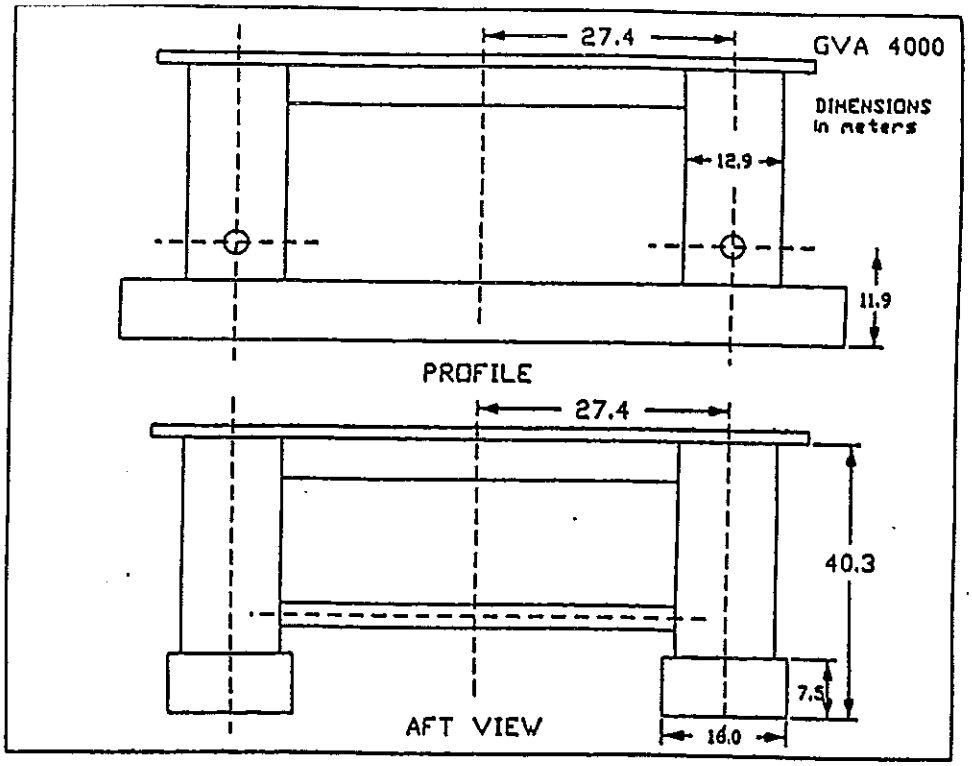

Fig 1 : Particulars of the GVA-4000

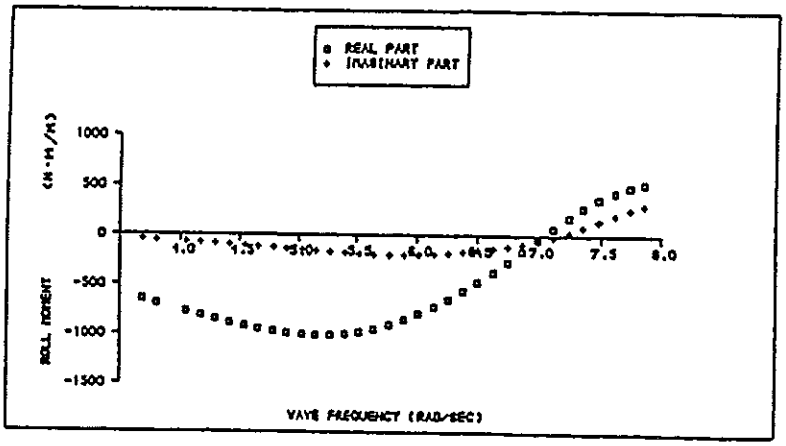

Fig 2 : First-order forces per unit wave height, model scale (1/60)

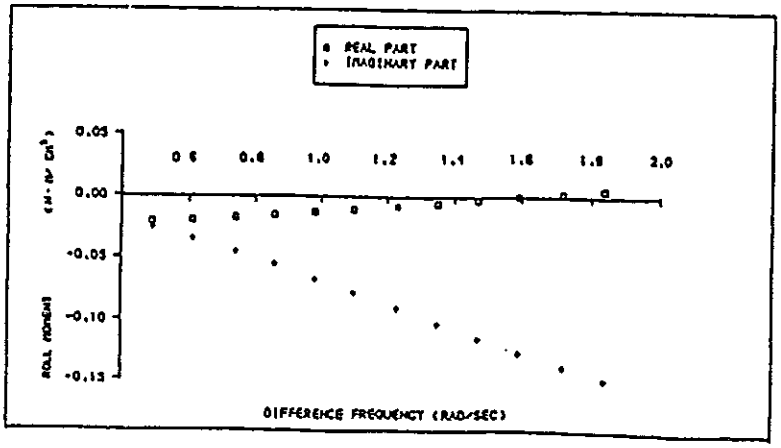

Fig 3 : Second-order roll moment wave height 1.0 cm, model scale (1/60)

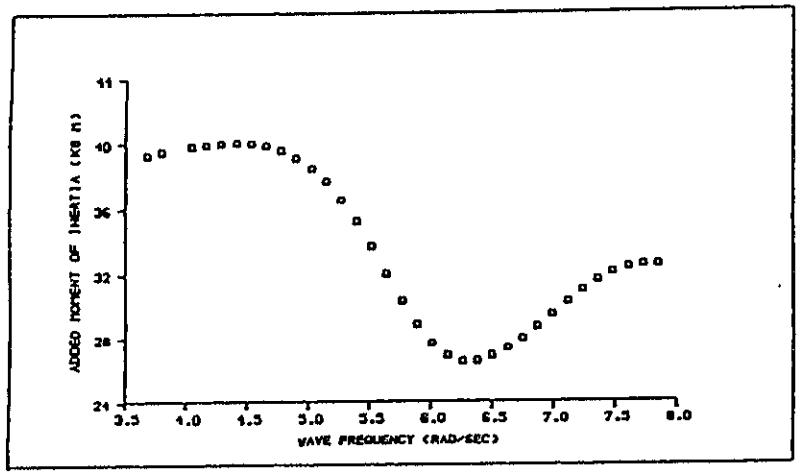

Fig 4 : Added-mass variation with frequency, model scale (1/60)

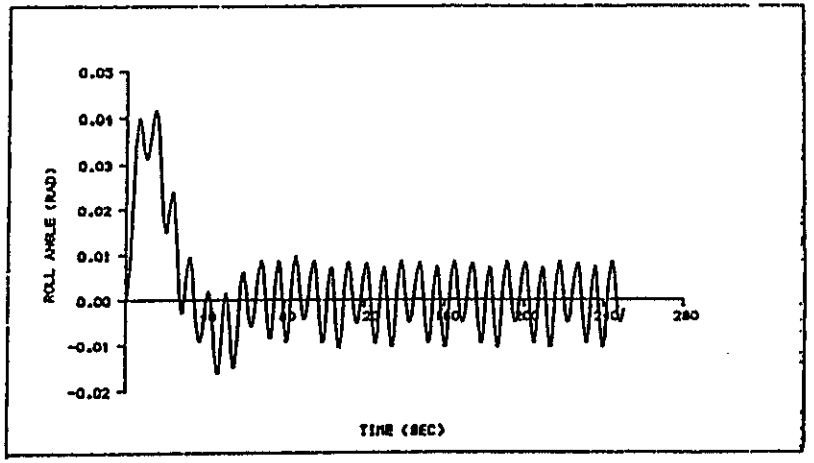

Fig 6a : ω_1=0.714 rad/sec, ω_2=0.9498 rad/sec, heavily damped

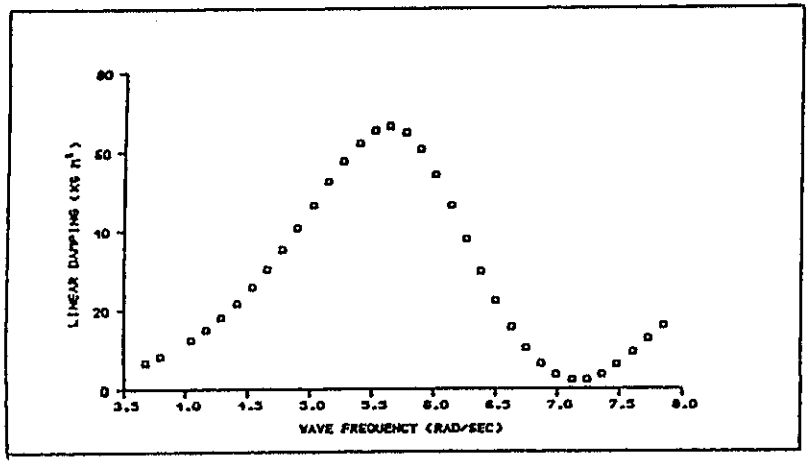

Fig 5 : Variation of roll damping with frequency, model scale (1/60)

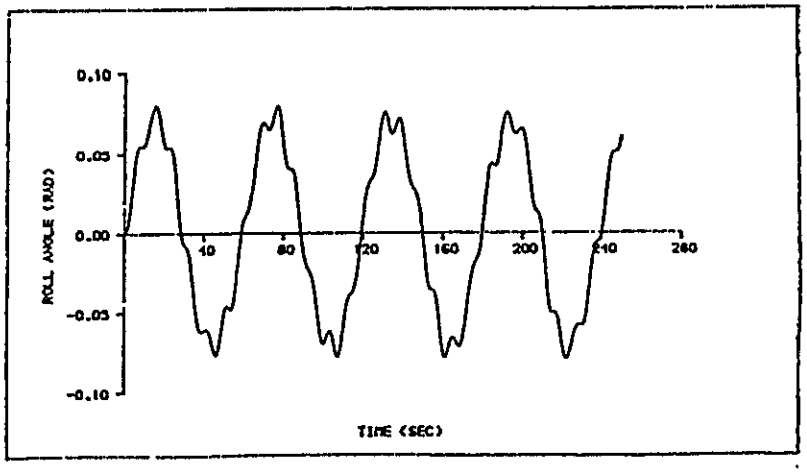

Fig 6b : ω_1=0.714 rad/sec, ω_2=0.9498 rad/sec, undamped

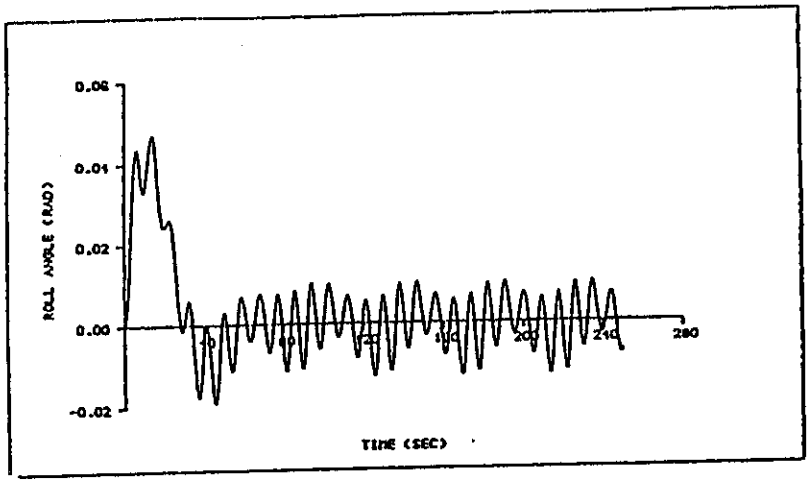

Fig 7a : ω_1=0.714 rad/sec, ω_2=0. 8548 rad/sec, heavily damped

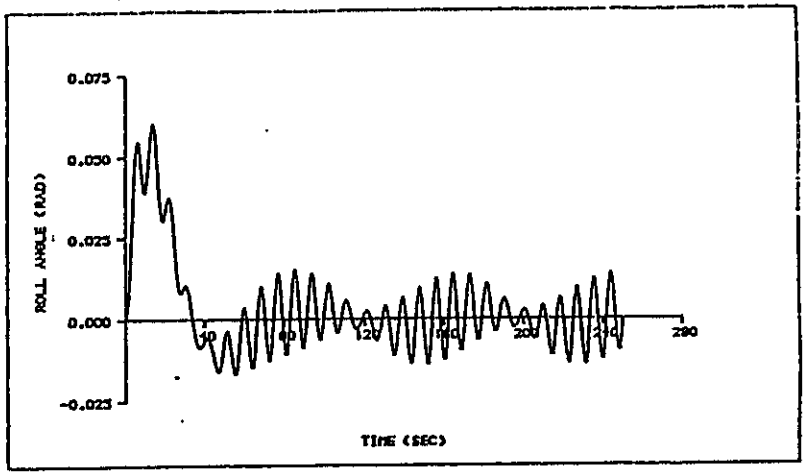

Fig 8a : ω_1=0.714 rad/sec, ω_2=0.7915 rad/sec, heavily damped

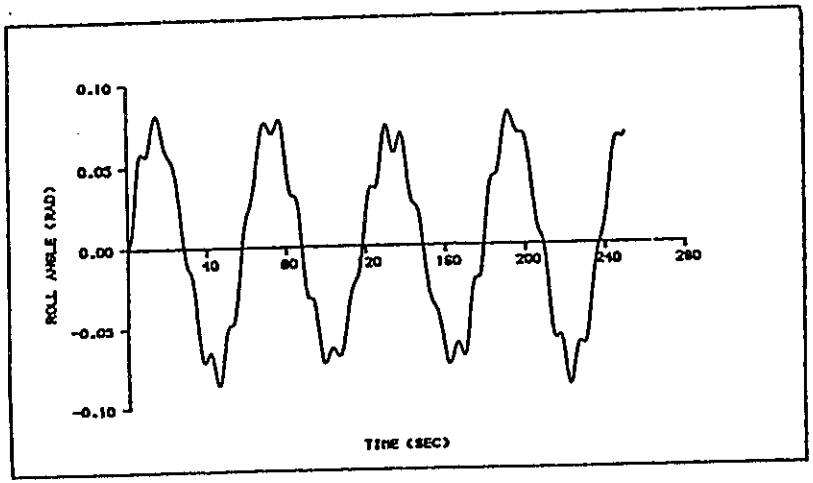

Fig 7b : ω_1=0.714 rad/sec, ω_2=0.8548 rad/sec, undamped

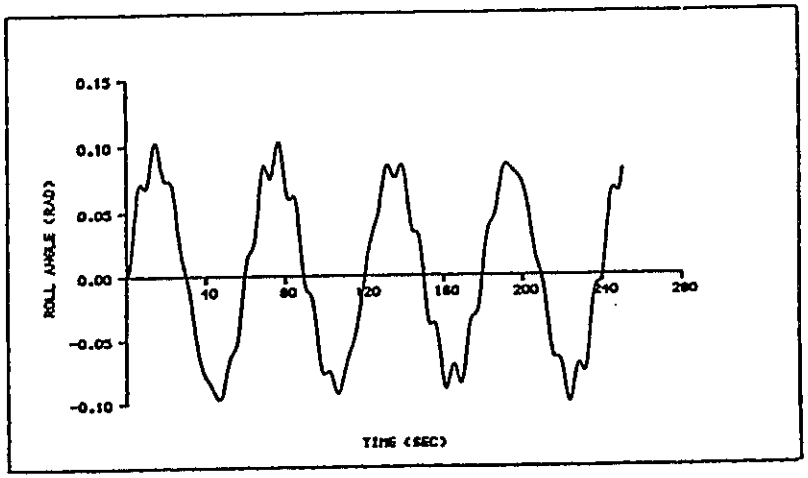

Fig 8b : ω_1=0.714 rad/sec, ω_2=0.7915 rad/sec, undamped

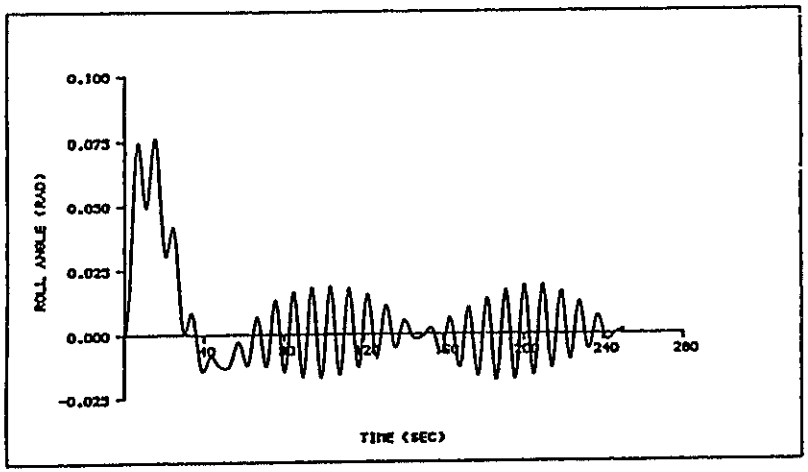

Fig 9a : ω_1=0.714 rad/sec, ω_2=0.6490 rad/sec, heavily damped

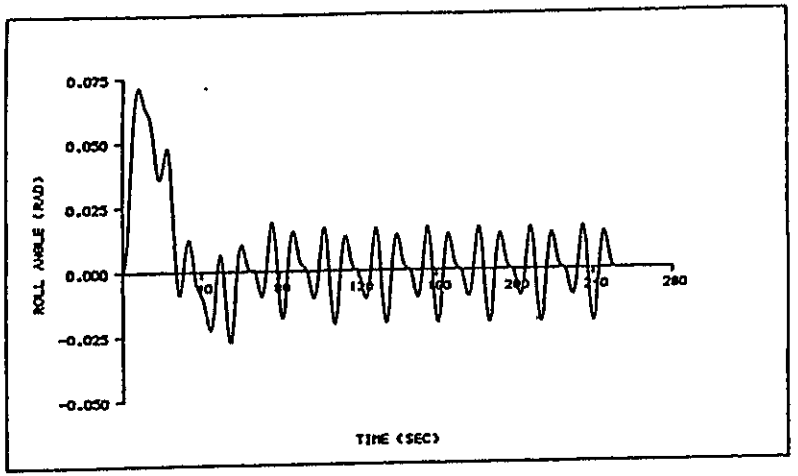

Fig 10a : ω_1=0.714 rad/sec, ω_2=0.4753 rad/sec, heavily damped

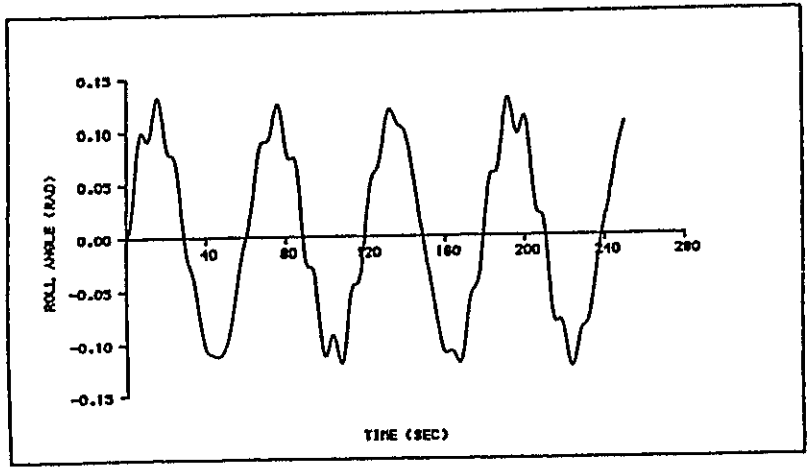

Fig 9b : ω_1=0.714 rad/sec, ω_2=0.6490 rad/sec, undamped

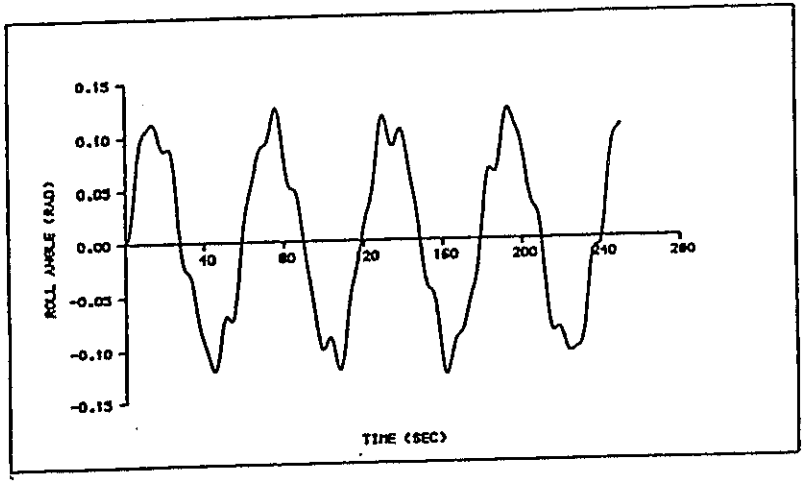

Fig 10b : ω_1=0.714 rad/sec, ω_2=0.4753 rad/sec undamped

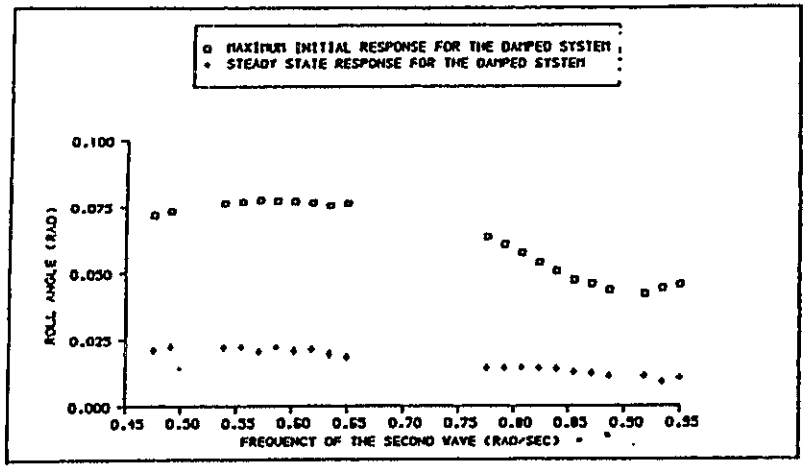

Fig 11 : Response as a function of frequency, ω_i=0.712 rad/sec

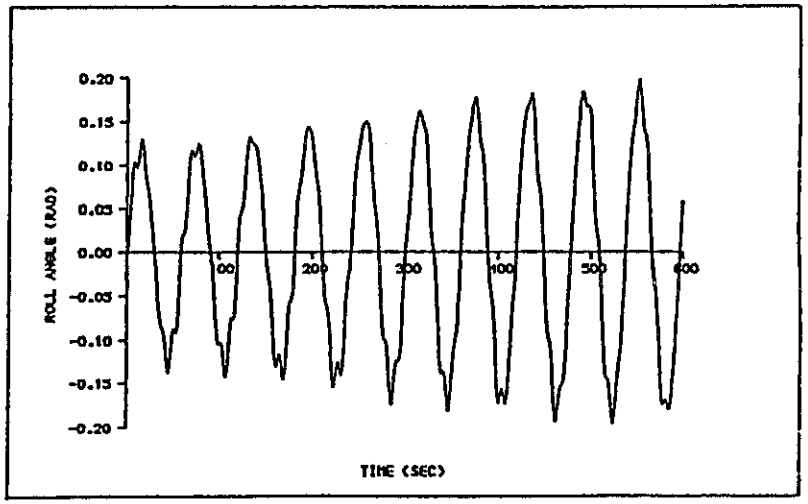

Fig 13 : Response at near-natural-frequency excitation, linear restoring

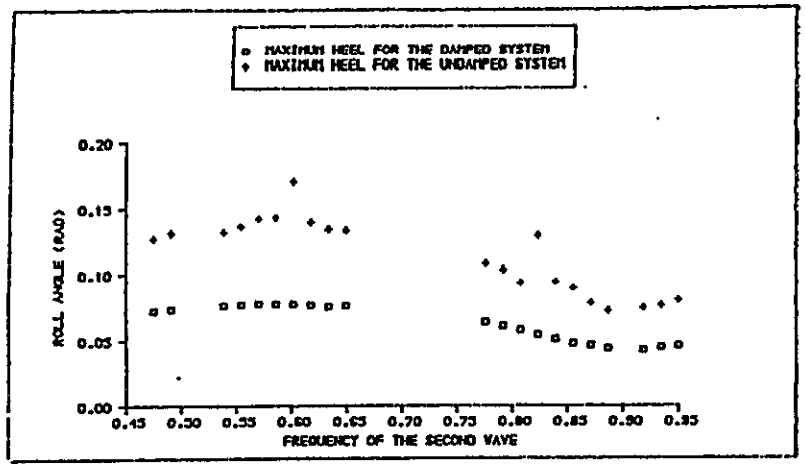

Fig 12 : Comparison of maximum heeling angles

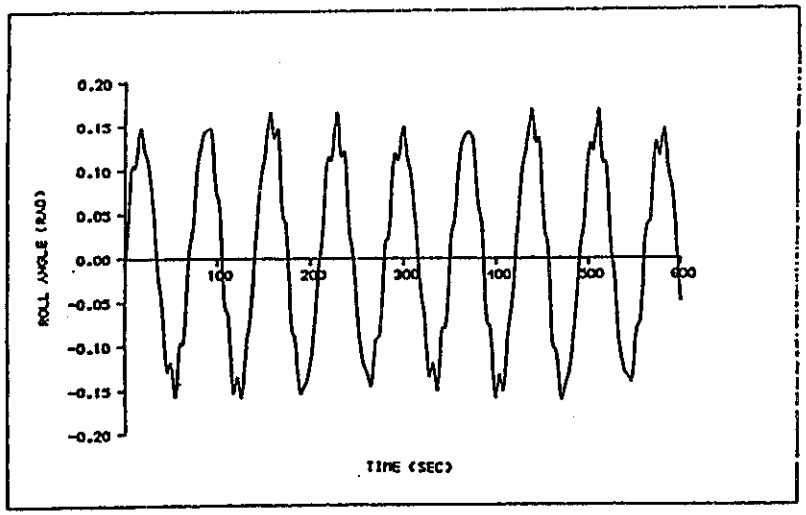

Fig 14 : Response at near-natural-frequency excitation, non-linear restori

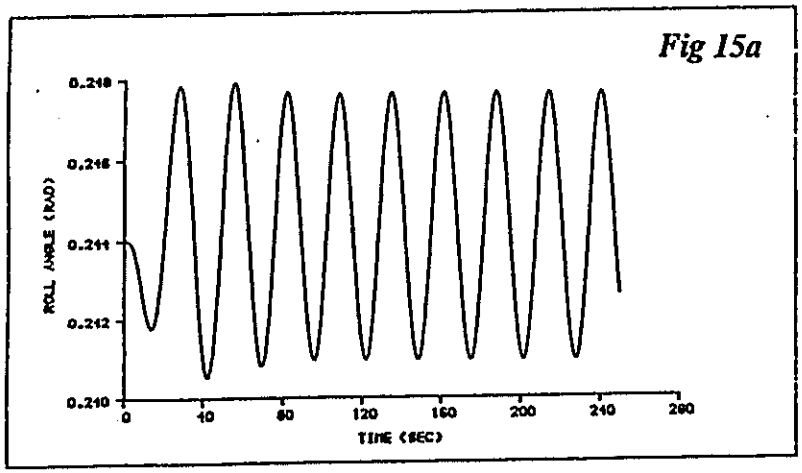

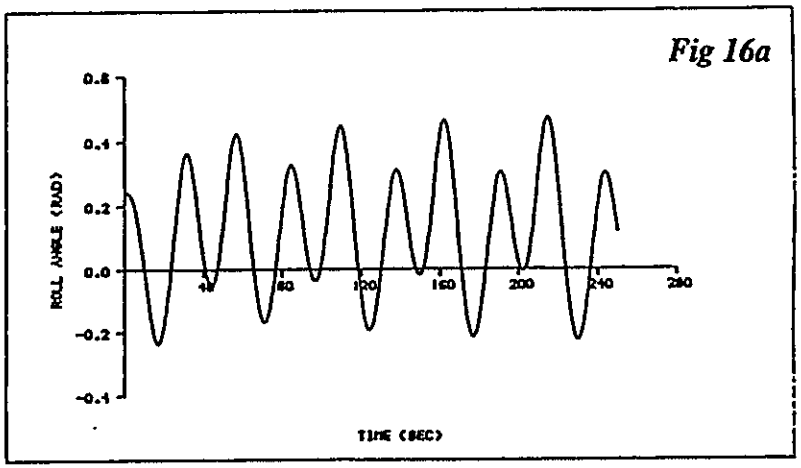

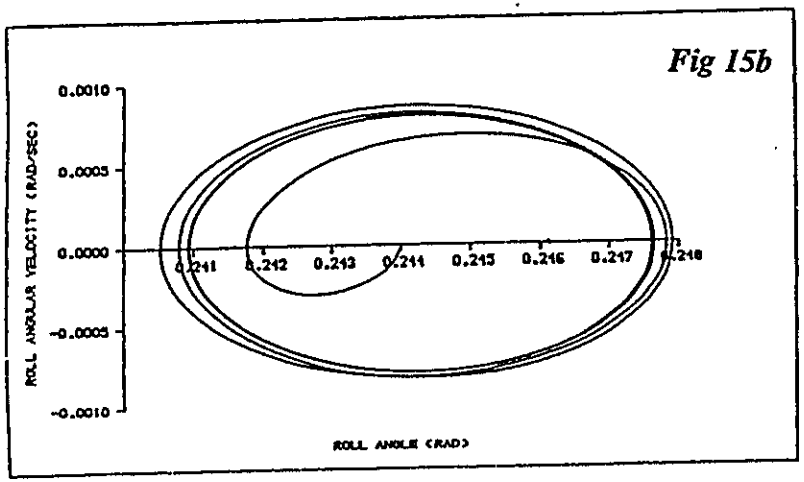

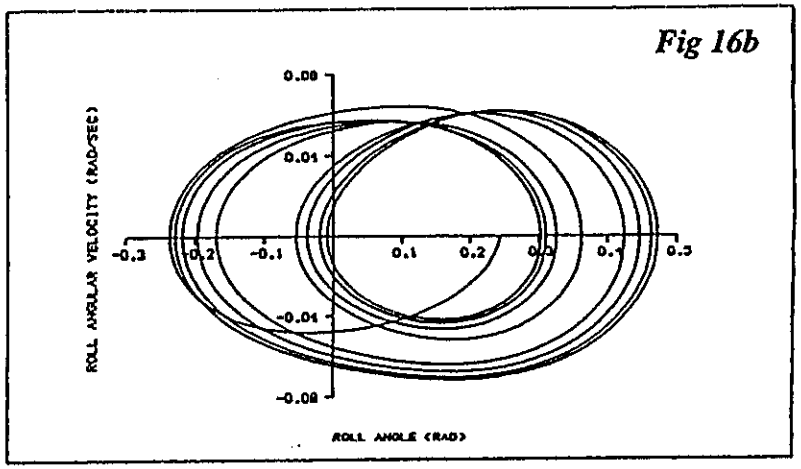

Fig 15 : 14 deg damage, $\omega_{-} = 0.2374632$ rad/sec

Fig 16 : 14 deg damage, $\omega_{-} = 0.2374632$ rad/sec, 10 m waves

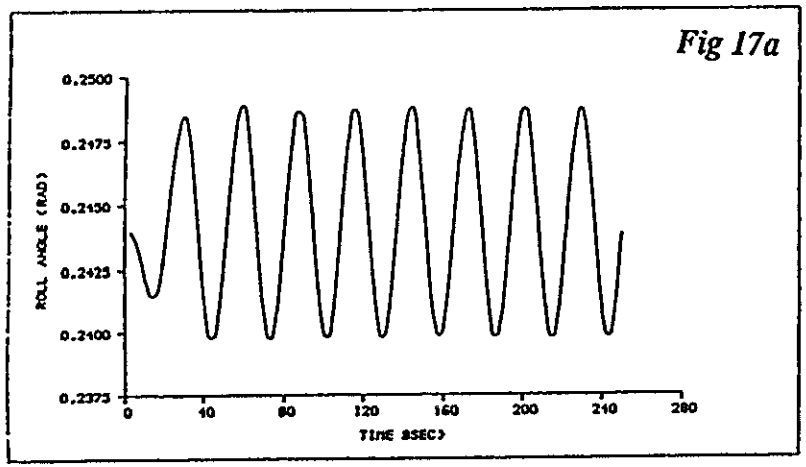

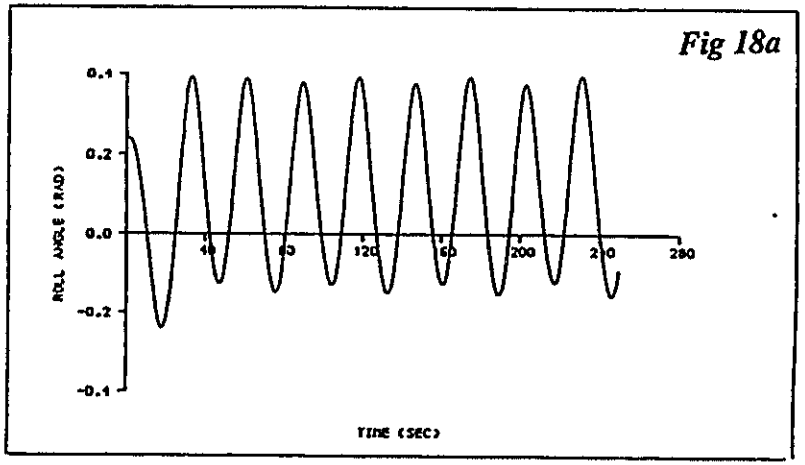

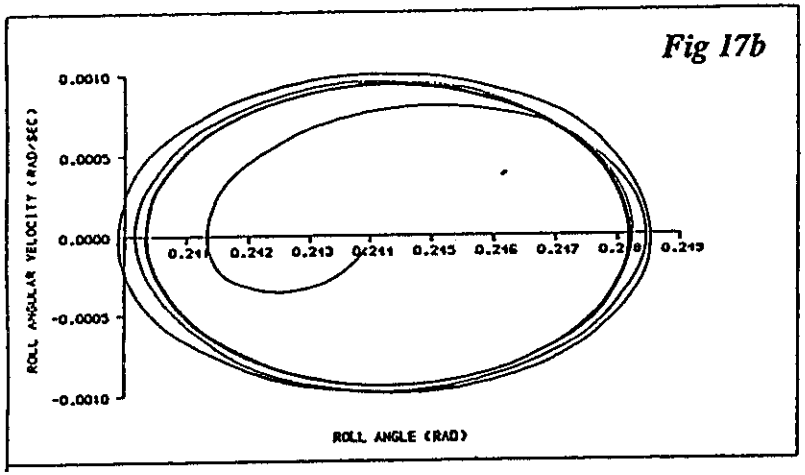

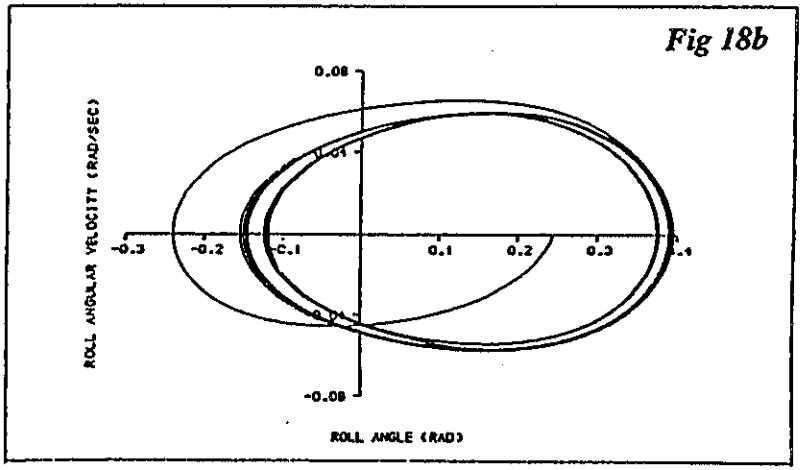

Fig 17 : 14 deg damage, ω_ = 0.2057989 rad/sec

Fig 18 : 14 deg damage, ω_ = 0.2057989 rad/sec, 10 m waves

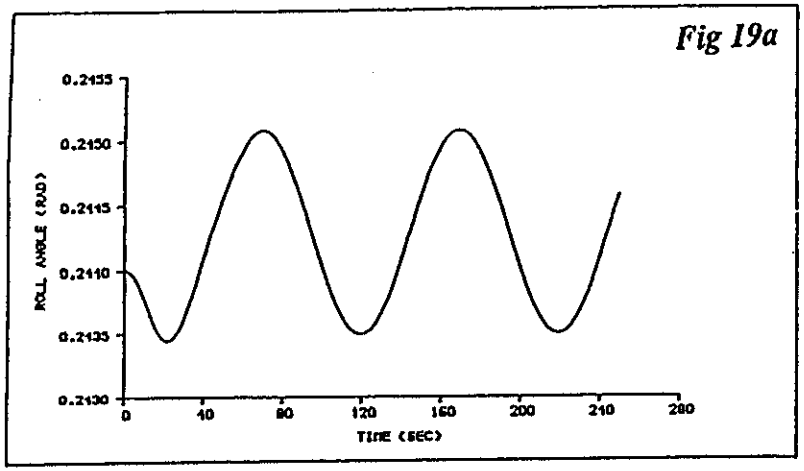

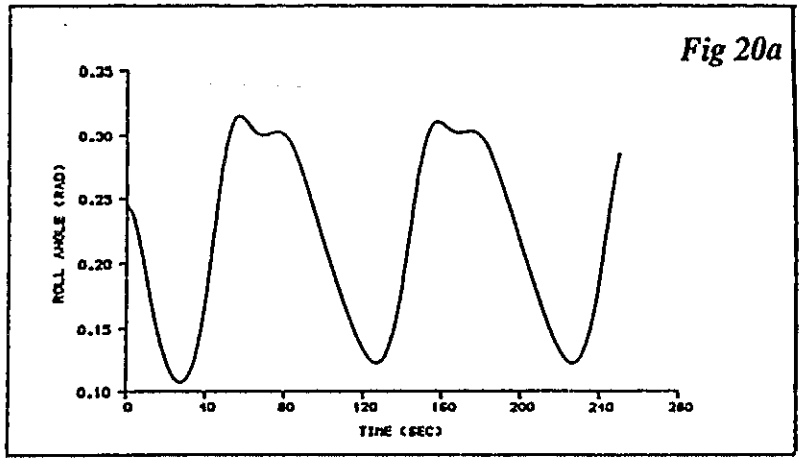

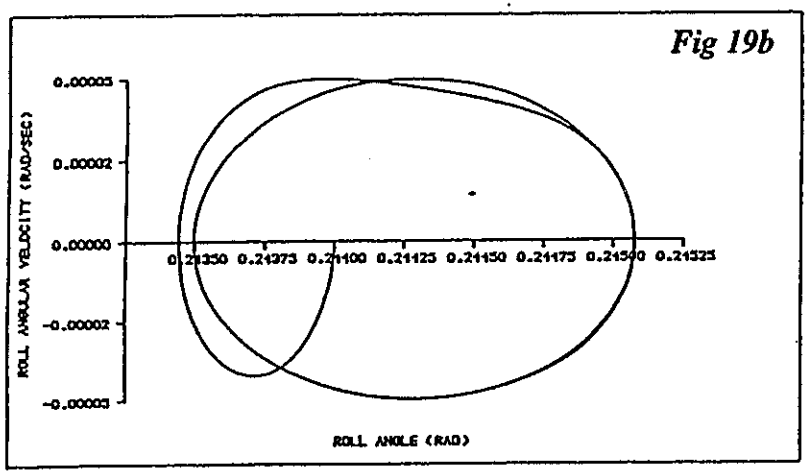

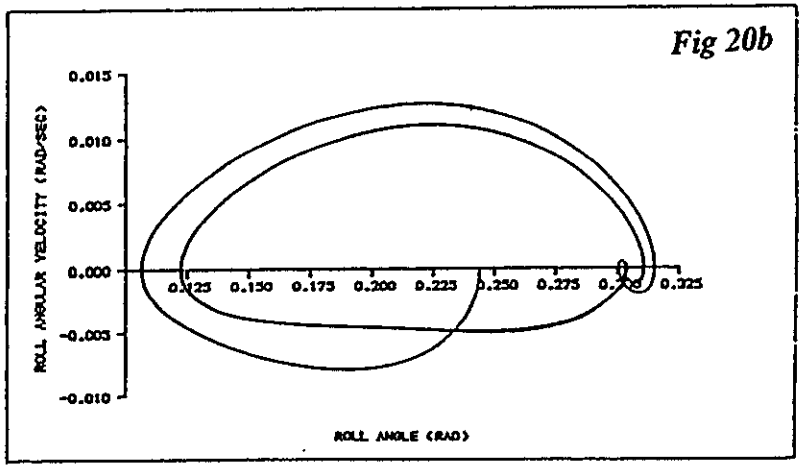

Fig 19 : 14 deg damage, $\omega_{-} = 0.063$ rad/sec

Fig 20 : 14 deg damage, $\omega_{-} = 0.063$ rad/sec, 10 m waves

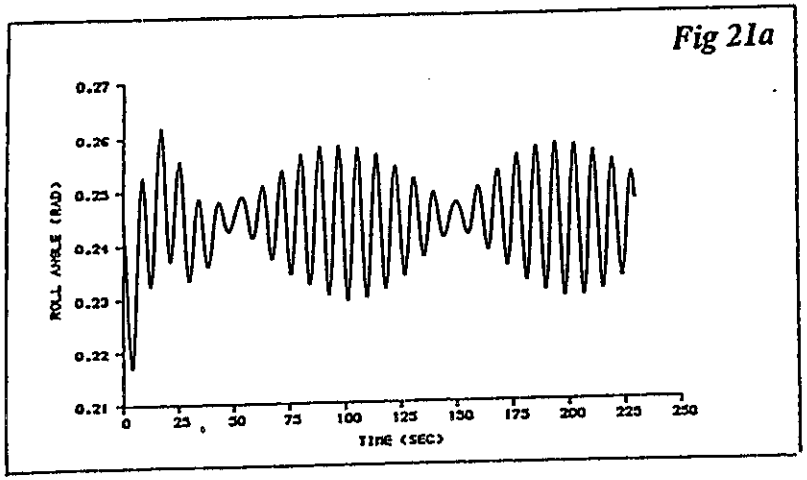

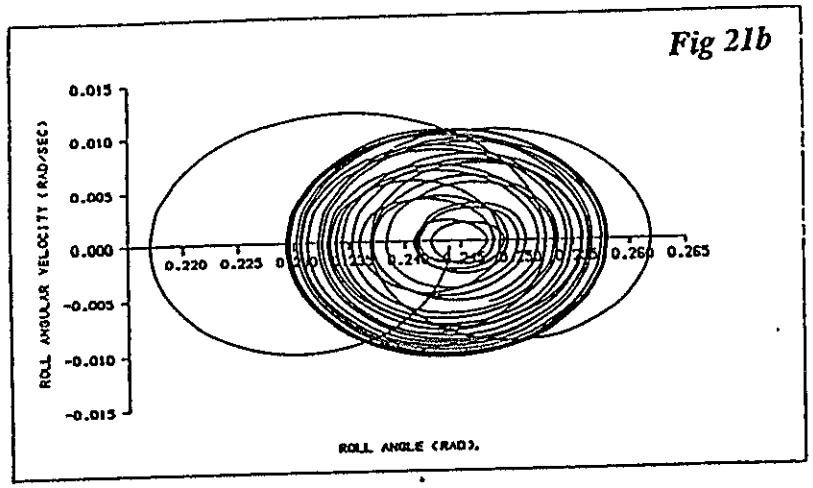

Fig 21 : 14 deg damage, $\omega_1 = 0.714$ rad/sec, $\omega_2 = 0.7757$ rad/sec, $b = 0.097958$

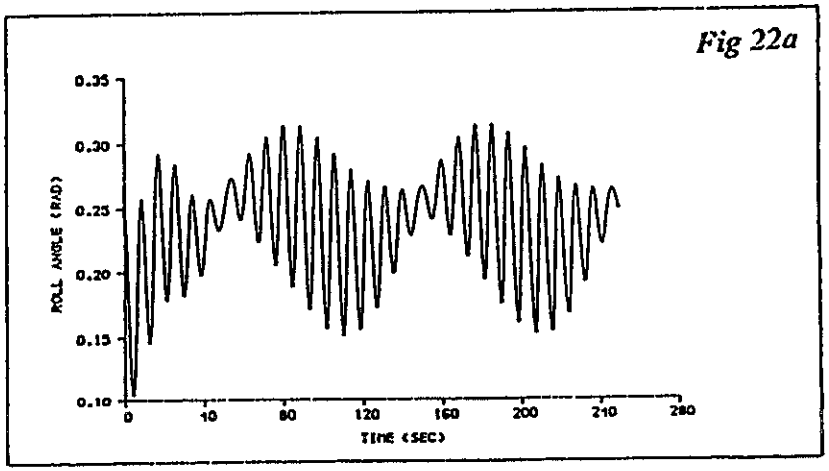

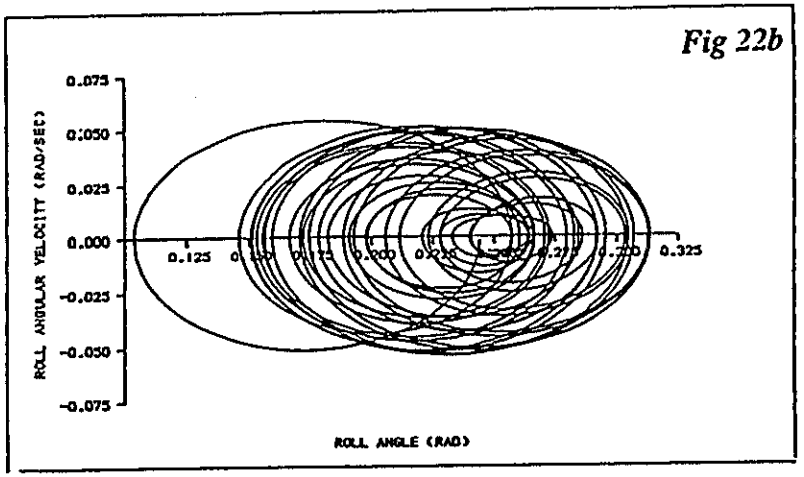

Fig 22 : 14 deg damage, $\omega_1 = 0.714$ rad/sec, $\omega_2 = 0.7757$ rad/sec, 5 m waves, $b = 0.097958$

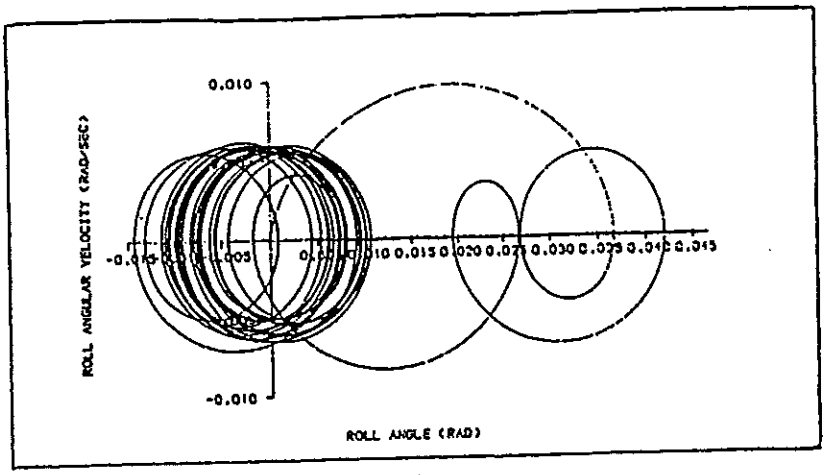

Fig 23a : $\omega_1 = 0.714$ rad/sec, $\omega_2 = 0.9181$ rad/sec, heavily damped

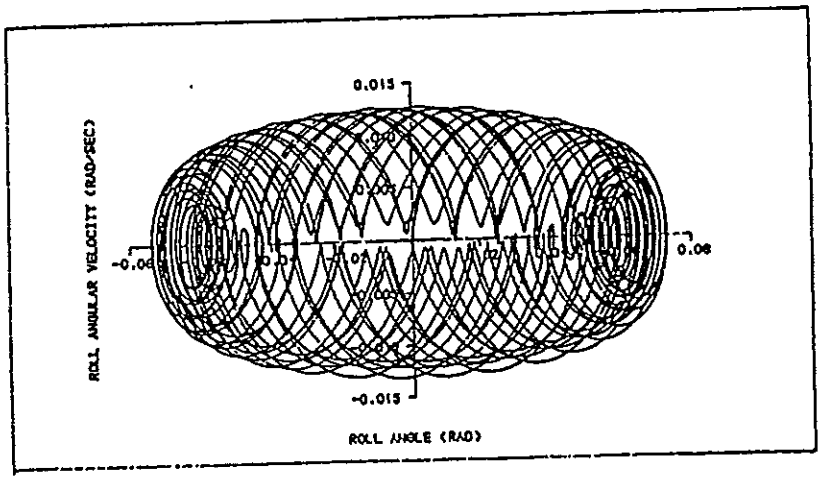

Fig 23b : $\omega_1 = 0.714$ rad/sec, $\omega_2 = 0.9181$ rad/sec, undamped

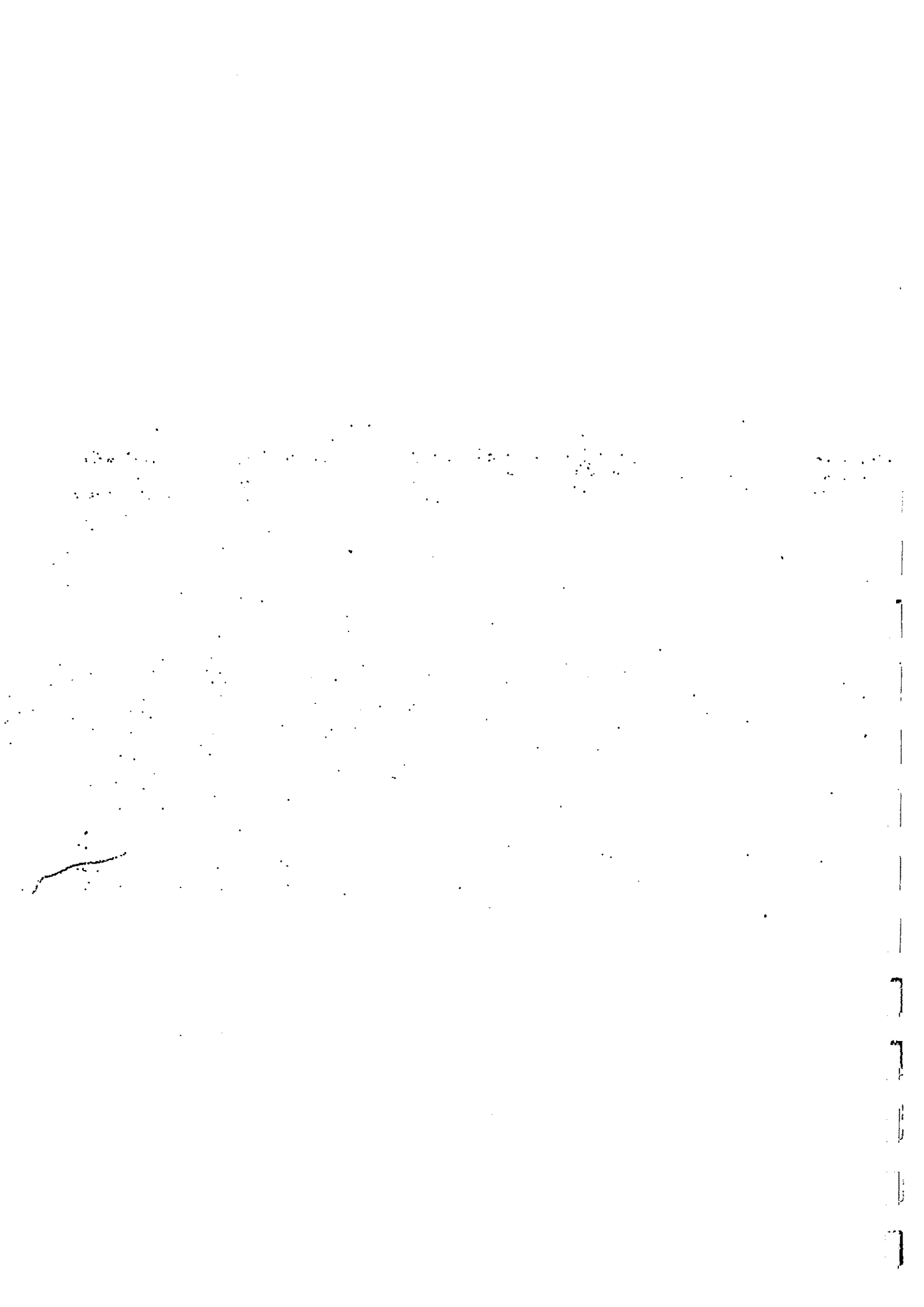

SHIP STABILITY IN FOLLOWING WAVES: THEORETICAL AND EXPERIMENTAL INVESTIGATIONS

Crudu L. (*), Nabergoj R. (**), Obreja D.C. (*), Trincas G. (**)

(*) Research and Design Institute for Shipbuilding ICEPRONAV S.A., Galati, Romania

(**) Department of Naval Architecture, Ocean and Environmental Engineering, University of Trieste, Trieste, Italy

Abstract

In the present paper the variation of transverse stability has been considered as an important factor for measuring the ship's ability to withstand unfavourable operating conditions in following waves. This problem has been considered both from theoretical and experimental point of view in the framework of a scientific cooperation between University of Trieste and ICEPRONAV S.A. Galati.

Numerical and experimental investigations have been carried out for a 2700 DWT cargo ship which actually suffered of violent rolling when operating in following waves.

Introduction

Three main factors must be taken into account in order to consider the ship safety problem: ship hull form, environmental conditions and ship operation. Due to the uncertainty of environmental conditions it is a dreadful task to provide the ship, during the design stage, with an absolute degree of safety. Generally, the most probable environmental conditions are considered according to the operational area. At the same time ship's handling is a problem of experience based on the information provided by the master. In this respect, it is very important for the designer to develop powerful tools, using theoretical as well as experimental results. As a connection among the three aforementioned factors, components of the general safety concept, the corresponding risk must be evaluated using a systematic investigation based on probabilistic and statistic analysis.

It was practically proved that the fulfilment of intact stability regulations in still-water hypothesis does not always represent an assurance for ship safety during navigation. Besides losses due to damage or to navigation errors, ship capsize is a consequence of an insufficient stability margin adopted in the design process together with an unfavorable combination of environmental conditions. Since statistics indicate that losses due to ship capsizing are frequent, it is obvious that the analysis of the dangerous situations as well as a deeper understanding of the complex phenomenon of capsizing are necessary. In studies of such a complicated dynamic phenomenon, it is essential to evaluate the contribution of different dynamic factors, to find a correlation between them and to select the most decisive ones from the

capsizing point of view. This cannot yet be done by theoretical considerations only. Appropriately designed model experiments can help not only to analyze and better understand physics of ship capsizing, but also to evaluate the quantitative influence of particular elements.

These were the reasons why a special experimental and theoretical program was proposed in the frame of the joint research between the University of Trieste and ICEPRONAV S.A. Galati. The objective is not to examine systematically the stability qualities of a certain vessel in various environmental conditions, but to investigate the physics of the capsize phenomenon in general and in most critical situations. Among the above mentioned situations the full loss of stability, the roll motion in beam sea, the main and parametric resonances in following sea, are being investigated. The results should help to define a mathematical model suitable for the prediction of capsizing in extreme quartering and following seas and to validate or calibrate the numerical simulation programs. In the present paper, only the most significant results obtained for ship stability in following waves are presented in detail.

Restoring moment in longitudinal wave

The transverse stability of a ship travelling in severe following seas is significantly affected by the change of the waterline geometry due to the relative position of the hull to the wave. This problem is even more complicated if the ship's own wave system is considered, and is typical for the well known case of small length ship (including cargo ships up to 100 m) as well as for displacement ships with high speed (close to following wave velocity). The full hydrodynamic problem of a ship moving in waves is extremely difficult to be solved since it involves consideration of non-stationary flow past solid body crossing the disturbed surface of a viscous fluid. However, from the point of view of the loss of stability, in certain conditions the hydrodynamic problem can be simplified.

According to several authors (Boroday and Netzvetaev, 1982; Boroday, 1990) the restoring moment in waves is defined as the moment of the time dependent hydrodynamic forces acting on the ship hull inclined at fixed heel angle but free to move otherwise. The problem is formulated and solved theoretically in the frame of the linear hydrodynamic theory of a non-viscous fluid, where the linearized velocity potential is presented in the form:

$$\Phi = \Phi_V + \Phi_1 + \Phi_2 + \Phi_3 \quad ,$$

where Φ_V denotes the potential of the steady motion in calm water, Φ_1 is the incident wave potential, Φ_2 is the forced motion potential, and Φ_3 is

the diffraction potential. Thus, by evaluating the fluid pressure in terms of the velocity potential, the total hydrodynamic moment can be expressed as:

$$M_W = M_V + M_1 + M_2 + M_3 \quad .$$

In the previous relation, M_V is due to the pressure field changes when the ship is running in calm water, M_1 is the Froude-Krilov component, M_2 is caused by ship forced motion in still water at fixed heel angle, and M_3 is the diffraction component. Every component is related to the corresponding fraction potential evaluated at fixed roll and the pressure integrated over the hull surface of the heeled ship. As a result, the additional restoring moment in waves is given by the relation:

$$M_{AW} = M_W - M_{SW} \quad ,$$

where M_{SW} is the righting moment in still water. The restoring moment M_{AW} in waves is a function of time and heel angle.

In the present investigation, the righting moment in following waves has been experimentally obtained by taking into account the interference between the incident-diffraction wave and the ship's own wave. A first method is based on the wave true profile measurement on the ship hull making use of photogrammetric records. The resulting wave profile is used as input data to a computer program which allows the determination of the instantaneous righting moment. A second method entails the use of a six component transducer which is connected to the towed model constrained at a fixed angle of heel in waves, allowing the measurements of the righting moment component due to incident-diffraction wave effects.

Research program

The knowledge of the ship dynamics and related phenomena could be completed if the components of both acting forces/moments generated by waves and the corresponding response of a ship are fully identified. The major problem lies in the fact that it is impossible to measure the exciting hydrodynamic forces and the model response at once. Therefore, the usual practice in experimental investigations of ship dynamics is to measure the behaviour of a free model in various wave configurations. This kind of tests may be very useful for stability estimation of a particular ship in specified environmental conditions but does not give any information about either the exciting forces or the force-response relationship during complicated motions and capsizing. Obviously, the well known identification methods based on linear theory and frequently used in seakeeping are not applicable to this case.

In order to reproduce the real capsizing mechanism, the free-running and the captive model tests must be correlated. For every instantaneous position of the model with respect to the wave profile in the free-running situation, the appropriate frozen situation in the captive tests must be found and the composition of the hydrodynamic forces has to be measured. Since this procedure requires experimental tools with special capacity, ICEPRONAV S.A. Hydrodynamic Laboratories in Galati have been charged to perform the measurements. The main characteristics of the facilities and the developed technique as well as the description of the experiments are presented below.

The experimental and theoretical results here reported, refer to a 2700 DWT cargo ship which actually suffered of violent rolling when operating at full load condition in following seas. The body plan is shown in Figure 1 while the main particulars and the mechanical characteristics of the model for the investigated case are listed in Table 1, respectively.

MAIN PARTICULARS	Full scale	Model (1/30)
Length over all	86.04 m	2.864 m
Length between pp.	79.84 m	2.661 m
Breadth	14.50 m	0.483 m
Draught aft	5.913 m	0.197 m
Draught fwd	4.578 m	0.153 m
Depth	6.700 m	0.223 m
Deadweight	2700.0 tf	100.0 kgf
Displacement	4404.4 tf	163.1 kgf
Speed	13.50 kn	1.25 m/s
Propeller diameter	3.00 m	0.105 m
Long. center of gravity from AP	37.702 m	1.290 m
Vert. center of gravity from BL	4.500 m	0.150 m
Metacentric height (still water)	1.600 m	0.053 m
Roll moment of inertia	82620 $t \cdot m^2$	3.4 $kg \cdot m^2$
Pitch moment of inertia	1540620 $t \cdot m^2$	63.4 $kg \cdot m^2$
Yaw moment of inertia	1433700 $t \cdot m^2$	59.0 $kg \cdot m^2$

Table 1 - Main particulars and mechanical characteristics at full load condition

Test facilities and experiments

The ICEPRONAV S.A. resistance, self-propulsion and seakeeping towing tank (276m x 12m x 6m) has been utilized for tests with self-propelled model and captive tests (two models with model scale 1/20 and 1/30, respectively). The tank has a hydraulic driven flap type wave generator both for regular and irregular waves (length 0.4÷25.0 m, height 0.04÷0.60

m), a straight metal multigrid beach, while wave measurements are made by capacitance probes on carriage and tank walls.

The standard onboard data acquisition system can provide recording of 2048 samples through 12 channels at a sampling frequency of 20 Hz, thus producing the length of recordings equal to 102.4 sec. To obtain the wave exciting forces and moments a six component transducer was used. The upper and lower parts of the transducer are stiffly connected to the carriage and to the ship model, respectively. A pre-established heel angle can be imposed to the ship model. Estimation of standard errors for different items measured during experimental tests is given in Table 2.

GENERAL		FORCES AND MOMENTS		MOTIONS	
Sampling/digitizing	0.1%	Surge force	0.58%	Surge motion	0.09%
Wave height	1.0%	Sway force	0.21%	Sway motion	0.11%
Vert. centre of gravity	3.5%	Heave force	0.85%	Heave motion	0.03%
Roll moment of inertia	2.3%	Roll moment	2.50%	Roll motion	3.10%
Pitch moment of inertia	0.8%	Pitch moment	0.09%	Pitch motion	0.21%
Yaw moment of inertia	1.0%	Yaw moment	0.27%	Yaw motion	0.35%

Table 2 - Standard errors of measurements

Self-propelled model

First still water tests have been performed to determine the own wave profile on ship hull (model scale 1/20). The ship model was self-propelled at design speed (Fn = 0.25) and connected to the carriage by means of long wires and soft coil springs, all the degrees of freedom being ensured with no influence on the motions. In order to determine the free surface profile on the ship hull in upright position two photogrammetric cameras were located on starboard to record the wave generated by the model running (ship's own wave). The obtained photoplates allow to create the so-called stereo model and to measure the free surface profile at each model station (Reti, 1990). The general arrangement of the set-up is schematically shown in Figure 2.

The present experimental procedure differs from the method adopted by Ferguson and Conn (1970) where the tests were carried out by means of towed models. Their procedure allowed to measure sinkage and trim as well as the restoring moment on models with an initial heel angle up to 7 degrees in the static condition. The measurements of the wave profiles showed a substantial difference on the two sides of the vessel only for fuller forms and at larger heel angles. In this respect, our procedure has been limited to recording the model's own wave profile in upright position only.

After carrying out experiments in still water, regular following waves with length equal to the ship's length and full scale height of 1.800 m were generated in the tank. Hence, the resulting wave profile on the running ship hull was determined (ship's actual wave in following sea). The most unfavourable situation for transverse stability when the ship is set with the midship station on wave crest, was investigated.

The wave profiles obtained during self-propulsion tests in still water and in following waves are presented in Figure 3, where for sake of simplicity the ratio between the vertical and horizontal unit corresponds to 5. Using these data, static stability computations were carried out for still-water condition ($GZ_{max} = 0.797$ m), for ship's own wave ($GZ_{max} = 0.898$ m), for ship's actual wave when crest at amidships ($GZ_{max} = 0.762$ m), and for undisturbed sinusoidal wave which represents a standard for stability computations in longitudinal waves ($GZ_{max} = 0.658$ m). The results obtained when considering the still-water displacement ($\Delta = 4404.4$ t) and full scale wave height are shown in Figure 4. It is worth to note that practically no difference between computations carried out for the experimental resulting wave and for the wave obtained by a simple superposition of ship's own wave and an undisturbed sinusoidal wave (ship's hybrid wave), has been found (-1.2% in GZ_{max}). This fact allows to use such a procedure for computing the righting arms for different positions of the wave crest with respect to the ship.

The diagram clearly shows a difference between the righting arms computed through standard naval architecture methods and the ones obtained for the real physical situation observed in the towing tank. In particular, for the ship under consideration the own wave produces a stabilizing effect at design speed both in still water (+12.7%) and in following sea (+15.8%). This result does not agree with the conclusions presented by Ferguson and Conn (1970), but is fully confirmed by older experiments (Baker and Keary, 1918).

It is worth to observe that by using the data obtained from the photogrammetric method a difference between the still-water displacement and the actual displacements, both for ship's own wave and for actual wave when the ship is running in following sea with crest at amidships, was observed. In the first case, the computed displacement was 3.0 percent lower as a result of the combined effects of experimental errors in model's own wave profile estimation and of the modified sinkage and trim, which were not recorded. In the second case, the decrease in displacement amounted to 6.4 percent, caused by previous errors and by the fact that the ship was recorded in a dynamic condition characterized by simultaneous heave and pitch motions. Therefore, the true physical situation in which the ship model is not statically sitting on the wave has not been taken into account. Would the measured displacements been used in hydrostatic

computations, there should have been an additional GZ_{max} increase of 5.5 percent and of 12.6 percent, respectively.

Captive model

The fully captive test arrangement is shown in Figure 5. The ship model (model scale 1/30) is connected by a six-component dynamometer and has no freedom to move relatively to the carriage. The model can be fixed at different heel angles to get the still-water displacement.

The tests have been carried out in regular following waves at zero (Fn = 0) and service speed and for wave frequencies ranging from 0.55 Hz up to 0.85 Hz, the wave height kept constant and equal to 0.09 m. The range of heel angles was selected between 0°+15° with a stepwise of 2.5°. The net effect due to wave excitation, that is, the effect of both the incident and diffraction components in all the six degrees of freedom has been measured.

The signals supplied by six dynamometer outputs and the wave probe have been stored on magnetic tape and later processed off-line. As an example, the non-dimensional transfer functions of heave force, roll and pitch moments are shown in Figures 6 through 8 at Fn = 0 and Fn = 0.25, respectively. The diagrams are built in axonometric view to display the influence of heel on excitation.

The frequency response functions of both sway force and yaw moment, which are not shown, were practically zero in upright position, while they present small values at larger heel angles. When the frequency response functions of heave force, roll and pitch moments are considered, it can be seen that only small differences have been measured at different heels. However, in upright position the roll moment does not reduce to zero but remains significant, being considerably reduced at service speed. At Fn = 0, a local maximum occurs for heave force, roll and pitch moments close to wave frequency 0.75 Hz, which is systematically observed at all heel angles. This tendency for the above mentioned forces and moments disappears at Fn = 0.25. Except for roll moment, this behaviour is in both qualitative and quantitative agreement with theoretical predictions based on linear seakeeping theory.

The information on ship stability in following waves with length equal to the ship length can be obtained by estimating the roll moment frequency response function at $\lambda/L = 1$. The results obtained are shown in Figure 9 for the two Froude numbers considered. The experiments show a non-zero roll excitation for the ship in upright position which should be zero according to theoretical predictions based on linear approximation. A rough explanation cannot relate this value to the model disalignment with the direction of wave propagation but probably to nonlinear effects which

cannot be accounted for theoretically. The non-zero roll moment is responsible for exciting a roll resonance which has been observed during the tests on free models and will be reported in the next section.

Summing up the incident-diffraction component with the hydrostatic component, theoretically determined by means of calculations in still water, the righting moment in following waves has been obtained. Since the measured values are limited to 15 degrees, it was necessary to extrapolate to higher angles the additional effect of incident and diffraction components. To simplify the procedure the mean value of the measured data has been assumed for the whole range of heel angles. Taking into account the proper phase relationship, the resulting righting arms in following waves ($H_w = 1.800$ m) are shown in Figures 10 and 11 at $Fn = 0$ and $Fn = 0.25$, respectively. It appears that the ship is subject to sinusoidal varying righting moment at upright position and thus will be forced into roll oscillation. The amplitude of the resulting motion will be higher at zero speed due to considerable excitation and proper frequency tuning with the waves.

Free model

The motions of the model in six degrees of freedom were measured mechanically by using a pantograph system with potentiometers forming an arrangement similar to the one shown in Figure 2. The moving parts of the pantograph have relatively negligeable weight, therefore reducing their influence on the dynamic behaviour of the model. The signals supplied by the potentiometers and the wave probe have been analyzed by using the data acquisition and processing system previously described. The motion amplitudes are determined by means of harmonic analysis.

While the experimental results for surge, heave, and pitch motions are in agreement with theoretical predictions based on linear seakeeping theory, the same is not valid for roll motion. The results obtained for roll response are shown in Figure 12, at $Fn = 0$ and $Fn = 0.25$, respectively. At zero speed the ship exhibits strong roll oscillations for $\lambda/L = 1.043$ at wave frequency equal to the natural roll frequency, i.e., the model oscillates in main resonance. At design speed, due to frequency shift related to ship wave encounter, this frequency is out of measuring range, and therefore the possibility of such a resonance cannot be confirmed. In addition, the presence of a parametric resonance has not been examined for the same reason. However, such a situation could be investigated by performing experiments with lower GM.

The previous conclusions are confirmed when evaluating the natural frequencies of the ship in heave, roll and pitch. Both main resonance and parametric resonance occurrence in terms of speed and metacentric height

combinations, together with the safe zones for ship running in following waves (Bogdanov, 1989), are shown in Figure 13. Here, the investigated experimental conditions have been marked by heavy and light dots for zero speed and design speed, respectively. For GM = 1.600 m and zero speed the resonant roll tuning occurs with waves of length close to ship length. Therefore, the ship will exhibit main roll resonance at very low speeds as confirmed by the ship master.

Comments and recommendations

It has been shown that ship's own wave can be responsible for significant changes of the righting arm curve. Therefore, it is advisable to record the wave profile on the hull and to use these data to perform more accurate hydrostatic computations. Such kind of measurements should be performed sistematically by the model basins when carrying out standard self-propulsion tests with minor extra charges.

In following waves the ship can exhibit both main and parametric resonances. While the evidence of parametric resonance has been fully recognized in the past (Paulling, 1961), the same does not hold for main resonance oscillations. Main resonance in following seas has not been investigated with the same emphasis, and only a qualitative confirmation of such resonances can be found in some authors (Boroday and Morenschildt, 1986). Our experiments show that also in the main frequency range a ship can be excited to roll resonance and that the subsequent oscillations can reach large amplitudes. Since the theoretical aspects of the phenomenon as well as the prediction of the roll exciting moment amplitude are not yet available, major research efforts should be advocated in this field. In this respect, also the classical concept of ship stability in longitudinal waves needs a critical review in order to provide the designer with more realistic indications necessary to assess stability in the real dynamic conditions.

References

Baker, G.S. and Keary, E.M. (1918), *The Effect of the Longitudinal Motion of a Ship on its Statical Transverse Stability*, Trans. Instit. Naval Architects, Vol. 60, pp. 74-82.

Bogdanov, A. (1989), *Stability Criterion: Safe Speed and Wave-to-Course Angle Diagram for a Ship Sailing in a Storm Following Sea*, Proceedings 18th Scientific and Methodological Seminar on Ship Hydrodynamics, Varna, Vol. 3, pp. 81/1-19.

Boroday, I.K. (1990), *Ship Stability in Waves: on the Problem of Righting Moment Estimations for Ships in Oblique Waves*, Proceedings Fourth International Conference on Stability of Ships and Ocean Vehicles, Naples, Vol. 2, pp. 441-451.

Boroday, I.K., Netzvetaev, Y.A. (1982), *Seakeeping of Ships* (in Russian), Sudostroenie, Leningrad.

Boroday, I.K. and Morenschildt, V.A. (1986), *Stability in Parametric Roll of Ships in Waves*, Proceedings Third International Conference on Stability of Ships and Ocean Vehicles, Gdansk, Vol. 1, pp. 19-26.

Ferguson, A.M., Conn, J.F.C. (1970), *The Effect of Forward Motion on the Transverse Stability of a Displacement Vessel*, Trans. Inst. Engineers and Shipbuilders in Scotland, Vol. 113, pp. 215-249.

Paulling, J.R. (1961), The Transverse Stability of a Ship in a Longitudinal Seaway, Journal of Ship Research, Vol. 5, pp. 37-49.

Reti, N. (1990), *Tests for Free Surface Determination on Ship Body Using Photogrammetric Method* (in Romanian), Internal Report, Ac 2261-2.1.2.3.1.

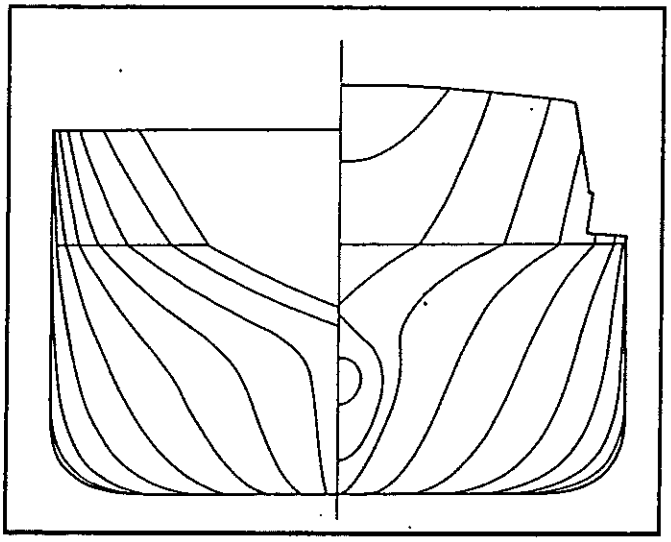

Fig. 1 - Body plan of 2700 DWT cargo ship

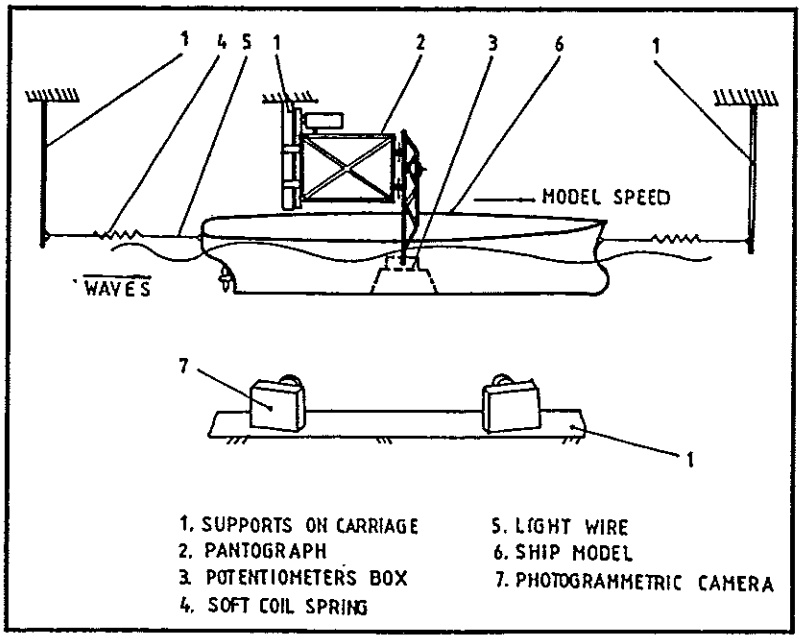

Fig. 2 - General arrangement of experimental set-up for self-propelled model tests

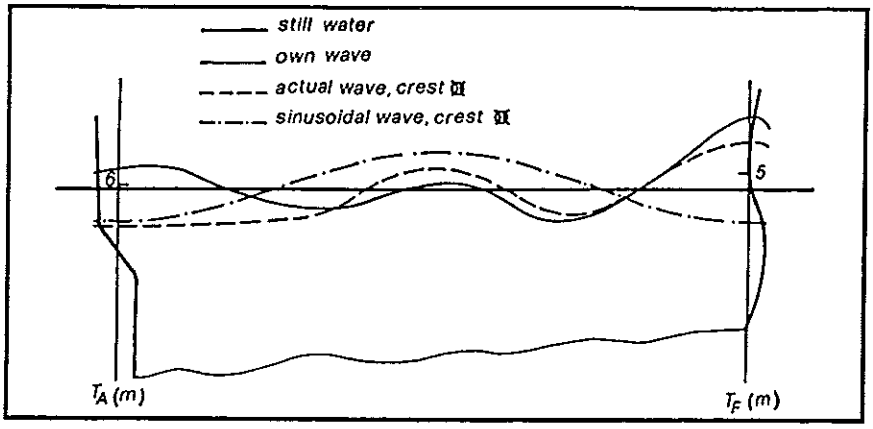

Fig. 3 - Wave profiles recorded during self-propelled model tests

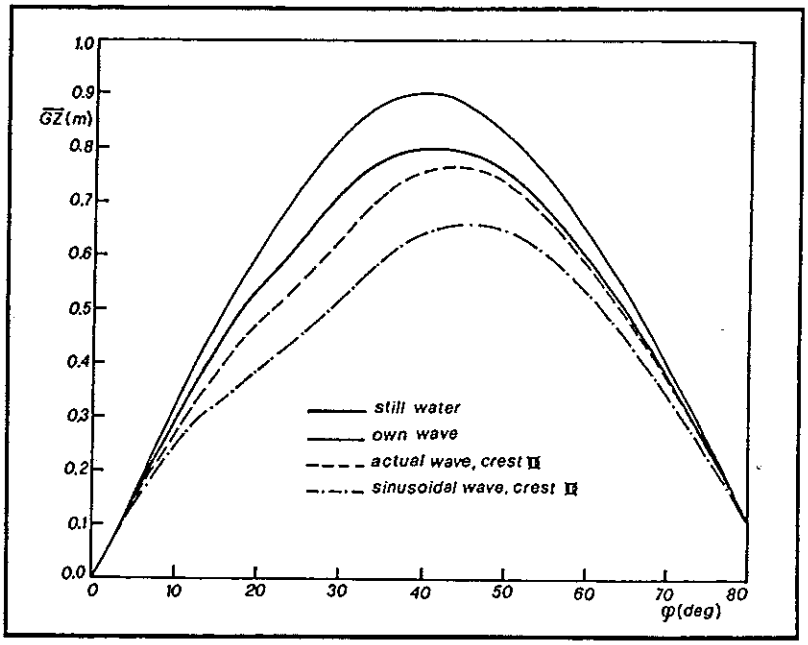

Fig. 4 - Righting arms

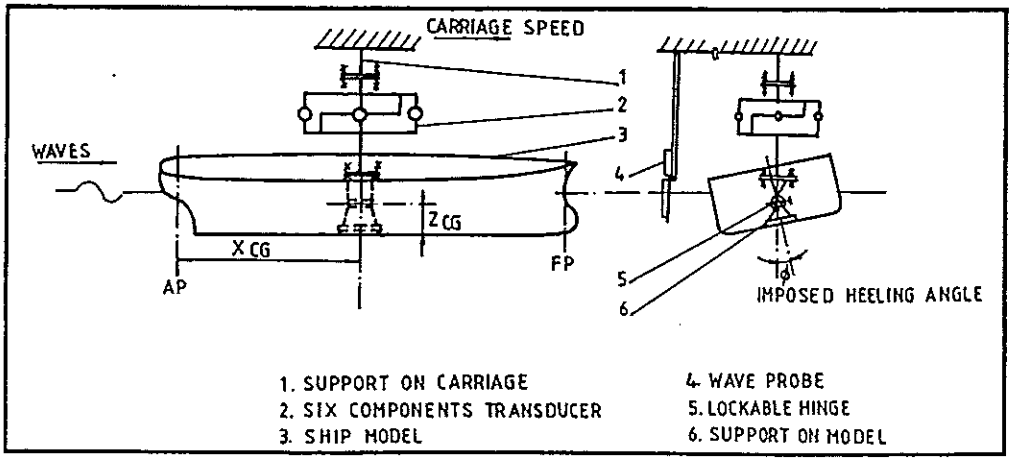

Fig. 5 - General arrangement of experimental set-up for captive model tests

FIFTH INTERNATIONAL CONFERENCE ON
STABILITY OF SHIPS AND OCEAN VEHICLES
FLORIDA, USA, NOVEMBER 1994

The Development of an ISO Stability Standard for Small Craft

by Andrew G. Blyth, BSc, CEng, MRINA.
Convener ISO/TC188 Working Group 22

ABSTRACT

The paper introduces some of the work of developing ISO Standards for small craft (ie: up to 24 metres length) as part of a programme prompted by the forthcoming European Union Directive on Recreational Boats.

It is intended to produce a rational Standard for the stability and buoyancy of small craft, containing requirements consistent with those for all forms of vessel and not solely addressed to recreational boats.

This Standard will embrace all forms of vessel whether powered by sail, motor, or muscle, of any speed range, and all hullforms. The exclusions are extremely limited, making the diversity of craft considerable. The current status of the draft Standard is described, showing how the various identified stability and buoyancy hazards are being addressed, and the development of boat type and operating categories in order to rationally subdivide the task. Projects being undertaken to validate the methods and criteria being developed are reported upon.

1 INTRODUCTION.

The European Union primarily exists to eliminate barriers to trade within its boundaries. About 1987 it was realised that free trade in small craft was being inhibited by the substantially different regulatory requirements existing in different countries, and so the idea of having a Directive to harmonise these requirements was put forward. This Directive will only apply to the design and manufacture of vessels first placed on the European market after the implementation date, currently expected to be 1996.

During 1994, the draft Directive has been extensively debated, and is currently on the point of being adopted [Ref 1]. The Directive itself identifies a number of Essential Safety Requirements, giving alternative methods of demonstrating compliance. In fact two basic methods are possible:

(a) by direct documentation in a Technical Data File, to the satisfaction of an Approved Body

or (b) by compliance with an agreed European Standard.

European Standards are often identical to International Standards.

In order to provide the technical detail not embodied in the Directive itself, the International Standards Organisation Small Craft Technical Committee (TC 188) has about 20 Working Groups developing International Standards intended to support the EU Directive. It is the intention that these standards will also be adopted as European Standards (CEN's). Because of the significance of Europe in the World Market for small craft, a number of non-EU countries are also participating in the development of these standards. A total of fourteen countries is actively involved, including USA, Canada, and Japan.

This paper is concerned with the development of:-

ISO 12217 - Small Craft - Stability and Buoyancy
- Methods of Assessment and Categorisation.

for which the author has been privileged to act as Convener.

It should be noted that the Standard identifies how to assess and categorise craft, based on their design and construction, and is NOT a REGULATION permitting or prohibiting the USE of vessels.

It is also emphasised that this paper merely summarises the state of development of the Standard as it stands in the Spring of 1994, and that further changes are to be expected before completion of the work.

2 SCOPE.

The scope of the Standard is the intact stability and buoyancy of all forms of small craft up to 24 metres Length of Hull, including the flotation characteristics of boats vulnerable to swamping. The following are excluded:-

- aquatic toys
- inflatable boats covered by ISO 6185
- personal watercraft (jetskis and similar)
- hydrofoils and hovercraft when operating in the dynamically supported mode

Not included in the terms of reference are the effects of damage to the hull on the stability and buoyancy nor the effects of unusual loads such as may be caused by lifting, towing, dredging or fishing.

3 EXISTING NATIONAL REQUIREMENTS.

The natural starting point for such a task is to review existing national requirements, in an endeavour to see whether these could be simply "editted" into one comprehensive document. However, it was quickly realised that this would not be a practical proposition in this instance, because closely similar vessels would often be required to meet substantially different criteria.

The requirements currently employed by different countries have mostly originated from a different viewpoint. National requirements naturally consider the types of vessel predominant in the country concerned, and in the interests of ease of application simplifying assumptions are frequently used which can be invalid for vessels originating from a different culture. Many national requirements are limited to types and series of craft with a history of accidents.

Further difficulties stem from the use of different definitions, different specific areas of safety concern, different backgrounds of boat users, and different attitudes to the abilities expected of the users. In the early stages, this led to some vigorous exchanges of opinion.

However, as members of the Working Group gradually became aware of the different experience and knowledge available in different countries, a commonality of purpose became established and preconceived ideas and positions were progressively abandoned in favour of a reasoned discussion of the logical merits of each aspect. It is believed that the resulting Standard will be as free of illogicalities as it is practically possible to achieve.

4 BASIC APPROACH.

The Standard is divided into two separate but coherent parts:-

Part 1 - Non-Sailing Vessels
Part 2 - Sailing Vessels

This division, apart from considerations of administrative convenience, has been made because the capsizing hazards for these two groups of vessels can be significantly different.

The purpose of the Standard is to enable any individual vessel to be assessed by a variety of methods, resulting in the allocation of a Stability Category which reflects the manner in which the vessel might be safely used by people of ordinary seamanship skills, ie: neither novice nor ocean veteran.

A number of basic principles are being followed in the development of the Standard:-

Wherever possible, distinctions are made on a rational basis, rather than arbitrary (eg: length) differences. This is in order to try to minimise illogical variations in requirements for closely similar craft resulting in "paragraph" boats.

Alternative methods of demonstrating compliance are allowed, varying from rigorous or approximate calculation, calculation plus experiment, or exclusively experimental, depending on the subject matter concerned. Some very simple methods are included, which incorporate appropriate margins for inaccuracy, but more sophisticated methods may also be used for greater accuracy (at greater cost).

Where possible, simple screening formulae are being developed, to enable those vessels which easily meet the requirements to be identified with minimum effort. By applying more sophisticated methods it may subsequently be possible to achieve a higher categorisation.

The aspects being considered in the criteria under developement include:-

- adequate freeboard when upright, for example in waves
- adequate freeboard when heeled due to offset load, wind forces or rolling in a seaway
- vulnerability to swamping, relating size of recesses or cockpit to reserve buoyancy of the hull
- buoyancy after swamping
- for sailing vessels: behaviour after knockdown to 90° or complete inversion

5 DEFINITIONS.

This work has generated a need for a whole series of new definitions, the more important of which are discussed below.

Stability Categories

Craft examined in accordance with the Standard will be assigned to one of six Stability Categories. Four of these relate to limiting environmental conditions, using limits which correspond to those for the Design Categories referred to in the EU Directive. The remaining two are used to classify those which fail to meet any of the first four categories. In brief, these Stability Categories are currently defined as:-

I - significant waveheight up to 8m, calculation wind speed 25m/s

II - significant waveheight up to 4m, calculation wind speed 21m/s

III- significant waveheight up to 2m, calculation wind speed 17m/s

IV - significant waveheight up to 0.5m, calcul'n wind speed 13m/s

V - vessels failing to meet Categories I to IV, which are required to be marked as being of limited stability and/or buoyancy properties

VI - vessels of Category V which would sink if swamped (as opposed to holed)

In defining these Categories, it is quite deliberate that no reference is made to geographical limits, for example distance from coast or refuge. Environmental conditions are the rational parameters for determining the suitability of a vessel in terms of stability and buoyancy. Geographical limits take no account of variations in conditions, whether daily or seasonal. Furthermore, applied on a worldwide basis where climatic conditions can vary enormously, fixed geographical limits do not allow for local conditions creating particular hazards. Half a mile off land in the Pentland Firth in summer, can be much more dangerous than fifty miles from land in the Pacific in winter.

If it ever became necessary, seasonal geographical limits could be set in relation to specific Stability Categories by the National Administration concerned, taking account of such local factors. But since it would be extremely difficult to police them effectively, it is expected that such limits would be advisory rather than mandatory.

Sailing/Non-Sailing

Although it may appear superfluous to have to define this, it should be remembered that there is a distinct group of craft which use sail for auxiliary propulsion, but which rely heavily on their engine, and another group which use sail purely for steadying what is essentially a power driven vessel.

Currently,

sailing vessels]		[	$As/Vd^{2/3} > 10$
motor sailing vessels]	are those where	[	$10 > As/Vd^{2/3} > 4$
non-sailing vessels]		[	$As/Vd^{2/3} < 4$

As = sail area, Vd = loaded displacement volume, in similar units

Recesses

"Recess" is the term used for any volume which may retain water, even temporarily, after a swamping event. Thus it includes cockpits, wells, and areas surrounded by bulwarks without sufficient freeing arrangements. A "Recess of Limited Volume" is a recess judged to be of a sufficiently limited volume in relation to the reserve buoyancy, that the effect of swamping is not considered to be hazardous. The size of such a Recess varies with the Stability Category, the volume of the watertight hull above the waterline, and whether or not the Recess is self-draining in accordance with ISO 11812 - Cockpits and Cockpit Drainage.

Downflooding Height

This expression is used to identify the minimum height of the lowest downflooding opening above the waterline, when the vessel is at the Loaded Displacement. The term "freeboard" is not used in the Standard on account of its usual association with the height of the main deck. This latter definition is used in the

Scantlings Standard, but is not meaningful in relation to stability and buoyancy. Since it is a more familiar term and for the convenience of readers, this paper uses the word "freeboard" to describe Downflooding Height.

Draught of Canoe Body

Unlike conventional ships, the draught of small craft is not always easy to define in a consistent manner, due to the variety of hullforms and appendages that abound. Some care has therefore been taken to adopt a particular methodology in this respect, so as to obtain a consistent estimation of the maximum draught of the main part of the hull(s).

Displacement

Two displacements are used in the Standard: Loaded Displacement, and Minimum Sailing Condition. Both are defined in detail. Most conventional ships have least margin of stability at maximum displacement, but in stark contrast, sailing vessels are usually most vulnerable at their lightest operational displacement.

Crew Limit

This term is used to describe the maximum number of people of 75kg mass which can be carried by the vessel, consistent with the requirements for the Stability Category under consideration. Therefore the Crew Limit may be different for different Stability Categories.

It is interesting to note that more than one fifth of the text of the Standard is devoted to Definitions!

6 NON-SAILING CRAFT.

These requirements are set out in Part 1 of the Standard. No distinction is made between mechanical and human powered craft, and motorsailers are required to be assessed under BOTH Part 1 and Part 2. The application of Part 1 is shown schematically in Figure 1.

Three methods of assessment are proposed:-

Method A

This method sets out requirements for small craft that are considered to be vulnerable to relatively frequent swamping. These comprise minimum "freeboard" and swamped stability and flotation standards, based to a large extent on existing Nordic and USA methods. The aim is to provide a basic minimum "freeboard" against over-frequent swamping, together with sufficient flotation to ensure that the vessel can adequately support the Crew Limit load, and have sufficient stability in the swamped condition for people to re-board after being in the water.

All vessels NOT being assessed under Method A, MUST meet downflooding requirements, which consider the reserve of Downflooding Angle above the angle of heel resulting when all the people on board are crowded to one side. The required margin increases with higher Stability Categories. Failure to meet this results in either being assessed under Method A, or being assigned to Categories V or VI.

Method B

Vessels which are fully decked and have Recesses of Limited Volume (ie: can cope adequately with a swamping event) do not have to meet a "freeboard" requirement, and only have to meet the additional requirements for resistance to wind and waves, as discussed below.

Method C

Vessels which meet the Downflooding Angle requirements, but which nevertheless have Recesses of a size which would mean that swamping would render the vessel vulnerable to foundering, are required to meet minimum "freeboard" requirements. These are similar in form but about 40% greater than the freeboard requirements under Method A. The required "freeboard" is a function of the volume of reserve buoyancy of the hull above the load waterline compared to the loaded displacement, with maximum and minimum limits for each Category. Experience has shown that light boats with good reserve buoyancy in relation to displacement need less "freeboard" than vessels which are relatively heavy and therefore tend to plough through waves rather than ride over them.

Additional Requirements

Craft being assessed by either Methods B or C must consider additional requirements for resistance to wind and sea.

Vessels aspiring to Stability Categories I and II are considered using a simplified and modified version of a weather criterion after the style of Sarchin and Goldberg [Reference 2]. The main modifications are that the wind gradient effect is ignored, and also that the wind heeling lever expression does NOT assume that the lever becomes zero at 90° heel.

Craft intended for Stability Categories III and IV are assessed for wind heeling only, with a maximum permitted angle of heel reducing with increasing Length of Hull, or half the minimum Downflooding Angle. Small craft with a low profile are not required to be assessed in this way.

For vessels with a maximum length Froude Number exceeding 0.82, a test to detect any loss of stability with increasing speed is included.

7 SAILING CRAFT.

These requirements are set out in Part 2 of the Standard, and the application is shown schematically in Figure 2.

Sailing vessels are classified into one of three types, depending on whether they are expected to avoid capsize or how they are designed to recover from such an event. Making these distinctions in rational, rather than prescriptive, terms has been quite challenging. These three types of sailing craft are assessed using Methods D, E and F.

Method D

Some craft can be expected to capsize relatively frequently no matter how skillfully they are sailed - eg: racing type dinghies. The vital factors with such vessels are that the crew are in fact able to right the boat without external assistance and that whilst swamped, minimum standards of flotation and stability are met. Thus to use this method, it must first be demonstrated that the crew can in fact right the boat, and the MINIMUM weight of crew necessary must also be established. In this unusual case insufficient crew weight may make the vessel less safe.

Method E

Seagoing monohull sailing vessels are normally designed to recover from a 90° knockdown without assistance, and to have a range of positive stability such that in the rare event of a complete inversion due to a large breaking wave, the probability of remaining inverted for an appreciable period of time is acceptably low. Since this type of seagoing sailing vessel is the most numerous, there is a tremendous body of information on its stability properties. Much investigation work was conducted after the infamous 1979 Fastnet Race, in which hurricane conditions were experienced by a fleet of 303 yachts, resulting in 15 deaths, the abandoning of 24 vessels, and the total loss of 5 vessels. References 3 to 8 represent a modest selection of the recently available knowledge in this area.

Criteria in this area are still being developed. It is currently envisaged that they will include:

- a minimum Angle of Vanishing Stability
- a minimum righting lever at 90° heel
- a minimum Dynamic Stability Factor

Alternative provision is made for vessels which have a history of safe operation in less exposed conditions ie: those which have sufficient stiffness to stand up to their sailplan, but which would founder if knocked down to 90°. This method is only available for Categories III and IV.

The Dynamic Stability Factor is a development of the SSS system of the Royal Ocean Racing Club and the STOPS system of the Royal Yachting Association. It comprises a number of elements multiplied together, which between them take account of the following parameters:

- length
- displacement length ratio
- beam displacement ratio
- sail area in relation to beam, displacement and length
- self-righting capability
- roll moment of inertia
- downflooding angle
- potential for loss of stability at high speeds

Method F

A number of types of sailing vessels which are unable to meet the requirements of Method E have nevertheless demonstrated a capability of making open sea passages with very adequate safety. These vessels all rely on hullform for their stability and are quite unable to recover from a 90° knockdown. Such vessels include catamarans, trimarans, and shoal draught barge-like monohulls.

The most important factor which renders such vessels adequately safe is that the user is provided with information to enable a sailplan appropriate to the wind strength to be used. The main requirement for such vessels is therefore that proper information on the maximum advised wind speed for each combination of sails is provided for the user, and that the wind speed at which the normal working sailplan should be reefed is placarded at the main control position. The method of calculating these wind speeds assumes that a gust of 50% higher than the mean wind speed will not quite cause the angle of maximum righting moment to be attained. This methodology is already widely used by multihull designers.

It is also considered important that such vessels should not sink if they are inadvertently capsized.

Other requirements are being developed to address the dynamic stability properties of these craft. One approach being considered is to classify them according to the heeling energy available under the righting moment curve. Other work is being conducted to develop a method of assessing the risk of pitchpoling (caused by too high a rig in relation to the pitch stiffness) and of cartwheeling (a combined yaw-pitch-roll capsize about the lee bow). Very little prior work exists in this area, but it is clear that it would be unsafe to consider only roll stability, since this could lead to craft which are extremely vulnerable in pitch.

It is intended that any vessel failing to meet Method E can alternatively be assessed under Method F.

8 VALIDATION.

In developing a totally new and comprehensive Standard for the stability of all kinds of small craft, it is obviously important that as much evidence as possible can be accumulated and that the requirements correlate sensibly with practical experience. All participating countries have been urged to use the Standard on a trial basis during its development. However, this is considered to be insufficient in itself.

In the UK a project has been set up, jointly funded by the Department of Trade and Industry and the British Marine Industries Federation (BMIF), to formally examine 20 non-sailing and 30 sailing boats, and to compare the results of assessment according to the Standard with the independent opinions of the designer, builder, and experienced assessors. This project employs boats from BMIF member companies, and naval architecture students from a number of academic and educational establishments to perform the experiments and calculations. This programme also has the following objectives:-

- to determine what changes to the draft Standard may be required
- to verify that the experimental and numerical methods employed are workable and produce adequately accurate results
- to compare the results obtained from permitted alternative methods in order to verify the adequacy of approximations
- to demonstrate that the text is readily and consistently comprehensible
- to gather data to assist in developing and verifying simple screening formulae

A suitable draft text for non-sailing boats was available for validation to commence in October 1993, and it is hoped that the comparable work on sailing vessels will begin in October 1994. The vessels being studied encompass the entire spectrum of craft covered by the Standard, from RNLI and ship's lifeboats to small dinghies and canal craft.

Another project is underway in the Netherlands, specifically examining whether the draft Standard would have been effective in indicating the vulnerability of known stability casualties.

It is hoped that further formal projects aimed at verifying the Standard will be established in other countries in the near future.

9 DIFFICULTIES EXPERIENCED.

As might be expected in tackling such an ambitious task, a number of difficulties have been experienced.

The most obvious difficulty is the very wide diversity of craft encompassed, some of which are illustrated in Figure 3.

Every attempt has been made to write the Standard in a way which does not leave gaps between different mainstream boat types, and also to write the requirements in such a way that they reflect the physical parameters that are important in each instance, rather than simply identify craft that do not conform to the currently accepted "norm".

Stability and buoyancy are relatively complex subjects to analyse with accuracy. Bearing in mind that the small craft construction industry often uses professional yacht designers rather than trained naval architects, methods considered routine by some appear impossibly complex to others. Many successful and respected yacht designers are not formally qualified in naval architecture and the analysis procedures normal in ship design. For this reason, the need to simplify this complex subject to an acceptable degree, whilst retaining maximum realism and flexibility has presented a real challenge.

Differences of background knowledge and experience can create problems in communication, especially when many participants in the Working Group do not have English as their native language. However, if these problems can be overcome, the resulting Standard benefits from this diversity. Everyone has different strengths and weaknesses in their knowledge, and by working as a team the best is hopefully obtained from each. It is interesting to note that some of the most useful contributions have been made by people not formally qualified in naval architecture.

The development of this Standard has taken nearly four years, and is not yet complete. In that time, representation of some countries has changed a number of times, for reasons connected with other pressing commitments. This lack of continuity of representation has led to a need for "re-education" of new appointees, in order to bring them "up to speed" with the detailed reasoning of the Working Group. However, in most cases, the delay caused by this has been offset by the fresh insight and experience which has been contributed.

10 SUMMARY.

The work of developing a comprehensive Standard for the intact stability and buoyancy of all forms of small craft is well advanced. Work to confirm that the draft text is appropriate and produces consistent results is being undertaken, and this will also yield information helping to simplify the application of the Standard to a large number of boats.

The author would like to see the scope extended to include the following, but funding is unlikely to permit this in the immediate future:-

- damaged stability and flotation
- towing and lifting loads
- effects of towing and using fishing gear

11 ACKNOWLEDGEMENTS.

The author would like to acknowledge the support and assistance of the following people and organisations, all of whom have played a vital role in the development of this draft Standard:-

- all members of ISO/TC188 Working Group 22 (see Appendix), for all their input, commitment and enthusiasm
- the British Marine Industries Federation, especially Tom Nighy, Technical Manager, for financial support, direction and encouragement
- the UK Department of Trade and Industry, for financial support
- the International Confederation of Marine Industries Associations (ICOMIA), especially Tim Donkin, Secretary General
- the British Standards Institution, especially Ron Spiers and Peter Gunns, successive secretaries to GME/33 Small Craft Committee
- the Secretariat of ISO/TC188, Johan Richert and Pia Sundin of SMS in Sweden
- all those students, staff and boatowners participating in the validation projects

Nevertheless, the opinions expressed in this paper are those of the author, for which he alone is responsible.

12 REFERENCES.

1. European Union, the Council, document 10699/1/93 Rev 1: Common Position of the Council of 16 December 1993 on the Proposal for a Directive .... relating to Recreational Craft.
2. Stability and Buoyancy Criteria for US Naval Surface Ships, T.H.Sarchin and L.L.Goldberg, SNAME, 1962.
3. 1979 Fastnet Race Enquiry Report, RYA and RORC, UK, 1979.
4. Safety from Capsizing - Interim and Final Reports, USYRU and SNAME, 1983 and 1985.
5. Seaworthiness - the Forgotten Factor, C.A.Marchaj, Adlard Coles Ltd, UK, 1986.
6. New England Sailing Yacht Symposium, 1988; USYRU, SNAME, USCG Academy, Eastern Connecticut Yacht Racing Association; New London, Connecticut, USA.
7. The Development of Stability Standards for UK Sailing Vessels, B.Deakin, RINA Spring Meetings, April 1990.
8. The Seaworthy Cruising Yacht, RINA Seminar, London, November 1991.

APPENDIX - MEMBERS OF ISO/TC188/WG22.

Names given in brackets are those who participate by correspondence only, or who have retired from representation.

Andrew G. Blyth,	Convener, UK
(Michael Kenyon),	BIN/Nautibell, Belgium
(Alexandre Trinas de Freitas),	ABNT/CB-07, Brasil
Dr Norm Vanstone,	CMMA, Canada
(Bent Andersen),	Denmark
David Taft,	Sea Ray Boats, Eire
(Roger Giles),	Sea Ray Boats, Eire
Gunnar Holm,	VTT, Finland
Gregoire Dolto,	Groupe GRAAL, France
Denis Bury,	Bureau Veritas, France
Andre Kobus,	Jeanneau S.A., France
Fritz Hartz,	I.C.O.M.I.A., Germany
Fabrizio di Luggo,	UCINA, Italy
Kensuke Sakamoto,	Japan Marine Standards Assoc.,
Ichiro Ogoh,	Japan Marine Standards Assoc.,
Koichi Fujiwara,	Japan Craft Inspection Organis'n
Dr Peter van Oossanen,	HISWA, Netherlands
Eivind Amble,	Amble & Stokke A/S, Norway
Luis Correia Lopes,	SPN, Portugal
Anders Wissler,	Sjofartsverket, Sweden
Rolf Eliasson,	RE Yacht Design AB, Sweden
(Yuri D. Zhukov),	Ukrainian Maritime University,
Ken Kershaw,	Royal Yachting Association, UK
John Moon,	Head of Falmouth Marine School, formerly Tech Manager, RORC, UK
Richard Woods,	Woods Designs (catamarans), UK
David W. Ralph,	Marine Safety Agency, UK
Lars Granholm,	Cert. & Standards, NMMA, USA
(David D. Beach),	SNAME Small Craft Group, USA
(Bill Cleary),	formerly USCG, USA
Richard Rounsevelle,	Recreational Boating, USCG
(Don Kerlin),	formerly USCG
(Donald Blount),	naval architect, USA
(Dudley Dawson),	Hatteras Yts/Dawson Marine, USA
Robert K. Johnson,	Island Packet Yachts, USA
Jack Riggleman,	NMMA, USA
Ralph Lambrecht,	NMMA, ABYC, USA

FIGURE 1

★ NON SAILING VESSEL REQUIREMENTS - SCHEMATIC FLOW CHART

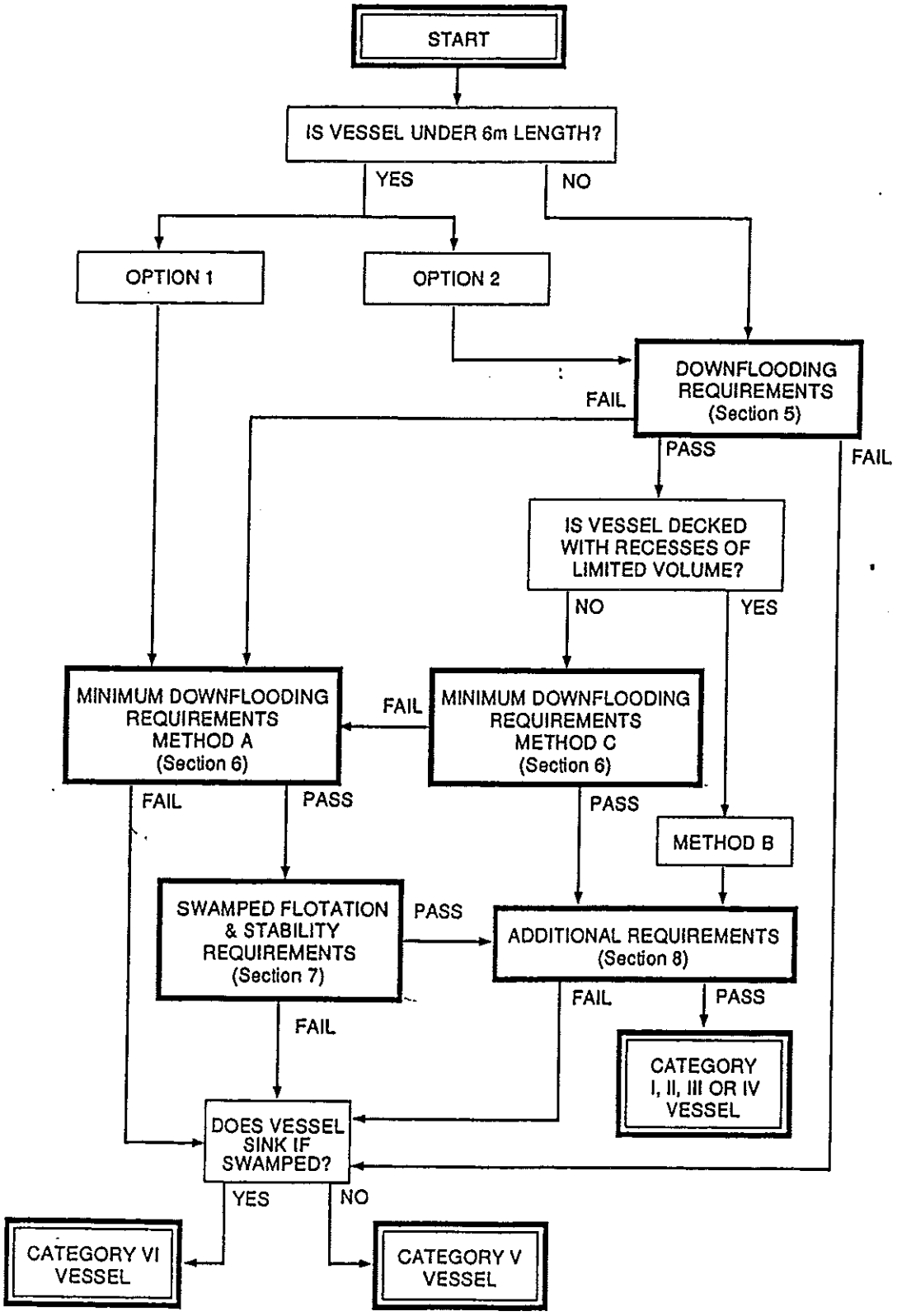

FIGURE 2

★ SAILING VESSEL REQUIREMENTS - SCHEMATIC FLOW CHART

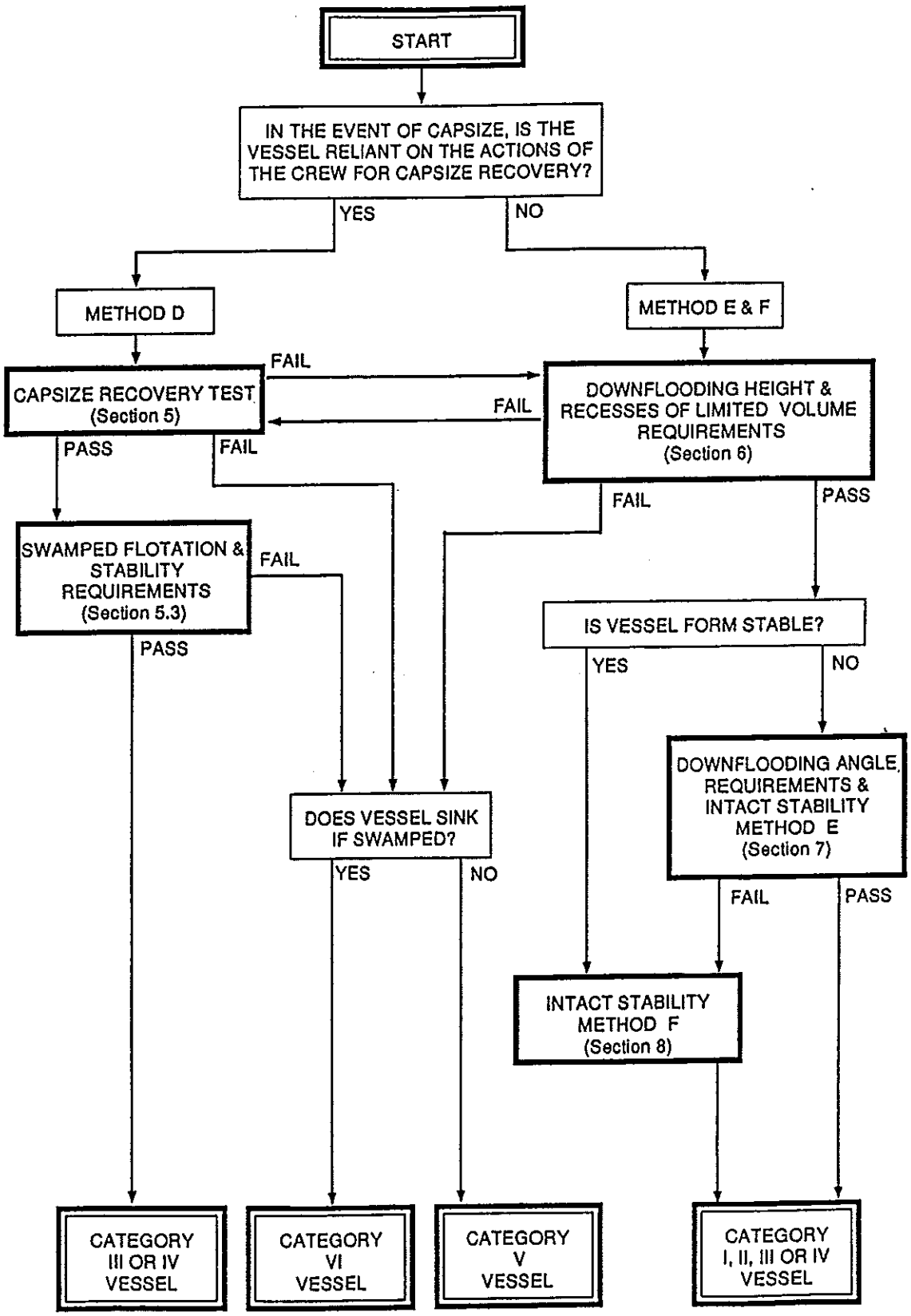

FIGURE 3

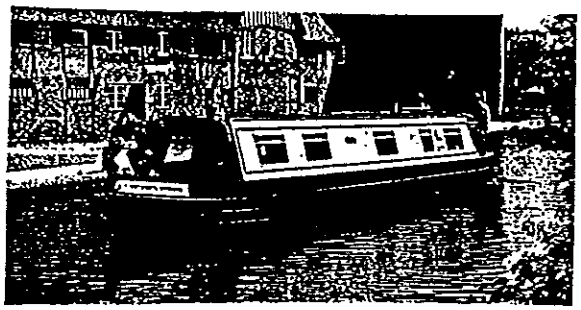

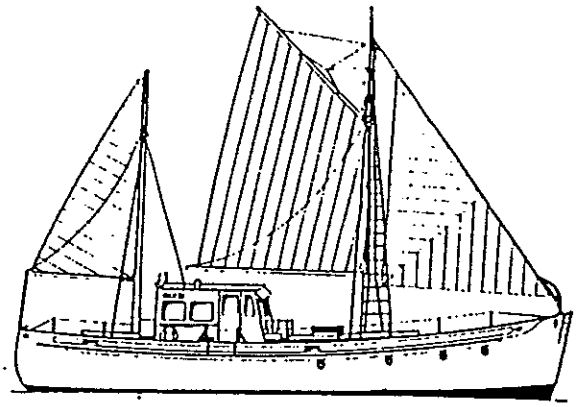

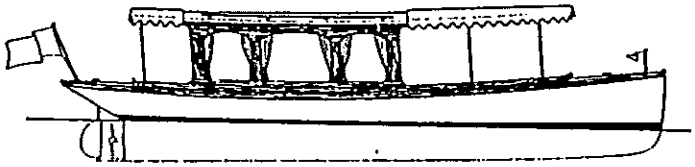

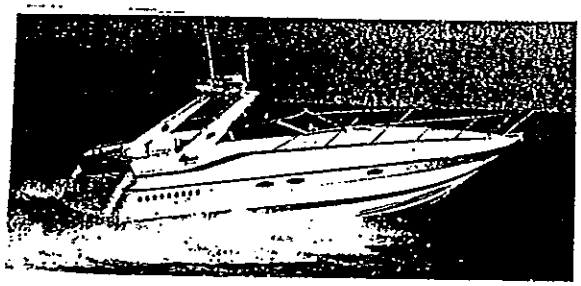

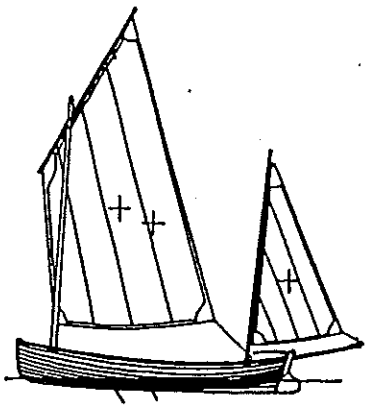

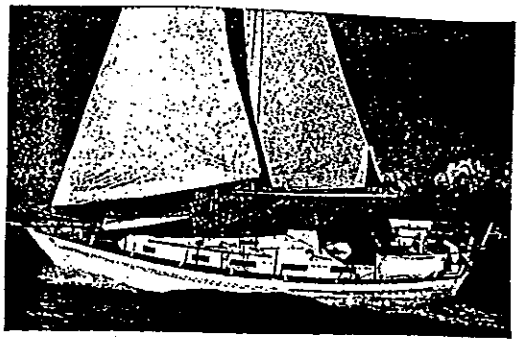

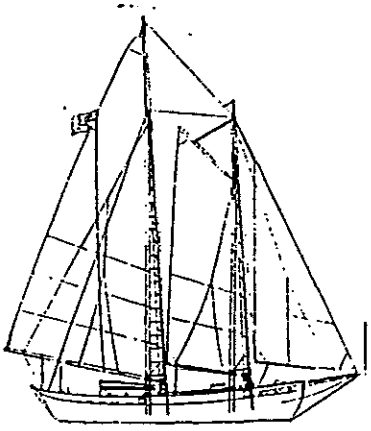

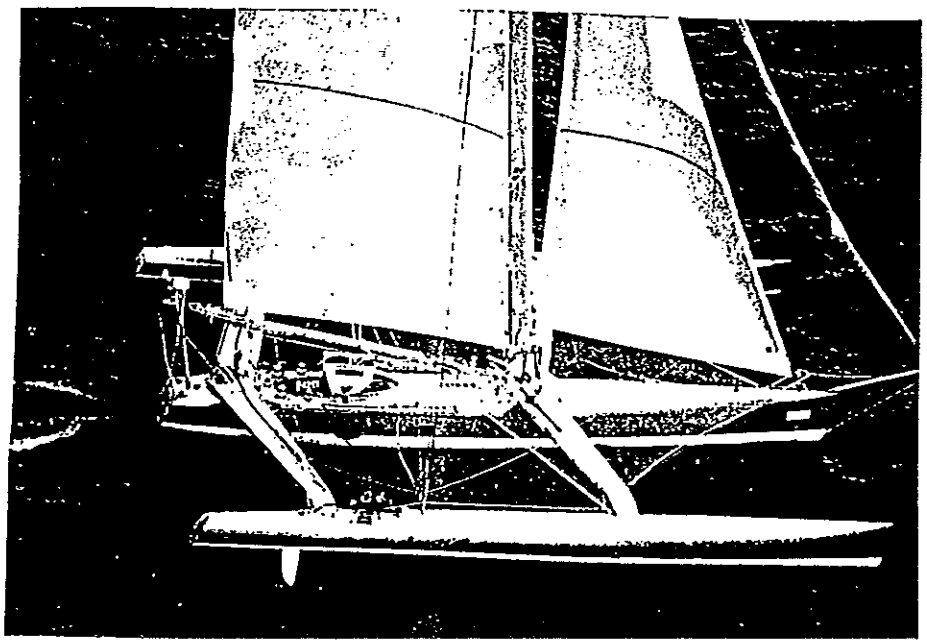

INTACT SHIP SURVIVABILITY IN EXTREME WAVES: NEW CRITERIA FROM A RESEARCH AND NAVY PERSPECTIVE

J.O. de Kat[1], R. Brouwer[2], K.A. McTaggart[3], W.L. Thomas[4]

ABSTRACT

This paper describes a joint navy research project on dynamic stability of intact ships. The main objective is the development of stability criteria that reflect the dynamic influence of waves on the safety against capsizing of intact frigates. A sound understanding of the physics involved and a practical ship motion simulation tool are essential elements in the approach taken. The first part of this paper provides an overview of the project approach and results, comprising a framework for developing dynamic stability criteria, physical aspects of waves and capsizing, and practical design and operational guidelines for frigates. The new guidelines apply in particular to astern sea conditions, which are typically not covered by existing criteria; this can have an important bearing on modern hull forms.

From a navy application perspective, the following issues related to dynamic stability are addressed in the second part of this paper: (1) implementation of operational guidelines aboard navy ships, (2) the role of probabilistic methods related to capsizing of intact ships, and (3) evaluation of new design concepts in operational and extreme conditions.

1. INTRODUCTION

Ships satisfying standard stability criteria can be considered safe with respect to capsizing, but little is known about their actual margin of safety. This applies especially to modern hull forms that have a significantly different hull shape, especially the aftbody with a notably wide transom, when compared with traditional hulls. Naval ships comply with stability criteria set by the individual navies. These criteria are in principle similar to (and typically more stringent than) the IMO criteria for intact ships, and they are typically based on calm water stability characteristics.

None of the presently used criteria represent the actual capsize behavior in waves. Furthermore, current stability criteria were developed decades ago, when ships from the '40s and '50s era provided the physical and statistical reference material. Consequently, these criteria will not necessarily result in the same level of safety for modern hull forms as for conventional ships. The commonly used Sarchin and Goldberg intact criteria, for example, are for a large part based on the capsizing of destroyers during World War II (in Pacific beam seas and wind). Reasons for considering a revision of stability criteria include:

- existing criteria do not reflect the dynamic behavior in waves
- existing criteria may not guarantee the same level of safety for modern hull forms as for conventional type ships
- existing criteria may be overly conservative

The first two items are a concern of an immediate nature, while the third is more difficult to quantify. Also, damaged stability requirements tend to govern stability related design parameters - at least for naval ships.

Besides the formal stability criteria, little or no written guidance exists on avoiding dangerous situations in heavy weather. For example, no information is available to operators as to what speed can be maintained in severe following seas without jeopardizing the ship. For normal operating conditions such information may not be relevant, but in critical, extreme situations practical information on safe ship handling will be useful.

In 1990, a 4-year joint effort was launched by five navies (from Australia, Canada, the Netherlands, United Kingdom and United States) and MARIN to investigate wave-induced capsizing of intact frigates. One of the final objectives of this Cooperative Research Navies Dynamic Stability project was to arrive at criteria that reflect the dynamic ship behavior in extreme wave conditions, while making extensive use of numerical simulations. To achieve these goals, activities focused on the following

[1] Maritime Research Institute Netherlands
[2] Royal Netherlands Navy
[3] Defence Research Establishment Atlantic, Canada
[4] David Taylor Model Basin, Carderock Division

framework:

- validation and updating of ship motion simulator
- modelling of wave climate
- capsize modes and mechanisms
- evaluation of existing stability criteria
- development of stability design guidelines
- development of operational guidelines
- capsize risk analysis

An essential part of the project is to develop a sound understanding of the physics involved with extreme ship motions. This comprises both extreme motion characteristics and the environment, in particular properties of extreme, irregular waves. Use is made of numerical simulations and data from physical model tests and (where possible) from full scale observations. Important properties of irregular seaways include limiting significant wave height as a function of peak period, joint distributions of wavelength and wave steepness, and encountered wave group properties. With the help of the simulation model and available model test data, a large range of potential capsize modes have been identified. The majority of capsize modes may occur for an intact frigate travelling in following to stern quartering seas, where the risk of capsizing increases with increasing speed. The combination of irregular waves in stern quartering conditions and high ship speed may unexpectedly present a critical situation within a short time period.

In essence the procedure for deriving design guidelines consists of performing a standard set of simulations with an extensive series of systematically varied hull forms. The aim is to quantify the effect of critical hull form parameters and loading condition on the extreme roll motion behavior. A so-called capsize index is derived from these simulations as a measure of the propensity to capsizing of a given vessel. Based on physical insights and simulations, operational guidance can be provided in a format suitable for on-board use. Practical guidelines have been developed for frigates of around 4,000 tonnes displacement. De Kat (1993) presents an interim overview of the above work.

An important conclusion is that the dynamic behavior of a ship in moderate to extreme waves is influenced to a large extent by its calm water stability characteristics. These are, however, not the same as those used in present stability criteria. The new guidelines highlight critical stability parameters. Application of the guidelines to modern hull forms should result in designs that are at least as safe as traditional vessels, which form the basis of present intact stability criteria.

The first part of this paper presents an overview of the above work and focuses on some of the most important findings (Section 2, 3 and 4):

- physics of capsizing (wave characteristics, simulator, capsize modes)
- new stability guidelines for the design and operation of intact frigates

The second part of the paper discusses from a navy perspective several applications related to dynamic stability (Sections 5, 6 and 7):

- operational guidelines
- role and application of capsize risk analysis
- evaluation of new design concepts

2. PHYSICS OF CAPSIZING

2.1. General

When modelling extreme sea states, it is necessary to have some information on limiting significant wave height and peak period, as well as associated spectral shape. As extreme roll motions or capsizing are particularly sensitive to wavelength and steepness, the joint distributions of relevant wave parameters are of interest. In the simulations, linear superposition is used to model long-crested irregular waves, thereby neglecting for example crest nonlinearities. Little is known about the range of applicability of the Gaussian wave model in relation to capsizing. Furthermore, wave characteristics encountered by a ship in astern i.e., following or stern quartering sea conditions can undergo significant changes by wave grouping effects.

The simulation tool (FREDYN) forms an essential part in understanding capsize physics. Throughout the project, the program was checked against model test results and the underlying physics were subjected to continuous examination. Theoretical improvements and programming changes were made where appropriate. The program is foremost a practical engineering tool, which runs quickly on a PC; this is a prerequisite in the present derivation methodology for design guidelines, the development of which requires an extensive number of simulations.

With knowledge of the critical environmental parameters and the availability of a suitable simulation tool, the next step is the investigation of the capsize process. This consists of the identification of potential capsize modes through simulations in regular and irregular waves. Where possible, use is made of available model test information. In the analysis of critical capsize conditions it is important to account for the irregular and random character of a seaway, and to determine to what extent the behavior in that seaway can be related to the behavior in equivalent regular waves.

This Section highlights some of the topics described above. More details on relevant wave characteristics and capsize modes in irregular waves are presented by De Kat (1994).

2.2. Extreme wave characteristics

Characteristic steepness

A sea state can be characterized roughly by a few spectral parameters: significant wave height, characteristic period and spectral shape; directional spreading of energy and crossing wave systems can occur, but these are not considered here, i.e., waves are assumed to long-crested. Depending on ocean area and season, there is a certain amount of statistical scatter between significant wave height and zero-crossing period. Ocean wave measurements suggest that the characteristic steepness of a seaway, s_{char}, defined as the ratio of significant wave height to wavelength associated with the spectral peak period, T_p, is bounded as follows (Le Méhauté and Hanes, 1990):

$$0.02 < \frac{H_s}{\lambda_p} < 0.05 \qquad (1)$$

Therefore, the maximum steepness is typically less than 0.05, and the steepest possible sea state occurs when the significant wave height in deep water is

$$H_{s,max} = 0.05 \frac{g T_p^2}{2\pi} \qquad (2)$$

The above maximum wave height is in agreement with the survivability envelope for storm waves with periods less than 15 s proposed by Buckley (1992). In an absolute sense, the highest H_s measured in the Northern Hemisphere is around 17 m, associated with a peak period of 18 s.

Spectral shape

For fully developed seas, the Bretschneider spectrum is traditionally used, and is the same as the JONSWAP formulation with a peak parameter γ equal to 1. Recent analysis of extreme North Sea wind seas suggests that JONSWAP spectra with γ = 1.9 apply (Torsethaugen, 1993), while Buckley (1992) suggests γ = 1.3 based on NOAA buoy data for extreme sea states with peak periods exceeding 13 s.

Steepness distribution of individual waves

Physical observations and simulations suggest that capsizing is sensitive to both wave height and steepness. Under certain conditions, encountered wave group properties also can be important. Statistical joint distributions of individual wave height and period for a given sea state are typically not part of ship performance assessment. Dahle and Myrhaug (1993) and Dahle *et al.* (1988) do consider the joint distributions of crest steepness and wave period in capsize risk analysis of small fishing vessels, for which wave breaking in beam seas is cited as the most likely cause for capsizing.

For larger intact ships, astern sea conditions tend to be the most onerous from the viewpoint of capsizing. The analysis of related capsize mechanisms suggests that the onset of capsizing will be governed by the wave as a whole (crest-to-trough height and spatial length), rather than by the individual crest properties. Individual crest properties are sensitive to wave steepening effects and tend to have a more nonlinear character than overall wave height properties.

Part of the present stability project is to compare full scale wave measurements with both model basin data and numerical simulations. Typical wave data consist of measurements made at one location; analysis based on such data is referred to as "temporal" analysis. A ship will be sensitive also to the *spatial* wave steepness. As temporal and spatial properties may differ rather significantly from each other (especially when the observer is moving with the waves), both aspects are considered in the statistical analysis of waves.

To illustrate some results, Figs. 1 and 2 show the joint distribution of temporal wave steepness and wavelength for the following sea state: H_s = 14.5 m, T_p = 14.7 s, JONSWAP with γ = 2, s_{char} = 0.043. Fig. 1 stems from MARIN model test data at scale 1 to 50 (basin dimensions: 200 x 4 x 3.7 m), Fig. 2 is based on simulations using the Gaussian model,

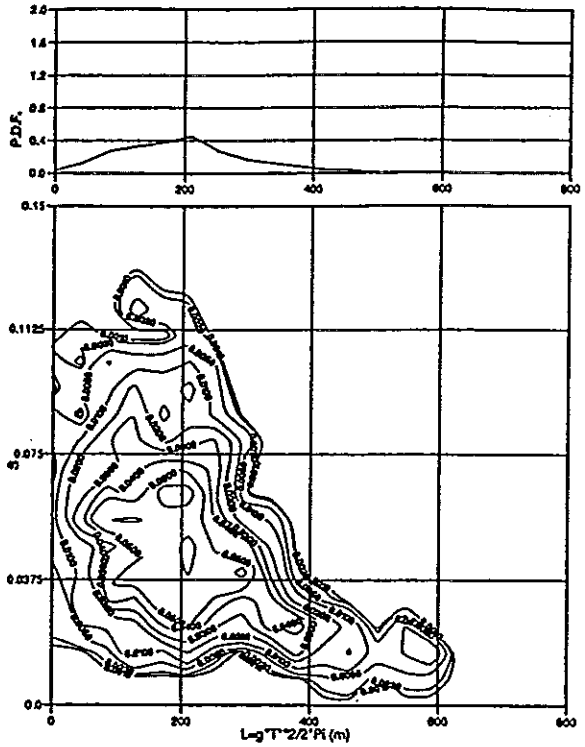

Fig. 1. Joint pdf of wavelength and steepness (model test, H_s = 14.5 m, T_p = 14.7 s). Upper graph represents the marginal pdf for wavelength.

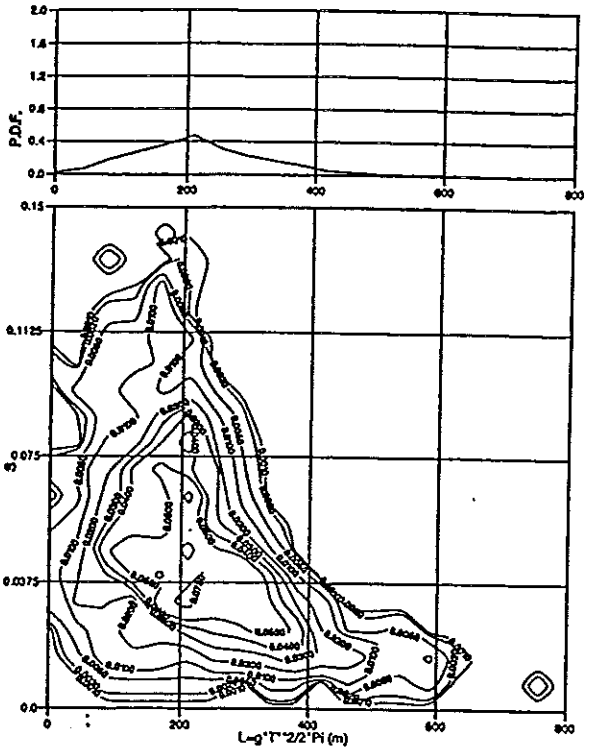

Fig. 2. Joint pdf of wavelength and steepness (simulation with Gaussian random wave model, H_s = 14.5 m, T_p = 14.7 s). Upper graph represents the marginal pdf for wavelength.

which uses linear superposition of sinusoids with random phases; both figures are derived from 3-hour duration data. The definition of individual wave steepness follows that of Myrhaug and Kjeldsen (1987), which is based on zero down-crossing analysis:

$$s = \frac{H}{\lambda} \tag{3}$$

where H is the crest-to-trough height and λ is the associated wavelength based on the zero-crossing period T_z:

$$\lambda = \frac{g T_z^2}{2\pi} \tag{4}$$

Even for this rather steep sea state, the linear simulation model predicts the same trends in wave steepness distribution as the model test; the discrepancies are larger when considering crest steepness, for example. De Kat (1994) discusses joint distributions in more detail, including some comparisons between temporal and spatial wave analysis.

Knowing the joint probability would enable one to determine the probability of occurrence of waves having a critical wavelength and steepness as a function of significant wave height and peak period:

$$P[(\lambda_{min} \le \lambda \le \lambda_{max}) \cap (s \ge s_{crit}) \mid H_s, T_p] = \int_{\lambda_{min}}^{\lambda_{max}} \int_{s_{crit}}^{s_{max}} p(\lambda, s)\, ds\, d\lambda \tag{5}$$

If this conditional probability is determined for a number of sea states, it can subsequently be used to estimate the probability of capsizing in a given operating area with known statistical distributions of H_s and T_p. A significant amount of information is available on theoretical and measured joint distributions for wave height and period, see for example Srokosz and Challenor (1987) and Tayfun (1993). Rather than using theoretical distributions, Sobey (1992) advocates the use of long-duration simulations employing the linear Gaussian model for the sea surface to derive joint distributions.

Myrhaug and Kjeldsen (1987) derived fitted joint distributions of crest steepness and wave height based on Weibull parameters.

We could argue that when extreme ship motion behavior is more sensitive to overall wave steepness than to individual crest steepness, linear random wave theory may be acceptable for simulating extreme ship motions even in relatively steep random seas. This hypothesis may not apply to hull girder loads, slamming, or green water effects on deck, which tend to be more sensitive to local wave characteristics. Local crest properties are critical when considering airgap or ringing effects of offshore platforms.

The critical influence of group speed in astern seas
As mentioned previously, astern (following and quartering) seas tend to be most critical with respect to capsizing of large ships. The perceived characteristics of the irregular seaway change drastically for such headings with forward speed; the effect on the encounter spectrum is discussed by Oakley *et al.* (1974) and De Kat (1990), among others. For a range of speeds the encounter spectrum collapses, i.e., it becomes very narrow-banded and average wave group lengths increase; the same applies to ship excitation forces and response. The effect of forward speed on measured encounter spectra of wave elevation and roll moment excitation in following seas is discussed by De Kat (1993). These measurements indicate that in irregular following seas the total wave excitation forces follow the same trend as the encountered wave characteristics at one location: the roll excitation moment becomes more narrow banded for a range of speeds. Furthermore, the roll excitation can be of a very regular nature and significant amplitude during the passage of a wave group, despite the inherent spatial wave irregularities; De Kat (1994) analyses this aspect in more detail. Tikka and Paulling (1990) discuss the influence of forward speed on encountered wave group properties and the effect on capsizing.

When a ship is subjected to narrow-banded, large amplitude roll excitation moments for extended time periods related to the length of the encountered wave groups, dynamic loss of transverse stability or parametric (low cycle) resonance, for example, could be the result. The group speed is defined as

$$C_{g,p} = \frac{g}{2\omega_p} = \frac{g\,T_p}{4\pi} \qquad (6)$$

which is the speed at which the main energy of the seaway travels. For ship speeds in the neighborhood of the group speed, substantial roll excitation of extended duration can occur (De Kat, 1994), which is of operational importance (see also Section 5).

2.3. Numerical model for extreme ship motions

In the present investigations, use is made of extended, nonlinear strip theory embodied in the computer program FREDYN. This program is used as an engineering tool, and is not computationally intensive. Time domain simulations can be carried out for a steered ship in regular or long-crested irregular waves, and with or without wind. In essence, the approach consists of superimposing all physically relevant force contributions in the equations of motion, schematically shown in Table 1.

INERTIA FORCE	=	*FROUDE-KRYLOV*
	+	*WAVE DIFFRACTION*
	+	*WAVE RADIATION*
	+	*VISCOUS*
	+	*HULL RESISTANCE*
	+	*PROPELLER*
	+	*RUDDER*
	+	*WIND*

Table 1. Force contributions in FREDYN

Because of the nature of the problem, the motions are solved in the time domain for six degrees of freedom. The Froude-Krylov forces are evaluated up to the instantaneous free surface at each time instant and include hydrostatic effects. Linear theory is used in the time domain to estimate the diffraction and radiation contributions, where a correction is made to the convolution integrals to account for large amplitude motions. Viscous effects comprise roll damping due to hull and bilge keels, wave-induced drag due to orbital velocities, and calm water maneuvring forces. Viscous drag due to cross flow velocities is estimated empirically; here we use local, section-dependent drag coefficients derived from segmented model test results. Propeller and rudder interaction are also modeled, including the effect of orbital velocities.

An autopilot or human navigator keeps the ship on course; alternatively, specific maneuvres such as a zig-zag test can be simulated. The model is in principle applicable to any type of ship; only the part related to the linear and nonlinear maneuvering forces in FREDYN has been adjusted specifically for frigate-type ships.

The advantage of this partially heuristic technique is the ease of adding physical phenomena to the model and the ease of computations. A major disadvantage is the lack of knowledge and control concerning the errors involved. The only way to instill confidence in this approach is to validate the method with a variety of model test results and full scale data. The present numerical model has been validated extensively by means of captive and free running model tests, as well as some full scale measurements. The model tests with various ship types comprised a large range of moderate and severe waves, including capsize conditions. Besides frigates, tests and simulations were also carried out with containership models to study parametric rolling.

2.4. Capsizing of intact ships in waves

Identification of capsize modes
Based on the analysis of (few) full scale accounts, model tests, and numerical simulations, two main categories of wave-induced capsizes are distinguished:

- *single* capsize modes in astern to beam seas
- *combined* capsize modes

In principle, capsizing can occur at heading angles other than astern to beam seas. Parametric resonance in head seas has for instance been observed experimentally as a cause of capsizing. The risk of such events occurring is, however, viewed as too small for practical concern. A single capsize mode is applicable when one particular phenomenon is clearly the cause of the capsize. An example is the pure loss of stability mode, where the (quasistatic) loss of transverse restoring moment is the sole reason for the capsize event. In many cases, capsizing cannot be attributed to one phenomenon only, but is often the result of a sequence of different events.

The "conventional" wave-induced capsize modes observed for large vessels in astern wave conditions comprise: pure loss of stability, low cycle resonance (due to parametric excitation), and broaching due to successive waves. These modes were first classified as such by Oakley et al. (1974) and simulated by De Kat and Paulling (1989). Loss of transverse stability is based on hydrostatic considerations in following waves and is not characterized by any particular motions. The last two items are distinct physical (motion) phenomena that may or may not lead to capsizing. Other modes of broaching can occur at higher ship speeds. Another capsize mode, classified as "period bifurcation", has been observed experimentally by Kan et al. (1990) for a containership model in stern quartering sea conditions.

Although waves from astern are generally regarded as most critical, capsizing in beam seas can also occur because of (1) steep, breaking waves, resulting in transverse impact loads and/or piling of green water on the side of the deck, (2) synchronized roll resonance, or (3) conditions resulting in an excessive wave-induced roll moment. It should be noted that capsizing due to resonance in beam seas has been studied in many instances to test theoretical models, but most ships will not capsize in such conditions. Small ships, such as fishing trawlers, are known to have capsized in steep beam sea conditions.

Water on deck and bulwark submergence can have a significant influence on capsizing, both in astern and beam seas. These effects can occur in conjunction with the modes discussed above; experimental and theoretical observations are presented by Grochowalski (1993).

So far, little attention has been paid to capsize modes that result from a sequence of conditions, where several distinct phenomena can finally lead to capsizing. For example, a vessel in stern quartering seas may first surfride, then broach and roll heavily, followed by deck submergence and loss of stability in the wave crest after getting back on course. Also, a ship may yaw violently, inducing large roll motions, followed by dynamic loss of stability. Invariably, a ship will in the end capsize in the absence of sufficient restoring moment, which may be quasi static (loss of righting arm) or dynamic (loss of restoring energy). Before capsize occurs, the ship should be viewed as a complete six degrees of freedom object with some steering mechanism. A summary of potential wave-induced capsize modes is given in Table 2.

SINGLE CAPSIZE MODES

Astern seas
- Pure loss of transverse stability
- Parametric excitation
- Broaching (in order of increasing ship speed with respect to wave phase speed)
  - Successive overtaking waves
  - Surfriding and bow trim/submergence
  - Surfriding on front slope of a long and steep wave
  - Bow plunging
  - Coupled pitch, roll and yaw instability

Beam seas
- Steep, breaking waves
- Resonant beam waves
- Excessive wave-induced roll moment

COMBINED CAPSIZE MODES

Astern seas
- Surfriding and loss of static stability
- Broaching and loss of stability
- Surging, yawing and rolling with loss of dynamic stability ("dynamic rolling")
- Water on deck and deck edge submergence effects combined with other modes

Table 2. Potential capsize modes

Broaching and capsizing in irregular waves

At first sight, the capsize behavior in simulated random seas is very different from that in regular waves. Numerous simulations have been carried out in random waves to study the capsize mechanisms. The analysis consists of identifying capsize modes and the conditions leading to capsizing, the determination of the influence of the random nature of waves and to what extent these random events can be related to more deterministic capsize behavior in regular waves. The problem of predicting the probability of the occurrence of critical waves is explored. A few modes of capsizing are shown below.

To investigate extreme motions and capsize occurrences of a ship in irregular waves, a certain sea state is selected. For a given loading condition (with low initial GM), calm water speed and heading angle, simulations are carried out in many realizations of the selected sea state: 25 runs of 20 min. full scale duration were performed with randomly selected seeds. This process is repeated for various Froude numbers: Fn = 0.2, 0.3, 0.4 at a critical heading angle. Analysis of the runs where capsizing occurs suggests that the mode of capsize depends strongly on the ship speed. For the case considered,, at a 15 degree heading angle for example, Fn = 0.4 always results in broaching and capsizing associated with surfriding, while Fn = 0.3 typically results in loss of stability in the wave crest. At the low Froude numbers hardly any capsize events were recorded.

For each capsize case, the time-dependent spatial wave conditions immediately prior to capsize were examined. The onset of capsizing was found to occur in a critical range of wavelengths above a certain associated wave steepness. For a ship with a length L = 125 m, surfriding and broaching at Fn = 0.4 occurred with the encountered wavelength between 1L to 2.5L and the spatial wave steepness H/λ exceeds 0.06; four different modes of broaching have been observed for one state and heading angle. As an example, the time series of a broach are shown in Fig. 3a.

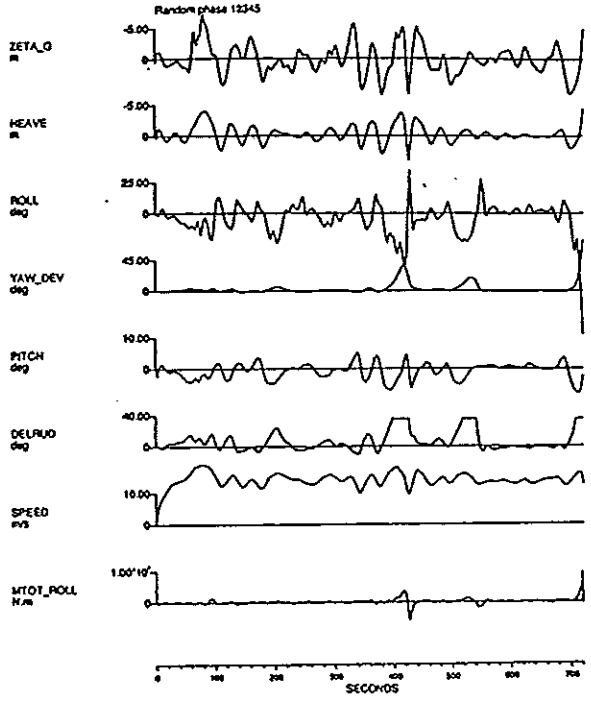

Fig. 3a. Time series of simulated capsize due to broaching (ζ_G is the wave height at the center of gravity). Test conditions: Fn = 0.4, ψ = 15°, GM/B = 0.05, Hs = 12.8 m, Tp = 13.4 s, JONSWAP with γ = 2.

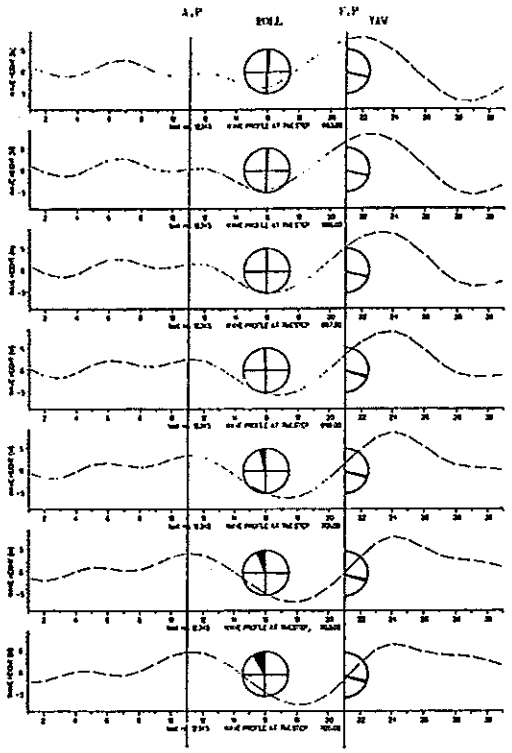

Fig. 3b. Sequence of spatial wave profiles spanning 3 ship lengths (L = 125 m) along direction of wave travel; first profile corresponds to the onset of the broach.

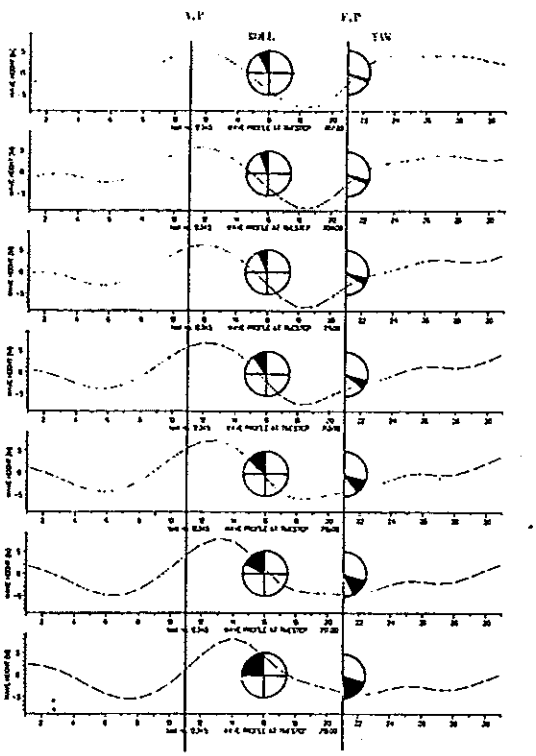

Fig. 3c. Sequence of spatial wave profiles spanning 3 ship lengths (L = 125 m) along direction of wave travel; last profile corresponds to the onset of the broach.

The sequence of the spatial wave profiles as of the onset of the final broach is shown in Figs. 3b and 3c (the profiles are shown over a distance spanning three ship lengths in the direction of wave travel, where position no. 16 corresponds to the location of the center of gravity of the ship at each time instant). Circle at station 16 indicates associated roll angle (clockwise is to starboard); semi circle at station 21 indicates associated course angle w.r.t. waves (clockwise is bow to starboard).

The broach from the above example would be classed as surfriding with bow trim. Here the ship is riding down the front slope of a steep wave with a length of about 1.5L. Gradually, the ship speed increases, yaw increases (ship more broadside to the wave), rudder is hard over; the bow is located in the trough region and in the back slope of the preceding wave, which adds to the broaching moment; the combined hydrodynamic yaw moment and inertia effects cause the final capsize. Other broaching modes are also observed; for example, broaching followed by loss of stability due to a steep trough at the stern.

Capsizing due to loss of stability at Fn = 0.3 is usually preceded by moderate roll motions and can occur suddenly when the encountered wavelength is between 0.8L (with a steepness exceeding 0.07) and 2L (with H/λ exceeding 0.04). Loss of stability in irregular waves can be attributed to several mechanisms: (1) "dynamic rolling" resulting in a capsize with the wave crest amidship, where the crest slowly overtakes the ship resulting in the loss of righting capabilities over an extended period of time, (2) the sudden formation of a steep wave trough at the stern, which for a ship with a wide aft body results in the sudden loss of buoyancy and righting capabilities. An example of loss of stability mode (1) is shown in Figs. 4a, 4b and 4c, where the same convention is used as in Fig. 3. At Fn = 0.2, some capsizes occurred because of dynamic rolling in a critical wave group combined with loss of stability in the wave crest.

Comparison with the behavior in regular waves suggests that if the spatial wave characteristics (height and length) leading to capsize in irregular waves were used to generate a regular wave, the ship would also capsize. By performing the same analysis for different sea states, an assessment can

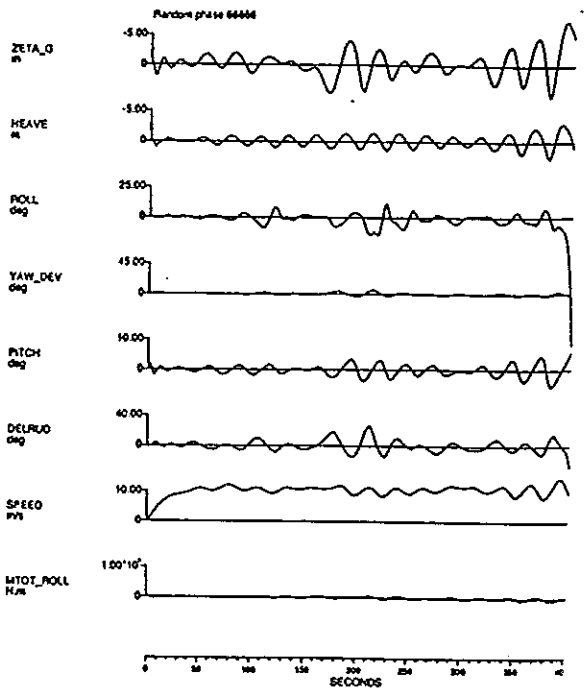

Fig. 4a. Time series of simulated capsize due to dynamic loss of stability in the wave crest (ζ_G is the wave height at the center of gravity, δ_{RUD} denotes rudder angle). Test conditions: Fn = 0.4, ψ = 15°, GM/B = 0.05, Hs = 12.8 m, Tp = 13.4 s, JONSWAP with γ = 2.

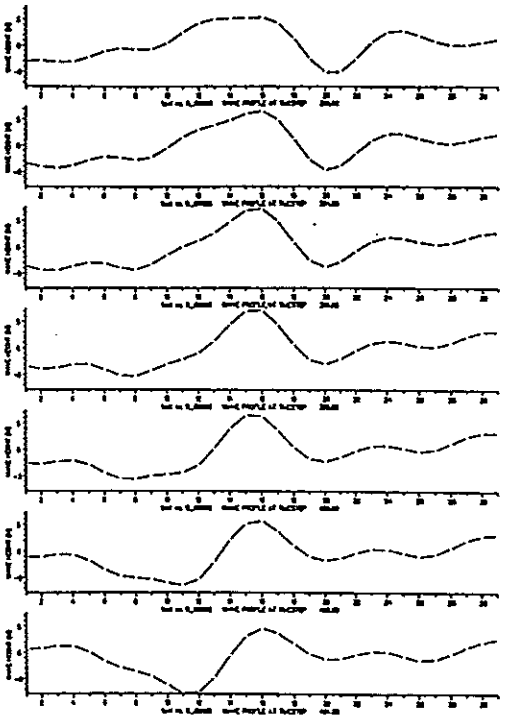

Fig. 4c. Sequence of spatial wave profiles spanning 3 ship lengths (L = 125 m) along direction of wave travel; last profile corresponds to actual capsize.

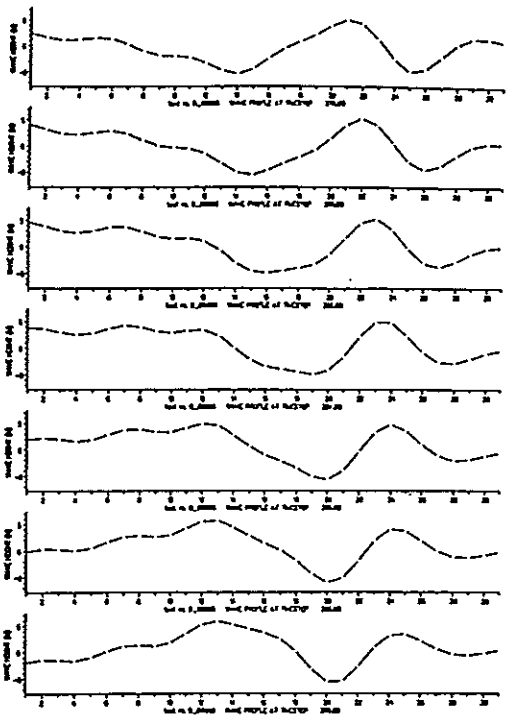

Fig. 4b. Sequence of spatial wave profiles spanning 3 ship lengths (L = 125 m) along direction of wave travel; first profile corresponds to the onset of the capsize.

be made of the critical conditions leading to capsize as a function of speed, heading angle and sea state. Combined with the joint distribution of wavelength and steepness, the probability of encountering critical conditions can be estimated. The suddenness

with which a capsize can occur at high ship speeds (Fn = 0.3 and higher) in astern seas indicates that caution is required when operating in severe sea states.

3. DEVELOPMENT OF NEW DESIGN GUIDELINES

3.1. General

The methodology pursued should result in dynamic stability criteria that can be used in the design stage, enabling one to assess the safety against capsizing as a function of hull and loading characteristics, while accounting for wave climate. Extensive use is made of numerical simulations.

Extreme roll behavior is considered as a function of both hull geometry parameters and stability properties, represented by the righting arm curve in calm water. A brief review of the parametric changes and relevant results is presented. The most

critical parameters are identified and their influence is discussed. This information forms the basis of new criteria aimed at minimizing the risk of wave-induced capsizing of intact ships in severe seas. These criteria should be regarded as supplementary to existing criteria.

In principle, the criteria are intended for intact frigates of around 4,000 tonnes displacement with lengths on the order of 100 to 130 m. Two generic parent hulls provide the starting point in the generation of a database of different hull forms; one hull is of the more traditional type with a cruiser stern, the other represents a modern hull characterized by a wide aft body and transom stern.

3.2. Variation of hull form parameters

To determine the capsize behavior as a function of design parameters, the procedure outlined below is used. Two parent hull forms are subjected to a systematic variation of the following geometric hull form parameters:

- L / B ▸ from 7.9 to 9.5
- B / T ▸ from 2.7 to 3.3
- D / T ▸ from 1.7 to 2.4
- C_B ▸ from 0.45 to 0.53
- C_{VP} ▸ from 0.57 to 0.66
- Aft body flare ▸ from 0 to 15 degrees

where L is the length between perpendiculars; B, T and D are the beam, draft and depth amidships, C_B is the block coefficient, C_{VP} vertical prismatic coefficient (= C_B / C_W), and C_W is the waterplane area coefficient.

Waterplane variations are effected in the aft body only, i.e., variations in the coefficients C_W and C_{VP} stem from changes in the waterlines aft. Flare in the aft body refers to flare extending above the waterline until the weather deck. The parent hulls are modified such that one parameter changes while all other parameters remain constant. For a number of cases, several parameters were changed simultaneously to generate a hull derivative (for example, combined freeboard and C_W variation). The displacement of the hull derivatives is maintained at approximately 4,000 tonnes. In addition to the parent hulls and their derivatives, 10 existing frigate-type ships are added to the database of 30 hull forms to serve as a reference.

All hull forms from the above database are subjected to a standard matrix of environmental and operational conditions, using the simulation program FREDYN. For each hull, the following conditions are varied:

- λ (from 0.75L to 2L)
- V_s (RPM) (Fn from 0.1 to 0.4)
- ψ (from 0 to 90 degrees)
- KG (GM/B from 0.05 to 0.1)

where λ is the wavelength, Fn is Froude number, ψ is the heading angle (0 degrees is following seas). KG represents the vertical location of the center of gravity above the keel, and GM is the initial metacentric height for small angles of heel; for each hull, three or four values of KG are applied. All simulations are performed in regular waves with a total (maximum) duration of 300 s. The wave steepness is the same for all conditions: $H/\lambda = 0.08$, which is considered as an expected maximum steepness. For a given KG, each hull is subjected to between 80 and 100 different simulations. For some critical speed/heading combinations, several initial conditions are used. The maximum roll angle obtained in each simulation is recorded and entered in the matrix of conditions for a particular hull form. The first 50 seconds of the simulation are skipped in the analysis to avoid the influence of possible transient effects.

Capsize index

To characterize the motion behavior in a nondimensional fashion, an extreme roll response index is defined. The capsize index represents a measure of the capsize risk in a given set of extreme conditions, and for a given hull form and loading condition it is defined using the above matrix of conditions as

$$CI = \frac{\text{no. of capsizes}}{\text{total no. of simulations}} \times 100\% \qquad (7)$$

Design parameters

To determine whether the complex motion response characteristics in extreme conditions can be related directly to practical design variables, a number of parameters are investigated. To describe the properties of a ship, two categories of hull form parameters are distinguished:

- 1) *Geometric* hull form parameters as described above
- 2) *Stability* parameters determined by hull shape and loading condition, for example:

- KG / D
- KG / B
- GM / B
- KG / T
- DST : dynamic stability (area underneath righting arm curve in calm water)
- RPS : the range of positive stability, limited by the angle of vanishing stability

Parameters belonging to category (1) are independent, while those in category (2) are dependent.

3.3. Determination of critical design parameters

Analysis of the simulation results obtained for all ships suggests that the possibility of capsizing in waves is governed by loading condition and calm water stability characteristics. Design parameters are labelled critical when they show a clear and consistent relationship with the capsize indices found for all hull forms considered in this study. The following parameters are found to have the most critical and consistent influence on extreme motion and capsizing behavior of frigates:

- KG / D
- total dynamic stability, DST_{TOT}
- dynamic stability beyond 40 degrees, DST_{40+}
- dynamic stability between 30 and 40 degrees, $DST_{30\text{-}40}$
- range of positive stability, RPS

Fig. 5 provides a schematic definition of the above parameters. Some hull parameters show strong correlation, as is the case for the ratio KG/D and total dynamic stability, shown in Fig. 6. Figs. 7, 8 and 9 show the capsize index as a function of the critical parameters KG/D, DST_{TOT} and RPS, respectively.

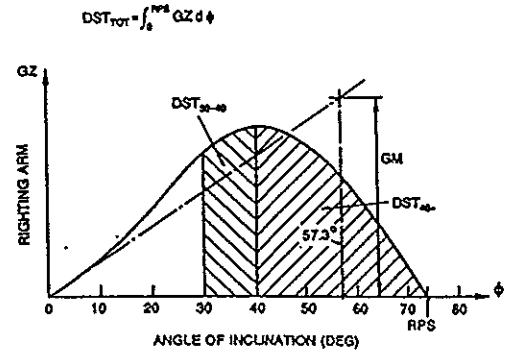

Fig. 5. Definition of critical stability parameters for design guidelines.

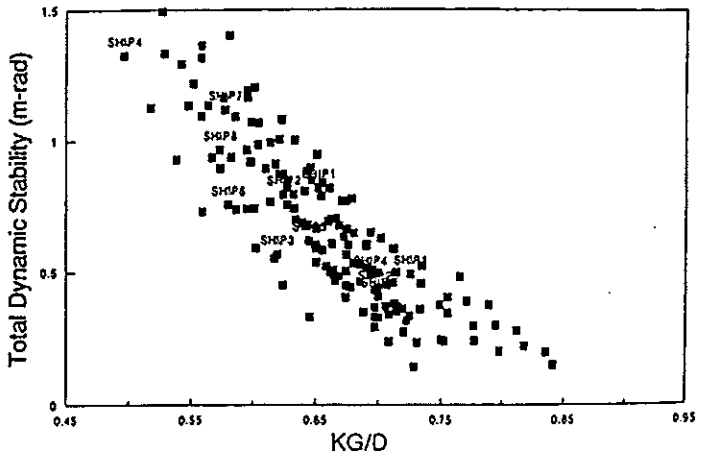

Fig. 6. Relationship between ratio KG/D and total dynamic stability.

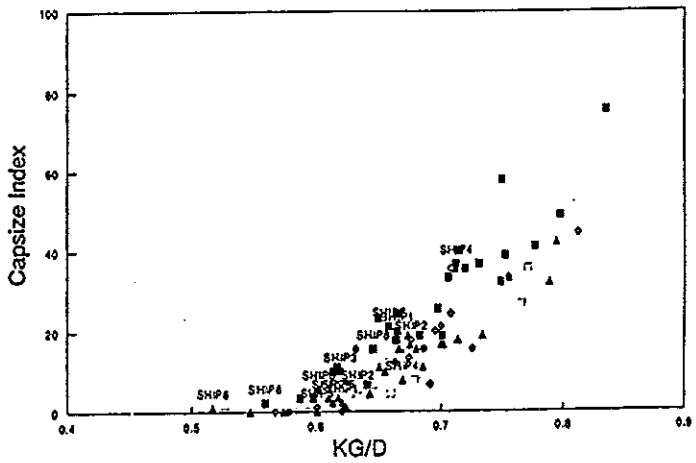

Fig. 7. Capsize Index for frigates as a function of KG/D ratio.

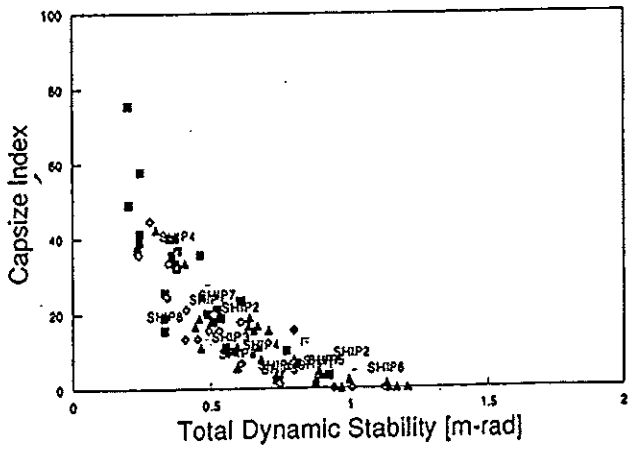

Fig. 8. Capsize Index for frigates as a function of total dynamic stability.

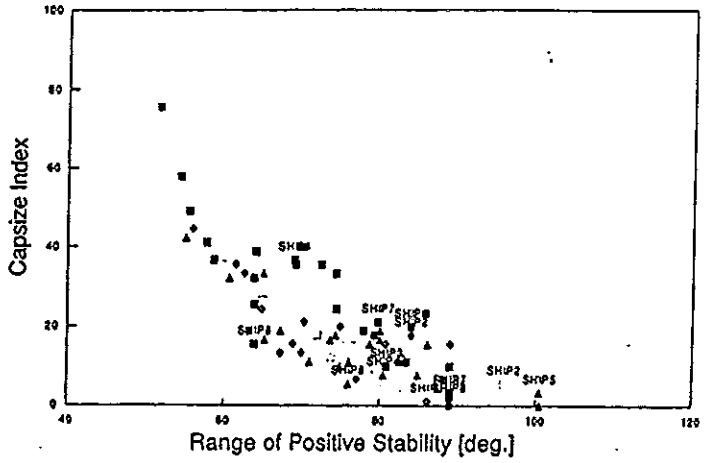

Fig. 9. Capsize Index for frigates as a function of range of positive stability (angle of vanishing stability).

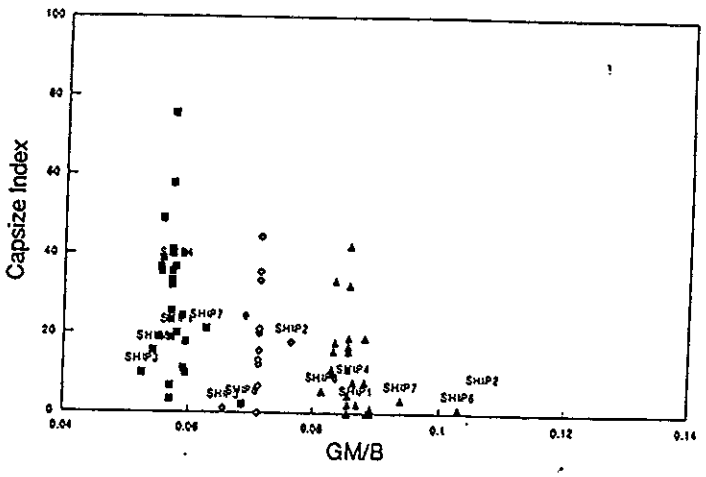

Fig. 10. Capsize Index for frigates as a function of ratio GM/B.

In the capsize index plots, each number refers to a hull derivative. The above critical parameters form the basis of the new design guidelines. Parameters having a more diffuse effect on capsizing include GM/B, KG/B, KG/T, and DST_{40} (dynamic stability up to 40 degrees of heel). As an example, Fig. 10 shows the capsize index as a function of GM/B, which suggests that a high value of GM alone does not necessarily result in a safe ship, and conversely, some ships with a relatively low GM could be quite safe.

An important conclusion is that wave-induced capsizing will be affected to a large extent by the calm water stability properties. From this we could infer that, fortunately, the traditional intact stability criteria indeed do provide a reasonable measure against capsizing in waves. However, most of the calm water properties identified in those criteria differ from those listed above, as the findings from the present project suggest that especially the stability properties *at large angles* are important. In contrast, present stability criteria consider righting arm properties typically up to angles of 40 or 50 degrees.

3.4. Influence of hull form on capsizing

For frigates, the following hull geometry parameters have an important influence on extreme roll behavior:

- B / T
- C_W and C_{VP}
- Aft body flare
- D / T

The influence of the block coefficient, C_B, is found to be less important but still significant, while the ratio L/B does not affect the capsize index significantly (at constant GM). It appears that ships allowing the highest possible KG at a comparable level of safety against capsizing are those with the following features:

- wide beam and corresponding high position of the metacentre, KM. This may compensate for low freeboard; however, such hull forms would have to be operated at a high value of GM
- considerable flare in the aft body; small flare angles have little effect
- low block coefficient and large reserve buoyancy
- ample freeboard

Frigates with a wide aft body and transom tend to have a higher capsize index than conventional ships with a narrow aft body, all other conditions (GM, for example) being equal. Some modern hull forms are characterized by wide aft bodies and have relatively high waterplane coefficients; this does not imply modern hull forms are less safe, as they typically will have more than sufficient intact calm water stability in conjunction with ample freeboard and possibly aftbody flare.

The vertical prismatic coefficient is also an

important parameter. If GM is kept constant, a higher vertical prismatic coefficient (and lower waterplane coefficient) tend to result in a lower capsize index. One should bear in mind that, given a sufficient amount of dynamic stability for example, a modern hull form with a wide aftbody and high C_W will typically have a higher "carrying capacity" than a conventional hull, i.e., for a given draft the KG for the modern hull can be higher than for a conventional hull. Ships with a high value of B/T tend to show a higher capsize index than ships with a low B/T at constant GM. Concerning freeboard, below a critical value of D/T the safety against capsizing deteriorates quickly.

In physical terms of stability, a wide aft body has a number of consequences:

- high initial GM
- while its contribution to transverse stability in calm water is relatively large, in the event of a steep wave trough located aft (due to e.g. wave crest amidships in steep following seas with wavelengths between 1L and 2L), the righting arm may undergo a significant reduction with possible loss of static stability; a sufficiently low KG or aft body flare sufficient will prevent too much loss of stability.
- during the passage of a steep overtaking wave, the waterplane area and shape aft can vary significantly, which may result in large stability (righting arm) fluctuations, which may result in dynamic roll excitation; a sufficiently low KG or aft body flare sufficient will result in relatively small stability fluctuations.
- combined roll and yaw excitation in stern quartering seas: a wide aft body can contribute to a large (wave-induced Froude-Krylov) roll exciting moment toward the lee side when the crest reaches the stern, at the same time a large volume aft will result in a large (Froude-Krylov) transverse force and yaw moment tending to yaw the ship broadside to the wave; sufficient rudder area will increase controllability and caution is required when operating in severe astern seas at high speed.

3.5. Capsize safety level of existing ships

It is of interest to determine if a relationship exists between current stability criteria and the capsize index. To this end, a number of existing frigate-type ships were evaluated using the same approach as for all ships in the database described in Section 2. For the selected existing ships, the minimum allowable metacentric height, GM_{crit}, was determined, i.e., the minimum value of GM, or maximum KG, for which the existing criteria are just satisfied. The weather criterion according to Sarchin and Goldberg (1962) was used for this purpose; the windage area and wind lever arms were assumed to be the same for all ships. By subjecting these ships with "marginal" loading condition to the standard set of environmental and operational conditions, through simulations the associated capsize indices were determined.

Table 3 lists values of GM_{crit} and the corresponding capsize index, denoted as CI_{crit}. Furthermore, for some ships the estimated GM in normal operating conditions (GM_{serv}) and the corresponding value of CI (CI_{serv}) are shown. The in-service results suggest that $CI_{serv} = 5$ is a typical safety level. The current regulations seem to result in a maximum value of CI_{crit} between 15 and 25.

	Sarchin & Goldberg criteria		Operating values (estimate)	
	GM_{crit}	CI_{crit}	GM_{serv}	CI_{serv}
SHIP1	1.00 m	17.8		
SHIP2	0.38 m	19.1		
SHIP3	0.67 m	18.0	~ 0.90 m	~5
SHIP4	0.87 m	16.0	~ 1.10 m	~5
SHIP5	0.86 m	17.5		
SHIP6	0.93 m	22.9	~ 1.30 m	~8
SHIP7	0.91 m	8.96		
SHIP8	0.72 m	9.20		
SHIP9	0.77 m	24.2		

Table 3. Critical values of GM and CI

The KG value that would be required to obtain an acceptable capsize safety level of CI = 5 has been estimated for all existing ships and hull derivatives. This value is referred to as KG_{CI5}. The ratio KG_{CI5}/KG_{crit} indicates the difference between the maximum allowable KG required to attain a given safety level and that according to the Sarchin and Goldberg criteria (associated with GM_{crit} from above). The KG ratio is equal to or less than 1.0 for all hull forms considered. For the majority of ships, this ratio lies around 0.95, which suggests that to attain a safety level of CI = 5, the maximum allowable KG could be approximately 5% lower than is required by the Sarchin and Goldberg criteria. The largest required reductions in KG to obtain CI = 5 with respect to current stability requirements apply to ships with a low value of C_{VP}

and to hull forms with little freeboard, i.e., ships with ratio D / T less than 2.0.

It can be concluded that for most ships the maximum allowable KG according to present Sarchin and Goldberg criteria results in a safety level that lies close to a capsize index of CI = 5, which seems acceptable. Some hull forms with a wide aft body, however, would possess a somewhat lower safety level, i.e., CI > 5, when marginally complying with the Sarchin and Goldberg criteria. Therefore, new guidelines should ensure an adequate level of safety against capsizing, especially for modern hull forms.

3.6. Proposed design guidelines for frigates

The information presented above is used in the development of guidelines for intact stability. These guidelines are based on the premise that new ships should be at least as safe as existing vessels. In other words, the capsize index should not be greater than 5 in the design service condition, and in no other loading condition should the capsize index exceed 25 (the level dictated by the weather criterion of Sarchin and Goldberg). When other values of CI are deemed necessary, the requirements will have to change correspondingly.

In view of the foregoing, the new guidelines should reflect hull form by incorporating a dependence on C_{VP}. It is proposed to define criteria with respect to the range of positive stability, total dynamic stability, and the dynamic stability between 30 and 40 degrees of heel. The combination of these three quantities is sufficient for obtaining dynamic stability against capsizing in waves, i.e., it is not necessary to include critical parameters such as KG/D and DST_{40+} in the criteria.

The proposed guidelines are illustrated in Figs. 11, 12 and 13 for additional verification. These plots show the capsize indices involving all hull derivatives and existing ships; each derivative is represented by a number, while existing ships are denoted by "SHIP1", "SHIP2", etc. A distinction is made here between regions where the conditions result in a CI value of 5 or less, conditions with CI values between 5 and 20, and conditions with a CI value higher than 20. These areas are labelled respectively as 'OK for design', 'Marginal' and 'Not allowed'. The design service condition should be in the first range, and any off-design condition should be in the second range, possibly with restrictions on sailing speed.

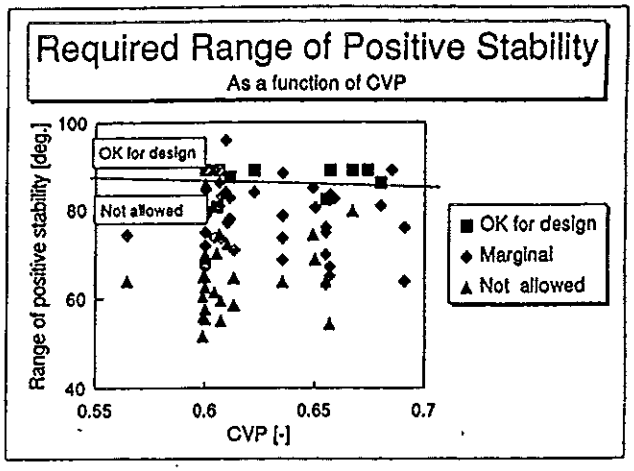

Fig. 11. Required range of positive stability (proposed design guidelines).

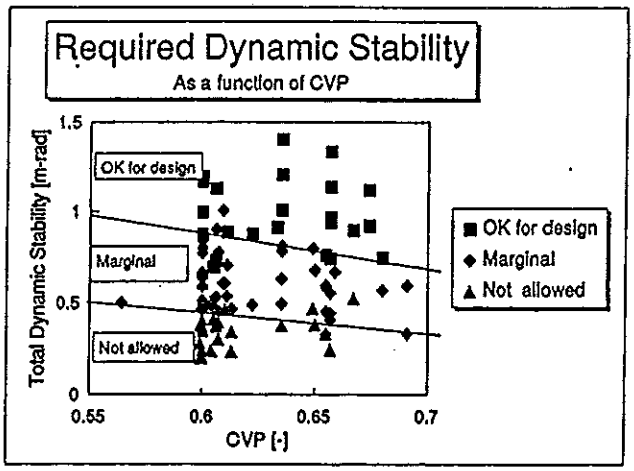

Fig. 12. Required total dynamic stability (proposed design guidelines).

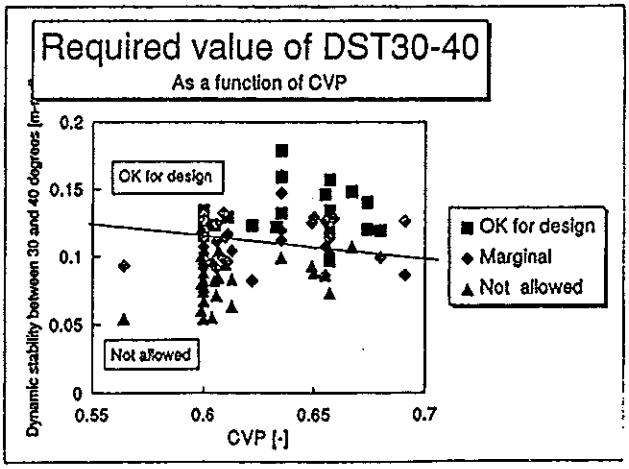

Fig. 13. Required dynamic stability between 30 and 40 degrees of heel (proposed design guidelines).

Conditions in the third range should be avoided under all circumstances.

Note
The guidelines formulated here do not replace, but supplement the criteria currently in use: they should be used for additional verification. They apply to frigates with a displacement in the range of 3,000 to 5,000 tonnes. New ships should still satisfy current stability criteria. It is important to note also that the new guidelines have been validated in a limited fashion only and are still under review. Therefore, the guidelines must be subjected to close scrutiny and future validation.

Range of positive stability
Fig. 11 shows the combinations of vertical prismatic coefficient and range of positive stability that are acceptable. The RPS required for a capsize index value of 5 is invariably about 90 degrees and does not depend on C_{VP}. It is advised to make RPS as large as possible, even beyond 90 degrees if feasible.

A positive stability righting lever at a heeling angle of 90 degrees is not an absolute guarantee against capsizing. Hull forms with a large freeboard (D/T = 2.4) may be vulnerable to capsizing even when the range of positive stability exceeds 90 degrees. In other words, a large freeboard will contribute to a low capsize index, but only when the initial stability (GM) is sufficient. The minimum range of positive stability for any hull form to give a capsize index less than 5 is 75 degrees. In the form of a criterion, the following formulation is proposed:

Criterion 1: The righting lever in calm water must remain positive up to an angle of at least 90 degrees.

Total dynamic stability
Fig. 12 shows the combinations of vertical prismatic coefficient and total dynamic stability that are acceptable. There is a definite minimum acceptable value for the total dynamic stability: no hull form has satisfactory values of CI when the total dynamic stability is less than 0.6 m-rad. Above that value, hull forms with a high vertical prismatic coefficient might possess sufficient safety against capsizing. For ships with a low C_{VP}, i.e., a full waterline in the aft body, the total dynamic stability may need to exceed to 1.00 m-rad. The following criterion is proposed.

Criterion 2: The area under the righting lever curve in the design condition must be at least as given in Table 4. For intermediate values of C_{VP} the required area under the curve must be obtained using linear interpolation.

	C_{VP} = 0.55	C_{VP} = 0.70
Required DST_{tot} in design condition, unlimited operation	1.00 m-rad	0.67 m-rad
Required DST_{tot} in any condition. Allowable sailing speed must be specified in operations manual.	0.50 m-rad	0.33 m-rad

Table 4. Required total dynamic stability

Dynamic stability between 30 and 40 degrees of heel.
The dynamic stability between 30 and 40 degrees represents a measure of the stability in both operational conditions (less than 30 degrees of roll amplitude) and extreme conditions where the roll angle can exceed 40 degrees. Fig. 13 shows the combinations of vertical prismatic coefficient and dynamic stability between 30 and 40 degrees that are acceptable; it shows the distribution of the cases

where CI is less than 5 and the cases where CI is greater than 20. There is a clear distinction between these areas, which leads to the following criterion.

Criterion 3: The dynamic stability between 30 and 40 degrees of heel should be at least as given in Table 5. For intermediate values of C_{VP} the required area under the curve must be obtained from linear interpolation.

When a triangular shape is assumed for the righting lever curve between 0 and 30 degrees, and a constant value of GZ between 30 and 40 degrees of heel, the corresponding value of GM would be 1.42 m for a ship with C_{VP} = 0.55 and 1.10 m for a ship with C_{VP} = 0.70. Due to the typical spring stiffening effect (added stability) for heel angles between 0 and 30 degrees, the required GM for a specific design will normally be less than these values.

	C_{VP} = 0.55	C_{VP} = 0.70
Required $DST_{30\text{-}40}$ in design condition, unlimited operation	0.13 m-rad	0.10 m-rad

Table 5. Required dynamic stability between 30 and 40 degrees of heel

4. DEVELOPMENT OF OPERATIONAL GUIDELINES FOR INTACT FRIGATES

When operating in severe sea conditions, it may be useful to a ship operator to know what speed can be maintained safely at a given course. Each ship, having its own specific hull form, size and loading characteristics, will feature its own extreme motion behavior. This makes it difficult to arrive at simple, generally applicable guidelines that would safeguard an arbitrary ship against any of its potential capsize modes. Nevertheless, it is possible to produce some general guidelines that would at least indicate the possibility of the occurrence of dangerous situations. For ships that satisfy the applicable stability criteria, additional guidance for ship handling in heavy weather can be provided through:

- polar plots
- surfriding avoidance indication
- indication of critical speed range for narrow-band wave energy concentration
- indication of minimum allowable speed for maneuvering in wind and waves

4.1. Polar survivability plots

To provide operational guidance aimed at avoiding capsize conditions, polar plots can be generated for a given ship and loading condition. The roll angle is considered as the critical criterion for stability performance. Although such plots could be generated for a range of loading conditions, a conservative approach would be to base them on the most critical loading condition for a selected draft. To generate a polar plot for a specific ship, systematic simulations are carried out in waves of varying length and steepness. Figs. 14 and 15 show some sample polar plots based on simulations in regular waves, where hatched areas indicate the exceedance of a specified roll angle. Polar plots based on irregular sea states are treated in the next Section.

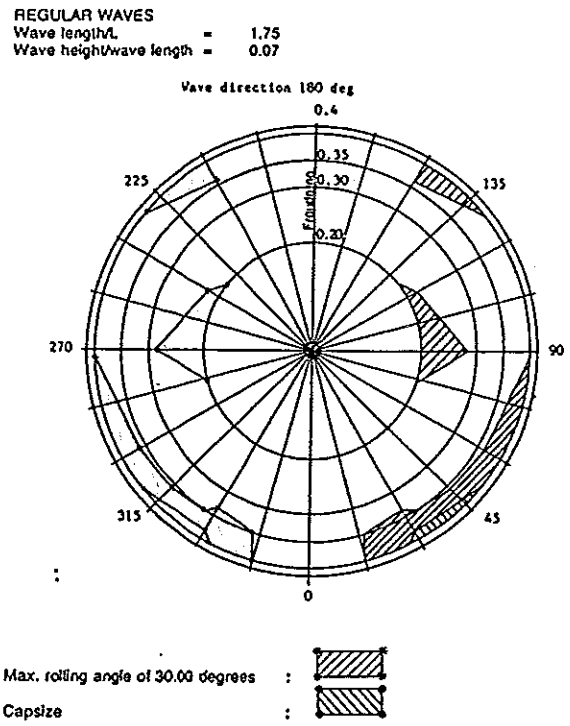

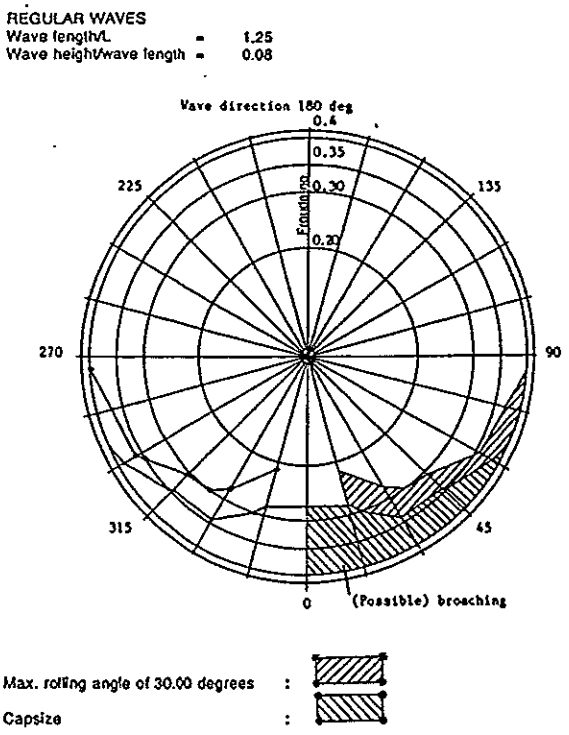

Figs. 14. and 15. Polar plots indicating critical operating conditions for example frigate.

4.2. Surfriding and broaching avoidance

From the polar plots it is evident that the combination of severe stern quartering seas and high ship speed (Fn ≥ 0.3) tends to be most critical as regards extreme roll motions. Surfriding does not necessarily result in broaching or capsizing, but is often a precursor to such events. Recent publications on surfriding include Kan (1990) and Thomas and Renilson (1992). To indicate the possibility of surfriding, use can be made of polar plots (see next Section). A simple criterion for avoiding surfriding and associated broaching possibilities could be based on the requirement that the Froude number be less than 0.3 in severe following to stern quartering seas:

$$V_s \leq 0.3 \times \sqrt{g.L} \quad \text{for } -45° \leq \psi \leq 45° \qquad (8)$$

where $\psi = 0$ degrees denotes following seas. If L is given in meters and V in knots, the criterion becomes

$$V \leq 1.8 \times \sqrt{L} \quad \text{for } -45° \leq \psi \leq 45° \qquad (9)$$

Seas could be defined severe when the dominant wavelength is of the order of L. Assuming a mean characteristic steepness of 0.035 for stern waves, a sea would be "severe" when $H_s > 0.035$ L.

4.3. Narrow-band wave energy concentration in irregular waves

When in irregular astern seas and when the ship speed lies close to the speed at which most of the wave energy travels, the ship can be expected to undergo significant roll excitation of a regular nature. This does not necessarily result in dangerous motion behavior, but it would be useful if the ship operator were at least aware the ship is operating in potentially critical conditions. In this context, a critical range of operating speeds in severe astern seas would be as follows:

$$0.6C_{g,p} \leq V_s \cos\psi \leq 1.3C_{g,p} \qquad (10)$$

where $C_{g,p}$ is the group speed defined by Eq. (6) and V_s is the ship speed in m/s. If a sea state has wave components containing significant energy with a wavelength of the order of the ship length, a ship speed corresponding to around Fn = 0.2 will result in the ship travelling at the group speed in overtaking seas, i.e., V_s would lie then in the critical range indicated by Eq. (10). If under these operating conditions the loading condition is such that parametric rolling may occur or the range of positive stability is limited, the ship is likely to experience large amplitude roll motions.

4.4. Minimum maneuvering speed in wind and waves

Simulations suggest that the ability to complete a turning circle in wind and waves strongly depends on the wind speed and ship speed. For a given wind speed, a certain minimum ship speed is required, below which the ship will drift without being able to complete the turning maneuver. Here it is assumed that the RPM is kept constant for a given rudder angle. Simulations were carried out for a range of significant wave heights and wind speeds. The results suggest that ship maneuvering is more sensitive to wind speed than to wave height. Fig. 16 shows a marginal turning circle trajectory, Fig. 17 the case where a turning circle cannot be completed and the ship starts to drift broadside to the waves and wind, and Fig. 18 illustrates the format of presentation for minimum required maneuvering speed as a function of sustained wind speed and rudder angle.

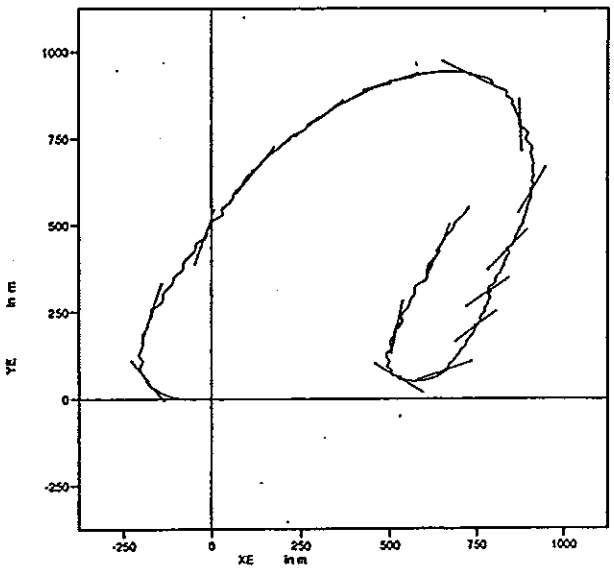

Fig. 16. Example of marginal turning circle in severe irregular waves and wind (collinear waves and wind along XE-axis in positive direction) H_s = 12.5m, T_p = 15.5 s, V_{wind} = 50 kn, V_s = 8 kn, rudder angle = 20 deg.

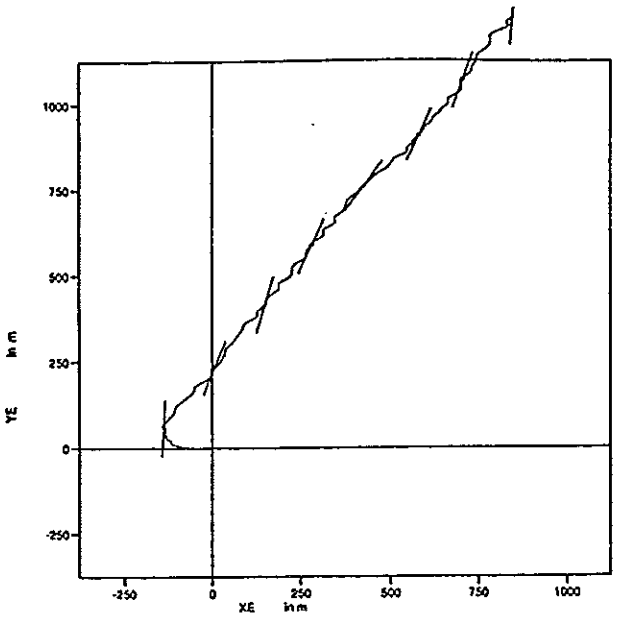

Fig. 17. Example of unsuccessful turning circle in severe irregular waves and wind (collinear waves and wind along XE-axis in positive direction) H_s = 15m, T_p = 16.5 s, V_{wind} = 60 kn, V_s = 8 kn, rudder angle = 35 deg.

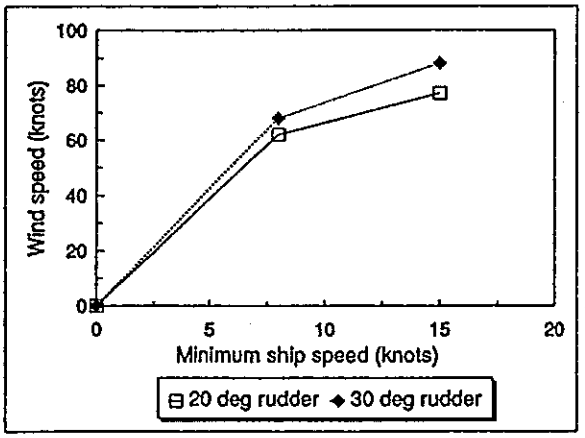

Fig. 18. Minimum required ship speed as a function of sustained wind speed for achieving a complete turning circle.

5. IMPLEMENTATION OF OPERATIONAL GUIDELINES FOR USE ABOARD NAVY SHIPS

Personnel aboard ship who are directly responsible for its control are typically referred to as ship operators in literature concerning naval architecture. This convention will be followed in this paper.

5.1. Background

In the past, operators of ships in the U.S. Navy and Coast Guard typically have been taught *ship dynamics* and *intact stability* as separate subjects. The content of classroom material concerning intact stability focuses on criteria that are primarily based on the work of Sarchin and Goldberg (1962).

Ship operators are trained to monitor the loading condition of a ship, and understand the need to maintain adequate metacentric height (GM). The assumption is made that as long as GM remains above the Sarchin and Goldberg minimum, a ship remains immune from capsizing in the undamaged condition.

Classroom training in *ship dynamics* exposes ship operators to the basic six degree of freedom ship motions. Emphasis is placed on the reduction of roll motions and the use of applicable hull appendages for this purpose. Basic concepts regarding the generation of ocean waves are discussed, with special emphasis placed on the avoidance of severe storms, such as hurricanes and typhoons.

Little or no classroom training is presently provided to prospective ship operators regarding nonlinear phenomena like capsizing, broaching and surfriding. When asked to describe the situation where a ship is most likely to capsize, a typical inexperienced ship operator will describe a scenario where a ship is "caught in the troughs" (in beam seas) at zero speed as very large, steep waves force the ship to roll at progressively larger and larger angles until it capsizes. There is no familiarity with the 10 modes of capsizing as defined in Section 2.

Steps are presently being taken to develop appropriate training materials that educate ship operators more extensively in the subject of dynamic stability.

5.2. Operator guidance

The development of Operator Guidance, analytical tools which can be used by ship operators to supplement existing knowledge gained from practical experience, has been an on-going effort in the U.S. Navy (Bales et al., 1985). Seakeeping Tactical Decision Aids (TDAs) which are based on frequency domain models display ship motions as a function of heading and speed for a particular seaway on a polar plot, an example of which is shown in Fig. 19 for a DDG2 frigate. The hatched areas enclosed by the contours in this polar plot identify combinations of ship headings and speeds where unacceptable ship motions exist.

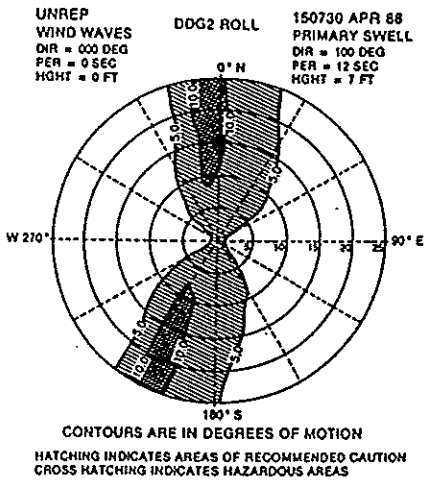

Fig. 19. DDG2 Speed Polar Plot of Limiting Roll Motions for Underway Replenishment.

In the TDA in Fig. 19, the DDG2 is predicted to have unacceptable ship motions to conduct Underway Replenishment Operations on Northerly and Southwesterly Courses in swells coming from the east. The limiting motion criterion is 5 degrees significant single amplitude roll for Connected Underway Replenishment (Smith and Thomas, 1989). Operator guidance in this TDA is shown as the range of choices in heading and speeds where acceptable motions are predicted in the nonshaded regions of this polar plot.

Seakeeping Tactical Decision Aids that use frequency domain ship motions predictions have shortcomings in roll predictions in stern quartering and following seas at high speeds due to the inability to model nonlinear phenomena such as capsizing, broaching and surfriding events. The development by the Cooperative Research Navies working group of the program FREDYN as a time domain seakeeping model, which is able to predict such events, is viewed to be significant because this numerical model can perform realistic calculations faster than real time.

FREDYN's special capabilities are being included in Tactical Decision Aids that focus on the avoidance of extreme ship motion events. Two examples of such TDAs are displayed in Figs. 20 and 21. The polar plots in these figures denote predictions for a 378 foot U.S. Coast Guard Cutter, in the full load condition with an unrealistically small GM. The plots are based on a range of simulations of 30 min. duration in irregular seas at 15 degree heading increments over 180 degrees of wave headings at speeds ranging from zero to maximum speed in 5 knot speed increments. The time series of the simulations are inspected for roll angle values, as well as for the occurrence of broaching and surfriding. Fig. 20 illustrates the prediction of large roll angles in stern quartering seas in Sea State 6 (H_s = 5 m). Fig. 21 predicts the occurrence of surfriding events in following seas for the same sea state.

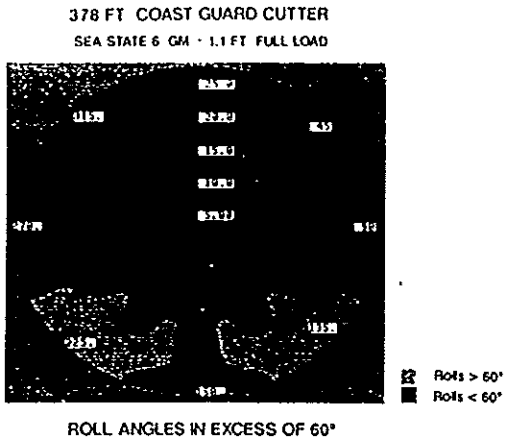

Fig. 20. Polar plot for 378 ft U.S. Coast Guard Cutter in Sea State 6 with low GM; roll angles in excess of 60 degrees (0 degrees heding is head seas)

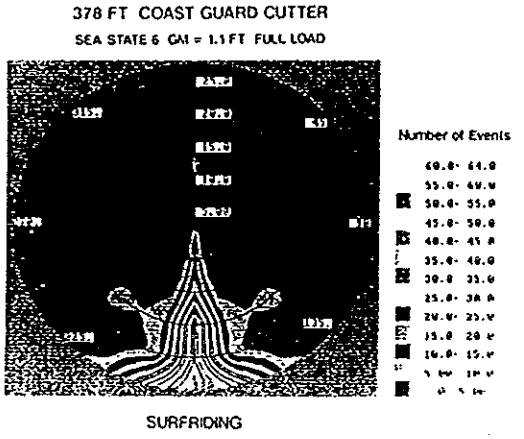

Fig. 21. Polar plot for 378 ft U.S. Coast Guard Cutter in Sea State 6 with low GM; surfriding predictions (0 degrees is heading is head seas).

5.3. Extreme operability evaluation

The information provided in polar plots can also be used to evaluate the stability performance of prototype hull forms in the design stage. The use of an assessment based on sea state is based on performance specifications, which measure satisfactory performance in terms of sea conditions. Examples of such specifications might be:

(a) Ship will not capsize at any heading or speed in Sea State 6 or less

(b) Ship will operate in Sea States 0 through 8 with a probability of capsizing of less than 10^{-4}

The sea state based assessments would be compiled in a manner similar to the polar plots used in the Operator Guidance tools using simulations. Inspection of the polar plots generated through Sea State 6 would indicate whether the new design was predicted to be in compliance with the Sea State 6 specification as listed above. The probability of capsizing in a given sea state can be estimated by evaluating the total matrix of simulation conditions. The probability of capsizing in Sea States 0 through 8 could be calculated by summation of the probabilities in the individual sea states.

Sea state based assessments can also relate the predicted performance to the environment at a particular geographic location for a specified season. This concept would be useful in estimating the risk of capsizing in terms of the operating region for which a ship is designed. The basic methodology has been applied by McCreight and Stahl (1985), where operability indices were based on ship performance predictions in wave environments, as defined by wave hindcast climatology. The assessment of capsize risk at a particular location would then be based on the probabilities of occurrence of the various sea states, combined with the conditional probabilities of capsizing. Ship designers could perform estimates of capsizing probability at locations having rough sea conditions. Operability assessments for the U.S. Navy, for example, typically choose a location in the North Atlantic Ocean during the winter season (Smith and Thomas, 1989). An application of capsize risk analysis is presented in the next Section.

6. PROBABILISTIC METHODS APPLIED TO CAPSIZING

The ultimate goal of any set of design criteria is to ensure that resulting designs have consistent, acceptably low probabilities of failure. Existing stability criteria (e.g. Sarchin and Goldberg (1962)) apply a simplified treatment to the very complex process of ship capsize. To compensate for this simplified treatment, such criteria are generally very conservative for most ships; however, the actual capsize risk for ships satisfying the criteria can vary widely, particularly for new design trends. As discussed above, for example, modern naval frigates having wide transom sterns are more likely to capsize in following seas than the narrow transom frigates that formed the basis for the Sarchin and Goldberg criteria. It is possible that a wide transom frigate could satisfy the Sarchin and Goldberg criteria but could capsize in following seas, for example due to loss of waterplane area while balanced on a wave crest.

Probabilistic methods coupled with a time domain ship motion code permit assessment of capsize risk in a rational manner which models the physics of ship capsize. For novel designs for which there is no design or operational experience, a probabilistic approach is the only viable method for achieving a safe design. This section outlines an approach for predicting ship capsize risk developed by McTaggart (1993).

Structural engineers have been using reliability methods for design, as discussed by Thoft-Christensen and Baker (1982) and Madsen, Krenk and Lind (1986). A given system is expressed in terms of a random "failure function" $G(\vec{X})$ which is less than zero when failure occurs:

$$G(\vec{X}) = R(\vec{X}) - L(\vec{X}) \qquad (11)$$

where $\vec{X}$ is a vector of input random variables, $\vec{R}$ is the system capacity or resistance, and $\vec{L}$ is the system load. The above two references describe efficient algorithms for computing the probability of the failure function $G(\vec{X})$ being less than zero. In structural engineering, the complexity of the failure function can range from being relatively simple to requiring a finite element code for evaluation. For a ship capsizing, the failure function can be written as:

$$G(\vec{X}) = \phi_R - \phi_{max}(\vec{X}) \qquad (12)$$

where ϕ_R is the maximum acceptable roll angle (e.g. 70 degrees or the angle of downflooding) and ϕ_{max} is maximum ship roll magnitude during a given time period (e.g. one year or the life of the ship).

6.1. Input Random Variables

When formulating the failure function, identification of input random variables is of key importance. The failure function should include all relevant input parameters. To assess failure probability accurately, the statistical distribution for each input random variable must be known. Ideally, the input random variables should be independent or have low correlation coefficients.

For evaluating ship safety, the failure function of Equation (12) can represent the probability of

capsize during the worst annual storm in a given operational area. Input statistical data are available for the following input random variables, which have low correlation:

1. annual maximum significant wave height, H_s,
2. nominal (characteristic) wave steepness, H/λ
3. desired ship heading ψ_s relative to direction of wave propagation,
4. calm water ship speed, V_s.

The annual maximum significant wave height usually represents the worst three hour recording period during a given year. The Canadian Climate Centre (1991) indicates that a Gumbel distribution provides a good fit to annual maximum wave height off Canada's East Coast. For the North Atlantic, H_s for the worst annual storm has a mean value of the order of 8 m and a standard deviation of the order of 1 m.

In addition to wave height, wave period is an important environmental parameter influencing capsize. Wave period tends to be strongly dependent on wave height, thus making it somewhat undesirable as an input random variable for the failure function of Equation (12). To maintain low correlation among input variables, the nominal wave steepness is introduced as an input variable:

$$H/\lambda = H_s\,(2\pi/gT_p^2) \qquad (13)$$

wich is the same as the characteristic steepness defined in Section 2.2., Equation (1). For worst annual storms in the North Atlantic, the mean and standard deviation of nominal steepness are of the order of 0.035 and 0.0037, respectively. Storm data for the North Atlantic indicate that a Weibull distribution gives an excellent fit to H/λ, and that very low correlation exists between H_s and H/λ.

Input distributions for desired ship heading ψ_s and calm water ship speed V_s depend on ship operational profile. A uniform distribution typically provides a suitable model for heading, with a range of 0-360 degrees, or 0-180 degrees if symmetry is applicable. During a time domain simulation evaluating the capsize failure function, actual ship speed and heading will deviate from the desired values of ψ_s and V_s due to wave forces (including added resistance) and loss of rudder effectiveness.

Wind forces strongly influence ship heel in severe conditions, suggesting that wind speed and direction could be introduced as input random variables; however, the failure function should consider the strong interrelationship between waves and wind for severe ocean conditions. Data from the North Atlantic suggest that the 1-hour mean wind speed can be approximated as a function of wave height as follows:

$$V_w = 1.823\,H_s + 3.45 \qquad \text{(m/s)} \qquad (14)$$

where V_w is mean wind speed at an elevation of 19.5 m and H_s is given in meters. For severe conditions, the winds can be assumed to be travelling in the same direction as the waves. More conservatively, the winds could be assumed to be approaching the ship from abeam.

6.2. Application of Reliability Methods

The time domain code FREDYN described previously was coupled with the reliability code CALREL (Liu, Lin and Der Kiureghian (1989)) to evaluate capsize probability using the failure function of Equation (12). Initial runs examined a frigate operating in both regular and irregular wave conditions. Unfortunately, the reliability algorithm failed to converge for any of the input conditions. This lack of convergence is likely due to the erratic nature of the capsize failure function, Equation (12). Reliability methods require that the failure function exhibit smooth variation with each of the input random variables, which does not occur with many complicated processes such as ship capsizing. For example, Fig. 22 shows the variation of maximum roll angle in irregular seas with significant wave height for a naval frigate in conditions given by Table 6. The variation of maximum roll angle with wave height is somewhat erratic. For the variation of other input random variables, maximum roll angle exhibits similar erratic tendencies.

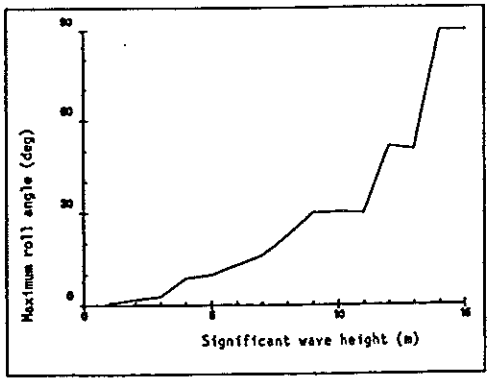

Fig. 22. Maximum roll angle versus significant wave height for example frigate in irregular seas.

Nominal wave steepness, H/λ	0.045
Desired ship heading, ψ_s	15 degrees
Calm water ship velocity, V_s	10 m/s
Simulation duration, T_s	30 minutes

6.3. Capsize Wave Height Method

One encouraging aspect of the results in Fig. 22 is that the wave height at which capsize occurs is relatively well defined. By conducting simulations for increasingly large wave heights (e.g. increasing by 1 m increments from an initial wave height of 5 m), it is possible to determine the capsize wave height as a function of other input variables:

$$H_C = F(H/\lambda, \psi_s, V_s) \tag{15}$$

where H_C is the lowest wave height at which the maximum roll angle exceeds the allowable value. Taking discretized distributions for input random variables, the total capsize probability is:

$$P(C) = \sum_{i=1}^{N_{V_s}} \sum_{j=1}^{N_{\psi_s}} \sum_{k=1}^{N_{H/\lambda}} p_{V_s}(V_{s-i})\, p_{\psi_s}(\psi_{s-j})\, p_{H/\lambda}(H/\lambda_k) \times [1 - F_{H_s}(H_C \mid V_{s-i}, \psi_{s-j}, H/\lambda_k)] \tag{16}$$

where N_X is the number of discretized values of variable X, $p_X(X)$ is the probability mass function of X, and $F_{H_s}(H_s)$ is the cumulative distribution function for annual maximum wave height. The above equation assumes that capsize will occur for all wave heights greater than H_C. In reality, it is possible for a ship to not capsize for certain wave heights greater than H_C; thus, Equation (16) is somewhat conservative.

Conditional probabilities related to ship capsize yield useful information regarding the likelihood of capsize under given conditions and the likelihood of given conditions being the cause of capsize. For example, the conditional probability of capsize given heading is:

$$P(C \mid \psi_s) = \sum_{i=1}^{N_{V_s}} \sum_{k=1}^{N_{H/\lambda}} p_{V_s}(V_{s-i})\, p_{H/\lambda}(H/\lambda_k) \times [1 - F_{H_s}(H_C \mid V_{s-i}, \psi_s, H/\lambda_k)] \tag{17}$$

Conversely, the conditional probability of heading given capsize is:

$$P(\psi_s \mid C) = \frac{p_{\psi_s}(\psi_s)\, P(C \mid \psi_s)}{P(C)} \tag{18}$$

The sum of the conditional probabilities $P(\psi_s \mid C)$ is equal to one. The conditional probability $P(\psi_s \mid C)$ indicates which heading is most likely to cause capsize and is very useful for design. The heading with the highest $P(C \mid \psi_s)$ value will not necessarily have the highest $P(\psi_s \mid C)$ value if the ship rarely travels at that heading. Conditional probabilities for ship speed and wave slope provide useful information regarding which speed and wave slope are most critical for capsize.

Capsize risk evaluations suggest that capsize wave heights should be computed for 7 nominal wave slopes ranging from 0.02 to 0.05 and 13 headings ranging from 0 to 180 degrees. The number of ship speeds will depend on operational profile. To obtain consistent capsize wave height values, simulation durations of 10 wave encounters are adequate for regular waves, while irregular wave conditions require simulation durations of the order of 30 minutes. Recent experience suggests that capsize wave heights in irregular seas are sensitive to the "random" phases of the individual wave components. Once capsize wave heights are computed for a given ship, capsize probabilities can be easily computed for any operating condition using Equation (16).

7. INCLUSION OF DYNAMIC STABILITY IN THE DESIGN OF FRIGATES

7.1. General

In the Cooperative Research Navies Research project on ultimate stability presented in this paper, several design parameters are identified that may have considerable influence on the dynamic stability performance of a ship in waves.

In present frigate design practice, the number of parameters that can be varied and the magnitudes of their variation are very limited. The *displacement* for example will be determined by the required payload, and the *depth* of the ship by the minimum number of decks needed. Another important parameter, the *length* of the ship, is the result of minimum relative distances required to avoid interference between weapon sensors and other electronic installations and of the increase in building cost with increasing ship length. A major design constraint is that most of the payload, such as weapons and helicopters, has to

be carried on deck, thus greatly restricting the location of the *vertical centre of gravity*.

Another important consideration is that a hull designed for optimal dynamic stability may have poor resistance and seakeeping properties.

This section of the paper considers the effects of limited variations of hull parameters on the seakeeping, resistance and dynamic stability of a frigate type ship.

7.2. Reference ship and derivatives

One of the parent hull forms from paragraph 3.2 is chosen as a reference ship. A small subset of those hull form derivatives is considered to be acceptable for practical design of frigate type ships. Table 6 shows identification and geometric hull form parameters of the reference hull form (referred to as hull "X") and its selected derivatives.
The displacement equals 4,000 tonnes for all hull forms and the vertical location of the centre of gravity (KG) is assumed to be a constant fraction of the depth. For all ships, the KG values are smaller than the maximum allowable KG according to the Sarchin and Goldberg criteria (i.e., all hull forms considered here satisfy the standard criteria).

ID	L/B	B/T	D/T	C_B	C_{WP}
X	8.7	3.05	2.17	0.49	0.81
L80	8.0				
C45				0.45	
W79					0.79
W75					0.75
B27 D20		2.7	2.0		
B33		3.3			
C53				0.53	
D24			2.4		

Table 6. Reference frigate "X" and derivatives

7.3. Ship resistance

The hydrodynamic resistance is calculated for a design speed of 30 knots, using the so-called FDS method developed by MARIN and based on regression data of several fast displacement hull forms. The results of these calculations are presented in Table 7. The relative ranking of the hull forms is shown in the second column.

ID	Resistance (kN)	Ranking
X	1255	5
L80	1425	9
C45	1246	4
W79	1237	3
W75	1219	2
B27 D20	1363	8
B33	1206	1
C53	1312	7
D24	1286	6

Table 7. Calculated hull resistance

7.4. Dynamic stability

The dynamic stability performance of the selected hull forms is taken into account by calculating the capsize index following the procedure explained in Section 3.2. The results calculated with the simulation tool FREDYN are shown in Table 8. A capsize index lying between 5 and 20 may be marginally acceptable for the design condition and might lead to restrictions on sailing speed in off-design conditions (see Section 3.6).

ID	Capsize index
X	1
L80	0
C45	0
W79	4.4
W75	6.7
B27 D20	12.2
B33	0
C53	15.6
D24	18

Table 8. Capsize indices of all derivatives

7.5. Seakeeping in operating conditions

To achieve maximum operability, for instance in performing helicopter operations, good seakeeping qualities are of utmost importance for a frigate type ship. The seakeeping performance of the hull forms considered is expressed in a percentage of downtime for helicopter-operations; this is determined in the following steps:

- 1) calculation of response amplitude operators of ship motions for 6 heading/speed combinations (headings: 135, 90 and 45 degrees; speeds: 15 and 25 knots) by means of a strip theory program.

- 2) calculation of significant motions, velocities and accelerations at the helicopter deck and of the probability of exceedance of given criteria using wave statistics for the North-Atlantic ocean for all heading and speed combinations.

- 3) the percentage of downtime for each hull for m is derived by taking the average of the downtime values calculated for each heading and speed combination. The following criteria are used as regards single significant amplitudes:

Roll	< 6.4 degrees
Vertical motion	< 1.20 m
Transverse accel.	< 1.0 m/s^2
Vertical acceleration	< 2.0 m/s^2

Table 9 shows the results of the downtime calculations, together with their relative ranking. Fig. 23 shows the average downtime due to transverse accelerations only as a function of the GM/B value. This figure also contains the calculated capsize indices for each hull.

ID	Downtime (%)	Ranking
X	40.1	4
L80	39.7	3
C45	40.4	5
W79	41.6	6
W75	47.7	9
B27 D20	39.6	2
B33	41.9	7
C53	39.5	1
D24	43.1	8

Table 9. Downtime analysis

Fig. 23 suggests that ships with an acceptable level of safety against capsize (i.e., capsize index < 5), also can have low downtime values as regards transverse accelerations, so long as the GM/B ratio (indicator of natural roll frequency) is not too high.

7.6. Overall performance

To compare the hull forms on the basis of their overall hydrodynamic performance, a method of weighting each aspect has to be used. Assuming that all three aspects considered are equally important, the following approach is applied to determine for example the "COST"-contribution of the resistance part:

$$\textit{COST FOR RESISTANCE} = \frac{\textit{actual resistance} - \textit{minimum resistance}}{\textit{maximum resistance} - \textit{minimum resistance}}$$

The "COST"-contributions related to the capsize index and downtime are determined in an analogous fashion. The sum of these three calculated cost contributions represents the "total cost" of a certain hull form. Fig. 24 shows the "total cost" and also the separate contributions. The number on top of each bar represents the final relative ranking.

Fig. 24 shows that the hull forms "C45", "B33" and "X" perform better than the other hull forms. Of these "good" hull forms, hull "C45" will perform best, but from the point of view of building cost this ship would be relatively expensive. The hull form with high B/T ratio (B33) is second best, but it has a rather high downtime related to transverse accelerations (see Fig. 23), which could be of importance when for example considering motion responses at the bridge.

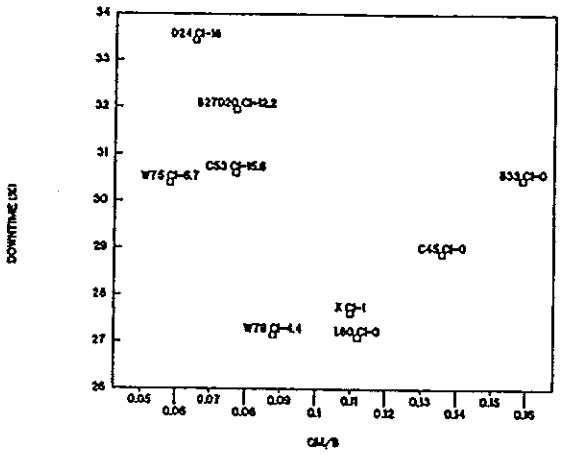

Fig. 23. Downtime due to transverse accelerations at helicopter deck.

A very important finding is that while trying to attain a high level of safety against capsizing in extreme wave conditions, it is possible to avoid a penalty on seakeeping and resistance. Moreover, the results for hull forms "C53" and "B27D20" shown in Fig. 24 suggest that a ship with good seakeeping performance is not necessarily a safe ship.

8. CONCLUSIONS

This paper presents an overview of the Cooperative Research Navies Dynamic Stability project related to intact frigate stability. The main objective is the

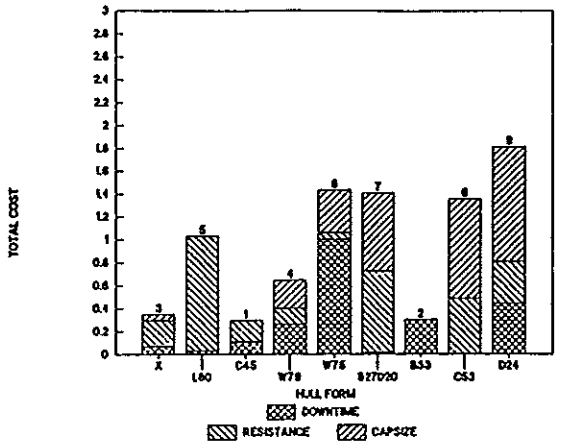

Fig. 24. Comparison of hull forms by equally weighting resistance, downtime and capsize index.

development of stability criteria that reflect the influence of capsize dynamics on ship safety. A sound understanding of the physics and a practical ship motion simulation tool are considered essential elements. Sections 1 through 4 of this paper provide an overview of the project approach and results, including:

- relevant characteristics of irregular waves
- mechanisms of capsizing
- influence of hull form on capsizing
- development of stability guidelines for the design and operation of intact frigates

The results show it is feasible to base a methodology for developing dynamic stability criteria against capsizing largely on numerical simulations. The complex behavior of capsizing in astern to beam seas is seen to depend to a large extent on the calm water stability characteristics at large angles of heel. The new guidelines proposed here apply in particular to astern sea conditions, which are typically not covered by existing criteria; this can have an important bearing on modern hull forms with a wide transom. Existing stability criteria seem to offer an acceptable level of safety against capsizing in waves, which is corroborated by the lack of capsize incidents involving navy ships. For modern hull forms, however, the new guidelines may be essential to maintain the same low risk of capsizing.

From a naval perspective, the following issues related to dynamic stability are addressed in Sections 5, 6 and 7: implementation of operational guidelines aboard navy ships, the role of probabilistic methods related to capsizing of intact ships, and the evaluation of new design concepts in operational and extreme conditions.

This joint research project will be continued for the next four years along with the addition of new topics, including damaged stability in waves and intact stability of ships with low L/B ratios.

ACKNOWLEDGEMENTS

The authors would like to express their thanks to all members of the Cooperative Research Navies Dynamic Stability group for their permission to publish this paper.

REFERENCES

Bales, S.L., Elliot, L.R. and Thomas III, W.L. (1985), "Degradation of Surface Ship Operations in Arctic/Cold Weather Regions," Paper presented at the *U. S. Navy Symposium on Arctic/Cold Weather Operations of Surface Ships*, Dec.

Buckley, W.H. (1992), "Matching Vehicle Characteristics to Seaway Environments," *Proc. Intersociety High Performance Marine Vehicle Conference, HPMV '92*, June, Arlington

Canadian Climate Centre (1991), "Wind/Wave Hindcast Extremes for the East Coast of Canada, Volume 1," Technical Report, Prepared under contract by MacLaren Plansearch Ltd. and Oceanweather Inc.

Dahle, E.Aa. and Myrhaug, D. (1993), "Risk analysis applied to capsize of smaller vessels in breaking waves", *Trans. R.I.N.A.*, Vol. 135, pp. 237-252

Dahle, E.Aa., Myrhaug, D. and Dahl, S.J. (1988), "Probability of capsizing in steep and high waves from the side in open sea and coastal waters", *Ocean Engineering*, Vol. 15, No. 2, pp. 139-151

De Kat, J.O. (1990), "The Modelling of Ship Motions and Capsizing in Severe Seas," *J. Ship Research*, Vol. 34, No. 4, Dec., pp. 289-301

De Kat, J.O. (1993), "The Development of Survivability Criteria Using Numerical Simulations," *Proc. U.S. Coast Guard Vessel Stability Symposium 93*, New London, March

De Kat, J.O. (1994), "Irregular Waves and Their Influence on Extreme Ship Motions", *Twentieth Symposium on Naval Hydrodynamics* (to be presented), Santa Barbara, August

De Kat, J.O. and Paulling, J.R. (1989), "The Simulation of Ship Motions and Capsizing in Severe Seas," *Trans. SNAME*, Vol. 97, pp. 139-168

Grochowalski, S. (1993), "Effect of Bulwark and Deck Edge Submergence in Dynamics of Ship Capsize," *Proc. U.S. Coast Guard Vessel Stability Symposium 93*, New London, March

Kan, M. (1990), "A Guideline to Avoid the Dangerous Surfriding," *Proc. Fourth International Conference on Stability of Ships and Ocean Vehicles STAB '90*, Naples, Sept. 24-28, pp. 90-97

Kan, M., Saruta, T., Taguchi, H., Yasuno, M. and Takaishi, Y. (1990), "Model Tests on Capsizing of a Ship in Quartering Waves," *Proc. Fourth International Conference on Stability of Ships and Ocean Vehicles STAB '90*, Naples, Sept. 24-28, pp. 109-116

Le Méhauté, B. and Hanes, D.M. (1990), Eds., *The Sea*, Ocean Engineering Science, Vol. 9, Part A, Wiley & Sons

Liu, P.-L., Lin, H.-Z. and Der Kiureghian, A. (1989), "CALREL User Manual," Technical Report UCB/SEMM-89-18, Department of Civil Engineering, University of California at Berkeley

Madsen, H.O., Krenk, S. and Lind, N.C. (1986), *Methods of Structural Safety*, Prentice-Hall

McCreight, K. K., and R. G. Stahl (1985), "Recent Advances in the Seakeeping Assessment of Ships," *Naval Engineers Journal*, May, pp. 224-233

McTaggart, K.A. (1993), "Risk Analysis of Intact Ship Capsizing", *Proc. U.S. Coast Guard Vessel Stability Symposium 93*, New London, March

Myrhaug, D. and Kjeldsen, S.P. (1987), "Prediction of Occurrences of Steep and High Waves in Deep Water," *J. Waterway, Port, Coastal, and Ocean Engineering*, Vol. 113, No. 2, March, pp. 122-138

Oakley, O.H., Paulling, J.R. and Wood, P. (1974), "Ship Motions and Capsizing in Astern Seas," *Proc. 10th Symposium on Naval Hydrodynamics*, Cambridge, June, pp. 297-350

Pierson, W.J. (1993), "Ship stability in heavy weather: the real situation and models thereof", *Proc. U.S. Coast Guard Vessel Stability Symposium*, Groton, March

Rahola, J. (1939), "The judging of the stability of ships and the determination of the minimum amount of stability," *Thesis*, Helsinki

Sarchin, T.H. and Goldberg, L.L. (1962), "Stability and Buoyancy Criteria for U.S. Naval Surface Ships," *Trans. S.N.A.M.E.*, Vol. 70, pp. 418-458

Smith, T.C. and Thomas III, W.L. (1989), "Underway Replenishment Investigation for Selected Surface Ships," David Taylor Model Basin, DTRC/SHD-1312-03, Oct.

Sobey, R.J. (1992), "The Distribution of zero-crossing Wave Heights and Periods in a Stationary Sea State," *Ocean Engineering*, Vol. 19, No. 2, pp. 10-118

Srokosz, M.A. and Challenor, P.G. (1987), "Joint distributions of wave height and period: a critical comparison", *Ocean Engineering*, Vol. 14, No. 4, pp. 295-311

Tayfun, A. (1993), "Joint distribution of large wave heights and associated periods", *J. Waterway, Port, Coastal and Ocean Engineering*, Vol. 119, No. 3, May/June, pp. 261-273

Thoft-Christensen, P. and Baker, M.J. (1982), *Structural Reliability and Its Applications*, Springer-Verlag

Thomas, G.A. and Renilson, M.R. (1992), "Surf-riding and Loss of Control of Fishing Vessels in Severe Following Waves," *Trans. R.I.N.A.*, Vol. 134

Tikka, K.K. and Paulling, J.R. (1990), "Prediction of Critical Wave Conditions for Extreme Vessel Response in Random Seas," *Proc. Fourth International Conference on Stability of Ships and Ocean Vehicles STAB '90*, Naples, Sept. 24-28, pp. 386-394

Torsethaugen, K. (1993), "A two peak wave spectrum model", *Proc. Offshore Mechanics and Arctic Engineering OMAE '93 Symposium*, Vol.2, Glasgow, June, pp. 175-180

Wind Heeling Loads on a Naval Frigate

Kevin McTaggart
Defence Research Establishment Atlantic
P.O. Box 1012
Dartmouth, Nova Scotia
B2Y 3Z7
Canada

Michael Savage
Applied Aerodynamics Laboratory
Institute for Aerospace Research
National Research Council of Canada
Ottawa, Ontario
K1A 0R6
Canada

Abstract

This paper describes a series of wind tunnel tests examining wind-induced heeling loads on a generic naval frigate. The objective of the experiments was to provide new data for improving stability criteria for naval frigates. The wind tunnel environment models the wind velocity profile over the ocean during storm conditions, which are of greatest interest for ship stability. A series of five different models represents the ship at heel angles of 0, 20, 40, 60, and 70 degrees. Wind directions for testing range from 0 to 360 degrees relative to the bow, thus giving results for the ship heeling to both leeward and windward. Measured wind heeling moments are shown to be much greater than those predicted by current naval stability criteria. Contrary to the existing criteria, wind heeling moment exhibits surprisingly little reduction as heel angle increases. The experimental data indicate that existing stability criteria should be revised to model more accurately actual wind loading.

1 Introduction

When designing a ship for safety against capsize, wind loading is of considerable importance, as demonstrated by intact stability standards for naval vessels [1, 2]. Although waves may play a more important role in ship capsize than wind, present intact stability standards likely emphasize wind loading because it is easier to quantify for design purposes. More rigourous examination of the relative importance of wind and wave loading is required.

This paper presents results from wind tunnel tests examining wind heeling loads on a naval frigate. The experiments, sponsored by the Canadian Department of National Defence, were motivated by Canada's involvement in an international project [3] to develop new stability guidelines for naval frigates. The new guidelines will more realistically consider the physics of ship capsize, thus leading to more consistent levels

of safety. The Dynamic Stability Criteria Project has been initially limited to frigates, but will be expanded to include other ship types.

A review of wind tunnel test literature revealed that few data were available for wind loads acting on naval frigates, particularly at non-zero angles of heel. References 4, 5, 6, and 7 provide useful lateral force coefficient data for various ships; however, only References 4 and 7 give data regarding the centre of lateral force, which is needed to calculate heeling moment. Kinoshita and Okada [7] give the only data for wind loads on heeled vessels. Most wind tunnel data in the open literature are limited to commercial vessels; thus, new experimental data are required for naval frigates.

2 Wind Criteria for Naval Vessels

Wind stability criteria for Canadian naval ships [2] are essentially the same as for American naval ships, and are based on the work of Sarchin and Goldberg [1]. Depending on the operational profile, the ship is subjected to winds of velocity between 50 and 100 knots. Wave-induced roll motions have a nominal amplitude of 25 degrees.

Figure 1 shows the main quantities that form the basis of the stability criteria. The wind heeling arm $K/(g\ \Delta)$ and the hydrostatic righting arm $\overline{GZ}$ represent moments acting on the ship divided by ship weight $g\ \Delta$, where K is wind heeling moment, g is gravity and Δ is ship displacement. The wind moment causes the ship to have a mean heel angle of ϕ_m. During wave-induced roll, the ship heels to windward and reaches a heel angle of $\phi_m - 25$ degrees. Wind and hydrostatic forces then cause the ship to heel to leeward, with the maximum heel angle being determined by conservation of energy. The area A_2 in Figure 1 represents the initial heeling energy, while area A_1 represents the available restoring energy. The maximum allowable heel angle ϕ_{max} is equal to the lesser of 70 degrees or the angle of unrestricted down-flooding for the ship, ϕ_f. To ensure that this angle is not exceeded, the ship must satisfy the following requirements:

1. $\overline{GZ}(\phi_m) \leq 0.6\ \overline{GZ}_{max}$,
2. $A_1 \geq 1.4\ A_2$,
3. $\phi_m \leq 30°$,
4. Metacentric height, $\overline{GM} \geq 0.05$ m,
5. Maximum $\overline{GZ} \geq 0.3$ m,
6. Angle of maximum $\overline{GZ} \geq 30$ degrees.

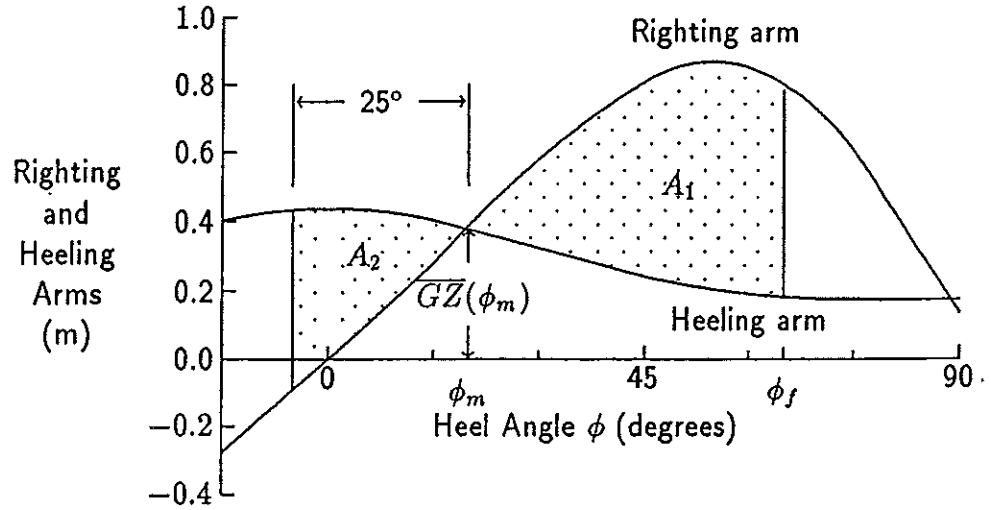

Figure 1: Wind and Righting Arms for Stability Criteria

Several operational conditions with varying displacement Δ and vertical centre of gravity $\overline{KG}$ are considered when determining righting moment curves $\overline{GZ}(\phi)$ for stability evaluation. The overturning wind moment can be expressed in terms of a dimensionless lateral force coefficient, C_Y, as follows:

$$K = \frac{1}{2} \rho_a \overline{U}_r^2 C_Y A_{ay} (h_{ay} + h_{wy}) \cos^2 \phi \tag{1}$$

where ρ_a is air density, $\overline{U}_r$ is the reference wind velocity, A_{ay} is the above-water lateral cross-sectional area of the ship, h_{ay} is the height of the centre of lateral force above the waterline, and h_{wy} is the depth of the centre of lateral resistance below the waterline. Dimensional values given in stability standards suggest that the dimensionless force coefficient C_Y has a value of 1.15. The height h_{ay} of the above-water lateral force is assumed to equal the height h_{cy} of the centroid of the above-water area. The lateral water force is assumed to act at a depth h_{wy} equal to half the ship draft. The reference wind velocity $\overline{U}_r$ accounts for the variation of wind velocity with elevation as follows:

$$\overline{U}_r^2 = \frac{\int_{A_{ay}} \overline{U}_a^2(z)\, dA}{A_{ay}} \tag{2}$$

where $\overline{U}_a$ is mean local wind speed and z is height above the water. The wind velocity profile can be represented using the following power law equation:

$$\overline{U}_a(z) = \overline{U}_a(z_1) \left(\frac{z}{z_1}\right)^{\alpha} \tag{3}$$

where z_1 is reference elevation and α is an exponent dependent on surface roughness. Reference 2 uses a reference elevation z_1 of 10 m, with mean wind velocity at that

elevation varying between 50 and 100 knots, depending on ship type and operational profile. The value of the exponent α for Canadian naval stability standards [2] appears to be 0.15, which is slightly higher than the range of 0.12-0.14 reported by Vickery and Pike [8] for stormy ocean conditions.

3 Wind Coefficients from Published Literature

Wind coefficients from published literature provide useful comparisons with values used in stability standards. Table 1 gives a summary of two separate sets of wind coefficients presented by Blendermann [4] and Gould [5].

Table 1: Published Force Coefficients for Beam Winds

	Blendermann [4]	Gould [5]
Ship types	Various	Merchant
Target wind profile	Uniform	Uniform, gradient
Reference wind speed	Uniform	Defined by Eq. 2
Lateral force coefficient C_Y		
Mean	0.87	0.95
Standard deviation	0.08	0.09
Number of ships	15	23
Height of centre of force h_{ay}/h_{cy}		
Mean	1.47	
Standard deviation	0.54	
Number of ships	17	

Despite the different wind conditions and reference velocities, the force coefficients values from Blendermann and Gould are quite similar. The small standard deviations for the data sets are surprising when one considers the large variety of ship geometries in each data set. Variability of force coefficients would likely be even smaller for a given ship type (e.g. naval frigates). The lateral force coefficient of 1.15 used in naval stability standards appears to be reasonable, but is greater than a value of 0.85 reported by Blendermann for a naval destroyer.

In contrast to the consistent force coefficient values, Table 1 indicates that the height of the centre of lateral force relative to the centre of area, h_{ay}/h_{cy}, varies greatly. The mean value of h_{ay}/h_{cy} is also much larger than the nominal value of unity suggested by stability standards. Consequently, naval stability standards probably under-estimate wind heeling moment. Wind tunnel studies by Kinoshita and Okada

[7] indicate h_{ay}/h_{cy} values of approximately 1.3. Relatively few other data for h_{ay}/h_{cy} exist in the open literature for confirmation of Blendermann's values. Note that Blendermann reports a relatively low value of 1.1 for a naval destroyer.

When modelling the variation of wind heeling moment with heel angle, Equation (1) assumes a $\cos^2\phi$ relationship, suggesting that heeling moment approaches 0 as heel angle approaches 90 degrees. It is likely that the $\cos^2\phi$ model under-estimates heeling moment at larger angles. Indeed, experimental results from Kinoshita and Okada suggest that the wind moment at large heel angles can be approximately 40 percent of the moment at zero heel angle, as shown in Figure 2.

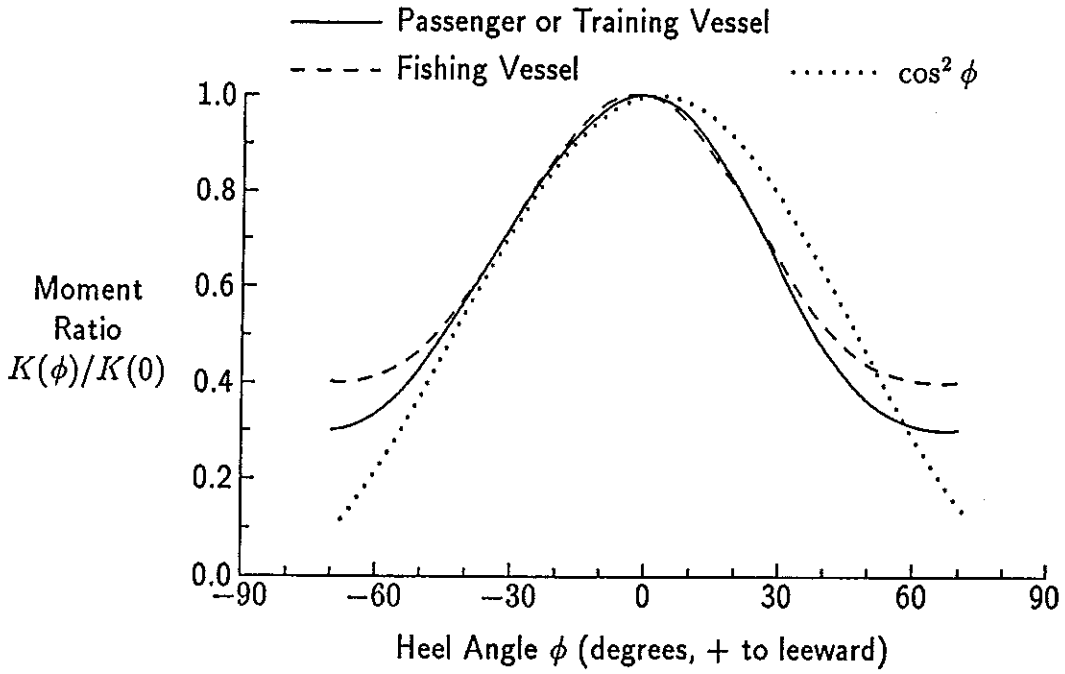

Figure 2: Observed Trends for Variation of Heeling Moment with Heel Angle (from Kinoshita and Okada [7])

4 Design of Experiments for Wind Loads on a Naval Frigate

The scarcity of experimental data for wind heeling loads prompted an experimental study to aid with assessment of wind load criteria for naval frigates. The location of the centre of heeling force and the variation of heeling moment with heel angle were the main parameters for which additional experimental data were considered necessary. Other areas of interest included lateral force coefficients, the variation of heeling moment with wind direction, and dynamic wind loading effects. References 8, 9, and 10 were very useful when designing the experiments.

4.1 Test Program

Wind tunnel tests were conducted in the 2 m by 3 m wind tunnel of the Applied Aerodynamics Laboratory of the National Research Council of Canada. Initial tests surveyed the test wind conditions, which were designed to simulate the wind profile over the ocean surface. The second phase of the experimental program measured wind loads acting on a generic frigate model for various heel angles and wind directions. Wind directions ranged from 0 to 360 degrees relative to the bow, with 15 degree increments. The third phase consisted of measurements of dynamic wind loads acting on the ship. The ship heel angles for both mean and dynamic load tests were 0, 20, 40, 60, and 70 degrees. The dynamic measurements were limited to beam winds because of the large amount of data collection and processing. Due to asymmetry, dynamic force measurements were made with the ship heeling to both leeward and windward.

The dynamic measurements have not yet been analysed and are not included in the present paper. Mean wind loads are generally much greater and more important than dynamic wind loads for stability analysis. An example calculation in Reference 11 for a naval destroyer in severe winds (80 knots) gives the RMS dynamic wind force as being only 15 percent of the mean wind force.

4.2 Generic Frigate Model

To encourage utilization of the wind tunnel test results, a relatively simple model representative of contemporary naval frigates was desired. A hull form from the open literature combined with a new superstructure design was considered to be the most viable approach. The basic hull form is Design 24 of the NRC Fast Surface Ship series, as reported by Schmitke and Murdey [12]. Design 24 is typical of contemporary frigates, and includes a wide transom. The wind tunnel model has less freeboard than the model of Design 24 for hydrodynamic testing, with a level deck from the transom to midships and a deck sloping upward from midships to the bow. By necessity, the wind tunnel model has a more realistic representation of the deck location for a real ship. Figure 3 shows the offset lines for the hull with the modified deck.

The superstructure consists of three modules representing a hangar, exhaust system, and bridge. Dimensions for the superstructure modules are based on a review of contemporary NATO frigates. Principal dimensions for the frigate are given in Table 2. Figure 4 shows plan and profile views of the frigate, including the superstructure, waterline, centroid of lateral above-water area, and wind direction convention. The average lateral height given in Table 2 is defined as:

$$\overline{H}_y = \frac{A_{ay}}{L} \tag{4}$$

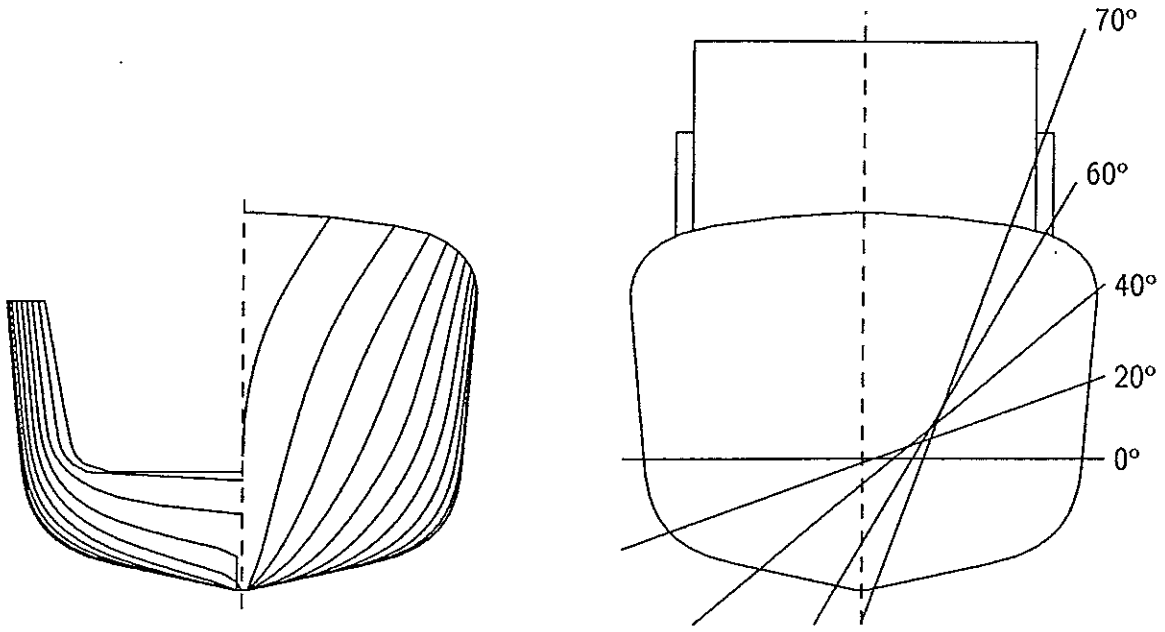

Figure 3: Body Plan and Waterlines for Frigate Wind Tunnel Model

Table 2: Principal Dimensions for Generic Frigate

Length between perpendiculars, L	108.5 m
Draft, T	3.89 m
Beam, B	12.8 m
Displacement, $\triangle$	2853 tonnes
Lateral wind area, A_{ay}	954 m^2
Height of area centroid, h_{cy}	4.83 m
Average lateral height, $\overline{H}_y$	8.79 m

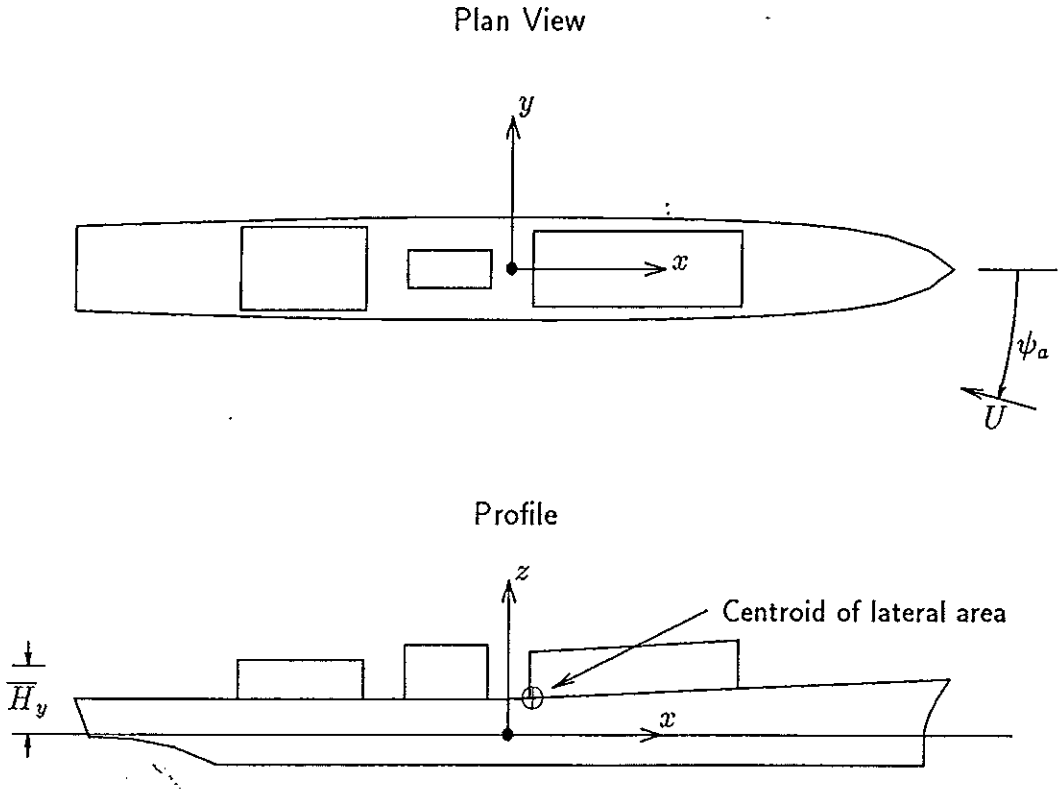

Figure 4: Plan View and Profile of Generic Frigate

A separate wind tunnel model of 1/300 scale was built for each heel angle. Each model was milled from high-density foam, into which an aluminum rib was inserted to permit mounting on a wind tunnel balance. Due to the light weight of each model, the natural frequency of the balance-model system was sufficiently high to not interfere with dynamic wind load measurements. Figure 3 shows waterline locations for the various ship heel angles. These waterline locations are based on constant displaced volume, but do not account for variation of longitudinal trim with heel angle. The ship could be expected to trim by the bow due to heel, which would have only a very small effect on lateral wind force and roll moment, but a larger effect on yaw moment due to changes to the longitudinal centre of lateral area.

4.3 Wind Environment

Two primary considerations influenced the selection of the wind tunnel conditions for the experiments. Firstly, experimental Reynolds numbers had to be sufficiently high to model the interaction between the wind and the ship. Secondly, the wind conditions generated by the wind tunnel had to be representative of winds over the open ocean. For measurements of mean wind loads, simulation of the mean wind velocity profile is necessary. Dynamic wind loads introduce additional requirements for modelling of turbulence intensity and the wind velocity spectrum.

For selection of a suitable model scale, gust sizes in the wind tunnel were of primary importance for matching model and prototype conditions during dynamic tests. Previous wind tunnel studies provided useful guidelines. Vickery and Pike [8] used a scale of 1/400 for determining dynamic wind loads on an offshore platform. Laurich [13] reports a model scale of 1/100 for dynamic testing of an offshore platform. A scale of 1/300 was selected for the present study, with a free-stream wind tunnel velocity of 60 m/s. The resulting Reynolds number of 0.41×10^6 based on $\sqrt{A_{ay}}$ was considered sufficiently high with the levels of turbulence present to model the wind flow around the ship.

Simulation of the wind velocity profile over the ocean surface can be achieved by placing vertical spires at the upstream end of the wind tunnel or by placing a rough surface on the wind tunnel floor. Due to the relatively short wind tunnel test section, spires were selected for the present set of experiments. A wind profile exponent α in the range of 0.12-0.14 was selected to model severe ocean wind conditions [8].

To simulate dynamic wind effects properly, it is necessary to model both turbulence intensity distribution and the turbulence spectrum. The turbulence intensity is expressed as a function of height:

$$I(z) = \frac{\sigma_{u_a}(z)}{\overline{U}_a(z)} \tag{5}$$

where I is turbulence intensity, and σ_{u_a} is the RMS velocity fluctuation. Observed wind profiles indicate that the fluctuation component σ_{u_a} can be considered independent of elevation in the vicinity of a ship, while $I(z)$ will vary due to variation of $\overline{U}_a$ with elevation. References 8 and 13 indicate that the turbulence intensity at a reference elevation of 10 m (full-scale) should be in the range of 0.12-0.15 for severe ocean environments.

The non-dimensional spectrum of longitudinal velocity fluctuations must be the same for model and prototype, such that:

$$\left[\frac{f\ S_{u_a}(f')}{\sigma^2_{u_a}}\right]_{model} \approx \left[\frac{f\ S_{u_a}(f')}{\sigma^2_{u_a}}\right]_{prototype} \quad (6)$$

where is f is frequency, S_{u_a} is spectral density, and f' is dimensionless frequency given by:

$$f' = \frac{f\ z}{\overline{U}_a(z)} \quad : \quad (7)$$

Based on wind spectra reported by Ochi [14], the peak frequency of the dimensionless spectrum $f\ S_{u_a}(f')/\sigma^2_{u_a}$ should fall in the following range:

$$0.004 \leq f'_{max} \leq 0.04 \quad (8)$$

A full-scale elevation of 10 m is suitable for matching of model and prototype spectra. The wind velocity spectrum is dependent on the properties of a given wind tunnel and often determines what model scale must be used for dynamic testing. For example, the model scale of 1/400 reported by Vickery and Pike [8] is commonly used for dynamic measurements of models within the earth boundary layer. A model scale of 1/300 provided suitable spectral modelling at the facility used for the current set of experiments.

4.4 Instrumentation

Measurement of the wind environment and forces acting on the ship were the two main areas for which instrumentation was required. A pitot tube monitored reference wind velocity near the model at an elevation corresponding to 10 m at full scale. Hot-wire anemometers mounted on a vertical traversing system measured wind speed for evaluating velocity profiles, turbulence intensity, and longitudinal velocity spectra.

A six-component dynamic balance having a fundamental frequency of 80 Hz was used to measure the mean and dynamic wind forces acting on the ship. The natural frequency of the balance was sufficiently high not to interfere with measured wind load spectra.

5 Experimental Results

5.1 Measured Wind Environment

Several different spire configurations were tested to obtain optimal modelling of the ocean wind environment. The final configuration consisted of six spires placed across the 3 m wide test section at a location 3 m upstream of the ship model. Each spire was a triangular plate, with a base width of 0.064 m and a height of 0.69 m. Figure 5 shows the resulting velocity profile, with the reference elevation being the top of the spires, height h_s. The fitted wind profile exponent $\alpha = 0.13$ is within the desired range of 0.12-0.14. The turbulence intensity was 0.11 at an elevation of 10 m full-scale, slightly below the desired range of 0.12-0.15. The peak frequency of the measured spectrum was within the desired range of $0.004 \leq f' \leq 0.04$.

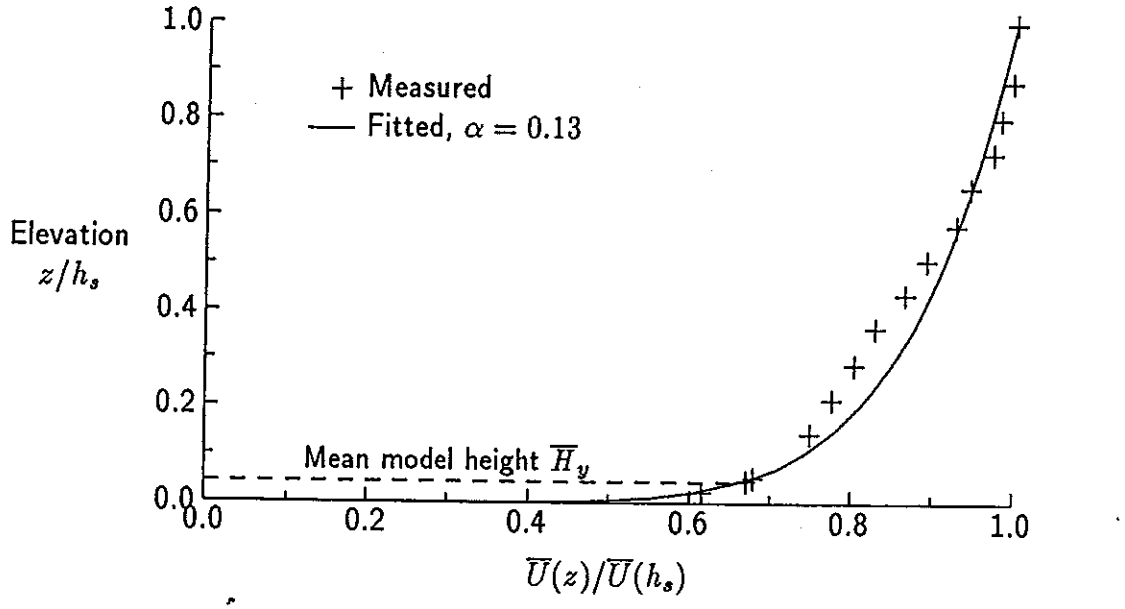

Figure 5: Profile of Mean Wind Velocity

5.2 Mean Wind Loads

Mean wind loads for all six degrees of freedom were measured during the experiments. The origin for the ship-based coordinate system was located in the waterline plane at midships as shown in Figure 4. Figure 4 also shows the direction convention for wind angle, with 0 degrees representing head winds. The coordinate system was always aligned horizontally/vertically and did not heel with the model. The moment components follow the right hand rule. The ship is heeling to leeward for wind angles of 0 - 180 degrees.

Lateral force and heeling moment are of primary concern in the present study; thus, lateral area A_{ay} and height of centroid of lateral wind area h_{cy} are used to non-dimensionalize forces and moments as follows:

$$C_Y = \frac{Y}{1/2\ \rho\ \overline{U}_r^2\ A_{ay}} \tag{9}$$

$$C_K = \frac{K}{1/2\ \rho\ \overline{U}_r^2\ A_{ay}\ h_{cy}} \tag{10}$$

where C_Y is the lateral force force coefficient, and C_K is the heeling moment coefficient. These coefficients allow the centre of lateral force relative to the centre of lateral area to be evaluated as follows:

$$\frac{h_{ay}}{h_{cy}} = \frac{C_K}{C_Y} \tag{11}$$

During on-line processing of data, force coefficients were output based on measured mean velocity $\overline{U}_{10}$ at a full-scale height of 10 m, which differs from the reference velocity given by Equation (2). The ratio $\overline{U}_r^2/\overline{U}_{10}^2$, which is the ratio between force coefficients computed using $\overline{U}_{10}$ and $\overline{U}_r$, is as follows:

$$\frac{\overline{U}_r^2}{\overline{U}_{10}^2} = \frac{1}{A_{ay}} \int \left(\frac{z}{10}\right)^{2\,\alpha} dA \tag{12}$$

If the ship area is integrated as a series of vertical strips of height h, then the velocity ratio is:

$$\frac{\overline{U}_r^2}{\overline{U}_{10}^2} = \frac{1}{A_{ay}\ 10^{2\alpha}\ (2\alpha+1)} \int_L h^{2\alpha+1}\ dx \tag{13}$$

For the frigate in beam winds with a velocity profile exponent of 0.13, $\overline{U}_r^2/\overline{U}_{10}^2$ has a value of 0.78. Consequently, the initial force and moment coefficients based on $\overline{U}_{10}$ were divided by 0.78 to obtain coefficients based on $\overline{U}_r$. This large factor provides an estimate of the force difference that would be measured between a uniform and a sheared profile, and demonstrates the importance of modelling the non-uniform velocity profile.

Figure 6 shows the lateral force coefficients versus wind direction at the five test heel angles. The force coefficients presented in Figure 6 are limited to wind directions with the ship heeling to leeward, which is the most common case. Figure 7 gives the lateral force coefficient versus heel angle for beam winds, and includes values for the ship heeling to both windward and leeward. The highest lateral force coefficient value of 1.36 occurred for a wind direction of 60 degrees with the ship heeling 20 degrees to leeward. Lateral force coefficients are relatively insensitive to wind direction for

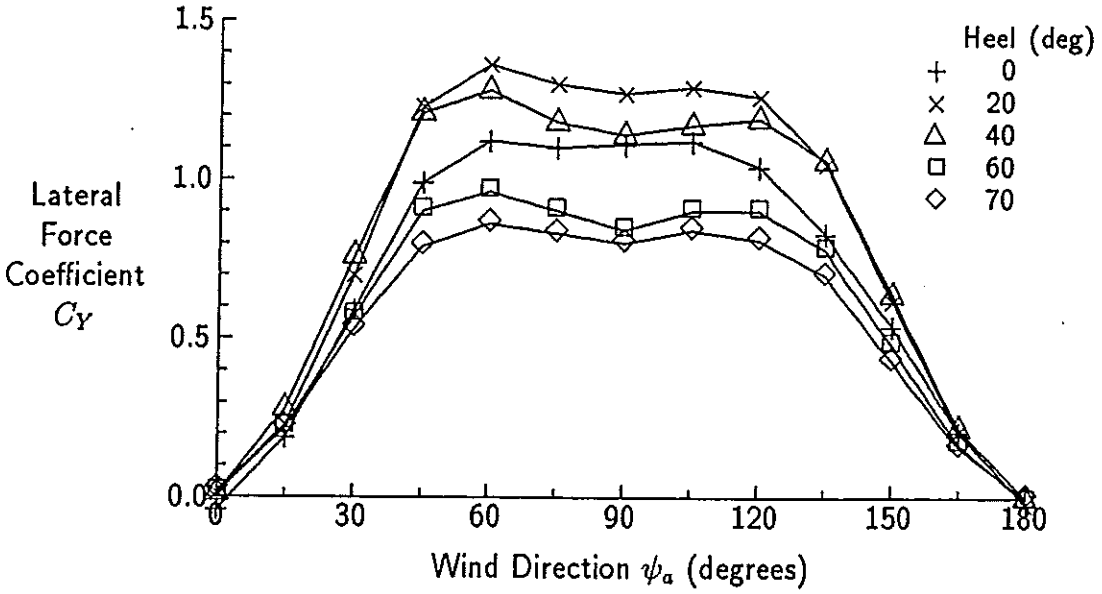

Figure 6: Lateral Force Coefficient Versus Wind Direction

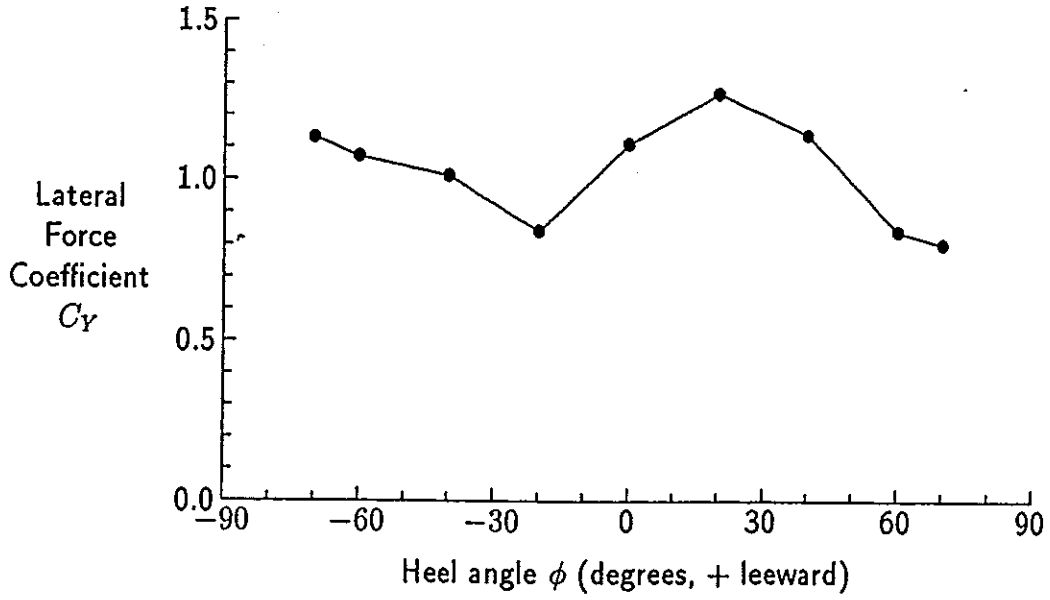

Figure 7: Lateral Force Coefficient Versus Heel Angle in Beam Winds

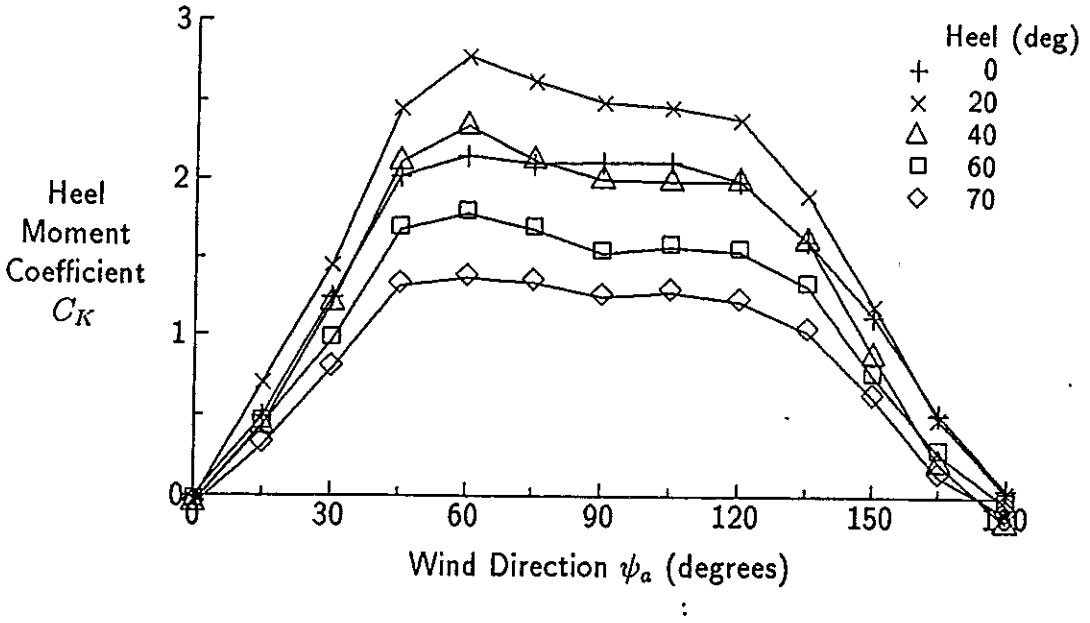

Figure 8: Heeling Moment Coefficient Versus Wind Direction

directions within 45 degrees of beam winds. The lateral force coefficients are also relatively insensitive to heel angle, likely because the lateral ship profile does not vary greatly with heel angle.

Heeling moment coefficients as functions of wind direction and heel angle are given in Figures 8 and 9 respectively. The largest heeling moment coefficient of 2.76 occurs at the same wind direction (60 degrees) and heel angle (20 degrees) as the largest lateral force coefficient. Like lateral force coefficients, moment coefficients are relatively insensitive to wind direction in the vicinity of beam winds. The moment coefficients are more sensitive than the force coefficients to heel angle.

Figures 10 and 11 give the dimensionless heeling moment arm h_{ay}/h_{cy} for all directions and for beam winds only. The dimensionless moment arm is relatively insensitive to wind direction and heel angle. The large variations of h_{ay}/h_{cy} near wind directions of 0 degrees and 180 degrees are relatively unimportant because the total heel moment is small at these directions, as shown in Figure 8. These large variations likely result from the effects of experimental errors on taking ratios of two small numbers.

6 Assessment of Current Wind Stability Criteria

The wind tunnel experimental results reported in this paper provide a useful source for verification of wind criteria used in current naval stability standards [1, 2].

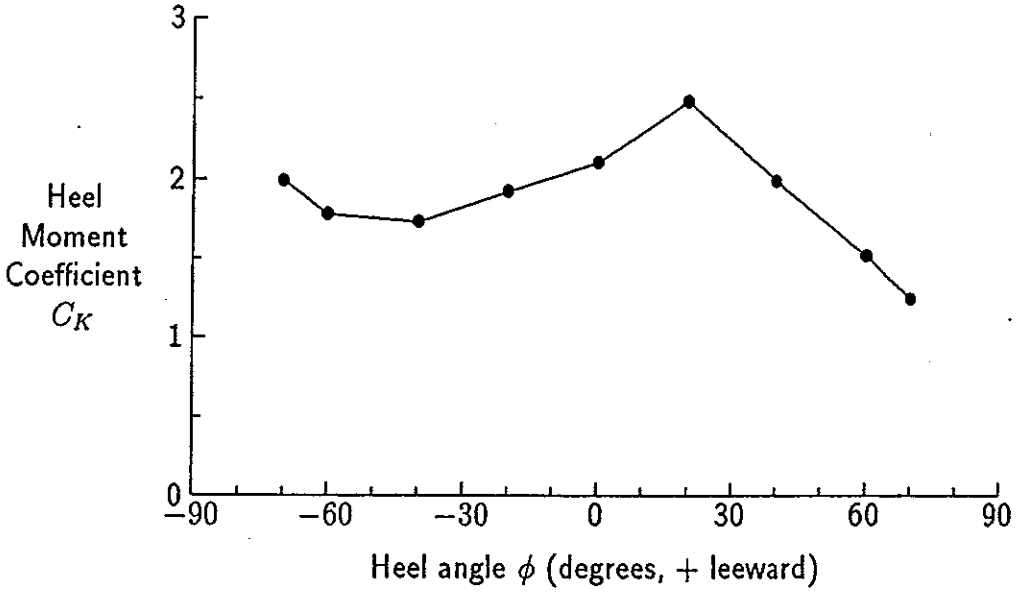

Figure 9: Heeling Moment Coefficient Versus Heel Angle in Beam Winds

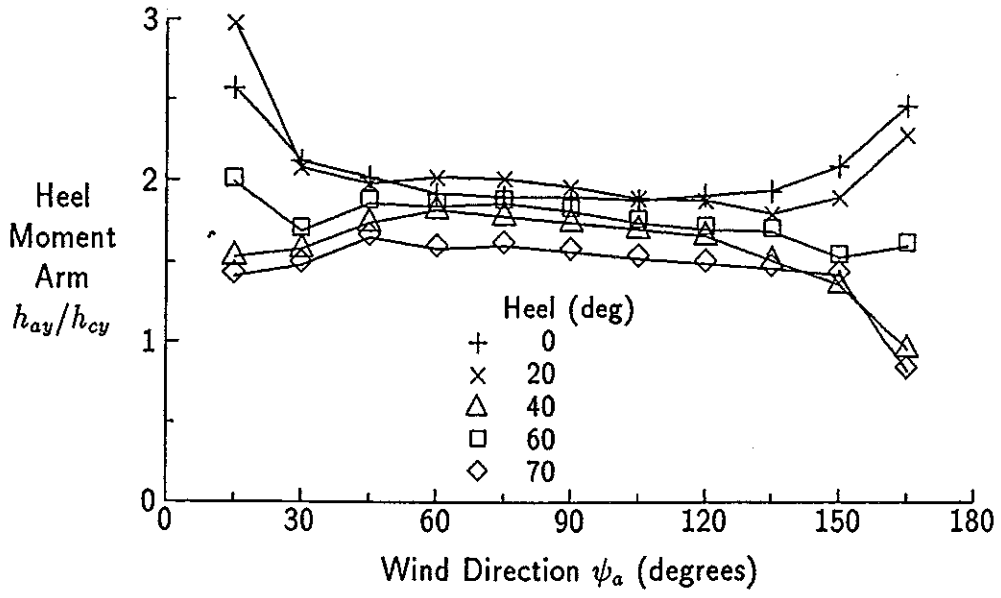

Figure 10: Dimensionless Heeling Moment Arm Versus Wind Direction

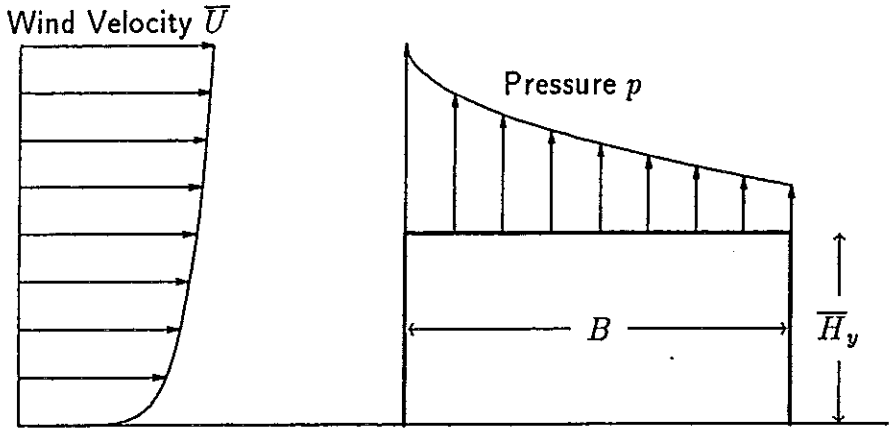

Figure 13: Schematic of Wind Pressure Distribution on Top of Ship in Beam Winds

arise from two sources. The first source is the wind velocity profile, which causes pressures to be greater near the top of the model. The second cause of the large moment arms is the wind pressure distribution along the top of the ship. Based on data in Simiu and Scanlan [9], Figure 13 shows a plausible form of the wind pressure distribution across a vertical cross-section of the ship in beam winds. The variation of suction across the top induces a heel moment in the same direction as the contribution from the lateral force, thus increasing the effective wind moment arm based on lateral force. This contribution would likely increase with increasing ship beam, as demonstrated by the experimental data of Figure 12.

Equation (1) from naval stability standards significantly under-estimates the wind heel arm acting on a ship. A more realistic approach would be to prescribe h_{ay}/h_{cy} as a function of dimensionless beam $B/\overline{H}_y$, as shown in Figure 12.

6.5 Influence of Heel Angle

Figure 9 shows that wind moment for the generic frigate exhibits little variation with heel angle. Experimental trends from Kinoshita and Okada [7] in Figure 2 show larger reductions in wind moment at larger heel angles. Both data sets indicate that the $\cos^2\phi$ term in Equation (1) causes the heeling moment to be greatly under-estimated at larger heel angles. Wind tunnel data should be obtained for additional ships to develop a suitable relationship for modelling the variation of wind moment with heel angle.

7 Conclusions

The present set of experiments provides further wind tunnel data for improving stability standards for naval frigates. The experimental conditions modelled the wind boundary layer over the ocean surface. The large observed heeling moment arms are consistent with other experimental investigations and are much greater than moment arms used in naval stability criteria. The current results and those from another investigation indicate that current stability criteria under-predict heeling moment, particularly at large heel angles. In general, the discrepancies between the present stability criteria and wind tunnel observations indicate that stability criteria need to be revised to model wind loading more accurately. Additional wind tunnel testing of naval vessels could provide a suitable basis for developing improved wind criteria.

References

[1] T.H. Sarchin and L.L. Goldberg, "Stability and Buoyancy Criteria for U.S. Naval Surface Ships," *Transactions, Society of Naval Architects and Marine Engineers* **70**, 418–458 (1962).

[2] "Stability and Buoyancy Requirements - Canadian Armed Forces Surface Ships," Technical Report C-03-001-024/MS-002, Department of National Defence (Canada), August 1991.

[3] J.O. de Kat, E.M. Krikke, K. McTaggart, and L. Thomas, "Intact Ship Survivability in Extreme Waves: Criteria from a Research and Navy Perspective," in *STAB '94, Fifth International Conference on Stability of Ships and Ocean Vehicles* (Melbourne, Florida, 1994).

[4] W. Blendermann, "Wind Loads on Moored and Manoeuvring Vessels," in *Twelfth International Symposium on Offshore Mechanics and Arctic Engineering* (Glasgow, 1993), Vol. 1, pp. 183–189.

[5] R.W.F. Gould, "The Estimation of Wind Loads on Ship Superstructures," Maritime Technology Monograph 8, Royal Institution of Naval Architects, 1982.

[6] R.M. Isherwood, "Wind Resistance of Merchant Ships," *Transactions, Royal Institution of Naval Architects* **115**, 327–338 (1973).

[7] M. Kinoshita and S. Okada, "Heeling Moment Due to the Wind Pressure on Small Vessels," in *Proceedings, Symposium on the Behaviour of Ships in a Seaway* (Wageningen, 1957), pp. 527–542.

[8] B.J. Vickery and P.J. Pike, "An Investigation of Dynamic Wind Loads on Offshore Platforms," in *Offshore Technology Conference* (Paper OTC 4955, Houston, 1985).

[9] E. Simiu and R.H. Scanlan, *Wind Effects on Structures - An Introduction to Wind Engineering*, John Wiley & Sons, 1978.

[10] SNAME Panel OC-1 (Stability and Motions Technology), "Guidelines for Wind Tunnel Testing of Mobile Offshore Drilling Units," SNAME Technical & Research Bulletin 5-4, Society of Naval Architects and Marine Engineers, August 1988.

[11] K.A. McTaggart, "Wind Effects on Intact Ship Stability in Beam Seas," in *Progress in Engineering, Proceedings of the Eighth International Conference on Wind Engineering* (London, Ontario, 1991), pp. 2487–2498. Proceedings published in Journal of Wind Engineering and Industrial Aerodynamics, Volumes 41-44 (1992).

[12] R.T. Schmitke and D.C. Murdey, "Seakeeping and Resistance Trade-Offs in Frigate Hull Form Design," in *Thirteenth Symposium on Naval Hydrodynamics* (Tokyo, 1980).

[13] P.H. Laurich, "A Wind Simulation System for the Ocean Ranger Hydrodynamic Model Study," in *Offshore Technology Conference* (Paper OTC 5361, Houston, 1987).

[14] M.K. Ochi, "Turbulent Winds and Forces for Consideration of Stability of Marine Systems," in *STAB '90, Fourth Conference on Stability of Ships and Marine Vehicles* (Naples, 1990).

Complete Six-degrees of Freedom Nonlinear Ship Rolling

J. M. Falzarano, Assistant Professor
Marine Dynamics Laboratory
Naval Architecture and Marine Engineering
University of New Orleans, New Orleans, LA 70148

In order to overcome difficulties in using solely perturbation methods or numerical simulations to analyze large amplitude (nonlinear) ship roll motion, an alternative approach was used to study the effect of linear coupling between sway and yaw, and nonlinear rolling motion and the frequency dependence of the hydrodynamics (Falzarano, et al, STAB '90). This approach utilized numerical path following techniques to directly study the nonlinear three degree of freedom (sway, roll and yaw) asymmetric ship motions equations with linear frequency domain hydrodynamics on a frequency by frequency basis.

This paper will describe recent research which expands the previous work to consider the complete six-degrees of freedom equations of nonlinear ship motion including Euler angle kinematics. The current status of the physical modeling is that frequency dependent linear added mass, damping and wave exciting forces are supplemented by nonlinear restoring moment curves and a harmonic (i.e., a one term) approximation to the parametric excitation due to vessel flare at the waterline. Although studying the bounded steady state behavior will be an important result of this project, this work will also include an assessment of the local stability of these bounded solutions.

Background and Motivation

One of the most fundamental concerns of an engineer is to evaluate the required level of accuracy of his/her design and analysis procedures. The practicing engineer must often compromise between highly accurate analysis techniques and approximate techniques. The more exact techniques require both that the design be finalized enough to describe the vessel in enough detail and subtsantail time to implement on the fastest of computers. While the approximate techniques may be time efficient they may not be able to adequately decribe the phenomenon under consideration. With the tremendous progress in computer software and hardware recently achieved, what was once unthinkable in terms of analysis is now common. As a result, engineers are no longer restricted to simple empirically based design formulas. It may now be possible to utilize physically based design and analysis techniques early on in the design spiral.

One of the most critical considerations in the design of any vessel or floating platform is that object's resistance to capsizing. To date, the state of the art in vessel stability regulation and therefore often design are statically based stability criteria. Although this may not be the case for floating offshore drilling units (Falzarano and Zhang, 1994). Alternatively, state-of-the-art ship motions design and analysis is usually done using linear ship motions computers programs. The linearity of small amplitude motions makes available relatively accessible linear systems theory and makes simplified random response analysis possible. However, ship capsizing is a highly nonlinear (global) transient dynamic phenomenon. Classical techniques of analyzing nonlinear systems using perturbation techniques and mathematical stability theory are therefore wholefully inadequate since they are both difficult to apply and restricted to weakly nonlinear systems.

An alternative which can solve much more general systems is numerical simulation. Using numerical simulation, much valuable insight can be gained into the underlying physics and the relative importance of various force contributions and response modes. By systematically varying vessel and environmental conditions parametric studies can be performed and an optimal hull-form can be selected; however this somewhat brute force approach can quickly become excessively time consuming unless a systematic method guided by some knowledge of the critical system behavior.

In order to avoid extensive computer simulation times or alternatively using excessively simplified modelling, an alternative approach which can be used to directly study critical system dynamics can be utilized. This methodology has recently been developed and applied to study various types of marine dynamical systems. This methodology consists of using two complementary approaches for a fixed vessel configuration; the first part consists of utilizing numerical path following techniques to track how steady state motion amplitudes vary with frequency and the second part consists of studying the safe basin boundary for a fixed environmental description. The first part identifies critical behavior by simply monitoring the character of the steady state solutions as frequency and wave amplitude are varied. Once the critical wave frequency and amplitude condition is identified, the Poincaré map is used analyze the system in detail.

Ship Dynamics Modelling

In this section, we briefly describe the various equations of motion studied. However, for the sake of brevity we neglect many details which can be found in previous works by the same authors (e.g., Falzarano, 1990). By considering Newton's laws of motion in a body fixed system (Figure 1), the full nonlinear coupled equations of rigid body motion are obtained,

$$X = m[\dot{u}+qw-rv-x_G(q^2+r^2)+z_G(pr+\dot{q})]$$

$$Y = m[\dot{v}+ru-pw+x_G(pq+\dot{r})+z_G(qr-\dot{p})]$$

$$Z = m[\dot{w}+pv-qu+x_G(rp-\dot{q})-z_G(p^2+q^2)] \qquad (1)$$

$$K = I_{44}\dot{p}-(I_{55}-I_{66})qr-I_{64}(\dot{r}+pq)-mz_G(\dot{v}+ru-pw)$$

$$M = I_{55}\dot{q}-(I_{66}-I_{44})rp-I_{64}(r^2-p^2)+mz_G(\dot{u}+qw-rv)-mx_G(\dot{w}+pv-qu)$$

$$N = I_{66}\dot{r}-(I_{44}-I_{55})pq-I_{64}(\dot{p}-qr)+mx_G(\dot{v}+ru-pw)$$

Where (u,v,w) are the body fixed translational velocities and (p,q,r) are the body fixed rotational velocities. These equations are often called Euler's equation of motion and are derived in a variety of references, (see e.g. Abkowitz, 1969). For small amplitudes of motion, it is sometimes possible to linearize these equations. The linearized equations of motion and are as follows,

$$X = m[\dot{u}+z_G\dot{q}]$$

$$Y = m[\dot{v}+x_G\dot{r}+z_G\dot{p}]$$

$$Z = m[\dot{w}-x_G\dot{q}] \qquad (2)$$

$$K = I_{44}\dot{p}-I_{64}\dot{r}-mz_G\dot{v}$$

$$M = I_{55}\dot{q}+m(z_G\dot{u}-x_G\dot{w})$$

$$N = I_{66}\dot{r}-I_{64}\dot{p}+mx_G\dot{v}$$

Although, various representations of the forces (X,Y,Z) and moments (K,M,N) on the left hand side of these systems of equations are possible, for simplicity, this analysis uses the standard seakeeping assumptions and considers small amplitudes of motion in an ideal fluid. These normal forces and moments are then obtained by integrating the pressure over the body surface. First order terms proportional to unit body motion (displacement, velocity and acceleration) and incident wave amplitude are obtained. Forces proportional to unit body displacement are the hydrostatic forces

C, forces proportional to unit body acceleration are called the added mass forces A, and forces proportional to unit body velocity are called damping forces B. The forces due to the incident wave are called wave exciting forces $\underline{F}(t)$. The matrix M is made up of the physical mass or inertias about the specific axis plus the inertial and coordinate coupling. The elements of the matrices A_{ij}, B_{ij}, and C_{ij} are the forces in the *i-th* mode of motion due to unit motion (displacement, velocity and acceleration) in the *j-th* direction. The mass matrix M_{ij} contains the appropriate mass, and inertial or coordinate coupling terms. The subscripts refer to the mode of motion and are: 1=surge, 2=sway, 3=heave, 4=roll, 5=pitch, 6=yaw. Considering all these forces, the well-known frequency domain representation of the seakeeping equations, a matrix representation of the system, are obtained,

$$(M + A(\omega))\ddot{X} + B(\omega)\dot{X} + CX = F(t) \qquad (3)$$

Note that in the linearized equations of motions, no inertial coupling exists between the symmetric (surge, heave and pitch) and asymmetric (sway, roll and yaw) modes of motion, moreover no other coupling exist between these two sets of modes. So only the sway, roll and yaw equations of motion need to be considered to study the small to moderate amplitude of motion in order to determine the effect of other modes on roll.

The decoupling process described by Webster (1989) and utilized by Falzarano and Zhang, (1993) is essentially determing the principle coordinates neglecting the nonlinearity, damping and forcing. It is unique because the sway and yaw have no restoring force. The process is accomplished in two steps. The first step is to move the origin of the coordinate system to the virtual center of gravity, i.e., that which includes the hydrodynamic added mass. The next step invloves rotating the x-z axes about the new y axis in order to eliminate the roll yaw cross-products of inertia again including the hydrodynamic added mass cross coupling coefficients. If the decoupling process is undertaken as mentioned previously it may be possible to accurately consider the single degree of freedom roll equation of motion,

$$(I_{44}+A_{44}(\omega))\ddot{\phi}+B_{44}(\omega)\dot{\phi}+B_{44}q\dot{\phi}|\dot{\phi}|+\Delta GZ(\phi)=F_4\cos(\omega t+\gamma_4) \qquad (4)$$

Results for Two Small Ships

In the remainder of this paper, we intend to report on some recent developments made in analyzing complicated systems by simplifying these to more manageable simplified systems. The emphasis of these

studies is to study the effect of additional degrees of freedom and reducing to approximate lower degree of freedom systems. Also we include some previously unpublished results (Falzarano, 1990), to compare to some of the new results.

One and three Degree of Freedom Analysis of *Patti-B*

The first set of results that are included herein are for the crab boat *Patti-B*. Most of the results are for the vessel very slowly turning in regular waves. The frequency variation occurs due to the frequency of encounter effect, the excitation frequency varies from ω_{min} in following seas, to ω_o in beam seas, to ω_{max} in head seas. The first figure (Figure 2) compares the nonlinear multiple (three) degree of freedom (MDOF) results to linear MDOF results. The nonlinear MDOF results were obtained with the path-following continuation computer program BIFPACK (Seydel, 1989). The linear results were obtained using a linear ship motions program with an equivalent linearization of the nonlinear damping (Beck and Troesch, 1989). The linear program well approximates the nonlinear response except in the multi-valued region. The continuation computer program is not only able to capture the high and low amplitude steady states but also the intermediate amplitude saddle type solution. The saddle type solutions are particularly important in determining the basin boundaries.

The next figure (Figure 3) compares roll magnification curves for a range of metacentric heights GM. The GM varies from 1.5 foot to 1.9 foot. One can see how the curves change qualitatively as the GM is varied. Not only does the GM change the linear natural frequency and therefore move the response peak but also the higher GM curves are single valued while the lower GM curves are multi-valued. Actually the higher GM curves have a disconnected unstable branch that was cut-off from the main curve as the GM was increased (Falzarano, 1990).

The next figure (Figure 4b) compares the nonlinear single degree of freedom (SDOF) modelling to the nonlinear MDOF modelling for two wave amplitudes. The smallest curve is for MDOF and η=5'. The MDOF η=7.5' and SDOF η=5' curves are almost coincident. The SDOF η=7.5' is the largest curve. Also note that the SDOF η=7.5', has a cut-off resonant peak and therefore a disconnected unstable branch.

The next two curves are for the vessel at a fixed speed and heading and the wave length and frequency are varied. Figure 4b is the analogous set of results as the previous figure, but instead of the vessel heading changing the wave length and frequency are varied. However, the qualitatively similar behavior is evident. That is the MDOF is smaller in magnitude than the SDOF.

The next set of curves (Figure 5) evaluates the effect of using constant hydrodynamics coefficients over the entire frequency range versus varying the coefficients on a frequency by frequency basis.

One can see that the simplest modeling, the SDOF constant coefficients, yields the largest magnitude overall. Although this greatly simple modelling over-predicts for the lower frequencies and somewhat under-predicts for higher frequencies.

The final curve (Figure 6) is a plot of the largest eigenvalue of the map for the vessel turning problem for two wave amplitudes, η= 5' and η =7.5'.The two curves are suprizingly coincident over the stable single valued region and only depart when the large amplitude becomes multi-valued.

Three and Six Degree of Freedom Analysis of T-AGOS Roll
The next set of results are for the US Navy ocean survey vessel T-AGOS. These results are also for the vessel slowly turning in waves (Taz Ul Mulk and Falzarano, 1994). The importance of the additional degrees of freedom upon the steady-state roll is only quantitative and qualitative. that is the additional degrees of freedom only effects the magnitude of the roll response and does not introduce any additional critical behavior in the roll response. This is in contrast to the effect of the roll on the sway and yaw which is a qualitative effect. The roll effects the sway and yaw in that though the added mass and damping coupling the sway and yaw become multi-valued over the same frequency range as the roll.

Again the nonlinear inertial coupling of pitch and heave to the roll in Euler's equations of motion, does not effect the roll qualitatively only quantitatively. Moreover, the heave and pitch coupling effect on the roll is only apparent as the amplitude of the motion is large.

Figure 7 compares the linear three degree of freedom system (3DOF) system to the nonlinear SDOF system and the nonlinear 3DOF system. The linear 3DOF uses an equivalent linearization of the damping so it is well able to approximate the amplitude of the nonlinear 3DOF system except in the resonance region. The nonlinear SDOF and 3DOF systems utilize and accurate polynomial representation of the roll restoring moment curve. However, the SDOF simply neglects the linear added mass and damping sway and yaw cross-coupling terms. It then solves an single degree of freedom with simply the original ship motions coordinate system roll added mass and damping. Also note that the nonlinear SDOF and 3DOF are coincident at the resonant peak. Considering this peak is the nonlinear analogue to linear resonance and damping is the only restoring force at resonance, this implys that the damping coupling must be less important than the added mass coupling.

The next two companion figures (Figures 8 and 9) are plot of the sway and yaw velocity at time zero. Since these figures are associated with the nonlinear 3DOF calculation of the previous figure, note that they are multi-valued over the same frequency range as the nonlinear 3DOF roll in the previous figure (Figure 7). The next figure (Figure 10) is a plot of the nonlinear 3DOF roll

response as a function of wave amplitude. One can see that for small amplitudes η = 2 ft, the roll is single valued; as the amplitude is increased to η = 3.5 ft the roll becomes multi-valued over a finite frequency range. However, as the amplitude is increased again to η = 5 ft, the multi-valued region is squeezed to the lower frequency following sea region.

The final two figures in this set of results (Figures 11 and 12), are a comparison of nonlinear 3DOF modelling to two six degree of freedom (6DOF) modellings. One 6DOF modelling with linear heave and pitch hydrostatics and one has nonlinear heave and pitch hydrostatics. One can see that for small amplitudes of external wave forcing the three curves are coincident and as the wave amplitude and therefore the motion amplitudes increase, so does the difference amongst the three modellings

Transient Analysis and Decoupling of Roll Motion for *Patti-B*

For the global analysis of the transient roll motion the situation is quite similar (Falzarano and Zhang, 1993). The sway and yaw coupling to roll does not introduce any critical phenomena in the roll motion. In order to accurately include the effect of the sway and yaw coupling onto the roll, one needs to undertake the decoupling procedure described by Webster (1989). This procedure is essentially equivalent to determining the principle coordinates for roll. That is statically determining the roll coordinates which are independent of the sway and yaw. After undertaking this procedure, the roll response obtained from either the single degree of freedom or multiple degree of freedom differential equations of motion are not only qualitatively similar but very closely quantitatively similar.

The next set of results should demonstrate the effectiveness decoupling the nonlinear 3DOF system using the technique described by Webster (1989). The first comparison (Figure 13a) is of the SDOF roll response with the projection of the 3DOF response onto the roll- roll velocity plane both using the standard ship motions coordinate system with origin at amidships and the design waterline. One can see that although they are close at this frequency and wave amplitude they are not coincident. The second comparison (Figure 13b) in this section is the same results using uncoupled coordinates. One can see that these two curves are almost exactly coincident. These results should demonstrate the effectiveness of the uncoupling process described by Webster (1989) and utilized by Falzarano and Zhang (1993). One should note that although it is in general only possible to exactly decouple undamped/unforced systems and that general damped and forced can only approximately be decoupled. However for the case studied herein, the undamped/unforced approximation is quite close.

Conclusions

This work should be useful in accurately assessing ship rolling motion to improve vessel operations in moderate seaways and should be especially valuable in assessing a vessel's ultimate survivability in extreme weather conditions. In addition, this technique could be used as a framework to provide guidance when planning nonlinear ship motions experiments and simulations, so that the possibility of critical behavior can be predicted prior to performing such physical or numerical experiments. The results of this project should provide new insight into previously unexplained phenomena observed in large amplitude (highly nonlinear) ship motions model tests and computer simulations.

Acknowledgements

The authors would like to acknowledge the support of various funding agencies throughout the years these include the US Coast Guard, the Office of Naval Research and the national Science Foundation. We would also like to acknowledge all the various students who have contributed to these results. These students include M. Taz Ul Mulk, F. Zhang and K. Holappa. We would also like to acknowledge Prof. Troger and Seydel and Dr. Steindl for their advice and making available BIFPACK and Prof. Troesch and Beck for their advice and making available SHIPMO.

References

Falzarano, J. and Papoulias, F. *Nonlinear Dynamics of Marine Vehicles: Modelling and Applications,* Bound Volume to sessions, ASME Winter Annual Meeting, November 1993.

J. Falzarano, S. Shaw, and A. Troesch, "Application of Global Methods for Analyzing Dynamical Systems to Ship Rolling Motion and Capsizing," *International Journal of Bifurcation and Chaos in Applied Sciences and Engineering,* Vol 2, No. 1, March 1992.

J. Falzarano and F. Zhang, "Multiple Degree of Freedom Global Analysis of Transient Ship Rolling Motion," *ASME Winter Annual Meeting,* Symposium on Nonlinear Dynamics of Marine Vehicles, November 1993.

J. Falzarano, K. Holappa, and M. Taz Ul Mulk, "A generalized Analysis of Stauration Induced Ship Rolling Motion,"*ASME Winter Annual Meeting,* Symposium on Nonlinear Dynamics of Marine Vehicles, November 1993.

J. Falzarano, A. Steindl, A. Troesch, and H. Troger, "Rolling Motion of Ships Treated as a Bifurcation Problem," *Bifurcation and Chaos: Analysis, Algorithms and Applications*, Ed. by R. Seydel, et al., Wuezburg, Germany, May 1990, published by Birkhauser, Basel, Switzerland, May 1991.

J. Falzarano, A. Stiendl, A. Troesch and H. Troger, "Bifurcation Analysis of a Vessel Slowly Turning in Waves," *4th International Conference on the Stability of Ships Ocean Vehicles*, Naples, Italy, September 1990.

J. M. Falzarano and A. W. Troesch, "Application of Modern Geometric Methods for Dynamical Systems to the Problem of Vessel Capsizing with Water-on-deck," presented at: *4th International Conference on the Stability of Ships and Ocean Vehicles*, Naples, Italy, September 1990.

Falzarano, J.M, *Predicting Complicated Dynamics Leading to Vessel Capsizing,* Doctoral Dissertation University of Michigan, 1990.

Taz Ul Mulk M., and J. Falzarano " Large Amplitude Rolling Motion of an Ocean Survey Vessel," Accepted for publication in: *SNAME Journal of Marine Technology*, February 1994.

M. Taz Ul Mulk and J. Falzarano, "Complete Six Degrees of Freedom Nonlinear Ship Rolling Motion," Submitted to *ASME Journal of Offshore Mechanics and Arctic Engineering* June 1993.

Webster, W., *Principles of Naval Architecture* "Transerse Motions,". Society of Naval Architects and Marine Engineers, 1989

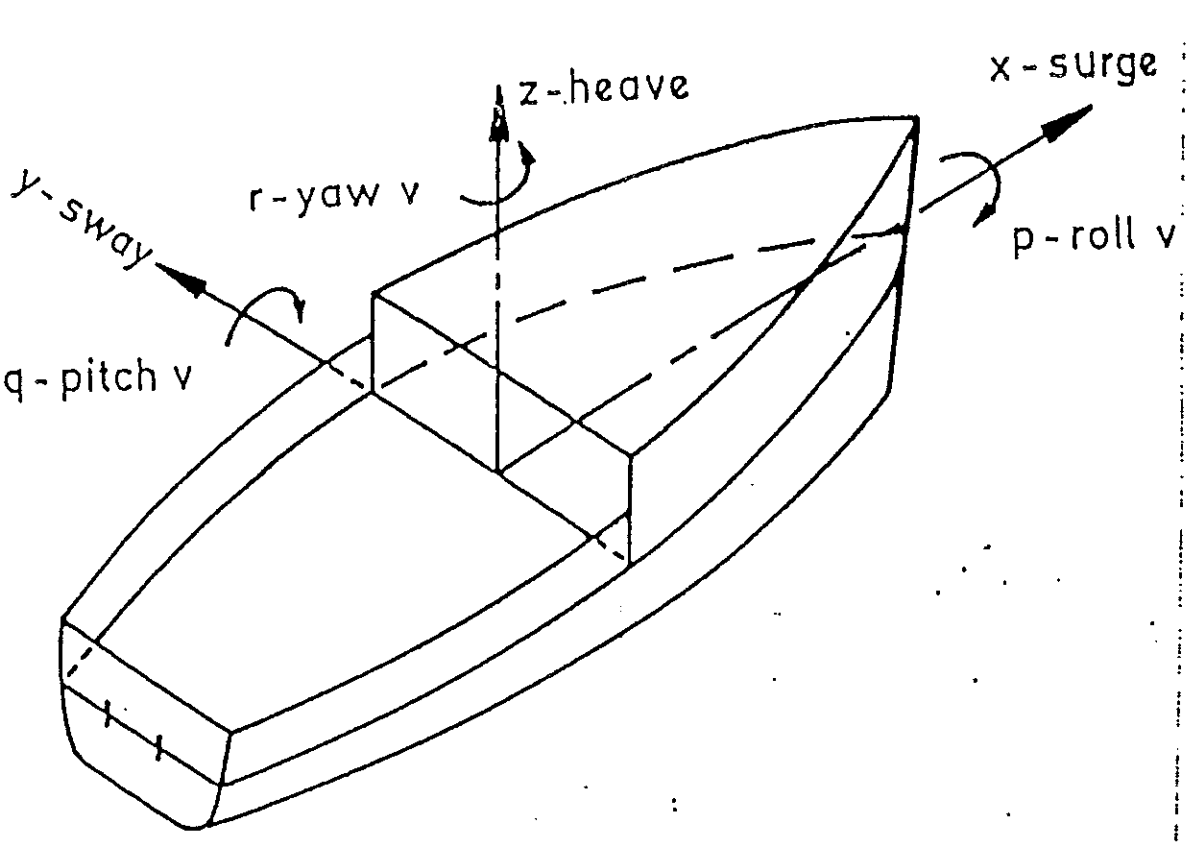

Figure 1 Standard ship motion coordinate system

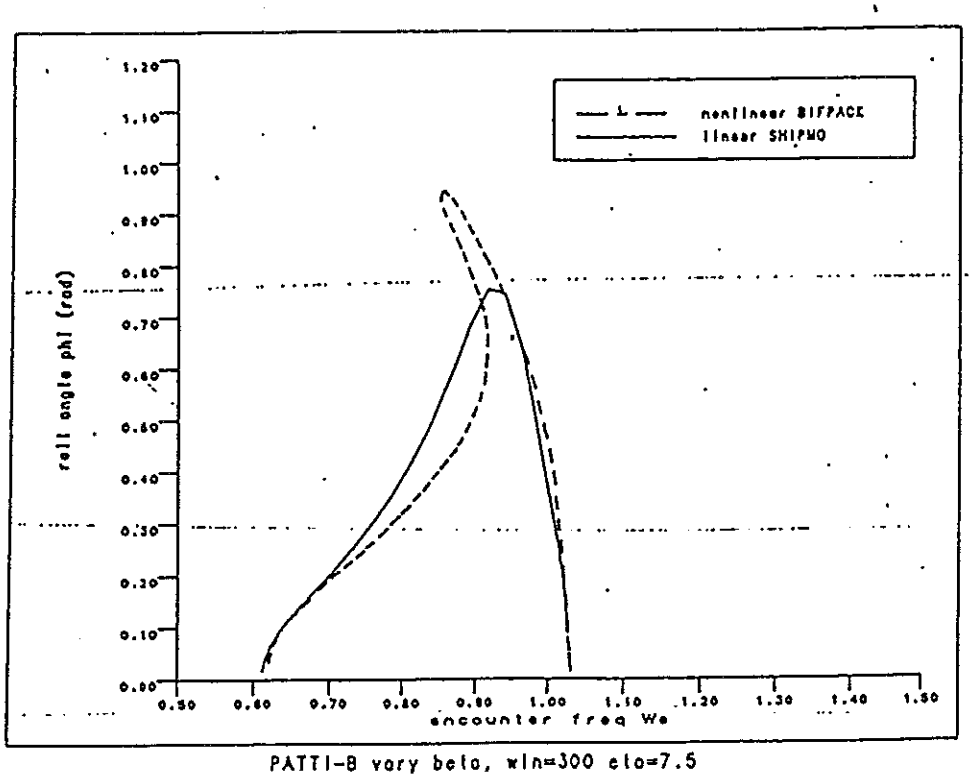

Figure 2 Comparison of linear and nonlinear solution

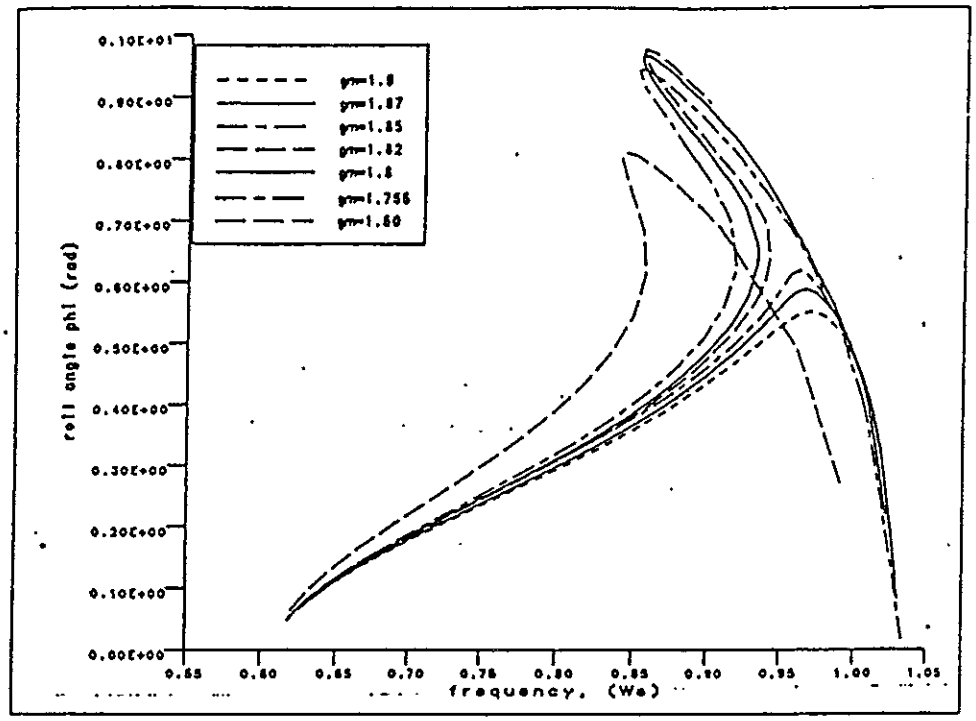

Figure 3 Nonlinear solution, note pinching off of the solution

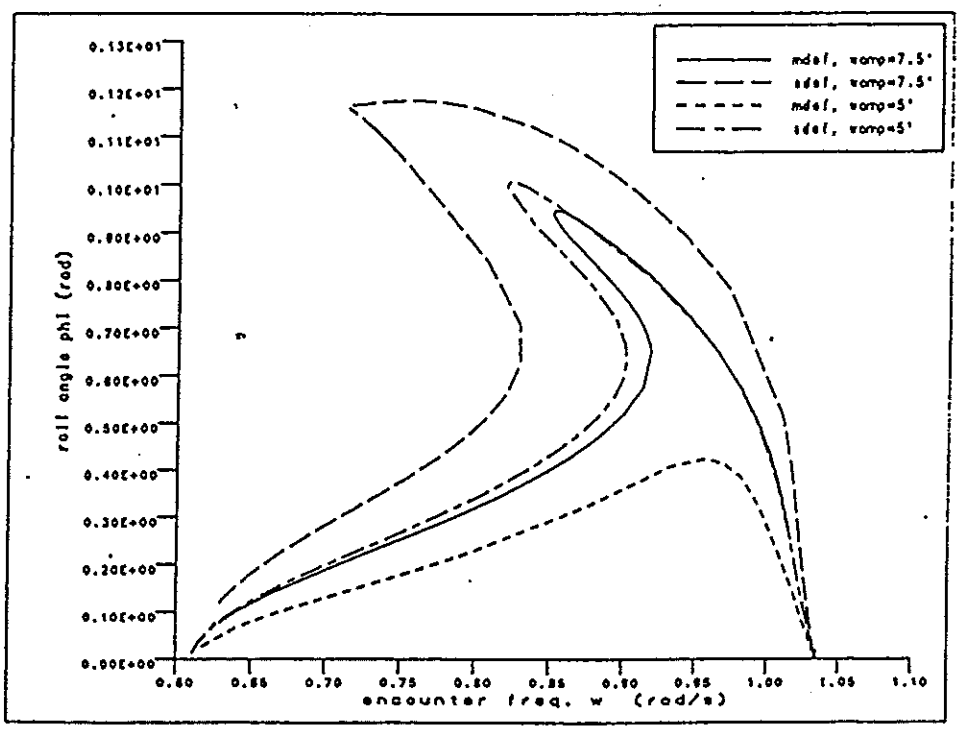

Figure 4a Single vs. multiple degree of freedom (vary β)

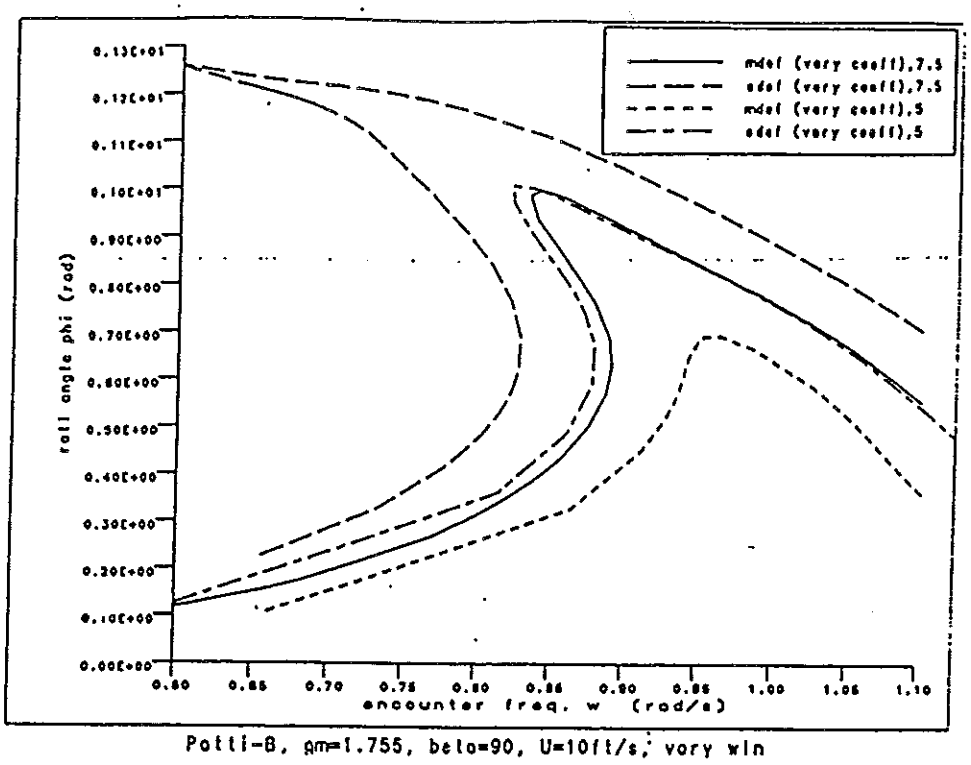

Figure 4b Single vs. multiple degree of freedom (vary λ)

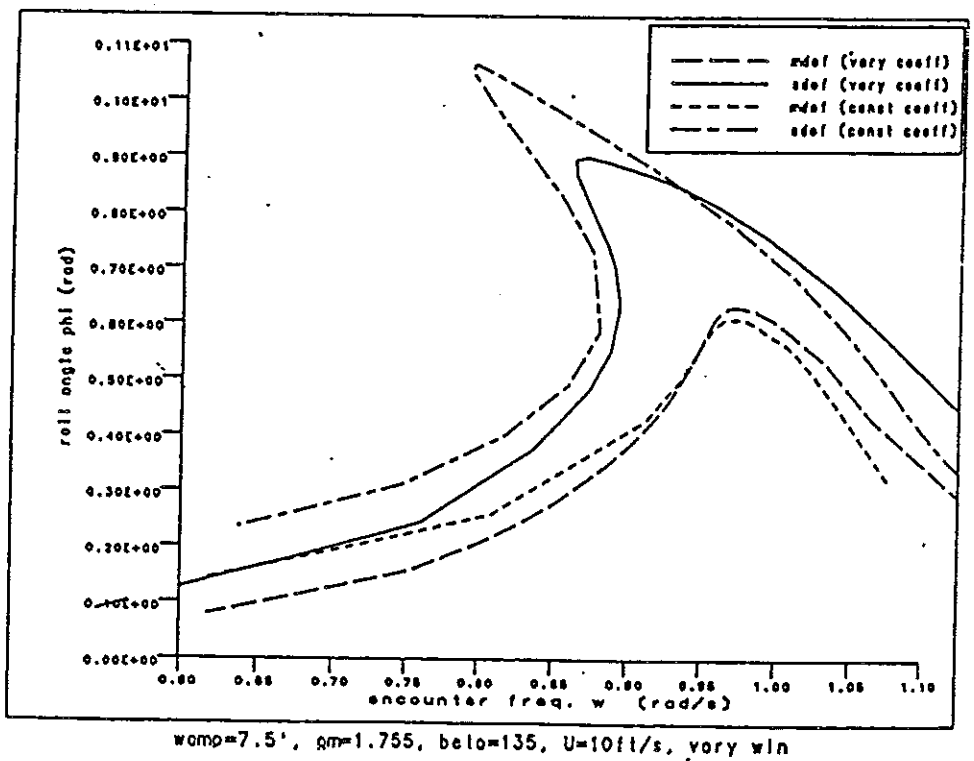

Figure 5 Fixed vs. frequency dependent hydrodynamics (vary λ)

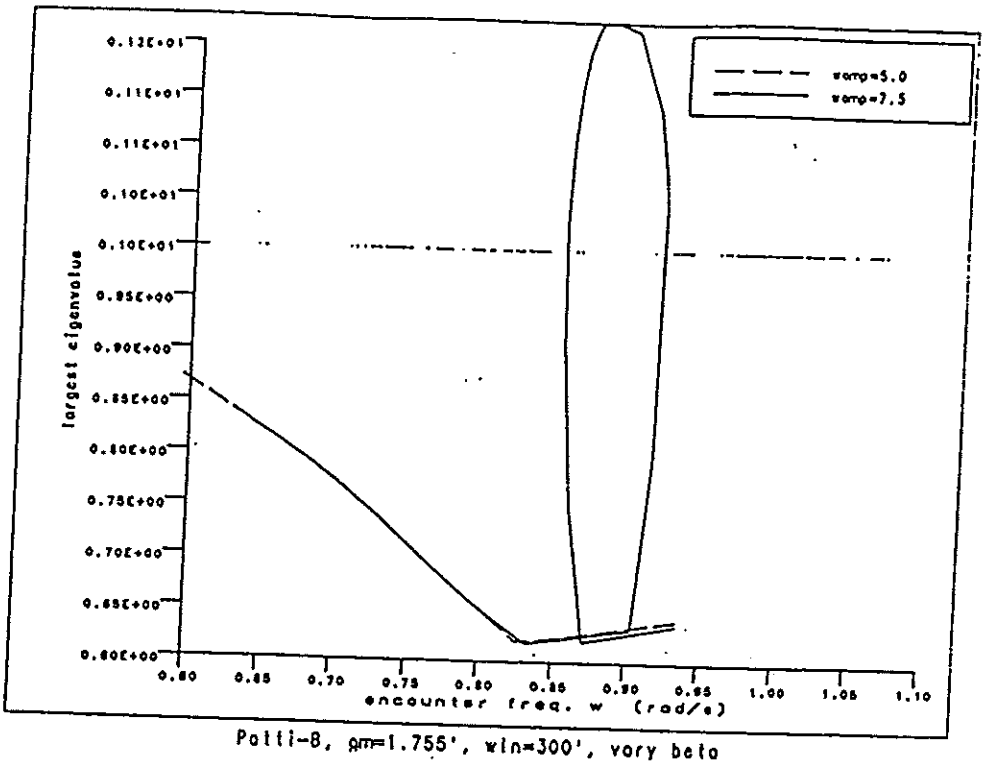

Figure 6 Typical result of stability calculation

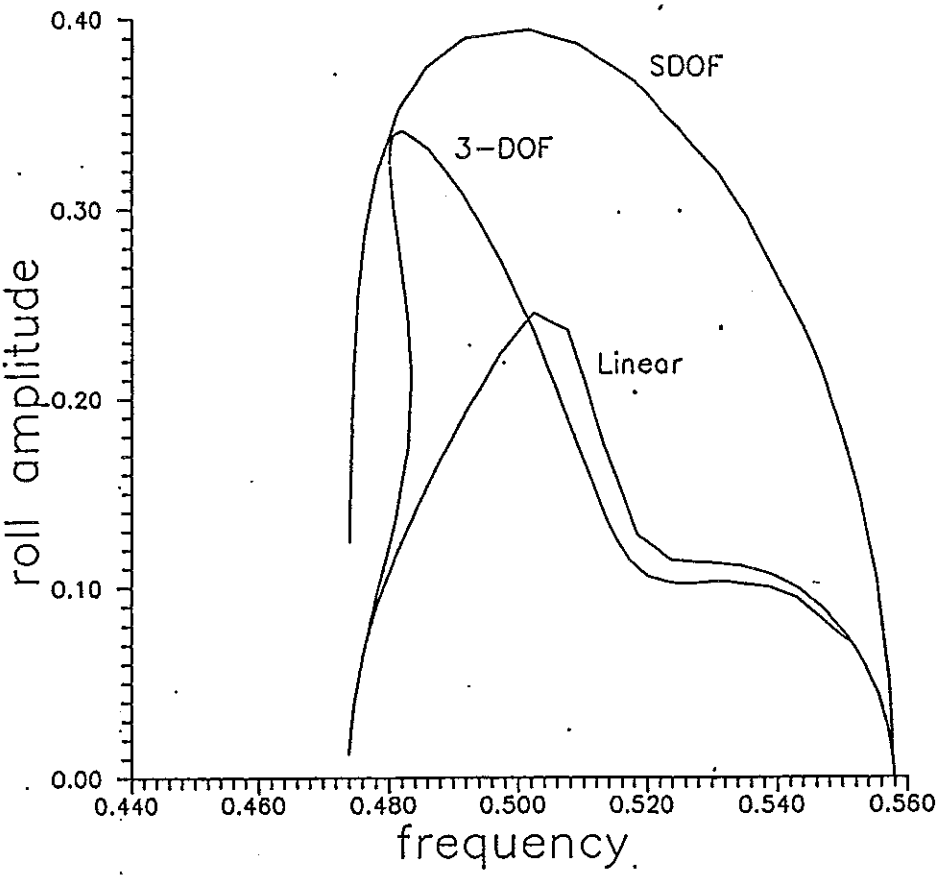

Figure 7 Comparison of various modelling approximations for steady state turning in waves. λ = 760', U= 3 Knots, η = 3.5'.

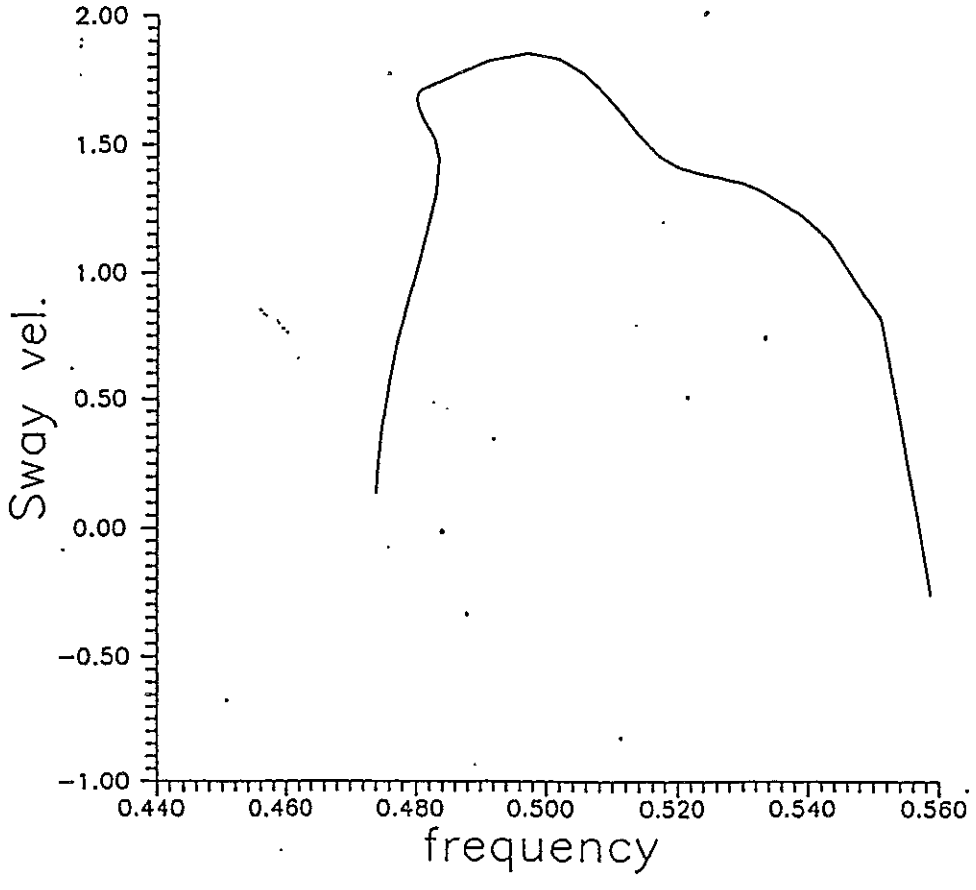

Figure 8 3-DOF, effect of nonlinear roll linearly coupled to sway velocity. λ = 760', U= 3 Knots, η = 3.5'.

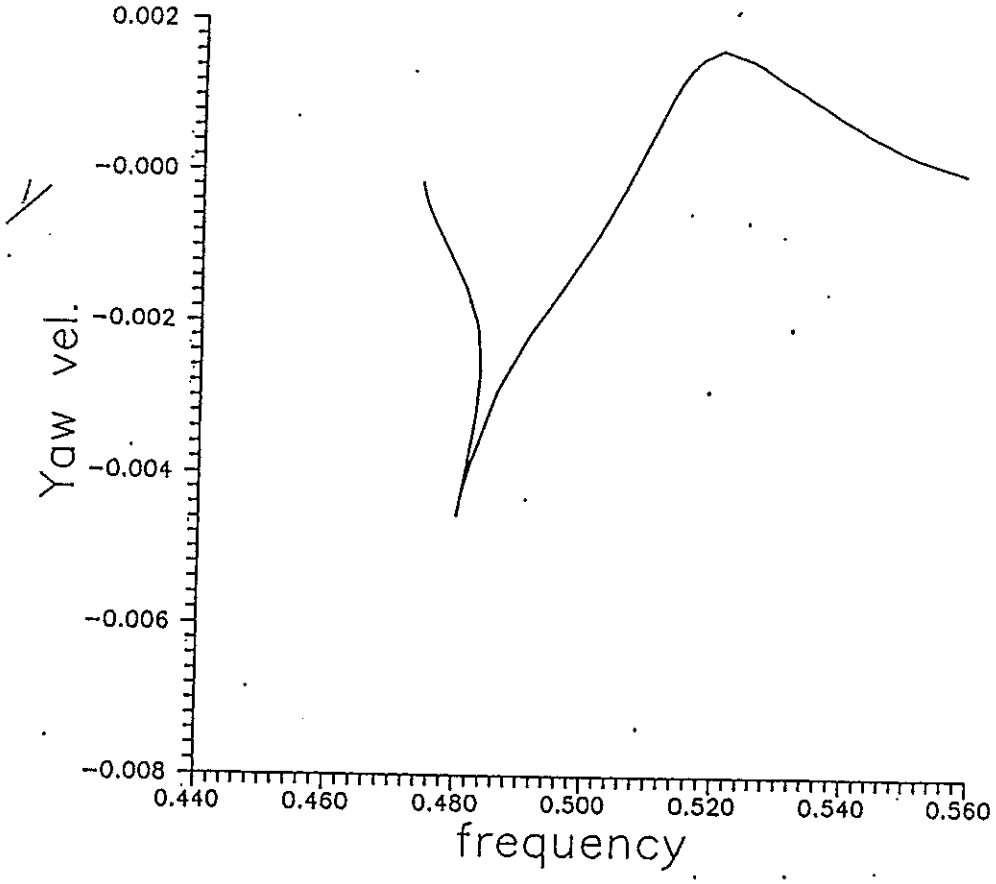

Figure 9 3-DOF, effect of nonlinear roll linearly coupled to yaw velocity. λ = 760', U= 3 Knots, η = 3.5'.

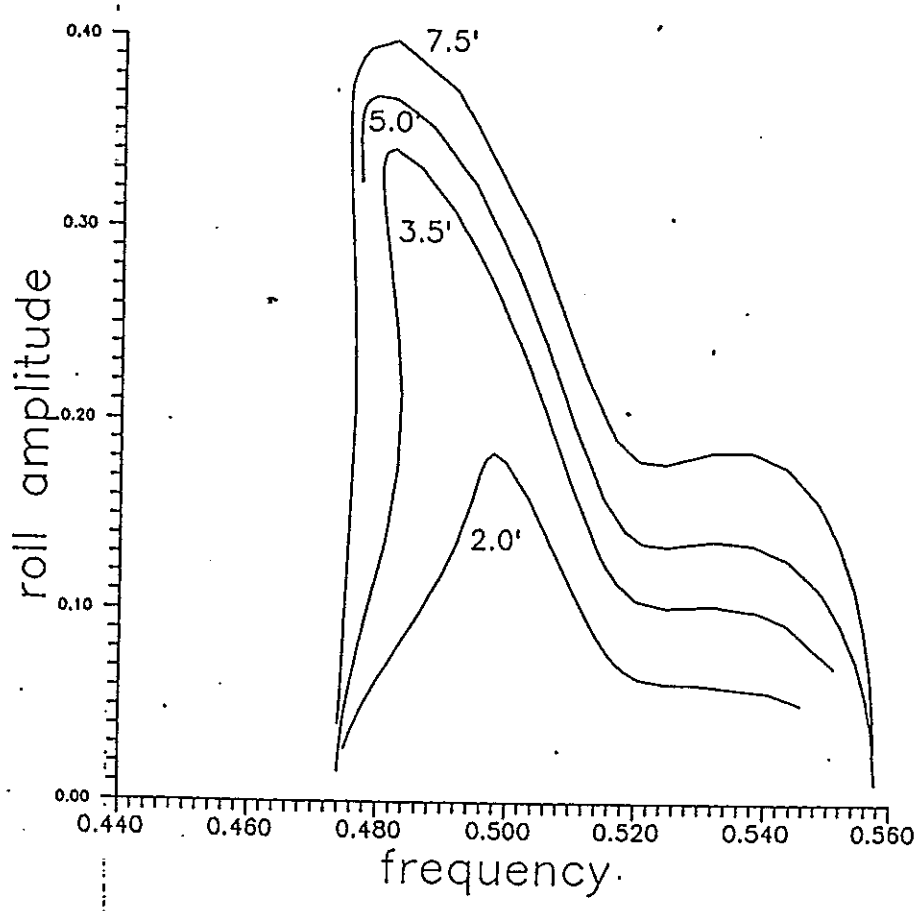

Figure 10 Effect of wave amplitude on 3-DOF roll. λ = 760', U= 3 Knots.

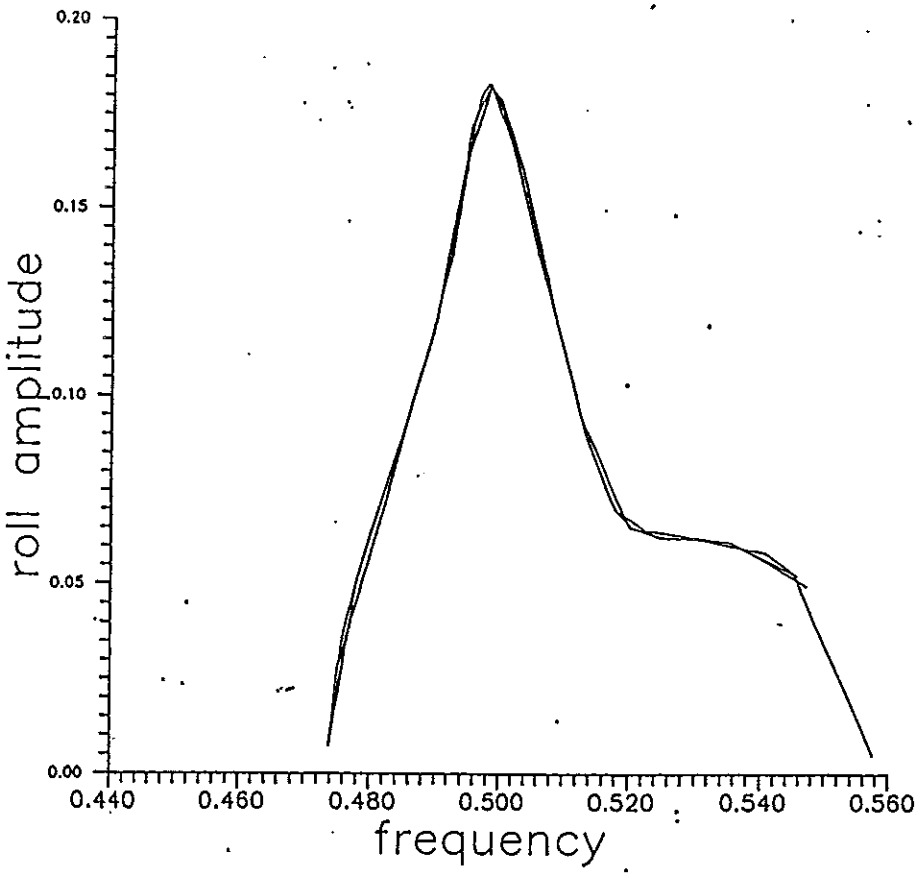

Figure 11 Effect of modelling approximations for low wave amplitude. (a) 3-DOF, (b) 6-DOF with and (c) 6-DOF without nonlinear heave/pitch hydrostatics. λ = 760', U= 3 Knots, η = 2'.

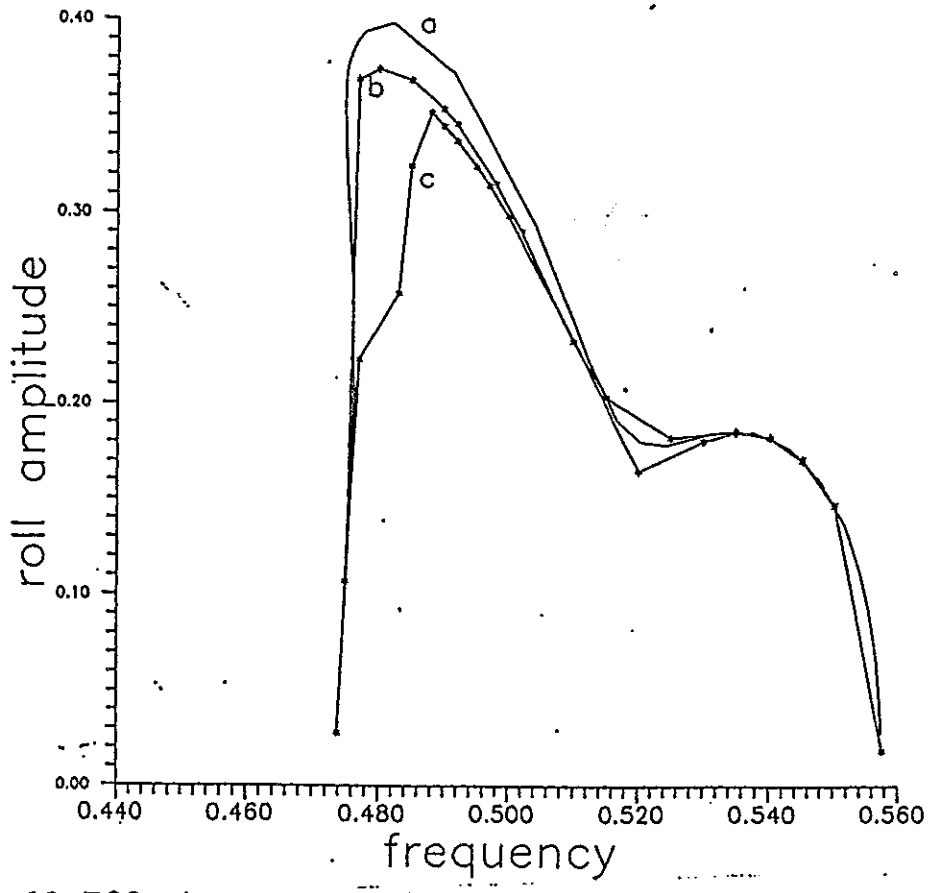

Figure 12 Effect of modelling approximations for high wave amplitude. (a) 3-DOF, (b) 6-DOF without and (c) 6-DOF with nonlinear heave/pitch hydrostatics. λ = 760', U= 3 Knots, η = 7'

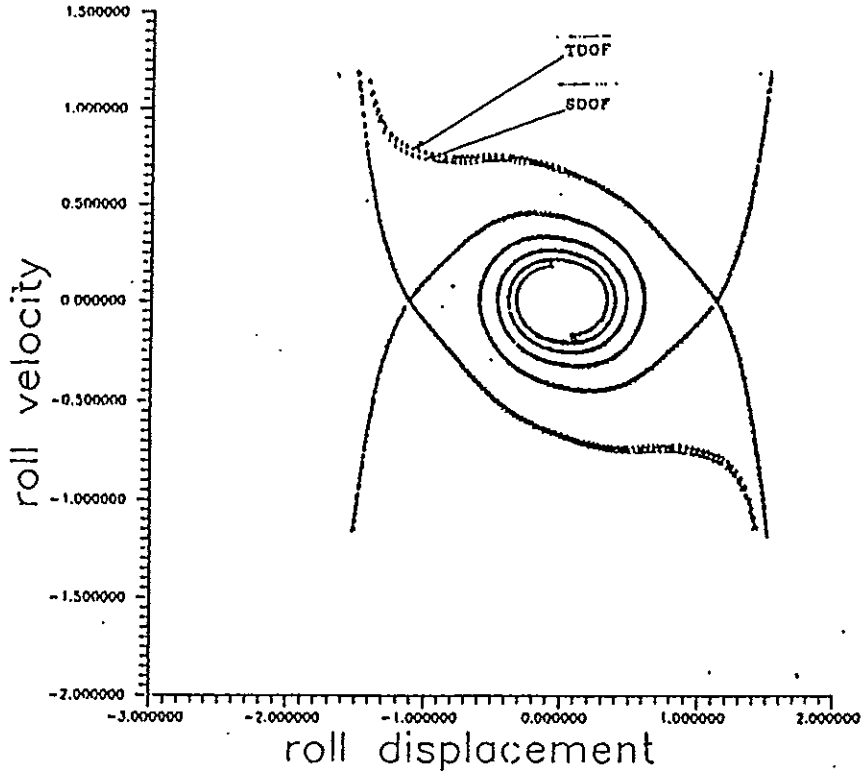

Figure 13a Comparison of coupled SDOF vs. TDOF projection.

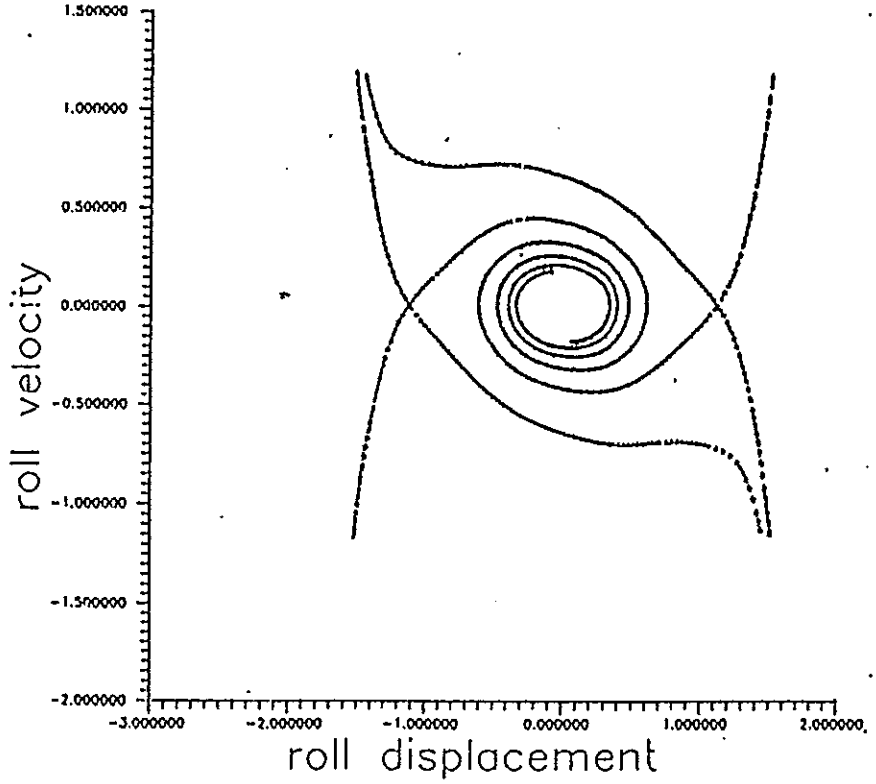

Figure 13b Comparison of uncoupled SDOF vs. TDOF projection.

EXPERIMENTAL EVIDENCE OF STRONG NONLINEAR EFFECTS IN THE ROLLING MOTION OF A DESTROYER IN BEAM SEA

Alberto FRANCESCUTTO (*), Giorgio CONTENTO (*) and Roberto PENNA (**)

(*) Department of Naval Architecture, Ocean and Environmental Engineering, University of Trieste, Trieste, Italy
(**) INSEAN, Italian Ship Model Basin, Roma, Italy

ABSTRACT

A campaign of experiments on ship rolling in regular beam sea has been conducted on scale models in the towing tank of the University of Trieste. The research was aimed at studying the features of nonlinear rolling and at obtaining realistic values for the parameters relevant to this motion as damping, excitation and stiffness. The experiments conducted on a 1:50 scale model of destroyer evidenced the presence of a bifurcation in the steady response. A jump from the low or anti-resonant oscillation to the high resonant state has been obtained by means of a schock while maintaining to a fixed value the wave excitation. The analysis of the phase lag between excitation and rolling confirmed the jump due to a bifurcation. The experimental results can be represented with satisfactory agreement by means of a perturbative solution of the nonlinear rolling equation.

1. INTRODUCTION

Rolling motion has been considered since long time the motion relevant to the hydrodynamic part of the ship safety [1]. Great interest has been and is presently being paid to both situations leading to large amplitude rolling, i.e. the rolling motion directly generated by the action of wind and waves as in the beam sea condition and the rolling motion indirectly generated by the action of waves as in the following sea conditions.
On the other hand, rolling motion is also the crucial motion in the context of seakeeping and the related features of seaworthiness and seakindliness. The reduction of the ship operational capability are evaluated considering the motion-induced task interruptions (MII) indicator, which is often approximated by means of the lateral force estimator (LFE) [2]. It is based on the consideration that large amplitude is not the only undesirable characteristics of roll motion. Large accelerations, often obtained as a side effect of a roll stabilizing system, are equally dangerous.
This twofold interest in ship rolling is due to the particular characteristics that this motion features for conventional ship forms. Roll motion is indeed the motion to which the ship opposes the minimum restoring moment and contemporarily the minimum damping ability. As a consequence, large amplitude

rolling can result also in moderate sea states, provided the sea spectrum is sufficiently narrow and the centerpeak frequency sufficiently close to the natural frequency of the ship [3,4]. Moreover the natural rolling frequency of the most part of existing ships is naturally included in the range of frequencies of the most energetic part of the sea spectrum. Finally, it is known that the rolling motion is a strongly nonlinear phenomenon.

A good comprehension of ship rolling thus means:

- resorting to perturbation approaches if analytical solutions are wanted;
- using sophisticated numerical techniques if very high reliability of the solution is searched in the extreme nonlinear domain;
- performing very complicated scale model experiments.

As far as the experiments are concerned, the difficulty in designing a realistic model test and in interpreting the obtained results explains the extreme lack of data in this field. Most of the results presented in literature refer indeed to forced rolling with internal excitation or to free decay tests, with an evident attempt to avoid the difficulties connected with the external wave excitation.

On the other hand, if the solution of the equation of motion is not straightforward, the draft of a realistic equation of motion is still an open problem. Approximate roll motion equations are often used in the practice. These equations use mixed hydrodynamic/hydrostatic approaches and consider that linear or quasilinear hydrodynamic assumptions allow reliable descriptions well beyond their intrinsic validity limit. This process shows often a good forecasting capability, provided that reliable coefficients are inserted in the equation of motion. In other words, even a mathematical model based on linear or quasilinear assumptions can often work well if used with parameter values obtained from experiments through a parameter identification technique, as will be described in the following. On the contrary, the state of art as regards the computation of the coefficients by using the methods of the theoretical or numerical hydrodynamics is still unsatisfactory [5]. This explains the generally poor forecasting capability of the conventional seakeeping codes when large amplitude rolling is concerned.

Recently, the methods to study the complex dynamics of nonlinear systems have received an extraordinary development. As a consequence, it is easier to study the possibilities of strange phenomena [6] (bifurcations, chaos, simmetry breaking, etc.) hidden in the rolling motion equation than to write down a correct nonlinear equation of motion for rolling. This explains the huge amount of published papers on complex roll dynamics. The results obtained in this field are very interesting as they disclose a new world of possibilities, some of them being very dangerous ones. On the other hand, there is often a great uncertainty in the coefficients of the mathematical model, while the possibility of the mentioned phenomena is usually tied to very precise values for these coefficients. Moreover,

bifurcations and chaos are usually studied in the deterministic case, i.e. in the presence of a regular excitation.
Recently, the possibility of bifurcations in nonlinear rolling in a stochastic sea has been proved [3,4] and analytical expressions for the probability density of the different states has been obtained. This constitutes a first step towards the evaluation of the practical probability of occurrence at sea.
Following the indications of the 20th ITTC Seakeeping Committee, experiments to indicate the effective possibility of the bifurcations have been undertaken at the towing tank of the Univerity of Trieste. These experiments are part of a campaign conducted on four different typologies (a frigate, a fishing vessel, a destroyer and a car ferry) to obtain informations on the damping model and coefficients [7].
In the following sections, some experimental results obtained for the destroyer in regular beam sea are presented and discussed in detail. In particular, a case of jump of the response between two steady-state oscillations with very different amplitude is evidenced.
The ability of an approximate analytical solution obtained long ago [8,9] in predicting the experimental results is also discussed.

2. EXPERIMENTAL SETUP

All the experiments have been conducted in the towing tank of the Department of Naval Architecture, Ocean and Environmental Engineering of the University of Trieste. Main dimensions are 50.00 m in length, 3.10 m in width, 1.60 m in depth. At one end it is equipped with 2 m long and 1 m wide beach with windows for checking the draft and trim of ship model. At the other end it is equipped with a Kempf & Remmers plunger type wave maker. It allows the generation of regular waves with wave length in the range 0.7-5.0 m and up to 200 mm height.

a) The model restraining

The scale models, with the maximum length compatible with tank breadth were disposed transversely and were loosely maintained in position by two elastic ropes connected with tank sides.
The ropes were fixed to the models at the bow and at the stern in correspondence to the flotation line. The ropes were sufficiently tensioned to restrain the model in excessive sway but not to interfere heavily with roll and heave. When excessive interference was suspected, from visual observation and/or from the analysis of the roll history recording, the measurement was repeated with a different pre-tensioning of the ropes.
Particular care was paid to avoid the undesirable phenomenon of frequency shift due to sway oscillations. In spite of this care, an oscillatory behaviour in the roll maxima was often observed in correspondence of the steep side of some measured resonance peaks. When this happened, the amplitude modulation of the response (due to beat phenomena) was included in the uncertainty interval of the experimental measurement.

At the extreme high frequency range moderate heave/pitch was observed. These motions introduced some modulation in the roll response as well. This modulation was also considered in the evaluation of the uncertainty level associated with the measurement.

b) The measurement system

The absolute roll angle was measured by using an Accustar clinometer of Lucas Sensing Systems. This type of device was chosen due to its relative simplicity of use, robustness, reliability, light weight, reduced size and low cost. Unfortunately, the upper frequency limit of the clinometer was very close to the lower frequency limit of the waves generated by the wavemaker. To overcome this difficulty, a complete dynamic calibration of the device has been performed taking into account the performance at high frequencies and when in positions different from the rotation axis. This operation allowed to obtain a correction factor at different frequencies and amplitudes of oscillation. A number of experiments was conducted checking the dynamic response of the device. It resulted that the clinometer can be used even in the moderately high frequency range, through the dynamic calibration, with high reliability. The uncertainty in the calibration was also introduced in the evaluation of the uncertainty level of the measurements.

The wave height was measured by means of a wave probe put at a fixed distance from the model on the wavemaker side. Due to the diffraction and radiation effects, the recording from the wave probe was not so meaningful. The quality of the waves generated by the wavemaker and of the calibration of the devices used to generate a wave of prescribed characteristics, in particular the steepness, was tested in the absence of the model. The results indicated an overall uncertainty in steepness of about 2-3% and the presence of a non negligible harmonic composition at the upper extreme of wave periods (T_W=1.8 s or more).

Both the roll and the wave height time histories were recorded on a multipen paper recorder. In addition the experiments were all video recorded. The paper records were used to obtain the steady roll amplitude, while the video recordings were used to obtain the phase lag of the response with respect to the excitation.

c) Experimental uncertainty.

Following the indications of 19th ITTC Panel on Validation Procedures, great attention has been paid to the evaluation of experimental uncertainty. This was estimated taking into account all the effects mentioned in sections a) and b). In the drawings it is represented generally as the maximum excursion of measured values around the average value.

3. THE TESTED MODEL

Only the results relative to the destroyer are shown and discussed in the following, as they present very peculiar

nonlinear characteristics. The information on damping model obtained through the experiments on the other tested ship typologies are reported elsewhere [7].
A 1:50 scale model has been ballasted so as to reproduce a complete mechanical similitude. The schematic body plan of the model is reported in Fig. 1, while the Table. 1 contains the main dimensions and the geometric and mechanical data. To avoid complications connected with unknown scale effects and to have data peculiar of the tested ship, the naked hull condition only was considered. In Fig. 2 the righting arm of the model in the actual loading condition is reported.
The tests have been coducted in a range of frequencies including the resonance peak at two values of the wave steepness: s_w=1/30 and s_w=1/50. The first value corresponds to the maximum value of wave steepness the wavemaker is able to generate in all the range of wave frequencies.
The use of a constant steepness was related to the need of having as much as possible a series of data at constant excitation moment amplitude. We will return later to this point. The use of an internal rolling moment generator has not been considered since this gives a more reliable frequency independent moment, but in a less realistic condition when experiments to simulate the actual behaviour at sea are planned.

4. EXPERIMENTAL RESULTS

The measured steady rolling amplitude ϕ as a function of frequency ω is reported in Fig. 3 for wave steepness s_w=1/50. Fig. 4a reports the experimental steady rolling amplitude ϕ obtained for s_w=1/30, while Fig. 4b contains the phase lag ψ of the response with respect to the excitation moment.
The arrow in Fig. 3 indicates a roll amplitude amplitude shift that took place, in the indicated direction without any external action. No explanation has been found for this phenomenon, except the possible presence of a beat due to the formation of a standing wave in the towing tank having a frequency very near to the roll frequency, so to give a long period modulation of the rolling oscillation.
More interesting is the effect indicated by the arrow in Fig. 4a and Fig. 4b. This indicates the jump of amplitude between two steady states as a result of an external action on the hull (at constant wave parameters). This action consisted in a shock excitation produced by knocking the deck at side by means of a rod. The evidence of a typical jump to another nonlinear resonant state was got by examining the time history of the rolling motion (Fig. 5). It exhibits the typical growing by resonance phenomenon. The measurement of phase lag indicated a sharp change of phase as shown in Fig. 4b. This phase change and the difference between the two states is also evident from the analysis of the videorecording of the event. Further knockings did'nt change the oscillation state. This proves that it is the state with the highest probability possible with the existing

wave parameters. Later on we will discuss the meaning of this probability assignement.

5. THE IDENTIFICATION OF THE MATHEMATICAL MODEL PARAMETERS

Analytic solutions of the equation of motion are usually employed to obtain values for the coefficients of the mathematical models from the experimental data through the use of identification techniques. Since the rolling motion equation is highly non linear, the analytical solutions, obtained through the use of perturbation methods or other approximate methods, contain as a rule some degree of approximation. This makes difficult their application to large amplitude experiments and can mask differencies among different models. Any change in the mathematical model implies tedious calculations and don't allow easily the inclusion of frequency dependent coefficients.
On the other hand, approximate analytical solutions work quite well once the proper values for the coefficients are used. In this way, these solutions can be used to develop semi-empirical approaches for the statement of upper limitations to the solutions to be used for safety criteria or in the improvement of seakeeping codes.
Having in mind an extensive research devoted to obtaining informations on the mathematical model suitable for the description of the different terms of the equation of motion and at the same time obtaining realistic values for the coefficients used in the models, a different approach was used. Following the idea of Haddara [10] that developed an identification technique based on the least squares fitting of the numerical solution of the equation of motion to roll decrements, this approach was extended to include all the cases of roll motion. In particular, the forced rolling experiments in beam sea have been analysed considering the following identification of parameters [11]. The best estimate of the model parameters (coefficients) are those minimizing the following function:

$$S(\vec{p}) = \sum_{i=1}^{N} \left[\phi(\vec{p},\omega_i) - \phi_i\right]^2$$

where $\vec{p}$ is the vector of parameters to be estimated, $\phi(\vec{p},\omega_i)$ is the stationary numerical solution of the equation of motion computed with the parameter values existing at the considered step of the minimization procedure and ω_i is the frequency corresponding to the experimental result ϕ_i.
The identification procedure can be efficiently dealt by means of a nonlinear least squares fitting computer code of the Marquardt type as for example the subroutine RNLIN of the IMSL mathematical library. Unfortunately the derivatives of the function $S(\vec{p})$ with respect to the parameters are not obtainable in analytic form, so that the computation is time consuming.

The advantages of the method consist in the use of the exact solution of the equation of motion and in the possibility of changing very easily the mathematical models and the number of parameters to be fitted. A practical problem during its use was constituted by the relatively slow convergence of the algorithm to this particular case. This resulted in frequent trapping of the solution far from the optimum solution and the consequent need of helping the search by varying the initial values of the parameters. This difficulty was not encountered during the fitting of the roll decay curves that on the contrary exhibited fast convergence and independence on initial estimates. Unfortunately but not surprinsingly, the parameter values estimated from roll decrement in calm sea were usually quite different from those estimated from forced roll in waves and could not be used for the simulation.
Several different nonlinear damping models were tried:

quadratic models

$$2\mu\dot{\phi}+\beta_1|\dot{\phi}|\dot{\phi}$$

$$2\mu\dot{\phi}+\beta_1|\dot{\phi}|\dot{\phi}+\beta_2|\phi|\dot{\phi}$$

and cubic models

$$2\mu\dot{\phi}+\delta_1\dot{\phi}^3$$

$$2\mu\dot{\phi}+\delta_1\dot{\phi}^3+\delta_2\phi^2\dot{\phi}$$

The analysis on all the tested ship models is still in progress. Preliminary results seem to indicate that all proposed damping models fit quite well the experimental data. The cubic model and the quadratic model with one nonlinear term fit equally well, both in terms of residual and of visual fit, the experiments. The inclusion of a second nonlinear term, angle-dependent, seems to improve slightly the fitting. As a consequence, the results of the identification for the destroyer are given in Table.2 with reference to the mathematical model represented by:

$$\ddot{\phi}+2\mu\dot{\phi}+\delta_1\dot{\phi}^3+\omega_0^2\phi+\alpha_3\phi^3=\alpha_0\omega_0^2\pi s_w\cos(\omega t) \qquad (1)$$

The damping moment was given in terms of cubic damping because this is easier to handle in the approximate analytical approach. To obtain an estimate of the uncertainty connected with the estimated values, a Monte Carlo approach has been developed extending the method proposed by Spouge [12] to forced roll. Due to the long time needed to get the statistics of the identified parameters and due to the above mentioned convergence difficulty of convergence of the identification procedure, the analysis of the uncertainty on the estimated parameters was postponed to a second phase of the research project.

6. THE ANALYTICAL SIMULATION

To have a deeper insight into the mechanisms leading to the jump evidenced in Fig. 4, an analytical study of the roll dynamics as forecasted by Eq. 1 has been performed.

a) Steady state solution.
Approximate solutions of Eq. 1 are quite difficult to obtain if resonance zones different from the synchronism are involved [8]. On the other hand, a good quality steady state solution in the region of synchronism can be obtained by means of different methods, assuming a solution of the form:

$$\phi(t) = C\cos(\omega t + \psi)$$

After substituting this function and its derivatives in Eq. 1, neglecting the rapidly varying terms of frequency 3ω and applying the harmonic balance method, a system of two equations in the unknowns C and ψ is obtained. This system can be easily generalized to include further terms in the polynomial representations of damping and restoring moments. The result can then be expressed in the compact form:

$$\begin{cases} \left(\omega_{0eq}{}^2 - \omega^2\right) C = \alpha_0\, \omega_0{}^2\, \pi\, s_W \cos(\psi) \\ -d_{eq}\, \omega\, C = \alpha_0\, \omega_0{}^2\, \pi\, s_W \sin(\psi) \end{cases} \qquad (2)$$

where the nonlinear deviation of the natural roll frequency $\omega_{0eq}{}^2$:

$$\omega_{0eq}{}^2 = \omega_0{}^2 + \alpha_3\, C^2 + \alpha_5\, C^4 + \alpha_7\, C^6 + \ldots$$

and the equivalent damping d_{eq}:

$$d_{eq} = 2\mu + \frac{1}{4}\left(\delta_1 + 3\delta_2\omega^2\right) C^2$$

have been introduced.
The steady roll amplitude as obtained by solving numerically the system of equations (2) is reported as a function of the circular frequency ω in Fig. 6a and Fig. 7a for s_W=1/50 and 1/30 respectively. In Fig. 7a and Fig. 7b the phase obtained by means of the system of equations is reported. For comparison, in the same figures the experimental results are also indicated.

b) Dependence on initial conditions - Domains of attraction.

When a bifurcation possibility is detected in the dynamic behaviour of a physical system, two strictly correlated questions arise. The problems to be solved can be shortly stated as:

- identification of the danger for the survival or for the operability of the system arising from the possibility of bifurcations;
- identification of the probability of falling in each of the stable steady states or of switching back and forth between them.

Both problems have no simple answer. In the following we will concentrate on the second problem, and particularly on the deterministic, non chaotic case. For a discussion on the implications of bifurcations in the presence of a stochastic excitation see Ref. [3,4].

The problem of which steady state is reachable is solved in terms of strict dependence on initial conditions of the motion, that in the case of Eq. 1 means $\phi_0 = \phi(t_0)$ and $\dot{\phi}_0 = \dot{\phi}(t_0)$, being t_0 the initial time.

The phase plane $(\phi,\dot{\phi})$ can then be divided in two domains depending on the steady state belonging to the given initial conditions.

Practically, the approach is not so simple in the phase plane because of the spiralling of the trajectories around the time axis. The picture is greatly simplified when the searched solution exhibits a dominant frequency, like in the considered case of Eq. 1 near synchronism or in the presence of a subharmonic oscillation.

We can thus separate the vector of coordinates $(\phi(t),\dot{\phi}(t))$ into two parts, a rotating one with frequency ω and a 'characteristic part' containing informations on amplitude and phase of the solution. This separation corresponds to the Van der Pol transformation:

$$\begin{cases} \phi = u\cos(\psi) - v\sin(\psi) \\ \dfrac{\dot{\phi}}{\omega} = u\sin(\psi) + v\cos(\psi) \end{cases}$$

All the necessary information on system dynamics is now contained in the Van der Pol plane (u,v).

The approximate behaviour of ship roll, as described by Eq. 1, can be obtained by means of the Bogolyubov-Krylov asymptotic method. This assumes that the transient solution of Eq. 1 is still in the form:

$$\phi(t) = C\cos(\omega t + \psi)$$

with C and ψ slowly varying functions of time. This assumption allows to obtain the evolutionary equations for C and ψ in the following form:

$$\begin{cases} \dot{C} = -\dfrac{1}{2\omega}\left[d_{eq}C + e_w \sin(\psi)\right] \\ \dot{\psi} = \dfrac{1}{2\omega}\left[\left(\omega_{0eq}{}^2 - \omega^2\right)C - e_w \cos(\psi)\right] \end{cases} \tag{3}$$

where $e_w = \alpha_0\, \omega_0{}^2\, \pi\, s_W$.
In the Bogolyubov-Krylov approach, the additional assumption

$$\dot{C}\cos(\omega t + \psi) - C\,\dot{\psi}\sin(\omega t + \psi) = 0$$

is made, so that one can write:

$$\dot{\phi} = -C\,\omega \sin(\omega t + \psi)$$

and

$$\begin{cases} u = C\cos(\psi) \\ v = C\sin(\psi) \end{cases}$$

The three steady state solutions (C_i, ψ_i), where i=1,2,3 ordered in ascending values of the roll amplitude C, can be represented in the Van der Pol plane. The plane is thus divided in two parts or 'domains of attraction' (DOA). The DOA of the antiresonant steady state is obtained considering the set of values of (C,ψ) which, assumed as initial conditions for the system (3), lead to the antiresonant solution as steady state, and analogously for the resonant steady state.
The identification of the DOA's can be quickly performed drawing the boundary line or 'separatrix. The most efficient way of obtaining the separatrix is to integrate backward in time the system (3) starting with initial conditions close to the unstable steady state.
In Fig. 8, the domains of attraction of the nonlinear rolling at a couple of frequencies lying in the bifurcation zone with the parameter values obtained through the experiments on the destroyer in beam sea are given.

7. DISCUSSION AND CONCLUSIONS

In spite of the quite strong hydrodynamic assumptions (quasilinear approach leading to the separability of contributions) underlying Eq. 1, there is a fair agreement of its approximate solution and experimental results when the

values obtained by means of the identification technique describen in Sect. 5 are employed (Fig. 7). The agreement is maintained at large amplitudes and in the evaluation of the phase lag too. In addition the correct roll dynamics is predicted since the analytical solution bifurcates in a narrow frequency zone. The presence of the bifurcation, with three different steady states, is the explanation of the experimentally observed jump (Fig. 4a) which took place between the lowest and the highest oscillation states, being the intermediate unstable.
The discrepancies observed in the fitting capability of Eq. 1 to experimental data at frequency far from the resonance frequency can be explained considering that Eq. 1 is written with coefficients constant in all the range of frequencies. Experiments are in progress [14] to get a deeper insight into this question. They are performed varying the exciting moment at constant frequency for a range of frequencies. Preliminary results indicate that the parameters assume values that tend to correct the observed discrepancies.
From the preceding analysis, the change in the oscillation state, experimentally found in the nonlinear rolling of a destroyer in beam sea, has been clearly identified as a jump in the presence of a bifurcation.
With the aid of the diagram of the DOA we are now in the position to say something about the question raised in Sec. 7b as regards the probabilistic approach to bifurcations.
Strictly speaking, this approach should be based on the following scheme:
- identification of the probability of the states given a probability distribution on the admissible set of initial conditions;
- identification of the resistance of the state to a perturbation (of internal or external origin);
- identification of the probability of the different perturbations, i.e. of their statistics.
Even a very simple approach to all of these topics would bring the discussion too far from the aim of this paper. We will thus give some hint to the explanation of the experimentally observed phenomena.
The important features can be obtained from the examination of the Van der Pol plane as representative of the dependence of the final steady state from the initial conditions and from a perturbation to an existing steady state, without changing the excitation parameters. Fig. 8 indicates that the DOA of the small amplitude solution includes the origin. As a consequence, starting from rest this solution as steady state is the most likely to be obtained. On the other hand, the separatrix is in some zone very close to the origin and tends to enclose a DOA centred on the small amplitude solution that is smaller and smaller as the frequency proceeds toward the upper point of the bifurcation range. In these conditions, that probably represent the actual experimental situation, the resistance of the small amplitude steady state to perturbations is very small, so that as a result the separatrix is crossed toward the large amplitude

solution. This in turn is very resistent to perturbations for the reasons just stated.

ACKNOWLEDGEMENTS

This research has been partially supported by Contract Code 77/NR between INSEAN, Roma and University of Trieste.

REFERENCES

[1] Francescutto, A., "Is it Really Impossible to Design Safe Ships?", The Naval Architect, October 1993.

[2] Sellars, F. H., Martin, J. P., "Selection and Evaluation of Ship Roll Stabilization Systems", Marine Technology, pp. 84-101. Vol. 29 1992.

[3] Francescutto, A., "On the Probability of Large Amplitude Rolling and Capsizing as a Consequence of Bifurcations", Proceedings 10th International Conference on Offshore Mechanics and Arctic Engineering 'OMAE', Stavanger, June 1991, Vol. 2, pp. 91-96.

[4] Francescutto, A., "Nonlinear Ship Rolling in the Presence of Narrow Band Excitation", in "Nonlinear Dynamics of Marine Vehicles", ASME/DSC Vol. 51, 1993, pp. 93-102.

[5] Brook, A. K., "Evaluation of Theoretical Methods for Determining Roll Damping Coefficients", Trans. RINA, Vol. 132, 1990, pp. 99-115.

[6] Falzarano, J. M., Shaw, S. W., Troesch, A. W., "Application of Global Methods for Analyzing Dynamical Systems to Ship Rolling Motion and Capsizing", Int. J. Bifurcations and Chaos, Vol. 2, pp. 101-115, 1992.

[7] Cardo, A., Coppola, C., Contento, G., Francescutto, A., Penna, R., "On the Nonlinear Ship Roll Damping Components", Accepted for presentation at International Symposium NAV'94, Roma, Ottobre 1994.

[8] Cardo, A., Francescutto, A., Nabergoj, R., "Ultraharmonics and Subharmonics in the Rolling Motion of a Ship: Steady-state Solution", International Shipbuilding Progress, Vol.28, 1981, pp.234-251.

[9] Cardo, A., Francescutto, A., Nabergoj, R., "On the Maximum Amplitudes in Nonlinear Rolling", Proceedings 2nd International Conference on Stability of Ships and Ocean Vehicles, Tokyo, The Society of Naval Architects of Japan, 1983, pp.93-102.

[10] Haddara, M. R., Bennett, P., "A Study of the Angle Dependence of Roll Damping Moment", Ocean Engng, Vol. 16, 1989, pp. 411-427.

[11] Contento, G., Francescutto, A., Coppola, C., Penna, R., "A Methodology for the Analysis of Roll Decay Curves", Tecnica Italiana, 1994.

[12] Spouge, J. R., "A Technique for Estimating the Accuracy of Experimental Roll Damping Measurements", Int. Shipb. Progress, Vol. 39, 1992, pp. 247-265.

[13] Krylov, N., Bogolyubov, N., "Introduction to Nonlinear Mechanics", Princeton University Press, New York, 1970.

[14] Contento, G., Francescutto, A., Piciullo, M., "On the effectiveness of constant coefficients roll motion equations", To appear.

FIGURE CAPTIONS

Fig. 1. Body plan of the destroyer.

Fig. 2. Righting arm of the destroyer scale model in the tested loading condition.

Fig. 3. Experimental results of rolling motion of the destroyer in a regular beam sea - stationary roll amplitude versus wave frequency. The excitation corresponds to a wave steepness s_W=1/50.

Fig. 4a. Experimental results of rolling motion of the destroyer in a regular beam sea - stationary roll amplitude versus wave frequency. The excitation corresponds to a wave steepness s_W=1/30.

Fig. 4b. Experimental results of rolling motion of the destroyer in a regular beam sea - phase lag of stationary roll motion with respect to excitation versus wave frequency. The excitation corresponds to a wave steepness s_W=1/30.

Fig. 5. Time history of roll motion in the presence of jump of amplitude.

Fig. 6a. Amplitude response curve versus wave frequency. The excitation corresponds to a wave steepness s_W=1/50. For comparison the experimental points are reported.

Fig. 6b. Analytical phase lag of stationary roll motion with respect to excitation versus wave frequency. The excitation corresponds to a wave steepness s_W=1/50.

Fig. 7a. Amplitude response curve versus wave frequency. The excitation corresponds to a wave steepness s_W=1/30. For comparison the experimental points are reported.

Fig. 7b. Analytical phase lag of stationary roll motion with respect to excitation versus wave frequency. The excitation corresponds to a wave steepness s_W=1/30. For comparison the experimental points are reported.

Fig. 8. Domains of attraction of roll motion in the Van der Pol plane for two different frequencies in the bifurcation range.

Model C 83-227 (scale 1:50.0)

Lbp	2.532 m
Loa	2.640 m
B	0.273 m
D	0.193 m
Displ (+/-0.01 kgf)	26.720 kgf
T (+/- 0.5 mm)	0.080 m
Trim (+/- 1.0 mm)	0.000 m
KG (+/- 1.0 mm)	0.133 m
GM (+/- 1.0 mm)	0.017 m
Mom. Inertia long. axis	0.2108 kg·m^2
Natural roll period	1.505 s
Natural roll angular frequency	4.175 rad/s

Table.1. Main dimensions and mechanical data of the destroyer

Wave steepness	s_w	1/50	1/30
Linear damping coefficient	μ	0.1701	0.1943
Nonlinear damping coefficient	δ_1	0.1004	0.1047
Nonlinear restoring coefficient	α_3	-28.440	-28.440
Wave steepness reduction factor	α_0	0.5800	0.5271

Table.2. Coefficients from the parametric identification

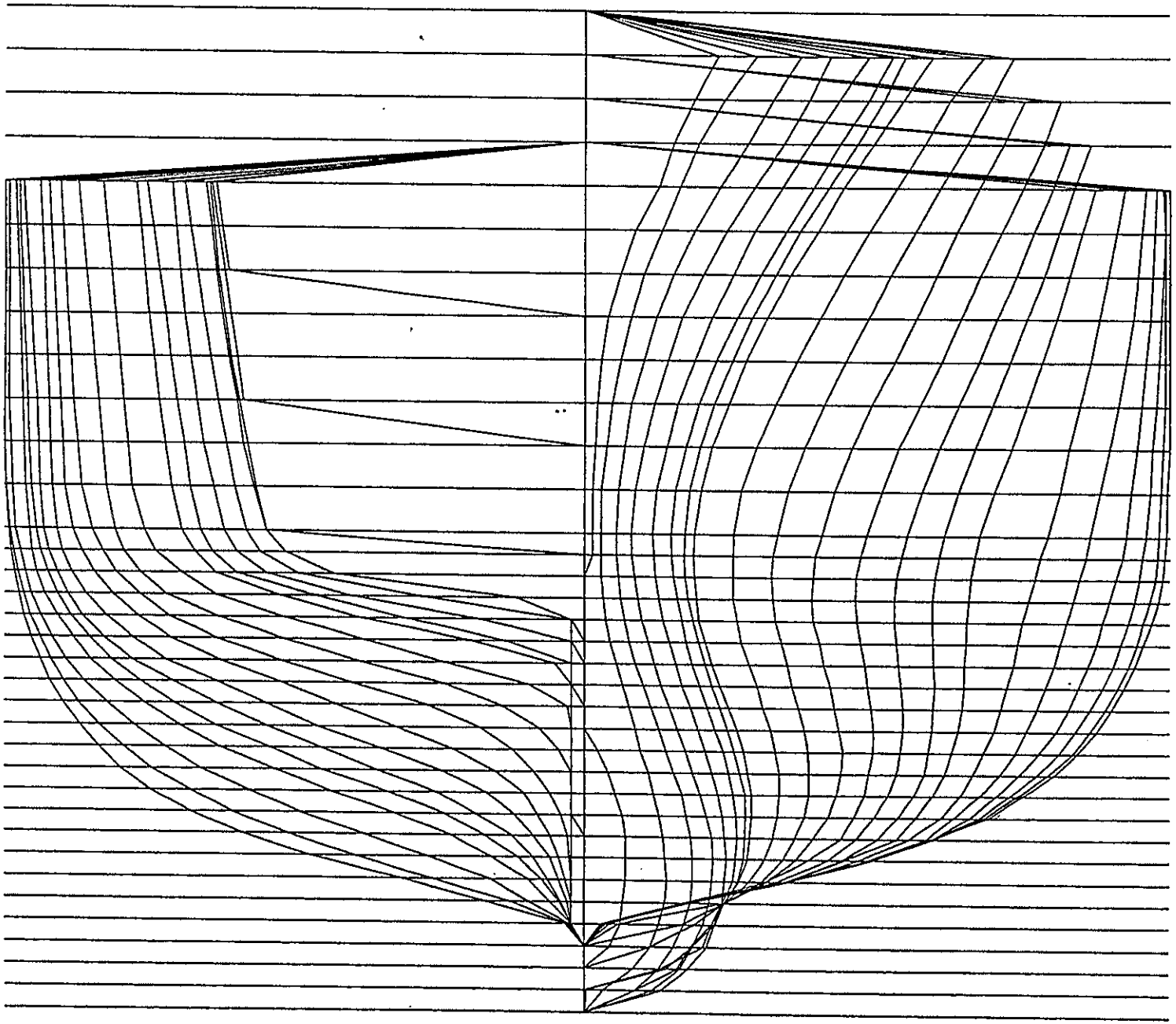

Fig. 1. Body plan of the destroyer

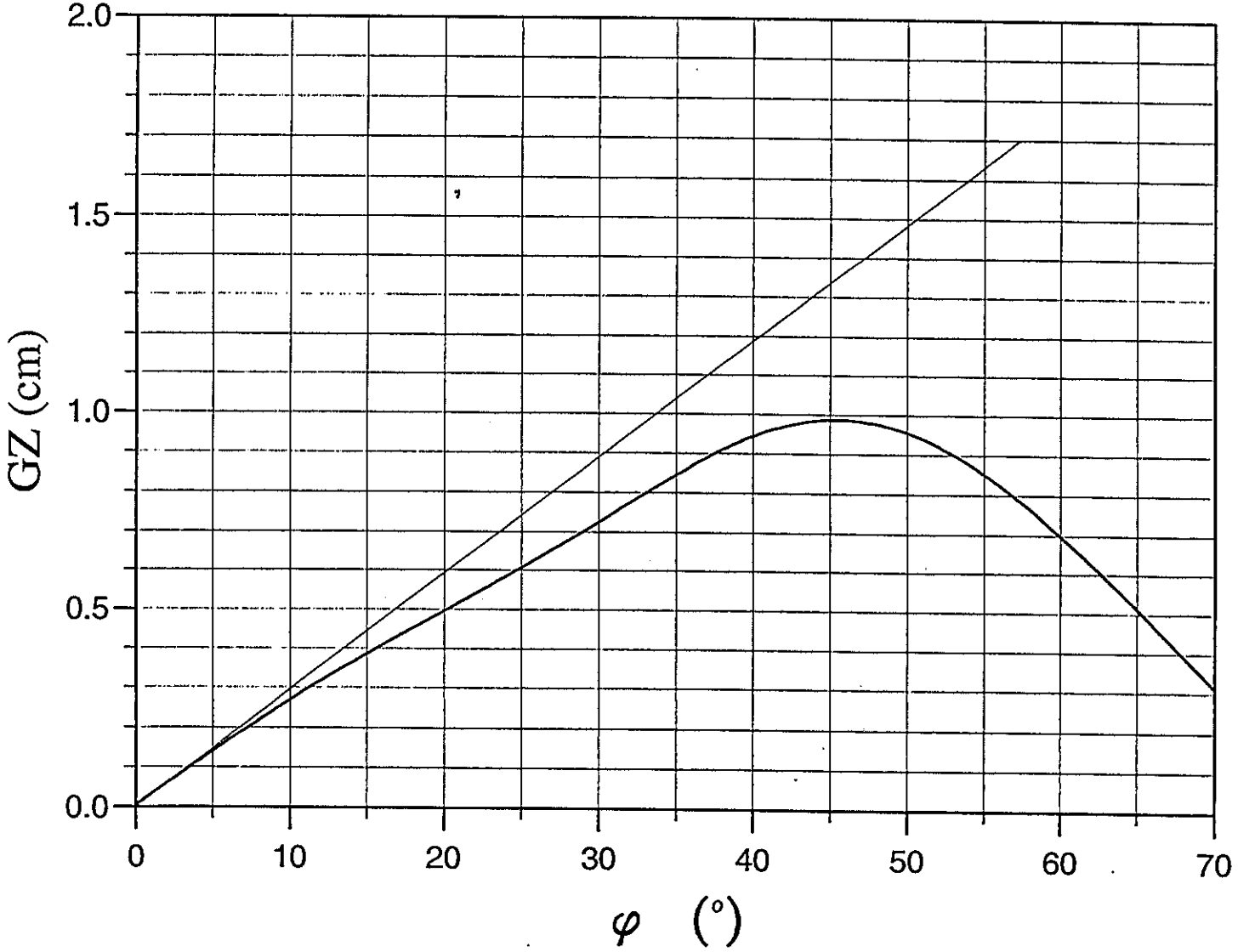

Fig. 2. Righting arm of the destroyer scale model in the tested load condition

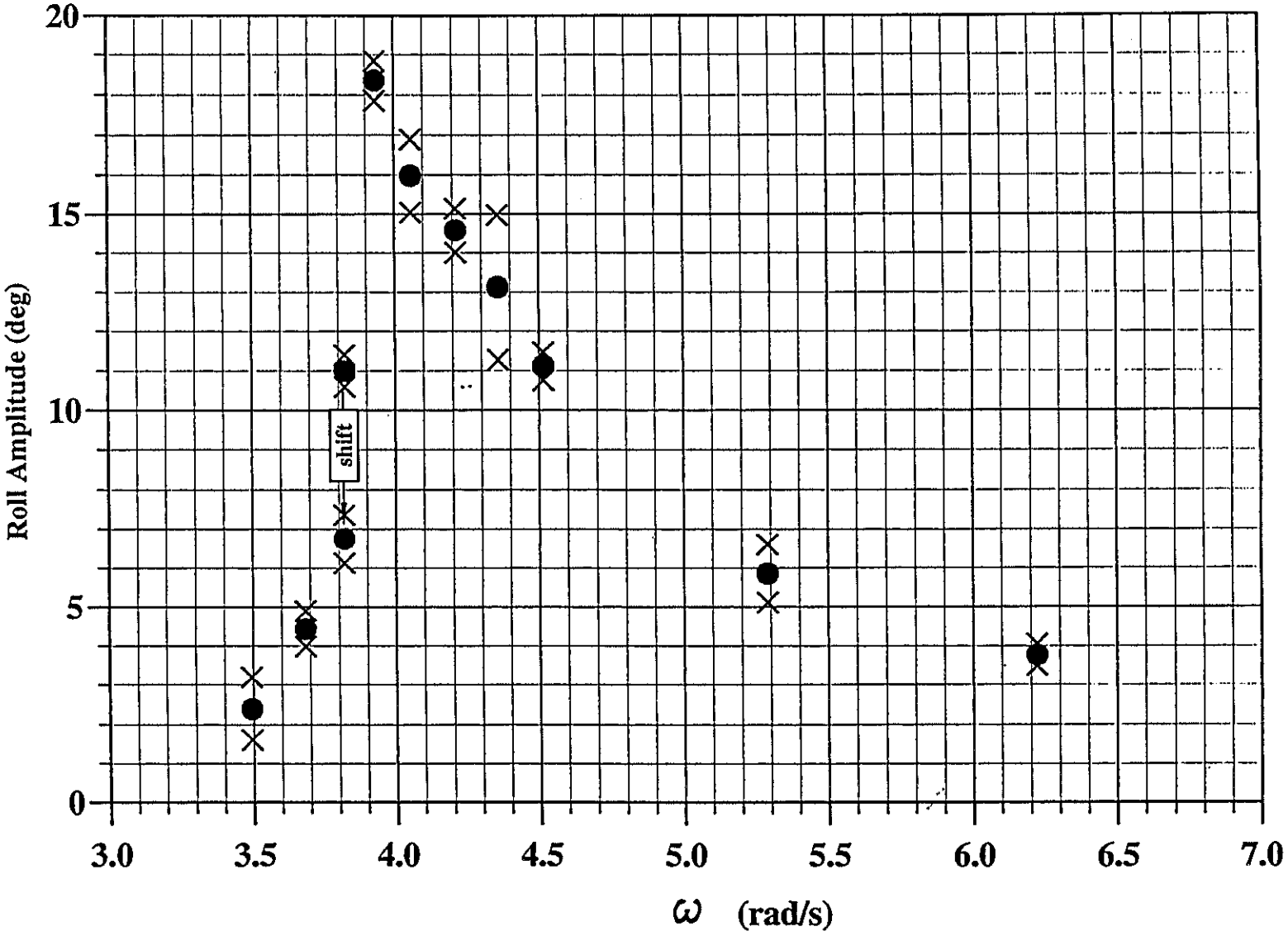

Fig. 3. Experimental results of rolling motion of the destroyer in regular beam sea - stationary roll amplitude versus wave frequency. The excitation corresponds to a wave steepness s_w=1/50.

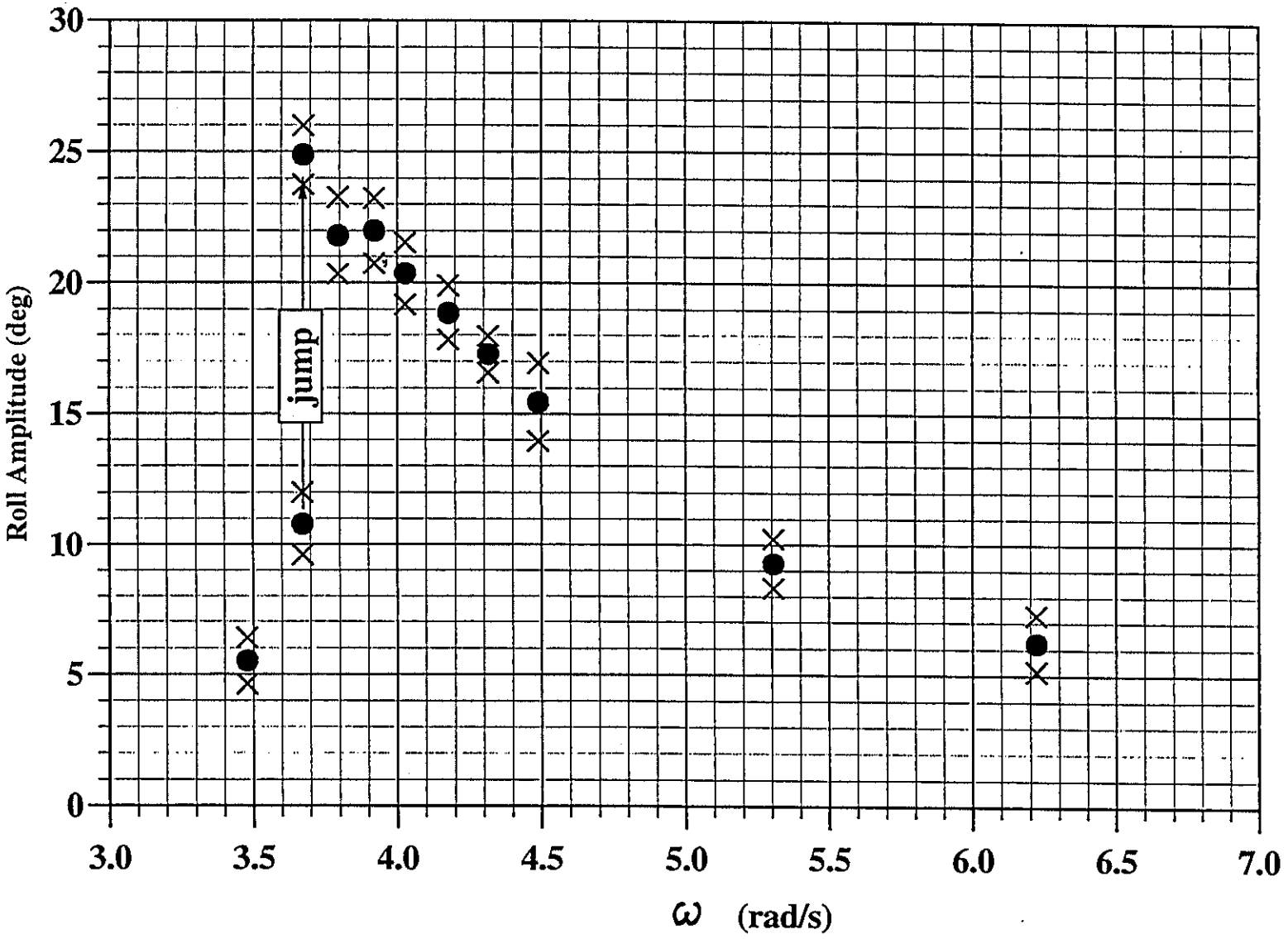

Fig. 4a. Experimental results of rolling motion of the destroyer in regular beam sea - stationary roll amplitude versus wave frequency. The excitation correspond to a wave steepness s_w=1/30.

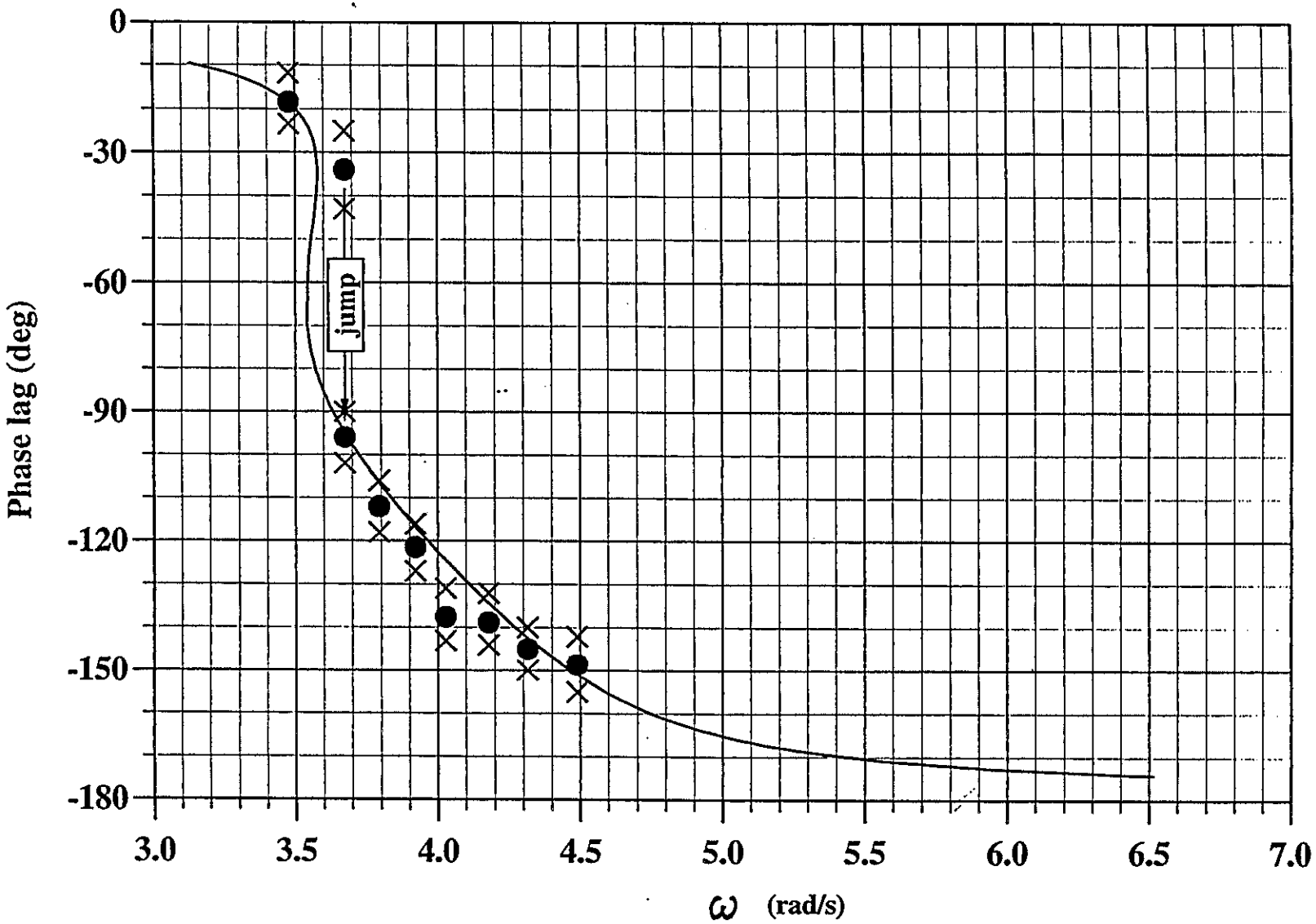

Fig. 4b. Experimental results of rolling motion of the destroyer in regular beam sea - phase lag of stationary roll motion with respect to excitation versus wave frequency. The excitation corresponds to a wave steepness s_w=1/30.

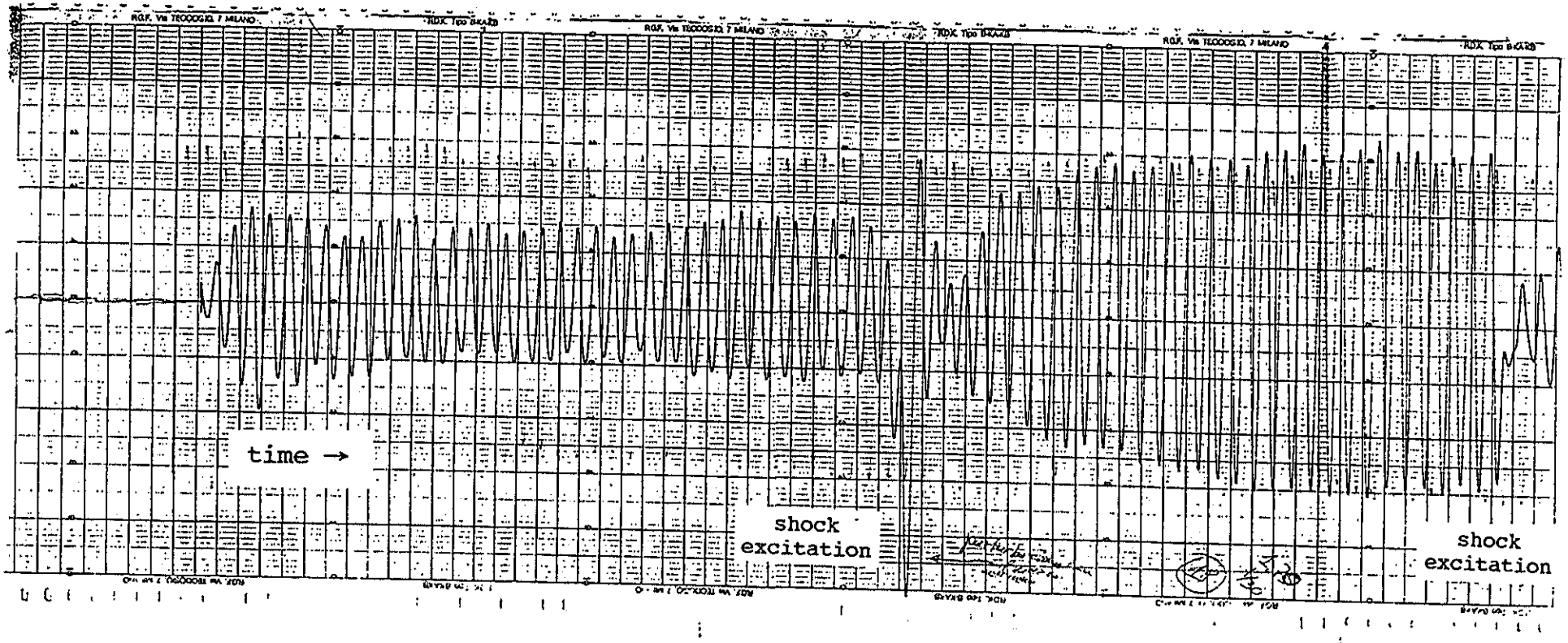

Fig. 5. Time history of roll motion in presence of jump of amplitude.

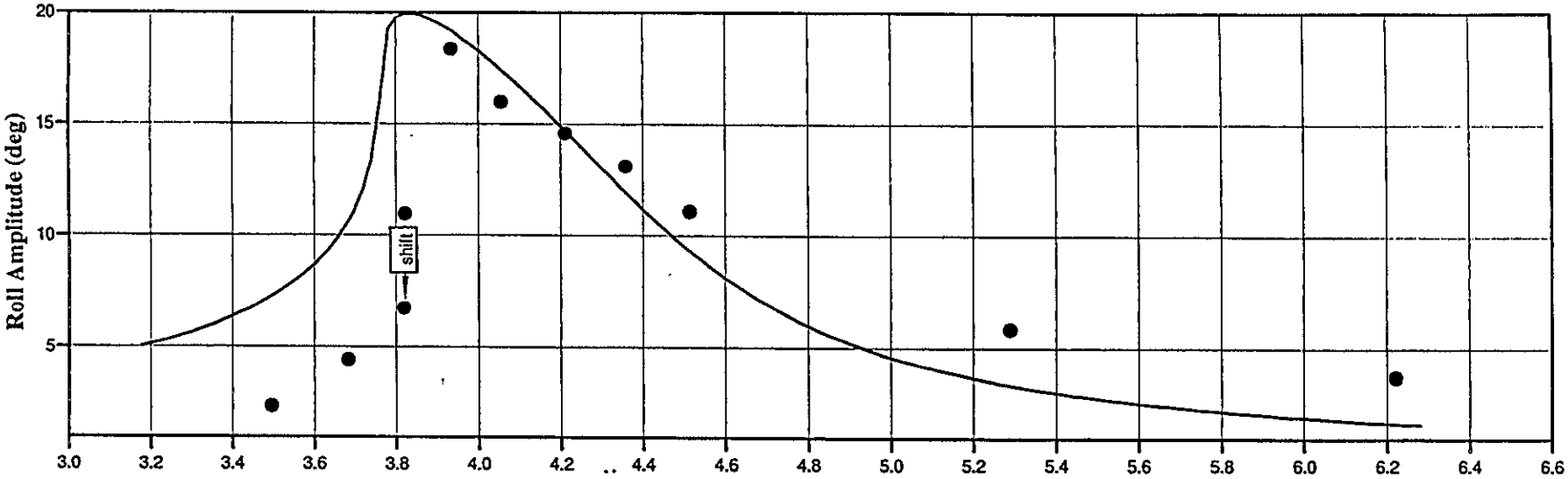

Fig. 6a. Amplitude response curve versus wave frequency.
For comparison experimental points are reported.

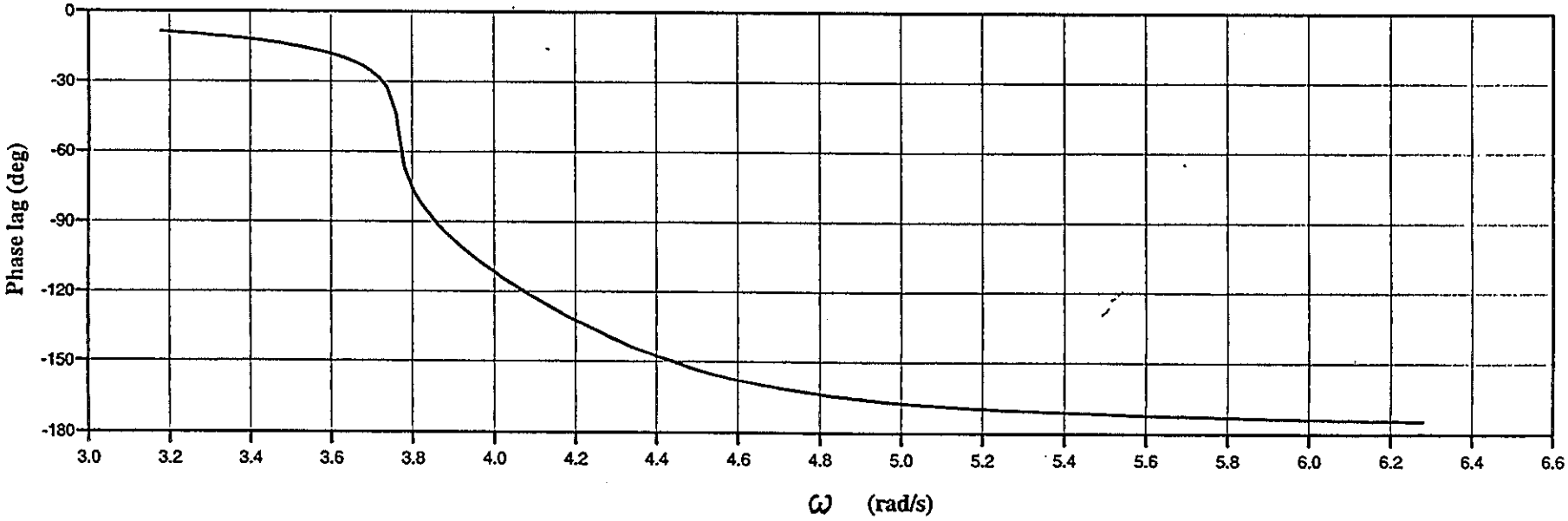

Fig. 6b. Analytical phase lag of stationary roll motion with respect to excitation versus wave frequency.

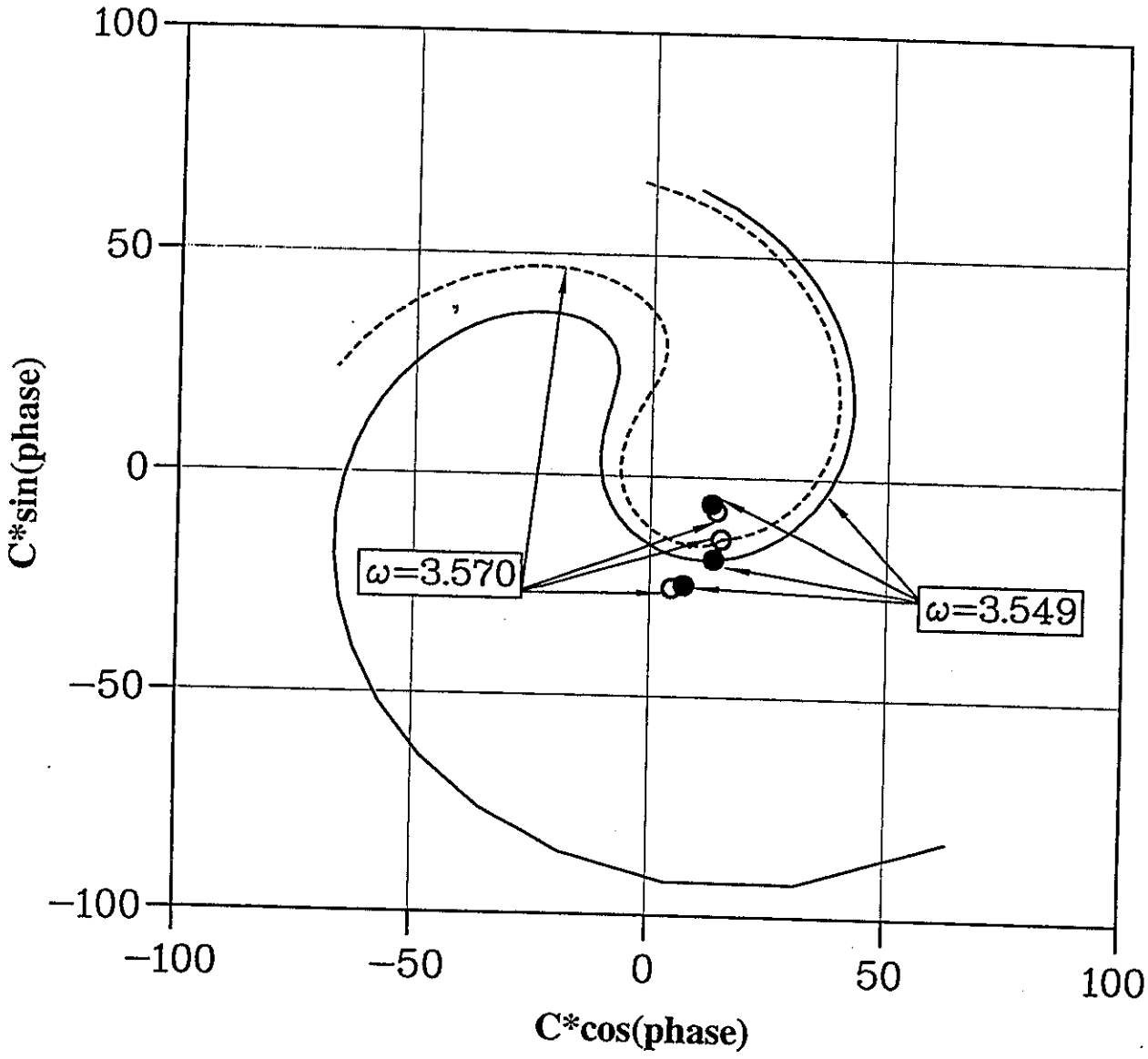

Fig. 8. Domains of attraction in the Van der Pol plane for two different frequencies in the bifurcation range

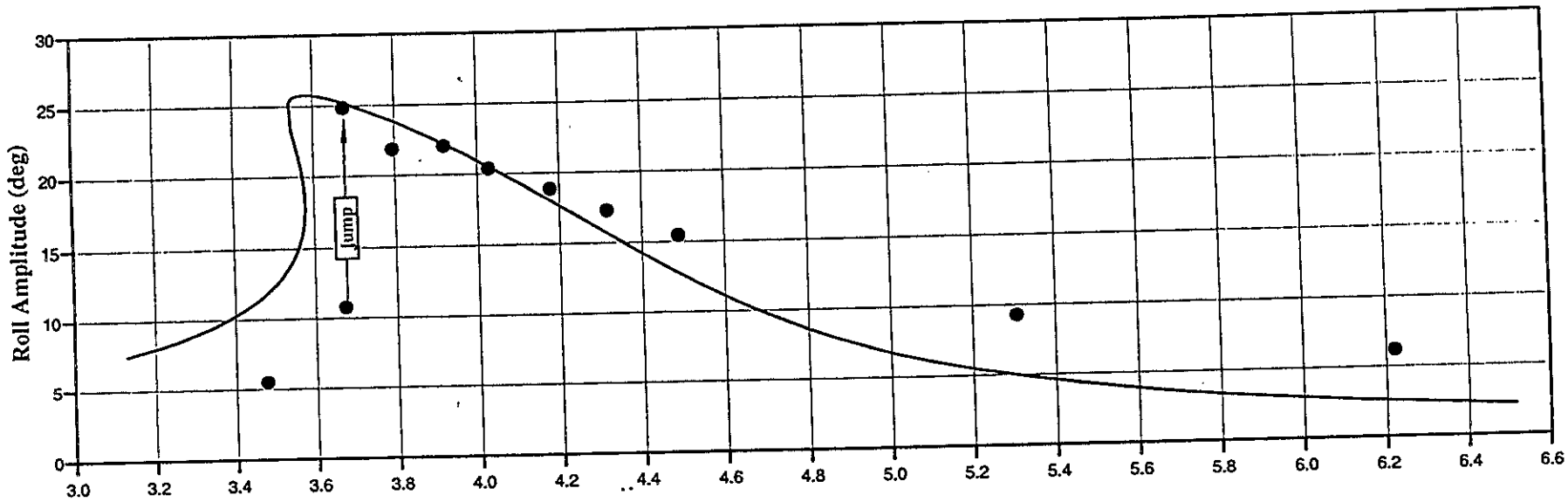

Fig. 7a. Amplitude response curve versus wave frequency.

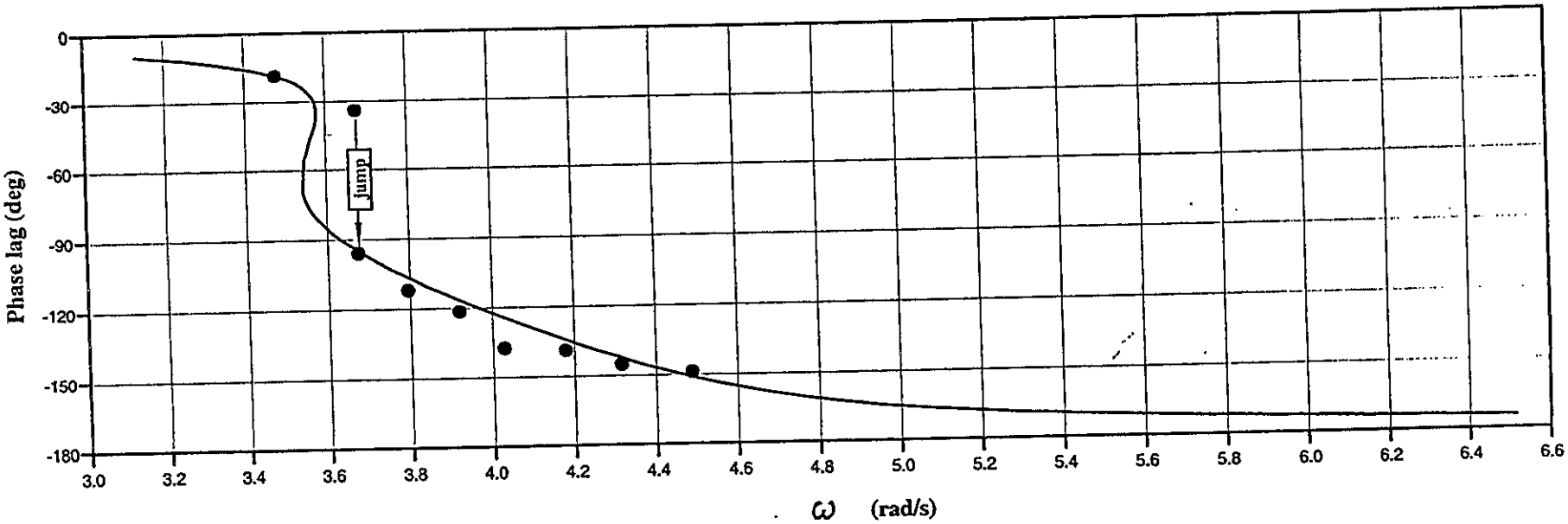

Fig. 7b. Analytical phase lag of stationary roll motion with respect to excitation versus wave frequency.
The excitation corresponds to a wave steepness s_w=1/30.
For comparison experimental points are reported.

ON THE DYNAMIC STABILITY OF A SWATH RESEARCH VESSEL IN FOLLOWING SEAS

A. D. Papanikolaou[1]

ABSTRACT

The paper addresses the dynamic stability and seakeeping behaviour of a SWATH Multipurpose Research Vessel, designed specifically to meet the needs of various institutions in the Mediterranean Area. The behaviour of the vessel, so-called SMURV, in head, oblique and following seas, has been studied systematically through alternative theoretical-numerical and experimental methods. On the basis of results of these studies, the stability and safety of SMURV is evaluated, considering its manifold operational profiles and the specific environmental conditions of the Mediterranean Sea.

1. INTRODUCTION

In recent time, a European Consortium , comprising of shipbuilders, ecological ship operators, an R & D center and an oceanographic institution and finally an university laboratory (see Table 1), has developed a SWATH (Small Waterplane Area Twin Hull) Multipurpose Research Vessel, which will hopefully play in the future an important role in environmental research and combat of marine pollution in the Mediterranean . The development of the vessel under consideration, so called SMURV, is implemented through a three phase EUREKA-EUROMAR project, as outlined in [1]. The first and second phase of the project (feasibility study and preliminary design) have been completed in July 1993, whereas the last stage (prototype realization - detailed design and construction, marketing of the system) is still pending.

The developed vessel SMURV is characterized by its relatively - for a research vessel - high top speed of abt 22-23 knots and the excellent seakeeping behaviour to cope with manifold operational profiles in partly severe seastate conditions , typical to the Mediterranean Sea (short and steep waves). Characteristic mission profiles of SMURV are the rapid marine data acquisition, the analysis and verification of gathered data to support airborne/remote sensing systems (sea truthing), the environmental monitoring (mainly: water quality control and initiation of alarms in case of marine pollution), traditional oceanographic research and finally emergency interventions (in case of natural disasters, marine pollution, accidents etc.). An outline of the general characteristics (initial and final design) and the arrangements of SMURV is given in Table 2 and in Fig. 1 *(see Papanikolaou, A. D. et al [2], 1993)*.

In the framework of the development of SMURV, the stability and seakeeping behaviour of the vessel in head, oblique and following seas has been studied systematically on the basis of theoretical - numerical methods and model experiments. It is this particular part of the SMURV project that will be reported in the following.

2. THEORETICAL PROBLEM BACKGROUND

In evaluating the stability and seakeeping behaviour of SWATH ships, two critical hydrodynamic conditions must be studied carefully, besides the calm water, intact and damaged hull hydrostatics: at first, the zero speed motion responses of the ship in waves of various headings and frequencies and at second, the high speed of advance seakeeping behaviour in following seas. It is this specific last problem that deserves particular attention, both from the theoretical and practical point of view. Namely, despite the excellent seakeeping behaviour of SWATH ships in short waves, and especially in head and bow-quartering seas, it is well known that SWATH-like hull forms tend to become unstable at high speed in following or stern-quartering long waves. This is because of the possible inception of resonances in specific modes of vertical plane motions, i.e. to the heave and pitch motions. Eventually these instabilities in the coupled heave-pitch motion, even enhanced by the possible coupling with the simultaneously excited surge motion, might lead to the so-called *"nose-diving"* situation and practically to the loss of the ship by bow-down capsizing.

The above unpleasant behaviour is due to the small restoring pitch moment and the reduced vertical plane stability of SWATH ships, because of their small waterplane area. The relatively high values of heave and pitch eigenperiods of SWATH ships, resulting from the

[1]Professor and Head of Laboratory of Ship Design, Dep. of Naval Architecture and Marine Engineering, National Technical University of Athens (NTUA)

small waterplane area, and the action of the destabilizing MUNK moments, eventually lead to the above dangerous situation at low frequencies of encounter, or long wave encounter periods, as given for following seas. Through the employment of stabilizing fins the action of the destabilizing MUNK moments at high speed is reduced and both the damping factors and the heave and pitch eigenperiods might be shifted to even higher values, not likely to be matched by the wave period of any probable incident waves in the specific region of operation. However, at small frequencies of encounter between the ship and the incident wave, like in following or stern seas, the effect of any stabilizing fins decreases substantially, because of the small onset (relative) fluid velocity to the fins. Thus it is of importance to study carefully the seakeeping and dynamic stability behaviour of SWATH ships in following seas by suitable theoretical-numerical and experimental technics. However, these studies tend to become very difficult in practice, because of many complications in both the theoretical-numerical, but also in the experimental procedures, when for following seas conditions (at very low frequency of encounter).

In the theoretical-numerical methods the well established, quasi-two dimensional strip theory concept fails in the critical for SWATH vessels following seas condition , because of the violation of at least one fundamental assumption of strip theory, namely that of the high frequency of encounter. but also due to the related failure of the strip theory, to predict correctly the values of the hydrodynamic coefficients at low frequencies. Also, the three-dimensional effects on motions and loads of twin hull vessels, especially in oblique seas and zero speed of advance (critical structural design case), cannot be predicted correctly by a strip theory approach, due to its failure to consider correctly the interaction between the two hulls. Thus it is of importance to develop three-dimensional approaches accounting better for the above failures of the common strip theory.

Such a 3-D method was introduced earlier by the present author (see *Papanikolaou, A. and Schellin, Th.*, 1991 [3], 1992 [4]) and was herein extended to account for the viscous, lift and fin effects typical to SWATH ships (see, especially, proposed procedures by *Lee, C. M., Curphey, R.*, 1977 [5] and *Mc Creight, K. K.* , 1987 [6]). The herein applied method is based on a zero-speed Green's function and accounts for the forward speed effects through the slender body theory assumptions, also governing the strip theory approach. However, in contrast to the strip theory, the present method has several advantages and proves to be sufficient for the seakeeping performance prediction of SWATH ships, for the following reasons. At zero speed the method is, to the possible extent of a linear[2] potential theory with viscosity corrections, exact, and proves to be a valuable tool for the correct estimation of the relevant motions and structural loads, as required by classification societies. Some improvements on the viscous damping and fin effects-terms, at zero or low speed, are necessary to better predict the resonance peaks, especially of the heave-pitch motion. These terms can be only predicted correctly after validation of the relevant semi-empirical formulas by systematic model experiments. Also the above water SWATH hull form, when with flared sections, must be considered through nonlinear terms, at least in the restoring coefficients. In any case, the present linear theory tends always, as can be expected, to overpredict the peaks at resonance, as compared with model experiments (*see Figs 9 to 24 later*).

At head, bow-quartering or beam seas at high or moderate or even low speed of advance -due to the high frequency of encounter and the slenderness of the SWATH hulls - the theory compares very well with model experiments and is fully satisfactory. However, at stern quartering or following seas some problems may arise with the present theory and a treatment is suggested for it in the following. Depending on the value of the frequency of encounter, i.e. to the values of wave frequency, wave heading and ship's speed, as well known, three distinct regions of operation of the ship might be defined (*see, e.g., [7]*). In the first region, the incident wave overtakes the ship and the wave's group velocity is greater than the ship's velocity, in the second region the ship is faster than the wave's group velocity but she is still overtaken by the incident wave, reaching, at certain speed, the point of zero frequency of encounter. At this point the ship is riding on the wave in a quasi-hydrostatic manner. Above this speed, what might be possible for a high speed vessel like SWATH, the ship is faster than the incident wave and the "head waves" situation is repeated, but at lower frequency of encounter, as compared to the incident wave's frequency.

The problems that the present theory might encounter , at very low frequencies of encounter, are related to two distinct effects, namely that of the evaluation of the hydrodynamic

---

[2] The present theoretical method and the related computer algorithm was earlier further developed to consider quasi-second-order drift force and drift motion effects (*see Papanikolaou, A. D., Zaraphonitis, G. N., Journal Schiffstechnik, 1987*) and finally full second-order hydrodynamic effects (*see Zaraphonitis, G. N., Papanikolaou, A. D., Proc. 3rd Int. Workshop on Water Waves and Floating Bodies, Woods Hole, 1988, and Journal Marine Structures, 1993*)

coefficients by potential theory at very low or zero frequency of encounter and the proper inclusion of the viscosity and fin effects for the same conditions. As to the first problem, namely that of the blowing-up of the forward speed effects on the hydrodynamic mass and damping coefficients at very low frequency, it is possible through the consideration of the limiting values of these effects on the hydrodynamic coefficients, for frequency of encounte: going to zero and after application of the rule of L' HOSPITAL, to numerically establish finite and correct values for the added mass, damping and excitation coefficients. However, as to the second problem, namely the proper coefficients for the viscosity and fin effects at low frequencies of encounter, it is necessary to perform in the future more systematic theoretical and experimental studies in order to validate the relevant semiempirical formulas for the hydrodynamic viscous-lift and cross flow drag coefficients, as suggested in [5] and [6].

In the following of the present paper after a brief description of present vessel's preliminary design data and operational requirements, an outline of the hydrostatic and hydrodynamic seakeeping analysis will be presented, including the design of the employed stabilizing fins. Finally, systematic comparisons between results of the above theoretical-numerical 3D method and model experimental data for the seakeeping performance of SMURV for various wave headings at zero and non zero speed of advance are presented and discussed.

3. PRELIMINARY DESIGN STUDY

The preliminary design phase of the presently reported research consisted of five main tasks, namely the General Requirement Definition (Task A), the Preliminary Design Study (Task B), the Design Specification (Task C) and the actual design of SMURV (Task D).

3.1 OUTLINE OF VESSEL'S REQUIREMENTS

In the framework of the first Task (A), an analysis of the requirements resulting from an earlier feasibility study of SMURV (see [8]) has been completed . In addition, an economic and technical market analysis was carried out based on a questionnaire distributed among 42 oceanographic institutions and ecological shipowners in the Mediterranean [9]. A market analysis for Greek institutions was prepared separately on the basis of a national hearing and questionnaire [10]. From the stability point of view, the requirements for SMURV might be summarized as following.

Operational Requirements:

On the operational side the vessel should be able to operate, on a regular basis, without loss of efficiency, in all sea state conditions, typical to the Mediterranean Sea, up to and including seastates 5-6 (annual sign. wave height H_S abt 2.0m). Efficiency means here that the vessel will be able to maintain its course at not significantly reduced top speed, at abt 20 knots, and the corresponding seakeeping behaviour should characteristically fulfil the following criteria, laid down for U.S. Navy designs *(see, e.g., Lamb, G. R. [11], 1987)*:

- significant single amplitude in roll .....≤ 8 deg.
- significant single amplitude in pitch .....≤ 3 deg.
- sign. single amplitude of vert. acceleration
  at any point of the upper (working) deck .....≤ 0.4 g.
  at the upper deck, for gear handling .....≤ 0.2 g.

The above criteria define the limits for the onset of degraded human performance and handling of oceanographic equipment at working deck level.

Survival Requirements:

On the damaged stability side the vessel is expected to be adequate in terms of the SOLAS criteria with every one separate compartment flooded, assuming the extend of damage in the vertical direction equal to the full side deck height (one compartment ship). The remaining quasistatic stability criteria, as to the combined wind-roll motion loads, are taken according to *Goldberg, L. L. and Tucker, R. C.* [12].Because of the multipurpose operational profile of SMURV, that is expected to serve also as rescue vessel in emergency situations (e.g. natural disasters in remotely located islands of the Mediterranean area), the survival requirements include the ability of the vessel to operate in marginal situations in seastates 7 to 8, without significant loss of its safety against capsizing or failure of its structural integrity.

3.2 STABILITY IN CALM WATER

3.2.1 Intact Stability

In Fig. 2 the lines plan and the main hydrostatic curves of a preliminary design of SMURV are shown. The bone like hull form of SMURV resulted from a multistage hydrodynamic optimization with respect to a least horsepower requirement of the vessel at top speed (Froude number over 0.6)(*see Papanikolaou, A. D. et al, FAST'93*) The cross curves of stability of SMURV are shown in Fig. 3, whereas its righting arm for a KG value of 8.0m (GM = 1.143m)is given in Fig. 4. Considering the inclined, balanced position of SMURV, due to a heeling by a crosswise wind of varying speed (variation between 4 and 11 Bft), and the resulting actually shaded area, the theoretical wind heeling arm was compared with the intact GZ restoring arm (see also Fig. 4) and the vessel was found satisfactory in terms of the standard balance procedure of the heeling against the restoring work ability of the ship, including a margin of at least 40% (area $A_1 \geq 1.40\ A_2$ acc. to *Goldberg and Tucker [12]*). It should be noted, that the angle of the ship's rolling into the wind, required by the above criteria, will never exceed 2 deg, in this particular case, because of the shortness and small height of typical Mediterranean seas (see Fig. 16, roll RAO for beam seas and wave frequency over 0.15 Hz). Note that SMURV's roll eigenperiod is quite high, namely over 15 sec (see Table 5).

3.2.2 Damage Stability

The damage stability of the projected vessel has been studied systematically using the well known hydrostatic software program ARCHIMEDES [13] and considering the criteria laid down in [12] for *'one compartment'* SWATH's. In Fig. 5 the definition of the various compartments (A to G) is outlined, each of them consisting of four sub-compartments, namely the (lower) hull, the strut, the sponson and the box region. It was herein assumed, as being the worst case, that the extent of damage covers all four regions of each compartment. The permeability in the various compartments has been varied, to some extent also systematically, between 0.85 for regular spaces, and 0.30 in some special cases, for which the partial use buoyancy materials is indicated. A part of the various studied flooding cases is outlined in Table 3, together with their effect on the heel, trim and metacentric heights (transverse and longitudinal) and local drafts.
Reviewing the herein presented cases, it is evident, that in all studied cases of damage the vessel gets strong heel and trim, but its stability characteristics (GMT and GML) never decrease. Instead of, they substantially increase giving the ship additional stiffness. Flooding of room E, e.g. case 5, seems to be the worst overall case, leading to an immersion of the forward starboard (FS) side - deck corner by 0.143m. This combined heel-trim might be easily balanced by counterflooding one of the many available ballast tank at the opposite, portside, with an amount of water being determined by the position (arm level) of the corresponding tank. The vessel meets the criteria laid down in [12] for the damage stability, considering a 60 kn, or even stronger, side wind and actually less than 2.0 degrees amplitude of roll motion due to the simultaneous action of typical beam waves (assumed significant wave height 3.0 m, modal period 9.0 sec, probability of exceedance for Mediterranean sea: 12%, see Fig. 16 for theoretical-experimental roll RAO). Note, that due to the increased GMT (and GML) in the damage stability case the restoring arms are much steeper, whereas the actual rolling of the damaged ship in waves has been not studied, so far. Finally it should be pointed out, that the reserve buoyancy of the projected vessel, provided by the watertight box structure, is sufficient to balance the total loss of buoyancy of the vessel's struts and lower hulls, in case of structural failure or severe damage due to collision. It must be, of course, assumed, that any openings in the sponson-box interconnection (longitudinal WT bulkhead) must have been closed in time to prevent flooding into the watertight box area.

4. DYNAMIC STABILITY AND ANALYSIS

4.1 HYDRODYNAMIC ANALYSIS

The hydrodynamic performance of the projected vessel in waves has been studied systematically by the use of both theoretical-numerical methods and through the execution of model experiments at the Towing Tanks of NTUA [17] and of the collaborating institution BMT Group Ltd [14]. The theoretical calculations have been based initially on strip theory only, but later also on three dimensional approaches, as outlined in the introduction of the present paper and is described in more details in *Papanikolaou, A. D., 1992, 1993, 1994*. In the present paper emphasis has been given to a sensitivity analysis of the motion responses and indirectly of all hydrodynamic quantities of interest, on the values of certain semiempirical coefficients, used in the theoretical model to account for the viscous lift and cross flow

drag effects (see [5] and [6]). Based on the available experimental data for the linearized damping coefficients in heave, pitch and roll, as they resulted from free decay tests at zero speed for the above modes (see Figs 7a, 7b, 7c), and comparing these values with the potentia theory (wave damping) values, resulting from application of the above mentioned 3D diffractio theory, the values of the cross flow drag coefficient of the lower hull for the vertical plan motion C_{DV} was estimated close to 1.0, whereas the corresponding value for the horizontal plane motion of the lower hull and strut C_{DH} can be assumed to be even higher, compared to a value between 0.4 and 0.7 suggested for all modes of motion and hull parts by *C. M. Lee in [5* on the basis of cross-flow experiments on airshiplike forms in uniform air flow [15]. Also, according to the theoretical-experimental study of *K. Mc Creight (1987)* for SWATH-like configurations , the value of the viscous-lift coefficient α_0 depends on the mode of motion and the hull form characteristics, reaching for SMURV a value of 0.14 for the B_{35} coefficient , 0.08 for the B_{55} and 0.04 for the B_{33} coefficient, compared to 0.07 used until now for al modes of motion according to *C. M. Lee - Thwaites* for airshiplike forms in small angle of incidence, uniform air flow *(see [5], [6])*. In addition, *K. Mc Creight* suggested a dependence of the viscous cross flow drag coefficient both on the hull form and the frequency of oscillation. Based on this, the values of the above coefficients have been varied, herein, systematically to assess their influence on the theoretically predicted motion responses, as compared to the performed model experiments. An outline of these comparisons for various wave headings, incident wave frequency and speed of advance of SMURV, with emphasis on the results for oblique and following seas, is shown later in Figs. 9 to 24.

4.2 DESIGN OF FINS

Because of the relatively high speed of SMURV and its small waterplane area, combined with the unique, for a conventional SWATH vessel, low slenderness ratio of the lower hulls (slenderness ratio $L/\nabla^{1/3}$ abt 5.2), it became necessary to consider the installation of control surfaces (fins) to increase the pitch restoring capability of the vessel and to counteract the destabilizing effect of the well known MUNK moments (see, *e.g., Lee, C. M. and Curphey, R., M., 1977*). The secondary and equally important reason for the employment of stabilizing fins is to increase the vessel's damping in the vertical direction, which will result in improved motion characteristics, especially in the resonance region. Finally, it should be remembered, that the employment of fins has an immediate impact on values of the eigenperiods in the main modes of motion (heave, pitch and roll), that are all shifted to even higher values, especially at higher speeds, compared to the bare hull condition or even to an equivalent monohull vessel design.

Preliminary theoretical calculations indicated that the speed of inception of the pitch instabilities for SMURV was at abt. 18 knots. It should be noted, that seakeeping model experiments at NTUA's Towing Tank at the above speed did not confirm, in practice, the above critical speed, that seems to be in reality above 20 knots. In any case, two design options have been considered at the collaborating institution BMT Cortec Ltd for the possible control surface configuration. The first option considered only one set of aft fin stabilizers, whereas the second option included a combination of a pair of aft fin stabilizers and forward canards. Comparative calculations, however, indicated that due to the relatively short and voluminous lower hull form of SMURV, combined with its high-speed requirement, the possible combination of the aft and forward fins requires a too large total control surface area, of abt. 28 m^2, resulting to an increased calm water resistance, together with an impractical fwd to aft fin ratio of 1:6. Therefore, the implementation of this design option was rejected and the first option associated with only one pair of aft fin stabilizers (tot. area 6.10 m^2/fin)was adopted and tested in model experiments. In Fig. 6 the two considered design options are shown, whereas Table 4 gives some details of the theoretical stability and response analysis for the bare hull and the two fin design options. One should bear in mind, that though the above analysis is based on a fixed fin assumption, the concept of active controlling of SMURV will eventually allow either the decrease of the required control surface area or even improved motion characteristics. Details of these studies can be found in *Atlar, M., 1992 [16]*.

4.3 EXPERIMENTAL STUDY

Besides the theoretical-numerical studies, extensive model tests were undertaken at the towing tanks of NTUA and BMT Group Ltd to assess the overall seakeeping performance and the dynamic station keeping ability of SMURV . The model experiments were aiming at gathering specific data on the motion responses, the wave, current and drift forces and concerned the following tests (see [14], [17]):

- Motion response decrement tests, in heave, pitch and roll, at zero speed (BMT Group Ltd , see Figs. 7a, 7b, 7c)
- Motion and wave drift force tests at zero speed and various headings in regular waves (BMT Group Ltd, NTUA only head and following seas)
- Motion tests at forward speed of 4.5, 18.0 and 25 knots in head and following regular and irregular waves corresponding three different average annual Mediterranean seaspectra (BMT Group Ltd : tested sign. wave height 2.0m and 3.0m and NTUA: tested sign. wave height 1.92m)
- Current drift forces measurements for various headings (BMT Group Ltd)

It should be noted, that though the two employed models by BMT Group Ltd and NTUA have been identical as to their underwater part, namely exactly in scale 1:17.5, they differed significantly in their above-water part : the BMT model was complete in the above water and transverse deck configuration, whereas the NTUA model was kept vertical in the struts and was crosswise simply connected through two fitted aluminium bars. Insofar, it could be expected, that comparing the results of theoretical predictions by NTUA, that are based on a linear theory, but also NTUA's model experiments with BMT's model experiments, especially in the regions of motion resonance for the main modes of motion, some differences might be justified due to the influence of the above water part on the motion responses.

4.4 DISCUSSION OF RESULTS

Some typical comparative results are discussed in the following. The comparisons concern specifically the motions of SMURV in heave, pitch and roll and the drift forces and moments for various wave headings and speeds of advance, with emphasis on the oblique and following seas case. The calculations have been performed at the Laboratory of Ship Design of NTUA with various discretization nets for the model of SMURV(see Fig. 8 for two typical examples). The model experiments have been performed in parallel with two similar models in scale 1:17.5 (model length : 2.0 m) at the Towing Tanks of British Maritime Technology Group Ltd (partner under the EUROMAR / EU 409- SMURV project) and of NTUA (Athens).
The theoretical-numerical results , Figs. 9 to 24 (here given for a discretization of 2x756 elements only) compare, in general, fairly well with the experimental data, except for wave frequencies near the motion resonances, where nonlinear effects (above water hull form and viscosity effects)are strong. In some of the BMT Group Ltd experiments, in particular, the incident wave height has been varied systematically, besides the wave frequency, in order to study any nonlinear motion behaviour (see, e.g., the heave RAO at zero speed, Fig. 9, for wave frequency abt 0.09 Hz, i.e. to the pitch resonance period). It is evident from the figure, that for a steep incident wave, e.g. wave height 3.4 m, the measured heave RAO is reduced, compared to the flat wave case of 0.8 m height, due to the action of the above water flared section of SMURV, what cannot be predicted correctly by the present linear approach. Also, it should be noted, that the vessel under investigation will be operating mostly in short period Mediterranean waves (sign. wave period abt 5 to 6 sec, corresponding wave frequency over 0.15 Hz), thus the designed ship is predicted to be perfectly suited for the required manifold operational profiles. Finally, it proves that the suggested 3D panel method is, at this stage, fully sufficient for evaluating the seakeeping and dynamic stability of SWATH ships, even under adverse conditions.

5. CONCLUSIONS

The reported work aimed to demonstrate the potentialities of the SWATH concept and to provide interested Mediterranean parties with the fundamentals for the development of a SWATH Multipurpose Research Vessel, to rationally manage the marine environment of the Mediterranean Sea. The undertaken theoretical and experimental hydrodynamic analysis confirmed the initial assumptions about the performance of the proposed vessel in calm water and in waves, especially in the relatively short and steep Mediterranean Sea waves, to the extent possible. In particular, in this present paper, it was demonstrated that the vessel can safely operate in high seastates and in adverse environmental conditions. Its intact and damaged stability is sufficient in terms of relevant criteria, as known from US Navy specifications for similar ships. The hydrodynamic performance of the vessel in the critical following seas condition is satisfactory and can be predicted sufficiently with the used 3D theoretical-numerical model. The final phase of the present project involves the preparation of the required documents to tender for the construction and marketing of SMURV. However, this depends upon the critical review of all preliminary design phase results and upon the identification of interested parties for securing the financing, the construction and the operation of SMURV.

6. ACKNOWLEDGEMENTS

The present work is based on results of the EUROMAR EU 409 project (code: SMURV). The author likes to thank the collaborating partners of SMURV, especially BMT Cortec Ltd, for the provision of data for the SMURV model experiments and the Greek Secretariat General for Research and Technology for the partial funding of the Greek partners of SMURV. Some concepts of the present theoretical work have been developed during the stay of the author as Visiting Professor at the Osaka University, Dep. of Naval Architecture and Ocean Engineering. The author likes to acknowledge the support of his colleague and friend, Professor S. Naito, who organized his sabbatical visit to Japan. Finally, the help of Mr. Chris Koskinas (Dr.-Eng. Candidate, NTUA) in completing in time several calculations for SMURV is acknowledged.

7. REFERENCES

[1] Team of Partners, "SMURV - SWATH MUltipurpose Research Vessel for the Mediterranean-EUREKA-EUROMAR Project EU 409, Project announced at the 7th Ministerial Conference, Vienna, 1989.
[2] Papanikolaou, A., Atlar, M., Khattab, O., "Hydrodynamic Analysis and Design of a SWATH Multipurpose Research Vessel", Proc. 2nd FAST'93 Conf., Yokohama, 1993.
[3] Papanikolaou, A., Schellin, Th. E., "On Seakeeping Calculations of a SWATH Passenger-Car Ferry", Proc. 1st FAST'91 Conf., Trondheim, 1991.
[4] Papanikolaou, A, Schellin, Th., E., "A Three Dimensional Panel Method for Motions and Loads of Ships with Forward Speed", Journ. Schiffstechnik, Vol. 39, 1992, pp 147 - 156.
[5] Lee, C. M., Curphey, R. M., "Prediction of Motion, Stability, and Wave Load of Small-Waterplane-Area, Twin-Hull Ships", Trans. SNAME, Vol. 87, 1977.
[6] Mc Creight, K. K., "Assessing the Seaworthiness of SWATH Ships", Trans. SNAME, 1987.
[7] Levis, E. V.,(ed.), "Principles of Naval Architecture", Vol. III : Motions in Waves and Controllability, by R. Beck, W. E. Cummins, J. F. Dalzell, W. C. Webster, Published by SNAME, New Jersey, 1989.
[8] Polydorou, G. and Gasparoni, G., "SMURV - SWATH MUltipurpose Research Vessel - Preliminary Study - Executive Summary", Cetena - Technomare Report No. 3291, 1988
[9] Longobardi, A., "SMURV EU 409 : Market Analysis - Technical and Economical Specification", Italmare s.p.A. Rep., 1992
[10] Papanikolaou, A., "SMURV EU 409 : 2nd Progress Report", NTUA Report, 1991.
[11] Lamb, G. R., "Influence of Seakeeping Requirements on SWATH Ship Geometry", pres. at SNAME Chesapeake Section, 1987.
[12] Goldberg, L. L., Tucker, R. G., "Current Status of Stability and Buoyancy Criteria used by the U.S. Navy for Advanced Marine Vehicles", Journal Naval Engineers, Vol. 87, 1975.
[13] Söding, H., "Hydrostatic Program ARCHIMEDES", publ. SET GmbH, Hamburg, 1989.
[14] Holland, B., "Seakeeping Tests for a SWATH Vessel", BMT Group Ltd, Draft-Report, 1993.
[15] Thwaites, B., "Incompressible Aerodynamics", Oxford Univ. Press, Oxford, 1960.
[16] Atlar, M., "SMURV Control Surface Design", BMT Corteç Rep. No. 289803.R14, 1992.
[17] Papanikolaou, A., Koskinas, Ch., Zaraphonitis, G., "Seakeeping Analysis of the SWATH Multipurpose Research Vessel - SMURV", Final Rep. Project EU 409 EUROMAR-SMURV, Lab. of Ship Design, Nat. Techn. Univ. Athens, 1993.
[18] Papanikolaou, A., "On the Seakeeping Performance of a SWATH Research Vessel in Oblique and Following Seas", Pres. at the Seakeeping Committee of The Soc. of Naval Architects of Japan, Osaka, February, 1994.

Table 1 : List of partners of SMURV-EU409
(updated list, as of November 1992).

1.	GB	:	BMT CORTEC Limited, Newcastle upon Tyne (*)
2.	GB	:	Swan Hunter International Ltd., Newcastle upon Tyne (**)
3.	GB	:	Vosper Thornycroft (UK) Ltd., Southampton (**)
4.	GERMANY	:	DMT Marinetechnik GmbH, Hamburg, (withdrawn)
5.	GREECE	:	ASD Marine Services - Alpha Marine Ltd., Piraeus (**)
6.	GREECE	:	National Center for Marine Research, Athens (**)
7.	GREECE	:	National Technical Univ. of Athens, Athens (*) (***)
8.	ITALY	:	CETENA SpA, Genoa (**)
9.	ITALY	:	ITALMARE SpA, Piano di Sorrento (*)
10.	SPAIN	:	ECOLMARE Iberica, Barcelona (**) (not active)

(*) : National Project Leaders, (**) : Industry partners;
(***) : Acting Project Leader

Table 2 : Main Characteristics of SMURV -
Feasibility Study & Preliminary Design (*)

Main Dimensions

Length of upper deck, LOA	39.00 m
Length between perpendiculars, LBP	33.00 m
Max breadth	18.00 m
Side deck height	11.20 m
Full load displacement (est.)	520 tons
Full load displacement (final)	610 tons
Payload (est.)	90 tons
Draft (max)	4.40 m
Draft (final)	4.50 m
Demihull-axes distance	14.00 m

Arrangements

Number of decks (incl. superstructures) : 4
Number of watertight bulkheads : 5

Hull Structure-Material

Main hull : normal steel altern. HT steel
Superstructure : light alloy/HT steel *(final: light alloy)*
Classification : RINA, G.L., ABS *(final ABS)*

Propulsion/Steering/Fins

Main Motors : 4 medium/high speed engines, 2 per lower hull, max. horse power abt. 11.000 HP.
final : *2 x MTU 16V 396 TE74L and 2 x MTU 12V 396 TE74L*
total MCR abt. 9.500 HP, all machinery at main-deck level.

Propellers : 2 CP propellers, 1 per hull.
final : *2 x 5 bladed CP propellers, 1 per hull.*

Side Thrusters : 2 lateral tunnel thrusters, 1 per hull at forebody
Rudders : 2 spade rudders, 1 per hull, behind CP propellers.

Stabilizers : 2 pairs of automatically/manually controlled aft and fwd fins.
final : *1 pair of automatically controlled aft fins.*

Electric Power : 3 x 220 kW power generators
final : *2 x 550 kW shaft generators*

Speed : max. continuous 25 knots *(final : 22 knots)*
: cruise 18 knots *(final : 15 knots)*
: towing 3-4 knots *(final : 4.5 knots)*

Autonomy : Bunkering 1000 nm, Max. Mission 15 days

Crew/Scientific
Personnel : 12 persons crew, 12 scientists (incl. 6 females)
Work space : Free main-deck abt. 430 m^2
Scient. modules : 6 x 10 ft containers or 2 x 10 ft and 2 x 20 ft (TEU)

Note (*) :
Initial values acc. to Feasibility Study-Final Values acc. to Preliminary Design.

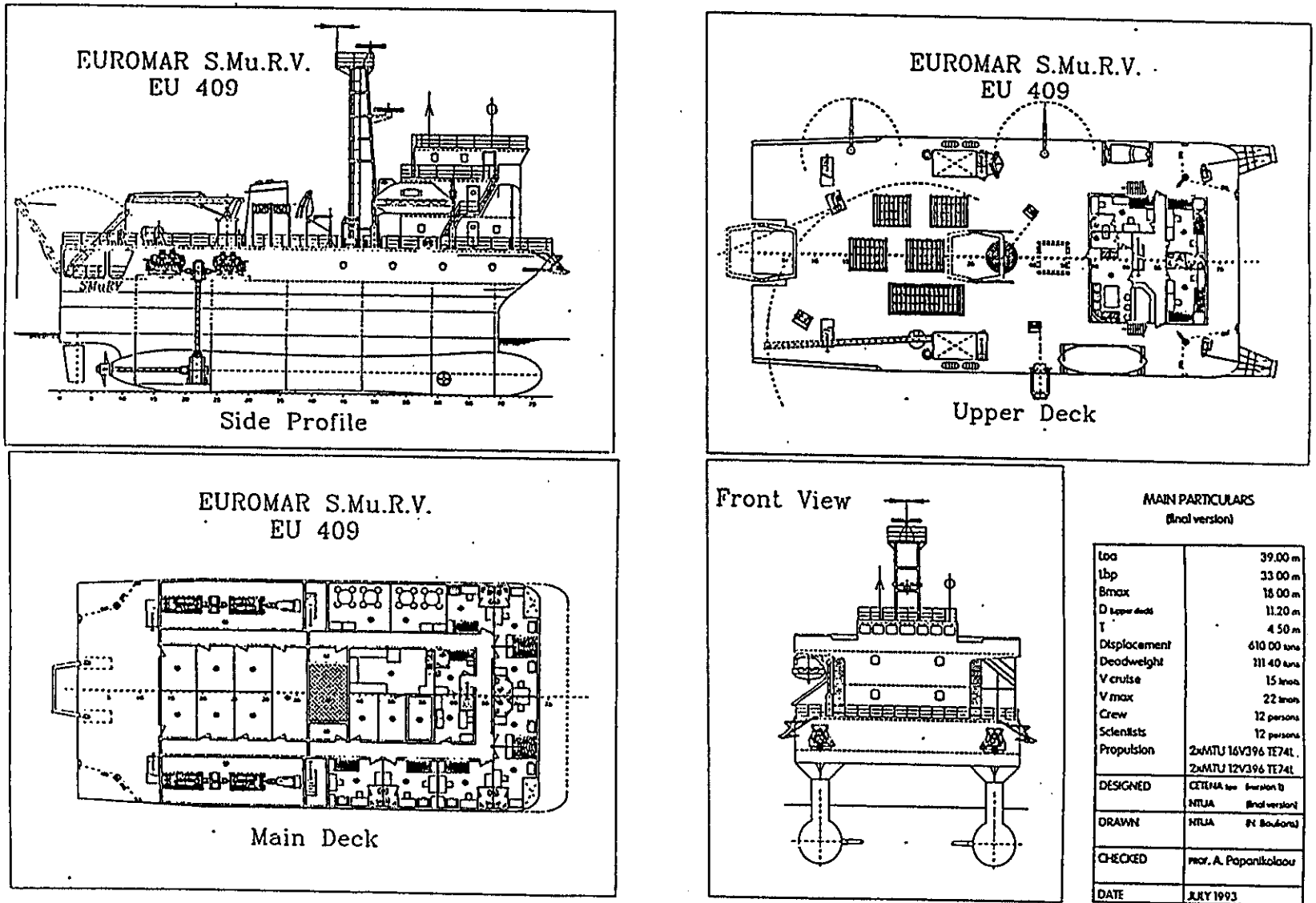

Fig. 1 : SMURV-SWATH Multipurpose Research Vessel General Arrangements

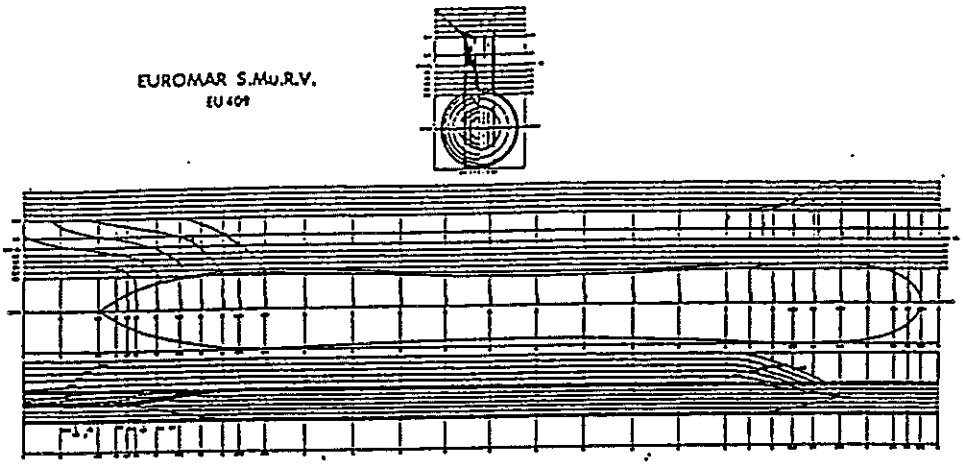

Lines Plan

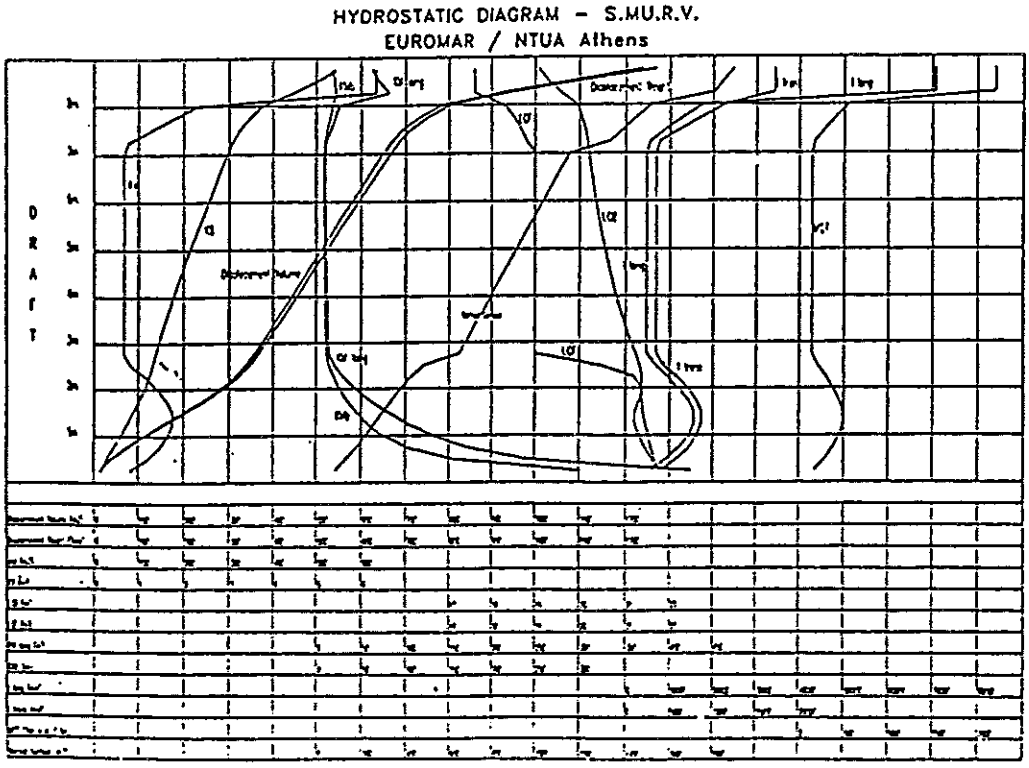

Fig. 2 : Lines Plan and Hydrostatic Diagram of a Preliminary SMURV Hull Form (NTUA-Lab. of Ship Design).

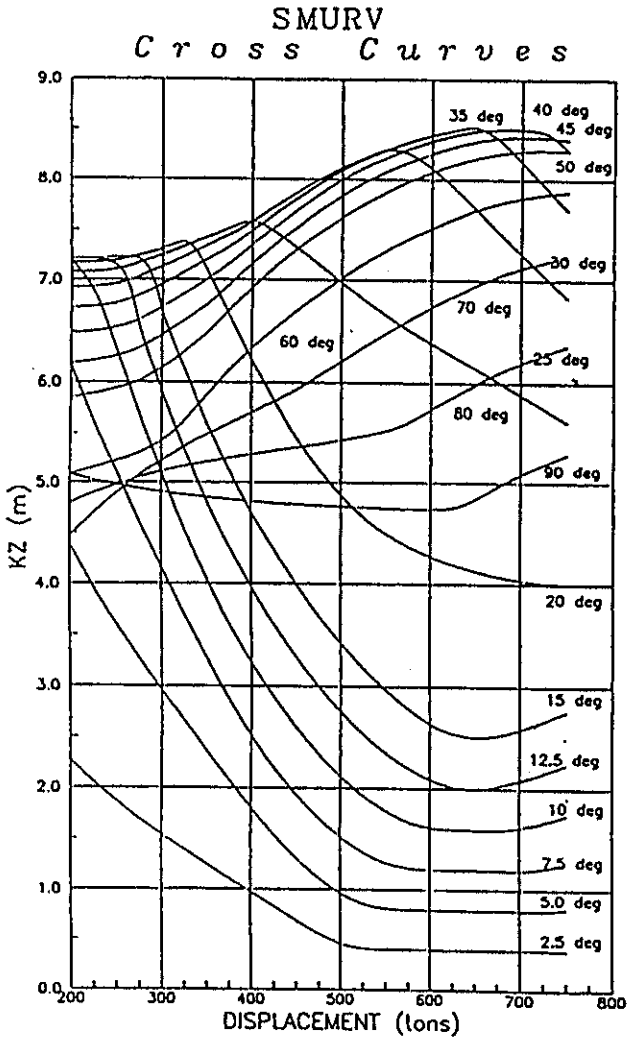

Fig. 3: Cross Curves of Stability of SMURV (NTUA-Lab. of Ship Design)

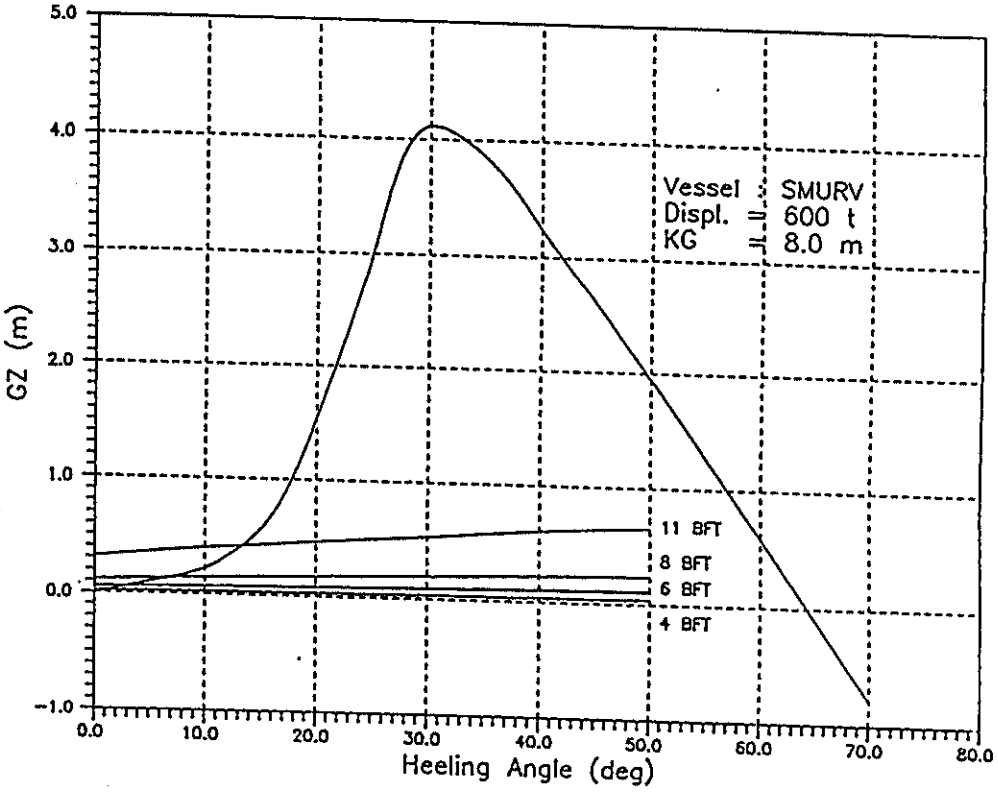

Fig. 4: Righting Arm Curve of SMURV at design condition, GM = 1.143m, vs. Wind Heeling Arms for Varying Side Wind Velocity (Bft 4 to 11)

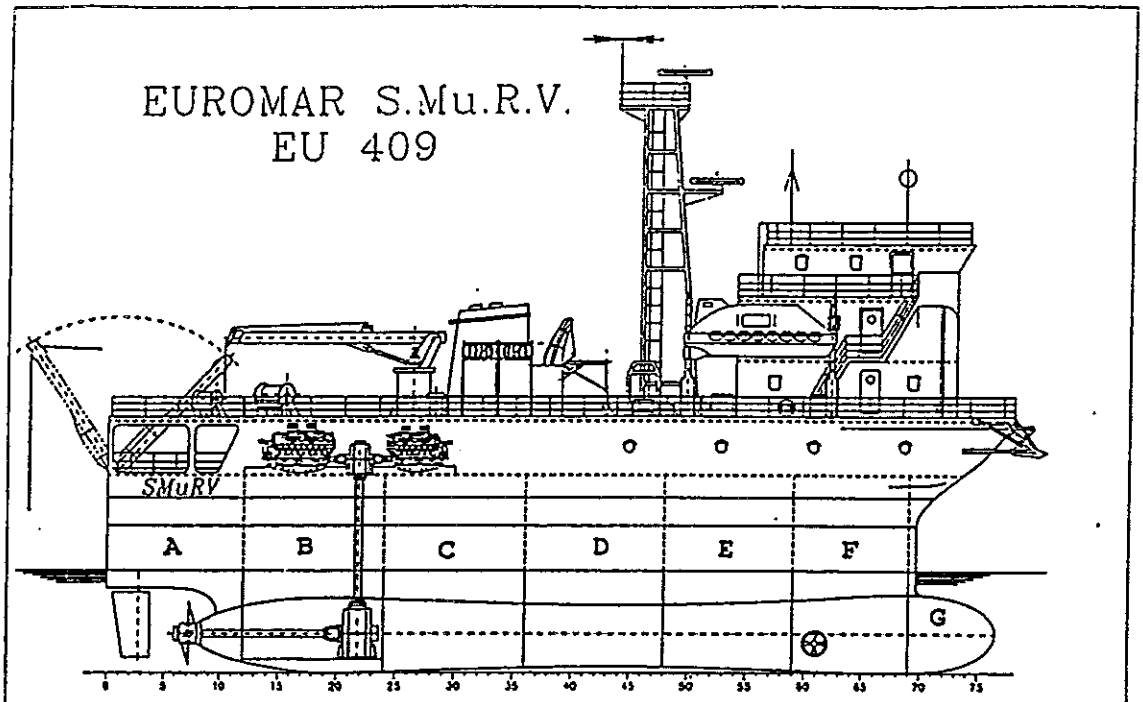

Fig. 5: SMURV - Definition of WT Compartments for Damage Stability Analysis

TABLE 3: DAMAGE STABILITY ANALYSIS OF SMURV
Systematic Case Studies

CASE	ROOM[8]	Permeability	Draft[9]	Trim[10]	Heel[11]	GMT	GML	FB[12](FP)	FB(FS)	FB(AP)	FB(AS)
1	A	H,ST,SP,B: 0.85	5.487	-4.157	-5.811	1.276	5.566	5.601	3.778	4.121	2.299
2	B	H,ST,SP,B: 0.85	6.022	-5.238	-13.68	4.162	12.88	6.416	2.159	4.596	0.339
3	C	H,ST,SP,B: 0.85	4.986	-0.348	-15.93	6.981	17.16	6.018	1.077	5.898	0.957
4	D	H,ST,SP,B: 0.85	4.175	3.749	-16.01	6.438	14.25	5.423	0.457	6.712	1.746
5	E	H,ST,SP,B: 0.85	3.276	8.676	-14.83	5.483	13.42	4.463	-0.143	7.454	2.847
6	E	H,ST,SP,B: 0.80	3.291	8.501	-14.56	5.294	13.04	4.474	-0.049	7.409	2.885
7	E	H,ST,SP,B: 0.75	3.304	8.332	-14.28	5.031	12.28	4.485	0.045	7.366	2.926
8	E	H: 0.85 ST,SP,B: 0.75	3.291	8.502	-14.50	5.301	13.02	4.467	-0.040	7.403	2.896
9	E	H: 0.85 ST,SP,B: 0.70	3.297	8.421	-14.34	5.177	12.62	4.469	0.010	7.379	2.921
10	F	H,ST,SP,B: 0.60	2.605	11.791	-11.77	3.789	10.17	3.633	-0.037	7.737	4.067
11	F	H,ST,SP,B: 0.55	2.663	11.389	-11.56	3.670	9.582	3.689	0.081	7.658	4.050
12	F	H: 0.85 ST,SP,B: 0.35	2.584	11.950	-11.59	3.869	10.60	3.574	-0.042	7.735	4.118
13	F	H: 0.85 ST,SP,B: 0.30	2.606	11.797	-11.48	3.825	10.39	3.591	0.007	7.701	4.117
14	G	H,ST,SP,B: 0.85	2.757	10.286	-9.24	2.560	6.780	3.663	0.773	7.279	4.389

Mass of ship: 610 tons, KG = 8.00 m, LCG = 21.145 m
[8]as defined in Fig. 5
[9]all lengths in [m]
[10] in [% L]
[11]in [deg]
[12]FB means: freebord, measured at main deck level,
FP: Forward - Portside, FS: Forward-Starboard, AP: Aftward-Portside, AS: Aftward-Starboard

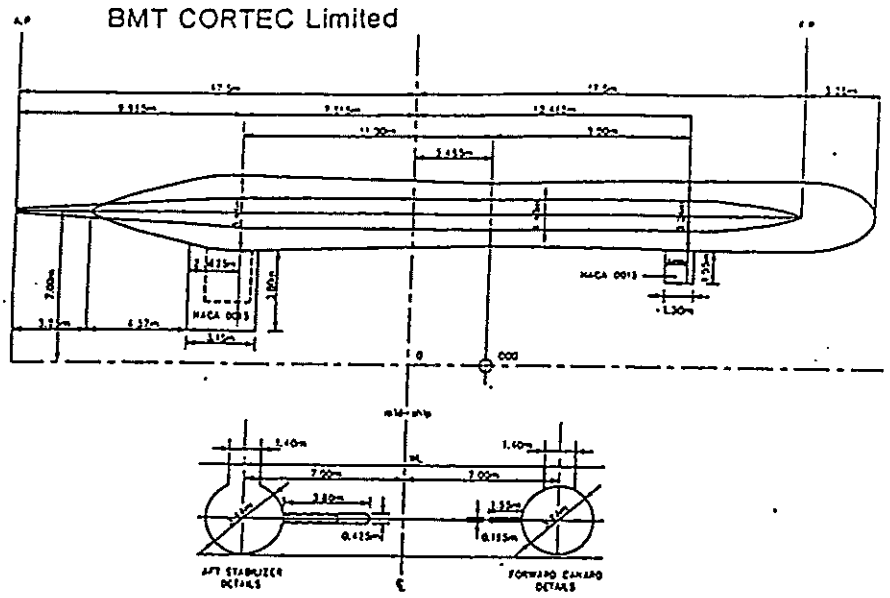

Fig.6 : Alternative Design Options for SMURV's Fin Stabilizer System

Table 4 : SMURV Transient Response Analysis Details for Alternative Fin Stabilizer Systems.

Coeff	Bare Hull				Bare Hull + All Stabilizers				Bare Hull + All Stabilizers + Canards			
	0	10	18	25	0	10	18	25	0	10	18	25
M	610.00	610.00	610.00	610.00	612.664	612.664	612.664	612.664	619.69	619.69	619.69	619.69
A_{33}	372.63	372.63	372.63	372.63	390.72	390.72	390.72	390.72	437.96	437.96	437.96	437.96
B_{33}	19.661	58.355	89.145	116.005	18.761	186.561	336.64	464.135	19.661	307.20	537.076	736.21
C_{33}	844.664	844.64	844.64	844.64	844.64	844.64	844.64	844.64	844.64	844.64	844.64	844.64
I_{55}	44906.	44906.	44906.	44906.	45319.65	45319.65	45319.65	45319.65	45374.97	45374.97	45374.97	45374.97
A_{55}	33473.26	33473.25	33,473.25	33473.26	35649.43	35649.43	35649.43	35649.43	41227.71	41227.71	41227.71	41227.71
B_{55}	1469.2	5118.773	8040.23	10505.63	1469.2	21564.92	36361.5	53706.50	1469.2	33331.37	56811.06	81250.13
C_{55}	34706.0	24799.63	2604.88	-27219.31	34706.0	32206.96	26611.12	19066.01	34706.0	32405.62	27248.28	20016.12
Stability	Stable	Stable	Stable	Unstable	Stable	Stable	Stable	Stable	Stable	Stable	Stable	Stable
T_{3n}	6.778	6.761	6.765	.	6.849	6.868	6.968	7.077	7.031	7.125	7.33	7.637
T_{5n}	0.443	11.188	25.92	.	8.597	10.20	12.035	17.458	9.963	10.876	14.12	48.363
$T_3^{(2)}$	86.83	23.35	15.26	.	70.03	7.040	4.094	2.997	73.825	4.77	2.73	1.566
$T_1^{(2)}$	73.975	21.22	13.51	.	78.405	5.11	2.926	2.1295	82.665	3.663	2.061	1.495
ζ_3	0.01058	0.0320	0.0488	.	0.0107	0.1073	0.184	0.252	0.0105	0.1625	0.413	0.3805
ζ_5	0.01408	0.0581	0.281	.	0.01387	0.215	0.413	0.6703	0.0133	0.3133	0.603	0.963

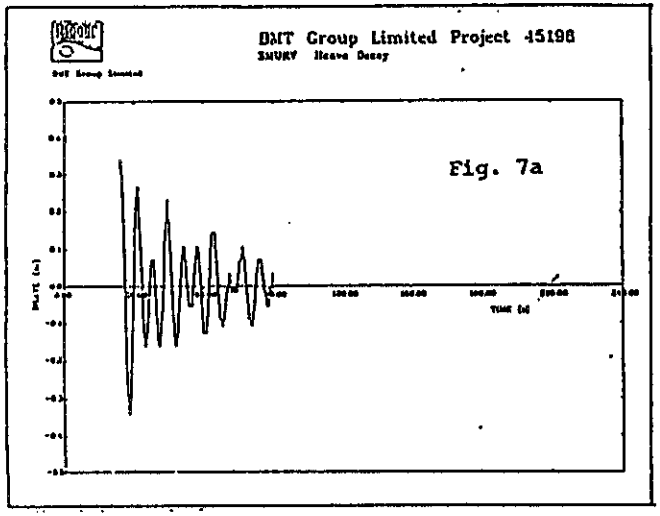

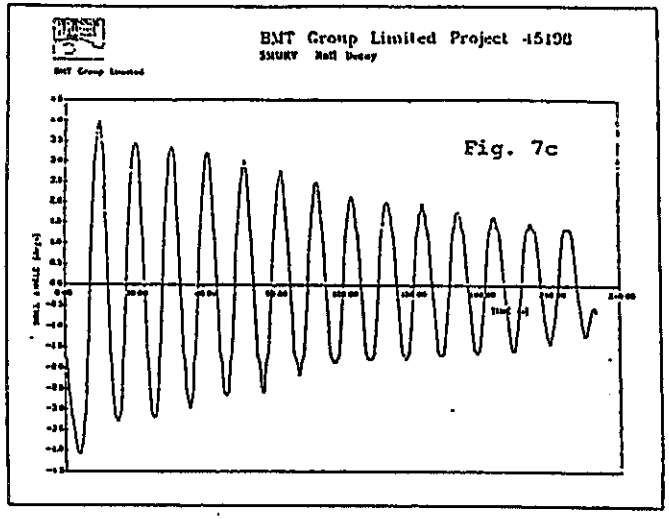

Fig. 7 : SMURV - Motion Response Decrement Tests
7a: heave, 7b: pitch, 7c: roll

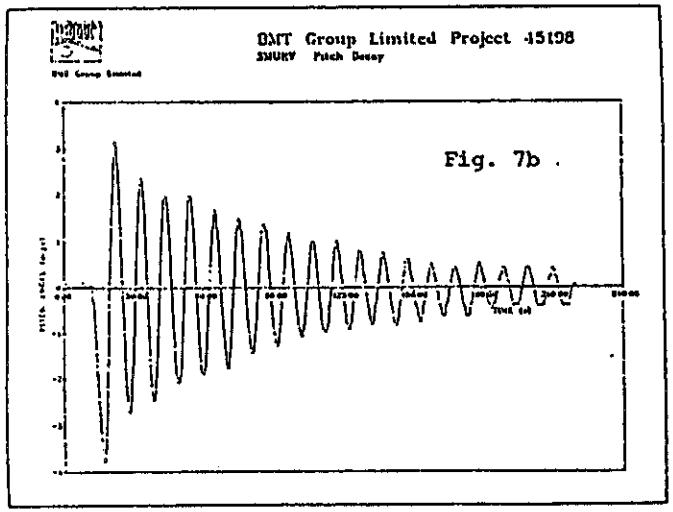

TABLE 5: Mean Values of Natural Periods and of Damping of SMURV acc. to Motion Response Decrement Tests of BMT Group Ltd

Mode	Mean Natural Period[sec]	Mean Natural Frequency [Hz]	Mean Linear. Damping Coeff. [% of crit.]
Heave	7.00	0.143	2.00
Pitch	10.65	0.095	1.74
Roll	15.90	0.063	1.14

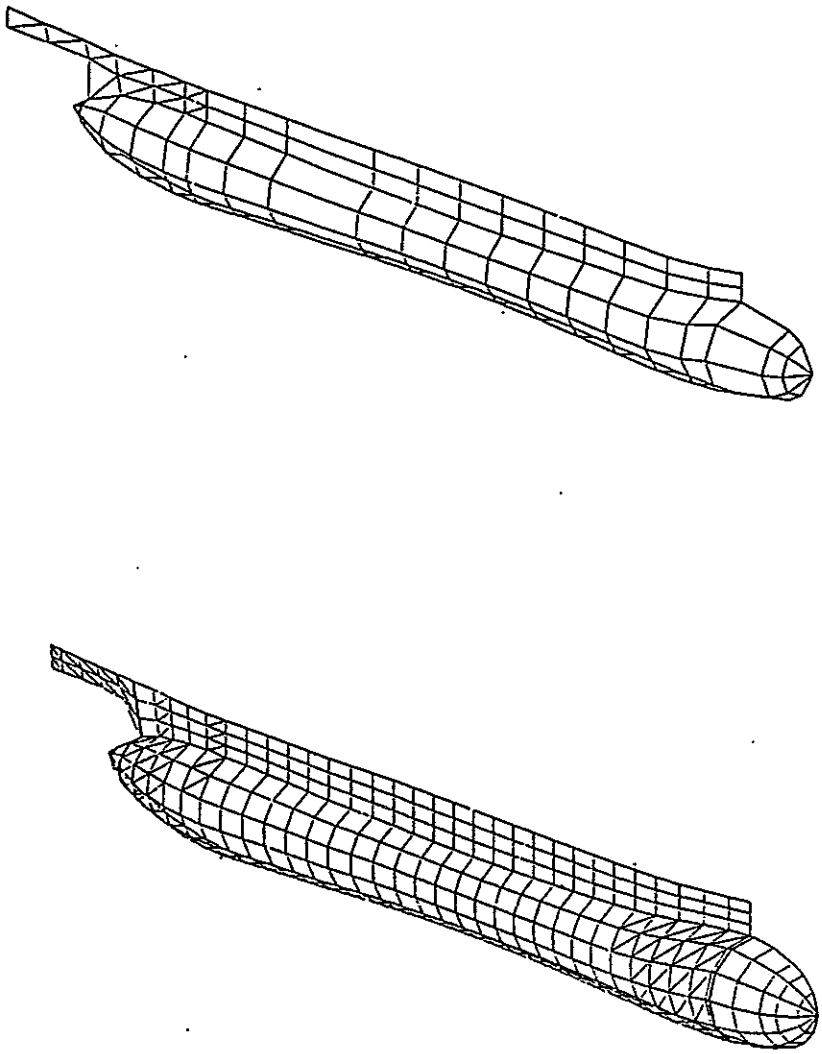

Fig.8: Alternative Discretization Nets for 3D Seakeeping Calculations of SMURV
Fig. 8a: No. of Elem 2x248, Fig. 8b: No. of Elem. 2x794

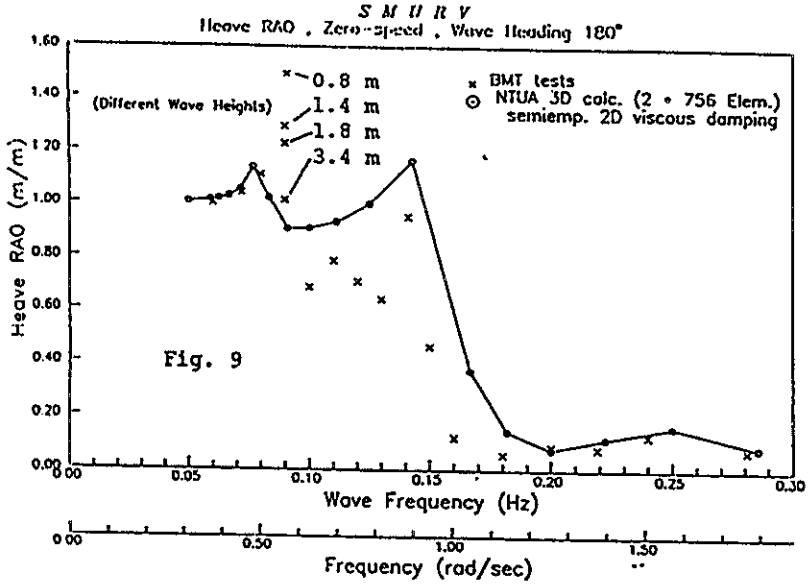
S M U R V
Heave RAO , Zero-speed , Wave Heading 180°
(Different Wave Heights)
0.8 m
1.4 m
1.8 m
3.4 m
BMT tests
NTUA 3D calc. (2 • 756 Elem.)
semiemp. 2D viscous damping
Heave RAO (m/m)
Wave Frequency (Hz)
Frequency (rad/sec)
Fig. 9

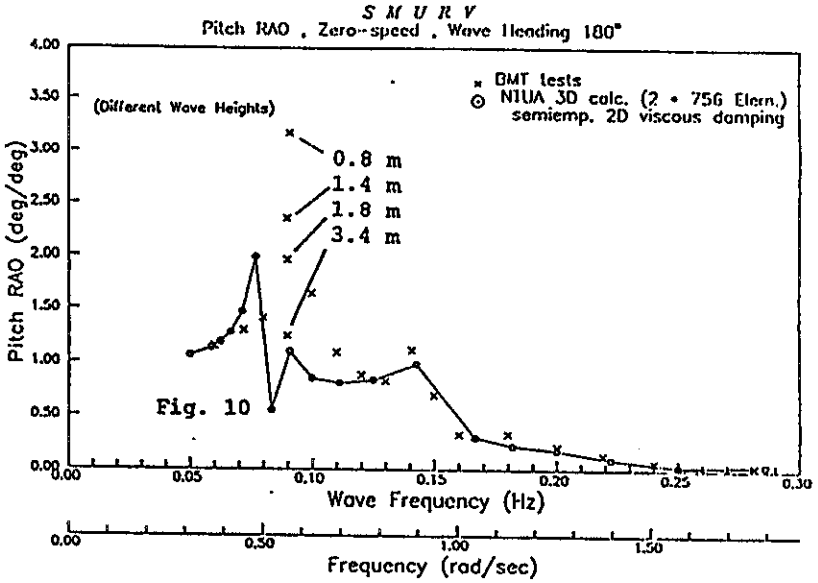
S M U R V
Pitch RAO , Zero-speed , Wave Heading 180°
(Different Wave Heights)
0.8 m
1.4 m
1.8 m
3.4 m
BMT tests
NTUA 3D calc. (2 • 756 Elem.)
semiemp. 2D viscous damping
Pitch RAO (deg/deg)
Wave Frequency (Hz)
Frequency (rad/sec)
Fig. 10

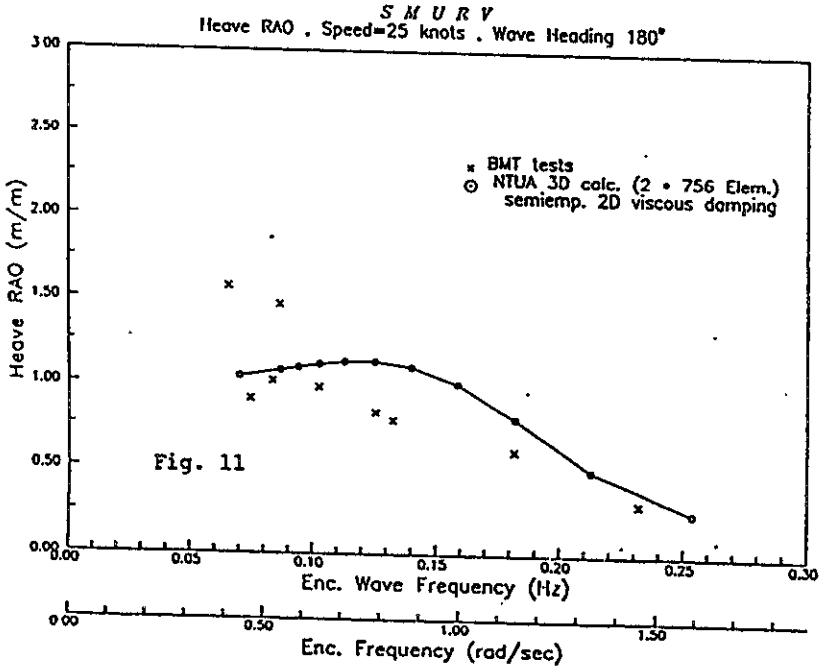
S M U R V
Heave RAO , Speed=25 knots , Wave Heading 180°
BMT tests
NTUA 3D calc. (2 • 756 Elem.)
semiemp. 2D viscous damping
Heave RAO (m/m)
Enc. Wave Frequency (Hz)
Enc. Frequency (rad/sec)
Fig. 11

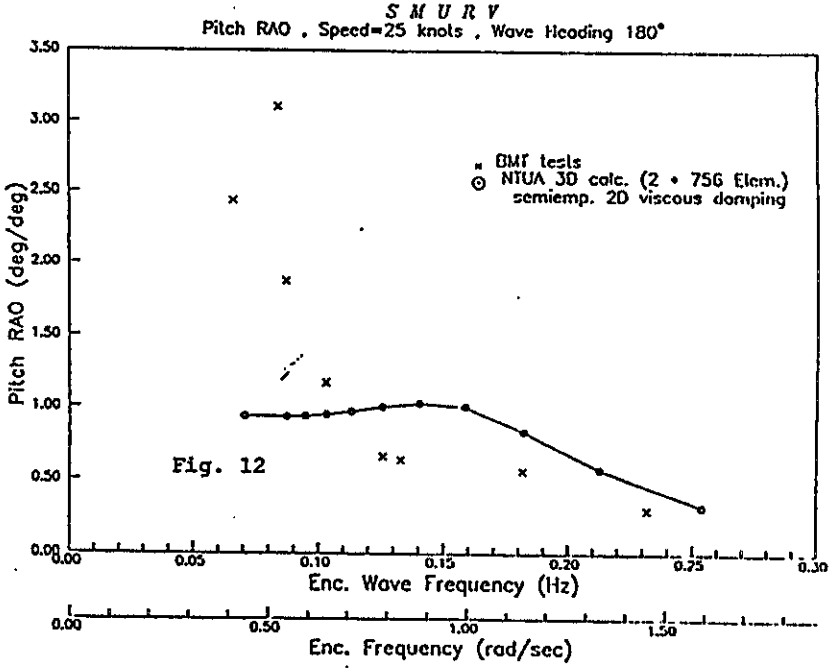
S M U R V
Pitch RAO , Speed=25 knots , Wave Heading 180°
BMT tests
NTUA 3D calc. (2 • 756 Elem.)
semiemp. 2D viscous damping
Pitch RAO (deg/deg)
Enc. Wave Frequency (Hz)
Enc. Frequency (rad/sec)
Fig. 12

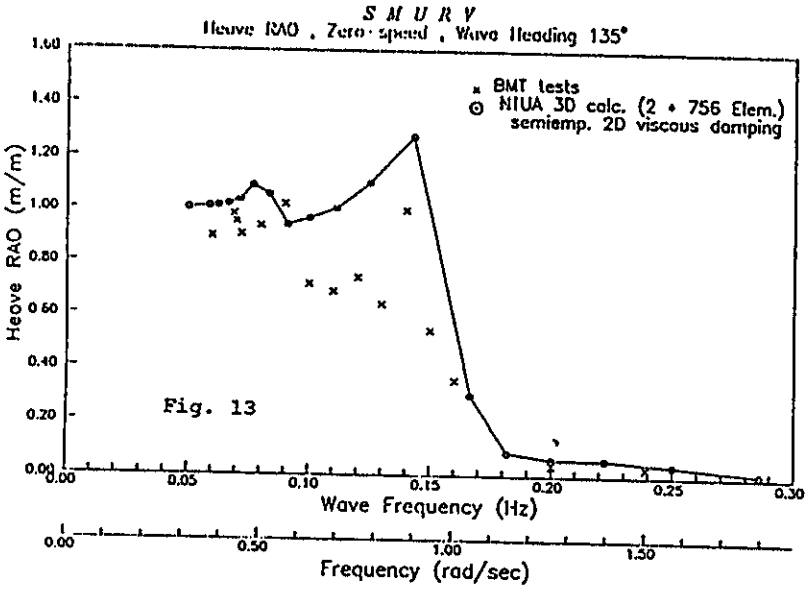
S M U R V
Heave RAO , Zero-speed , Wave Heading 135°
BMT tests
NTUA 3D calc. (2 + 756 Elem.)
semiemp. 2D viscous damping
Heave RAO (m/m)
Wave Frequency (Hz)
Frequency (rad/sec)
Fig. 13

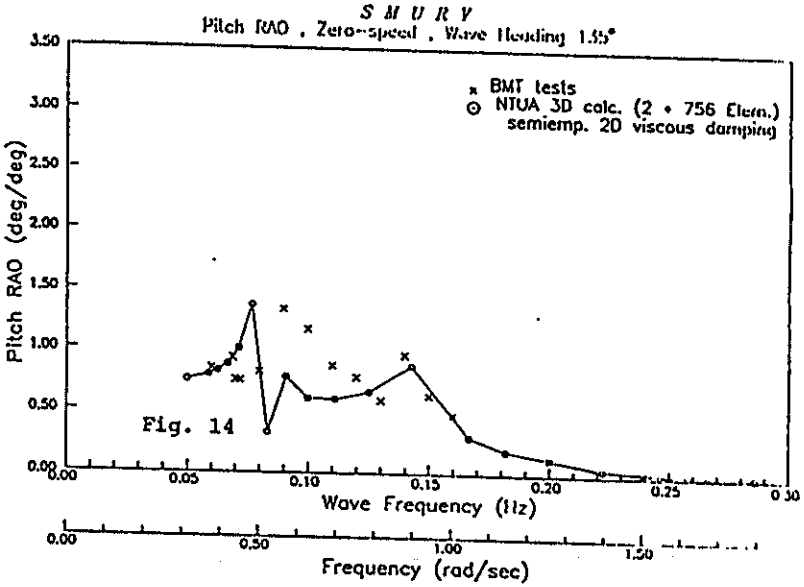
S M U R V
Pitch RAO , Zero-speed , Wave Heading 135°
BMT tests
NTUA 3D calc. (2 + 756 Elem.)
semiemp. 2D viscous damping
Pitch RAO (deg/deg)
Wave Frequency (Hz)
Frequency (rad/sec)
Fig. 14

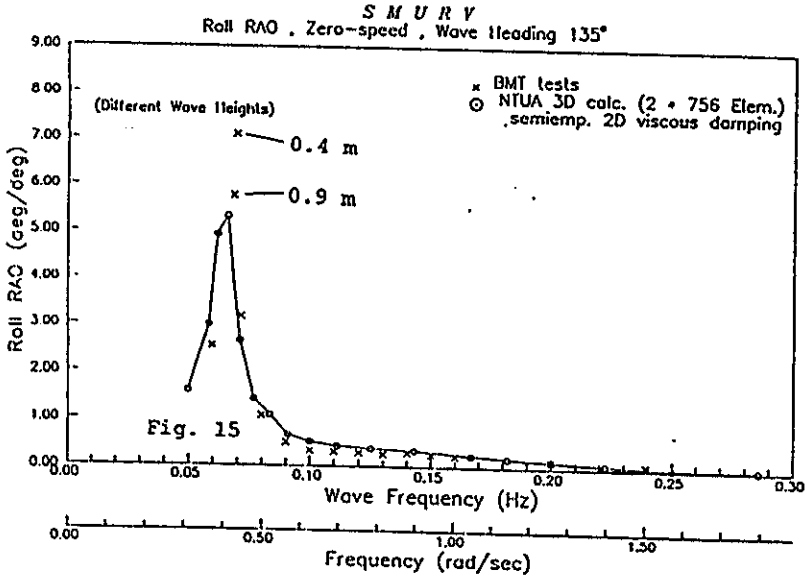
S M U R V
Roll RAO , Zero-speed , Wave Heading 135°
(Different Wave Heights)
0.4 m
0.9 m
BMT tests
NTUA 3D calc. (2 + 756 Elem.)
,semiemp. 2D viscous damping
Roll RAO (deg/deg)
Wave Frequency (Hz)
Frequency (rad/sec)
Fig. 15

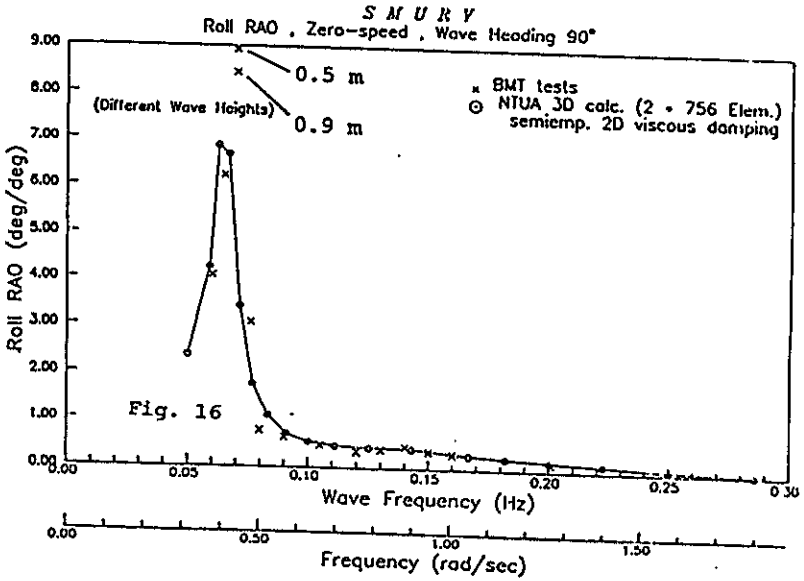
S M U R V
Roll RAO , Zero-speed , Wave Heading 90°
(Different Wave Heights)
0.5 m
0.9 m
BMT tests
NTUA 3D calc. (2 + 756 Elem.)
semiemp. 2D viscous damping
Roll RAO (deg/deg)
Wave Frequency (Hz)
Frequency (rad/sec)
Fig. 16

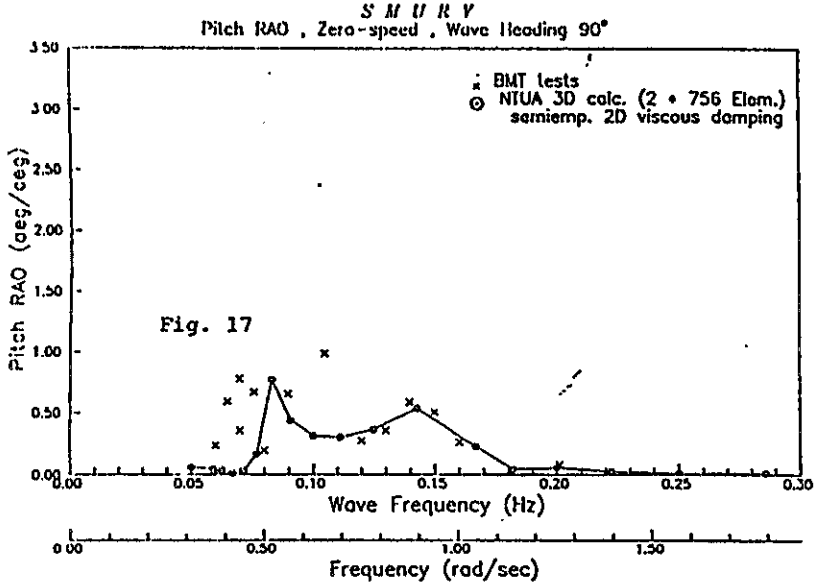

Fig. 17

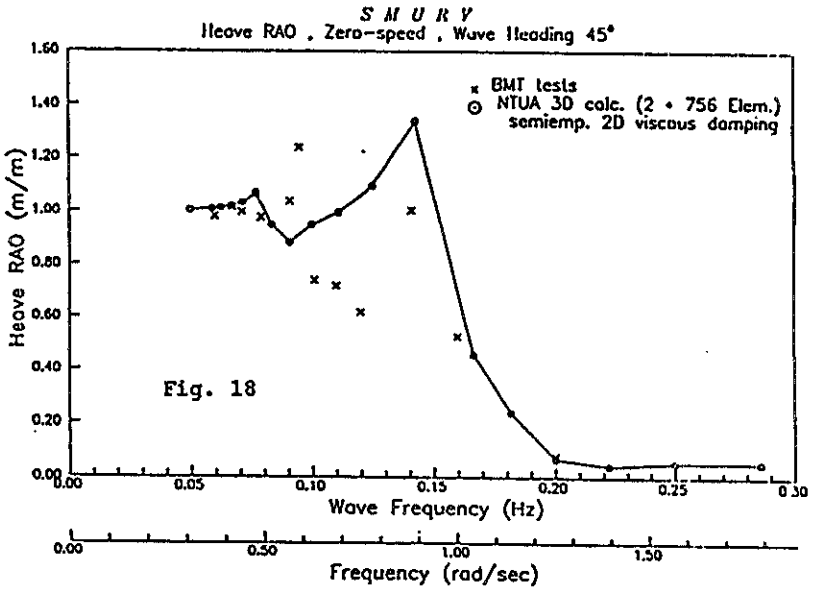

Fig. 18

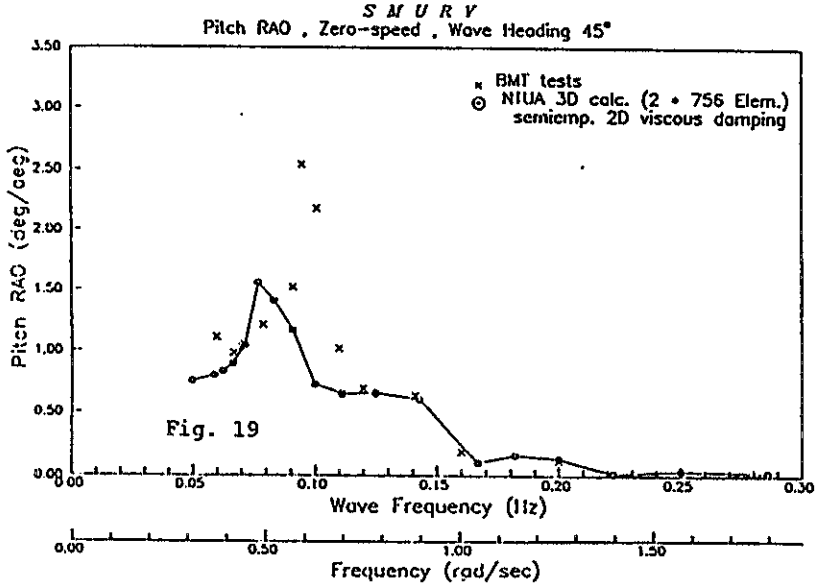

Fig. 19

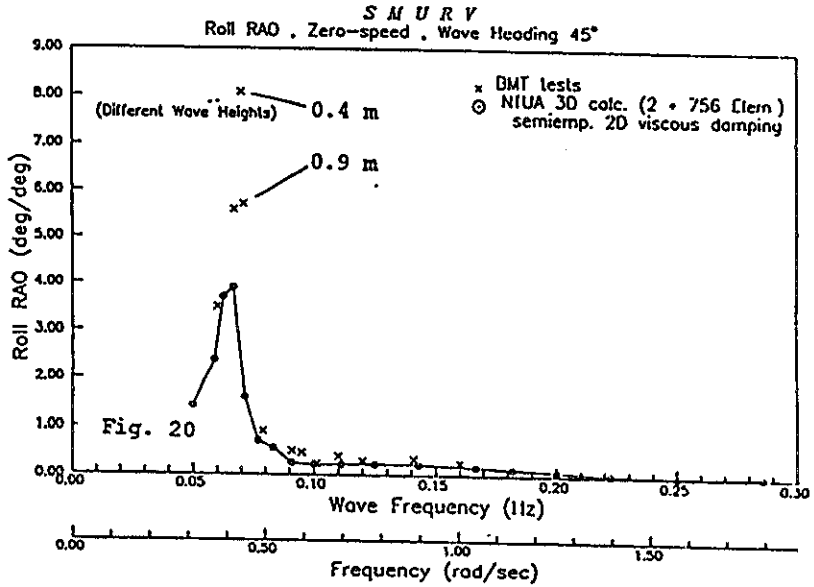

Fig. 20

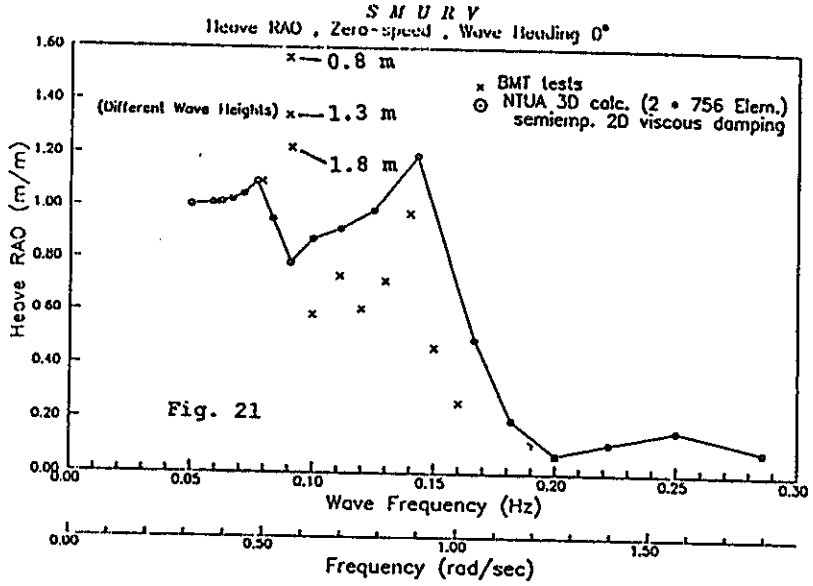
S M U R Y
Heave RAO , Zero-speed , Wave Heading 0°
(Different Wave Heights)
0.8 m
1.3 m
1.8 m
BMT tests
NTUA 3D calc. (2 • 756 Elem.)
semiemp. 2D viscous damping
Heave RAO (m/m)
Wave Frequency (Hz)
Frequency (rad/sec)
Fig. 21

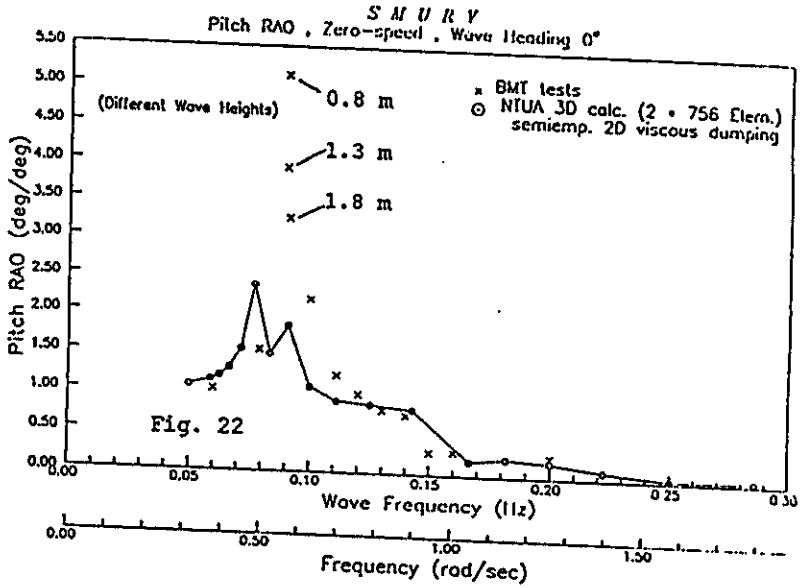
S M U R Y
Pitch RAO , Zero-speed , Wave Heading 0°
(Different Wave Heights)
0.8 m
1.3 m
1.8 m
BMT tests
NTUA 3D calc. (2 • 756 Elem.)
semiemp. 2D viscous damping
Pitch RAO (deg/deg)
Wave Frequency (Hz)
Frequency (rad/sec)
Fig. 22

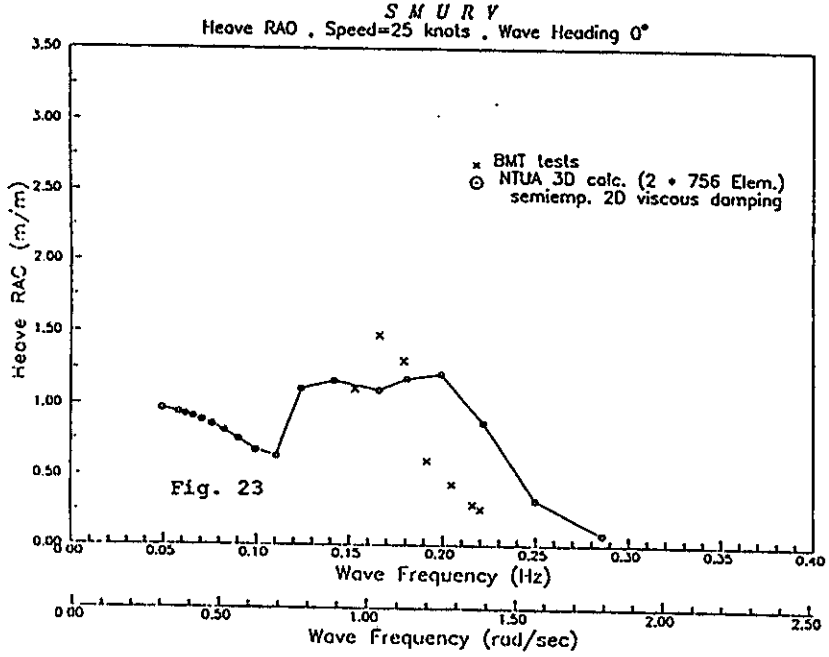
S M U R Y
Heave RAO , Speed=25 knots , Wave Heading 0°
BMT tests
NTUA 3D calc. (2 • 756 Elem.)
semiemp. 2D viscous damping
Heave RAC (m/m)
Wave Frequency (Hz)
Wave Frequency (rad/sec)
Fig. 23

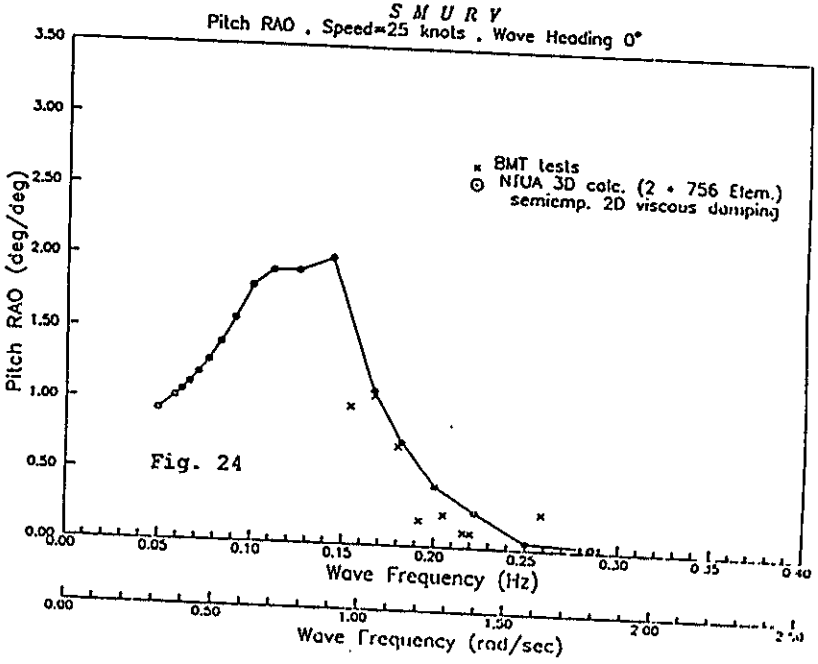
S M U R Y
Pitch RAO , Speed=25 knots , Wave Heading 0°
BMT tests
NTUA 3D calc. (2 • 756 Elem.)
semiemp. 2D viscous damping
Pitch RAO (deg/deg)
Wave Frequency (Hz)
Wave Frequency (rad/sec)
Fig. 24

Roll Motion Characteristics of High Speed Slender Vessels

Yoshiho IKEDA
University of Osaka Prefecuture, Sakai, Osaka, Japan
and
Toru KATAYAMA
Graduate Student, University of Osaka Prefecture, Sakai, Osaka, Japan

Keywords: High Speed Slender Vessel, Roll Damping, Stability, Dynamic Instability

Abstract

In this study experimental investigations on the roll damping and the high-speed stability losses are carried out for displacement-type slender vessels with round bilge. A modified method for predicting the roll damping of such vessels method is proposed on the basis Ikeda's prediction method for conventional cargo vessels.

1. INTRODUCTION

Roll motion is the most important factor for the safety of all kinds of ships. To determine the characteristics of roll motion of a ship, terms of a equation of motion, for examples, the exciting forces, the damping forces, the restoring forces and the others, play important roles. Therefore it is necessary for assessing the roll motion to know the characteristics of each term relating to hydrodynamic and hydrostatic forces for each type of ships.

The roll damping plays a very important role for large amplitude roll motion in resonance, and sometimes causes capsizing of a ship. In the heave, pitch, sway and yaw dampings, the wave damping component is dominant and the viscous damping components can be usually ignored. Therefore these dampings can be calculated by a potential-flow theory. In the roll damping, however, the viscous damping components play an important role, because the wave damping component is usually much smaller than other components due to the viscosity of fluid. Then the theoretical calculation is difficult to predict the roll damping.

One of the authors proposed a prediction method of the roll damping of a conventional cargo ship[1]~[5], and the method is widely used to predict the roll damping of a conventional cargo ship. The roll damping is assumed to be divided into five components, that is, the friction, the wave, the eddy and the lift components for a naked hull, and the bilge keel one. Furthermore, the author proposed a method for a hard-chine hull with a large skeg[6]~[8] by modifying the method mentioned above.

In the present paper, some problems which occur when the original prediction method of the roll damping of a conventional cargo ship is applied to a high speed slender vessel are experimentally revealed, and some modifications of the method to improve the accuracy are proposed.

In the second part of the paper, the restoring force of such a slender vessel at high advance speed are experimentally investigated to clarify the characteristics of the roll induced instability in calm water.

2. PREDICTION METHOD FOR SHIP ROLL DAMPING

As mentioned in the previous chapter, in Ikeda's prediction method, the roll damping is predicted by summing up the predicted values of the following components; the friction, the wave, the eddy, the lift and the bilge keel components. In the present paper, the suffixes F, W, E, L and BK express the friction, the wave, the eddy, the lift and the bilge keel components, respectively.

The friction, wave and lift components are linear components which are in proportion to roll angular velocity. The eddy and bilge keel components are nonlinear components which are in proportion to square of roll angular velocity. Then the roll damping of a ship can be expressed as a function of roll angular velocity as follows.

$$M_R = M_F\dot{\phi} + M_W\dot{\phi} + M_L\dot{\phi} + M_E\left|\dot{\phi}\right|\dot{\phi} + M_{BK}\left|\dot{\phi}\right|\dot{\phi} \tag{2.1}$$

The equivalent roll damping coefficient in linear form B_{44} can be expressed as follows

$$B_{44} = B_F + B_W + B_E + B_L + B_{BK} \tag{2.2}$$

where B_{44} is the roll damping coefficient which is defined by dividing the roll damping moment M_R by the roll angular velocity $\dot{\phi}$. The nonlinear components in Eq.(2.1) can be linearized as $B_E = \frac{8}{3\pi}M_E\phi_a\omega$ and $B_{BK} = \frac{8}{3\pi}M_{BK}\phi_a\omega$ respectively. ϕ_a and ω in Eq.(2.2) denote the amplitude and the circular frequency of roll motion, respectively. Note that all coefficients in Eq.(2.1) depend on roll frequency and advance speed, and that M_E and M_{BK} sometimes depend on roll amplitude as well as roll frequency because of the K_c number effect in vortex shedding problem. The roll damping coefficient B_{44} is non-dimensionalized as follows.

$$\hat{B}_{44} = \frac{B_{44}}{\rho\nabla B^2}\sqrt{\frac{B}{2g}} \tag{2.3}$$

The circular frequency of roll motion, ω, is also non-dimensionalized as follows,

$$\hat{\omega} = \omega\sqrt{\frac{B}{2g}} \tag{2.4}$$

where ρ, g, ∇ and B denote density of fluid, acceleration of gravity, displacement and breadth of a ship respectively. The roll damping coefficient B_{44} is able to be translated into the Bertin's N-coefficient on the condition that the energy losses of them in one period coincide with each other,

$$\hat{B}_{44} = \frac{GM\phi_a}{\pi B\hat{\omega}_0}N \tag{2.5}$$

In the equation Eq.(2.5), ϕ_a is expressed in degree.

3. METHOD OF EXPERIMENT AND ANALYSIS

Measurements of the roll damping of models of two high speed slender vessels with round bilge and a skeg are carried out by a forced rolling test. The models are forced to roll about the location of the center of gravity which is the standard for each vessel. The roll period and amplitude are systematically changed in the experiments.

Both ships are slender vessels with twin-propeller and twin-rudder for high speed cruising. Ship A has a big bulbous bow and Ship B has not it. The principal particulars of the models are shown in Table 1.

In the analysis of these experiments, the roll motion's equation in one degree of freedom as follows is used, in which nonlinear terms are replaced by equivalent linear terms,

$$(J_{44} + A_{44})\ddot{\phi} + B_{44}\dot{\phi} + C_{44}\phi = M_R \tag{3.1}$$

where A_{44} and J_{44} denote the added moment of inertia and the moment of inertia of the center about the roll axis, C_{44} and M_R the restoring force coefficient and the roll exciting moment respectively. The model is forced to move in regular roll motion as $\phi = \phi_a \sin\omega t$ by the forced rolling mechanism. The measured roll moment is expanded into a Fourier series. Using the amplitude M_{RF} of the Fourier series with the basic frequency in phase of the roll angular velocity(cosine component), the roll damping coefficient B_{44} can be obtained as follows.

$$B_{44} = \frac{M_{RF}}{\phi_a\omega} \tag{3.2}$$

4. RESULTS OF EXPERIMENT

4. 1 Comparison between predicted and experimental results

4. 1. 1 Roll damping of naked hull

The measured roll damping of Ship A in naked hull condition is shown in Figs.1 and 2. The measured results are in fairly good agreement with the predicted ones in short roll period of T = 1sec as shown in Fig.1. In longer roll period of T = 1.39sec, however, the prediction method underestimates the experimental results as the Froude number

increases as shown in Fig.2. Fig.3 in which the measured results is arranged on the based of the non-dimensional circular frequency, shows that the roll damping coefficient is almost constant at high Froude number. On the contrary the predicted result shown in the same figure increases with increasing the circular frequency. The tendencies of the predicted and measured roll dampings are different from each other. It is especially a serious problem for predicting the ship motions that in the case of $T = 1.39$sec ($\hat{\omega} = 4.52$), which is corresponding to the natural period of Ship A, the predicted results of the method overestimate the damping of about 70% at Froude number of 0.4.

In Fig.4 the results of Ship B are shown. In the case of Ship B, the measured roll damping of the naked hull are fairly in good agreement with the predicted results at high Froude number. At lower advance speed, however, the predicted one slightly overestimates.

These discrepancies of the predicted and measured roll dampings of Ships A and B may be caused by some problems in the prediction methods of the lift and wave components in Ikeda's method.

In Fig.5 the effect of roll amplitude on the roll damping of Ship A at zero advance speed is shown. From this figure, it is found that the experimental result is in fairly good agreement with the predicted results at $\phi_a = 10$ and 15 degree. Over $\phi_a = 15$deg the experimental result increases with increasing the roll amplitude, and at $\phi_a = 20$deg it is over twice as large as the predicted result. One of the causes of this discrepancy may be that the huge bulbous bow of Ship A creates the large eddy induced damping.

4. 1. 2 Bilge keel component

The comparison between the experimental and predicted results of the bilge keel component of Ship A at zero advance speed is shown in Fig.6. The comparisons between the experimental and predicted results of the bilge keel components of Ship A and Ship B at advance speed are shown in Figs.7 and 8. The bilge keel components in these figures are defined by the difference between the measured roll dampings with and without bilge keels.

From Fig.6 it is found that the experimental result of Ship A increases with increasing roll amplitude at zero advance speed, and that Ikeda's method underestimates the experimental results by about 30%. On the contrary, for Ship B, the experimental value at $Fn = 0$ in Fig.8 is much smaller than the predicted one. This may be because that the calculation method of the bilge keel component uses a simple hull form assumption.

In Fig.7 which shows the effect of advance speed on the bilge keel component of Ship A, the measured roll damping of bilge keels is in fairly good agreement with the predicted results in small Froude number region. The experimental result, however, rapidly increases with increasing advance speed, and much larger than the predicted one at high speed. Such a tendency is not found in the results of Ship B which are shown

in Fig.8. This difference may be caused by the difference of aspect ratio of the bilge keels of them. The results demonstrate that the effect of advance speed on the bilge keel component due to the lift force acting on it can not be ignored when bilge keels with large aspect ratio are attached.

4. 2 Improvement of the prediction method

To correct some defects of the prediction method proposed by Ikeda et al. for applying it to a slender high speed vessel, the contributions of the lift component of a naked hull, the bilge keel component and the viscous component due to a bulbous bow are investigated in this chapter.

4. 2. 1 Eddy component due to bulbous bow

In the case of $Fn = 0$, the roll damping moment M_R about the center of gravity generated by a bulbous bow can be expressed as follows

$$M_R = F \times r \tag{4.1}$$

where F denotes the drag force acting on the bulbous bow and r the distance between the roll axis and the center of the bow. The drag force F can be expressed using a drag coefficient C_D as follows

$$F = \frac{1}{2}\rho C_D S U_B{}^2 \tag{4.2}$$

where S and U_B denote the projected area of the bulbous bow and the tangential velocity due to roll motion at the center of the bulbous bow respectively. U_B is expressed as follows.

$$U_B = r\dot{\phi} = r\phi_a\omega\cos\omega t \tag{4.3}$$

Finally, the roll damping coefficient due to a bulbous bow is obtained as follows.

$$\hat{B}_{MR} = \frac{M_R}{\rho B^2\nabla\dot{\phi}}\sqrt{\frac{B}{2g}} = (\frac{C_D S r^3}{2B^2\nabla}\sqrt{\frac{B}{2g}})\phi_a\omega \tag{4.4}$$

The roll damping coefficient due to the bulbous bow of Ship A is calculated by Eq.(4.4) as follows

$$\hat{B}_{MR} = 1.113 \times 10^{-3}\omega\phi_a \tag{4.5}$$

The calculated result by Eq(4.5) is shown by a broken line in Fig.9 to compare it with experimental results. The predicted results including the bulbous bow effect show better agreement with experimental results. However, the disagreement between both results remains at large roll amplitude yet.

4. 2. 2 The effect of advance speed

The difference between the predicted and experimental results for a naked hull at lower frequency increases with increasing advance speed as shown in Fig.2. In order to clarify the reason of the disagreement, the prediction methods of the lift and wave components in Ikeda's method are reexamined.

Ikeda's method uses Inoue's formula to determine the lift coefficient of a ship. It may be a problem to apply it to such a slender vessel with a large skeg.

The lift coefficients of Ship A and Ship B are measured by an oblique towing method to compare with the predicted value by Inoue's formula. In Fig.10 the measured lift coefficient of Ship B is shown with the results by the formula. The experimental result shows significant nonlinearity with increasing the attack angle. The results demonstrate that nonlinearity of the lift coefficients should be taken into account in the prediction of the lift component of such ships.

Figs.11, 12 and 13 show the comparisons between the results of original Ikeda's method(rigid line) and modified one(broken line) including the effect of nonlinear lift coefficient of the ships obtained by the experiments. The predicted results for Ship A are in fairly good agreement with the experimental results at T = 1.0sec as shown in Fig.11. At T = 1.39sec, however, as shown in Fig.12 the predicted results are not in good agreement with the experimental results at high advance speed. The predicted results for Ship B shown in Fig.13 overestimate the experimental ones. These results may suggest that the agreement between the predicted and measured roll dampings can be improved to some extent by using measured lift coefficient of each ship in the prediction. However, the quantitative disagreement between them remains at high advance speed yet.

The wave component is also affected by an advance speed. The wave components of Ship A and Ship B significantly contribute to the roll dampings at advance speed although the component is inferior to the viscous induced components for a conventional cargo ship. To investigate the wave component from experimental results at advance speed, the residual values are calculated by subtracting the friction, eddy and lift components predicted by Ikeda's method using the measured lift coefficient from the measured roll damping. If the predicted values of other components is accurate, the residual one can be regarded as the wave component. The result is shown in Fig.14. It is found that the experimental result have a hump at Fn = 0.4. The hump may be caused by the interference between the bow and stern waves as pointed out by Ikeda's et al.[4]. Ikeda's method does not include the effect of the interference, because the effect is usually small for a conventional cargo ship. The present results may demonstrate that the effect of interference between the bow and stern waves created by roll motion should be taken into account in the prediction of the wave component of such a high-speed slender vessel.

4. 2. 3 Improvement of prediction method of bilge keel component

To predict the bilge keel component, Ikeda's method assumes that a cross section consists of a vertical side wall, a horizontal bottom and a bilge circle of a quarter circle for simplicity. The fitting position and the angle of the bilge keel are supposed to be the middle point of the arc of quarter circle and perpendicular to the hull surface. It may be impossible that these hull shape assumptions are applied to the real cross section of a high speed slender vessel with large bilge circle. These assumptions must cause some error in the calculation of the moment levers of the normal force of the bilge keel and of the pressure force distributing on the hull surface created by the bilge keel.

In this study a computer program has been developed in which the real cross section is used to calculate the bilge keel components. The pressure distribution used in the calculation is the same as that in Ikeda's method.

The calculated result of Ship A by the program is shown in Fig.15. The measured bilge keel component is in fairly good agreement with the predicted results.

4. 2. 4 Lift force acting on bilge keels

Ikeda's method supposes that the effect of advance speed on the bilge keel component is too small to be ignored. For Ship A, however, it is found that the lift force acting on bilge keels can't be ignored because of the large aspect ratio of them. In this section a simple method to predict the effect of advance speed on the bilge keel component is shown.

Since a bilge keel can be regarded as a small aspect ratio wing, Jones's theory can be applied to it. When a bilge keel is in the flow composed by the advance speed $U = F_n\sqrt{gL}$ and the roll angular velocity $u = r\dot{\phi} = r\phi_a\omega$ (where r denote distance between the center of roll axis and the center of bilge keel), the attack angle and the resultant flow velocity are obtained as $\alpha = \tan^{-1}(u/U)$ and $V = \sqrt{U^2 + u^2}$ respectively.

On the basis of Jones's theory, the lift force acting on a bilge keel is obtained as

$$L = \frac{\pi\rho\alpha V^2 b^2}{2} \tag{4.6}$$

where c and b denote the length and the maximum breadth of a bilge keel. The roll damping coefficient due to a pair of bilge keels B_{BKL} can be obtained as follows in non-dimensional form.

$$\hat{B}_{BKL} = \frac{2Lr}{\rho B^2 \nabla \phi_a \omega}\sqrt{\frac{B}{2g}} \tag{4.7}$$

Fig.16 shows the comparison between the measured results and the predicted results including the lift force contribution acting on the bilge keels of Ship A. The predicted results including the lift effect show better agreement with experimental results than that of Ikeda's method. However, the disagreement between both results remains at high advance speed yet.

4. 3 Interference between appendages

Interferences between appendages are sometimes important for the roll damping of a ship. In the present research project interference among appendages, that is bilge keels, fin stabilizers, shaft brackets and rudders are experimentally investigated. The results have been published in our paper[9] in detail. In this chapter, the interference between a set of fin stabilizers and a set of bilge keels is briefly summarized.

The models which are used in the present study have a set of fin stabilizers behind a set of bilge keels. In such a case, the induced flow to the stabilizer is disturbed by the bilge keels. To clarity the interference, the roll dampings of the models with and without a set of fin stabilizers behind the bilge keels and of the naked hull models with and without a set of fin stabilizers are measured. The difference between them shows the increase of the roll damping of the ship due to the fin stabilizers. The obtained results for Ship A and Ship B are shown in Figs.17 and 18.

The difference between the roll damping coefficients of the ships with and without a set of fin stabilizers is considered to be the pure performance of the fin stabilizers, and the difference between those of the ships with and without a set of fin stabilizers in addition to a set of the bilge keels is considered to be the performance of the fin stabilizer interfered by bilge keels. In the case of Ship A, the performance of the fin stabilizer is significantly interfered by bilge keels. The effect of the fin stabilizer becomes to be almost halved due to bilge keels at the Froude number of 0.45. This may be caused that the distance between a bilge keel and a fin stabilizer is too close. On the contrary, for Ship B in which the distance is almost twice comparing with that for Ship A, the effect of fin stabilizer is not affected by bilge keels. These results suggest that the distance between a bilge keel and a fin should be carefully examined in the design stage.

5. STABILITY CHARACTERISTICS AT HIGH ADVANCE SPEED

5. 1 Stability losses at high speed

Stability quality of a ship cruising at high speed is one of important problem for its safety and operation. In the following seas it is well known that the stability sometimes becomes worse. In calm water, similar stability losses at high speed have been also reported for planing craft[15]~[19] and displacement-type vessels[12]~[14].

Tanaka et. al.[12] reported that natural frequencies of displacement-type cargo vessels decreases at advance speed over Fn=0.3, and Tamiya et. al.[13] pointed out that the reasons of the stability losses at high speed are caused by steady waves created by the hull. Washio et.al.[14] pointed out that instability phenomena occurs for a round-bilge high speed vessel at Froude number over 0.8, and that the phenomena occasionally causes capsizing of a ship at high speed.

5. 2 Measurements of stability

The restoring moment, the lift force and the transverse force (or sway force)acting on Ships A and B are measured by towing tests for various heel angles. The models are fixed to a load-cell of three components on a towing carriage as shown in Fig.19, and towing speed, heel angle and draft (or sinkage) are systematically changed.

Measured forces are the difference between those at zero advance speed and those at advance speed. This means that the measured forces include only dynamic forces. The lift and transverse forces are non-dimensionalized by dividing them by the displacement. From the measured roll moment, GZ values are obtained by calculating adding static roll moment at zero advance speed to the measured one.

Measured results for Ships A and B are shown in Figs.20~25. The GZ values of Ship A shown in Fig.20 rapidly decreases with increasing advance speed, and become to be almost one-half of those at zero advance speed. On the contrary, the measured GZ values of Ship B slowly decreases with advance speed at large heel angle, and be almost constant at moderate heel angle as shown in Fig.21. These results suggest that the characteristics of high-speed stability losses significantly sensitive to hull shape.

The lift and transverse forces are shown in Figs.22 and 23 for Ship A and in Figs.24 and 25 for Ship B. These figures show that the lift forces do not depend on heel angle, and decrease with advance speed. The transverse forces depend on heel angle significantly. In free running condition these forces should be balanced by the increase of displacement by sinkage, and by the drifting resistance, respectively.

Finally, the effect of sinkage on restoring moment at high speed are shown in Fig.26. The restoring moment of Ship A decreases with advance speed all over the sinkage. On the contrary, the change of the moment of Ship B depends on sinkage of the ship. The results also suggest that the high-speed stability losses are sensitive to hull shape even if they have similar slender hulls.

6. CONCLUSION

The roll damping and the high-speed stability losses of a displacement-type slender vessel have been experimentally investigated, and the following conclusions have been reached:

1. The wave component of the roll damping of high-speed slender vessels plays an important role. In low frequency region, the interference between the bow and stern waves can not be ignored to get an accurate prediction of the roll damping.

2. Using the measured lift coefficient of a ship, the prediction of the lift component becomes better than that by Ikeda's prediction method.

3. The effect of the lift forces acting on bilge keels should be taken into account when the bilge keels have large aspect ratio.

4. The interferences between appendages, for example between bilge keels and fin stabilizers, are sometimes important.

5. High-speed stability losses occur for a displacement-type slender vessel as well as a semi-planing craft. The stability losses significantly depend on hull shape.

7. ACKNOWLEDGMENTS

The authors wish to express their appreciation to Mr.Y.Hasegawa and Mr.M.Segawa of Hitachi Zosen Co.Ltd. for their cooperation and support for this study, and prof.T.Okuno and Dr.K.Otsuka of University of Osaka Prefecture for their important advice and assistance.

REFERENCE

[1] Y.Ikeda, Y.Himeno and N.Tanaka : On Roll Damping Force of Ship -Effect of Friction of Hull and Normal Force of Bilge Keels-, Jour. of the Kansai Soc. of Naval Arch. Japan, No.161(1976), p.41

[2] Y.Ikeda, K.Komatu, Y.Himeno and N.Tanaka : On Roll Damping Force of Ship -Effect of Hull Surface Pressure Created by Bilge Keels-, Jour. of the Kansai Soc. of Naval Arch. Japan, No.165(1977), p.31

[3] Y.Ikeda, Y.Himeno and N.Tanaka : On Eddy Making Component of Roll Damping Force on Naked Hull, Jour. Soc. of Naval Arch. Japan, Vol.142(1977), p.54

[4] Y.Ikeda, Y.Himeno and N.Tanaka : Components of Roll Damping of Ship at Forward Speed, Jour. Soc. of Naval Arch. Japan, Vol.143(1978), p.113

[5] Y.Ikeda : A Prediction Method for Ship Roll Damping , Report of Dept. of Naval artitecture, University of Osaka Prefecture, No.405(1978)

[6] Y.Ikeda, N.Umeda and N.Tanaka : Effect of Forward Speed on Roll Damping of a High-Speed Craft, Jour. of the Kansai Soc. of Naval Arch. Japan, No.208(1988), p.27

[7] Y.Ikeda and N.Umeda : A Prediction Method of Roll Damping a Hardchine Boat at Zero Forward Speed, Jour. of the Kansai Soc. of Naval Arch. Japan, No.213(1990), p.57

[8] Y.Ikeda, Y.Kawahara and K.Yokomizo, A Study on Roll Characteristics of a Hard-chain Craft, Jour. of the Kansai Soc. of Naval Arch. Japan, No.218(1992), p.215

[9] Y.Ikeda, T.Katayama, Y.Hasegawa and M.Segawa : Roll Damping of High Speed Slender Vessels , Jour. of the Kansai Soc. of Naval Arch. Japan, No.222(1994)

[10] H.Kobayashi, A.Ishibashi, Y.Hasegawa and Y.Nakanishi : A Study on the Maneuverability of Twin-propeller Twin-rudder Ship, The Jour. of Japan Institute of Navigation, No.86(1992), p.205

[11] H.Kobayashi, A.Ishibashi and Y.Hasegawa : A Study on the Interaction among the Hull, Propeller and Rudder for the Twin Propeller Twin Rudder Ship, The Jour. of Japan Institute of Navigation, No.87(1992), p.171

[12] N.Tanaka, Y.Himeno, M.Ogura and K.Masuyama : Free Rolling Test at Forward Speed, Jour. of the Kansai Soc. of Naval Arch. Japan, No.146(1972), p.63

[13] M.Tamiya and T.Komura : Topics on Ship Rolling Characteristics with Advance Speed, Jour. Soc. of Naval Arch. Japan, (1972), p.159

[14] Y.Washio and A.Doi : A Study on the Dynamical Stability of High-Speed Craft, Transaction of the West-Japan Society of Naval Architects, (1991), p.53

[15] A Millward : Preminary Measurements of Pressure Distribution to Determine the Transverse Stability of a Fast Round Bilge Hull, International Shipbuilding Progress, Vol.26, No.297, May 1979

[16] Steven H. Cohen and Donald L. Blount : Research Plan for the Investigation of Dynamic Instability of Small High-Speed Craft, SNAME Transaction, Vol.94(1986), p.197

[17] Louis T. Codega and James Lewis : A Case Study of Dynamic Instability in a Planing Hull, Marine Technology, Vol.24, No.2, April 1987, p.143

[18] Donald L. Blount and Louis T. Codega : Dynamic Stability of Planing Boats, Marine Technology, Vol.29, No.1, Jan. 1992, p.4

[19] The High-Speed Marine Vehicles Committee Report, Proc. of the 20th ITTC, 1993

Table 1 Principal particulars of models

	Ship A	Ship B
L(m)	2.010	1.910
Lpp(m)	1.870	1.787
B(m)	0.245	0.235
D(m)	0.145	0.164
d(m)	0.070	0.061
W(kgf)	13.75	11.99
Cb	0.433	0.424
KG(m)	0.0867	0.088
GM(m)	0.019	0.033
Ts(sec)	1.39	1.18
bilge keel		
breadth(m)	0.018	0.0146
location(ss)	4.77-6.04	4.35-6.58

Ts: roll natural period

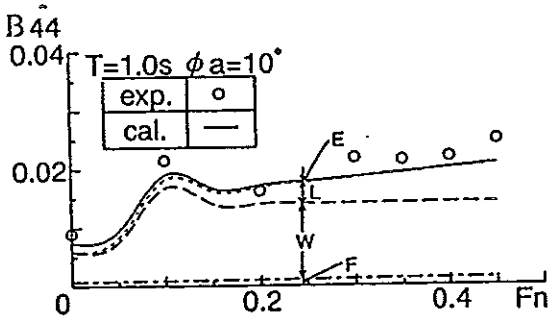

Fig.1 Effect of advance speed on roll damping of Ship A without appendages

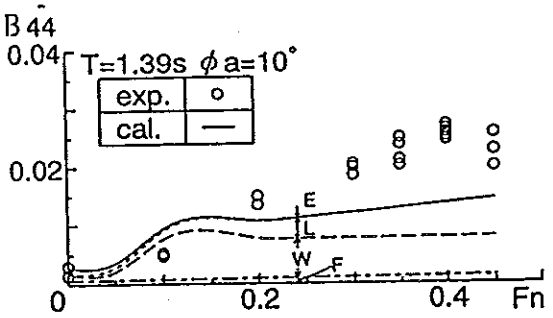

Fig.2 Effect of advance speed on roll damping of Ship A without appendages

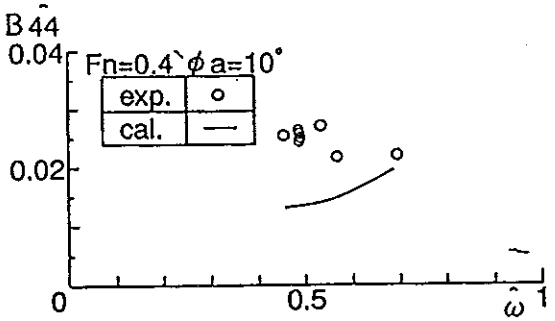

Fig.3 Effect of roll frequency on roll damping of Ship A without appendges

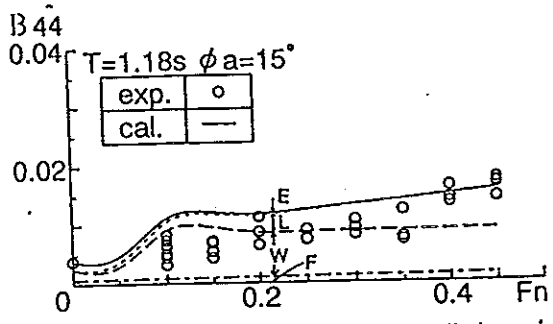

Fig.4 Effect of advance speed on roll damping of Ship B without appendages

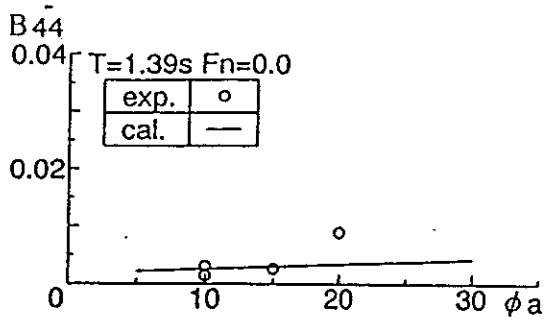

Fig.5 Efect of roll angle on roll damping of Ship A without appendages

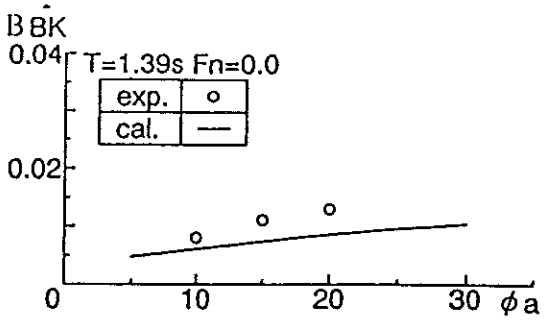

Fig.6 Effect of roll angle on bilge keel component of Ship A

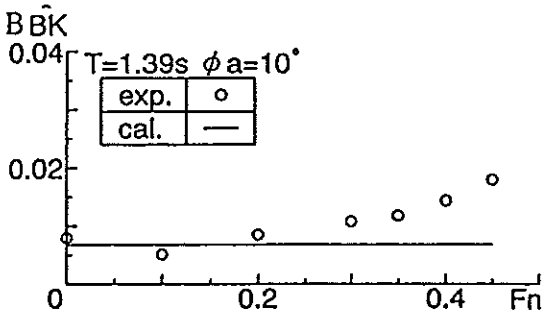

Fig.7 Effect of advance speed on bilge keel component of Ship A

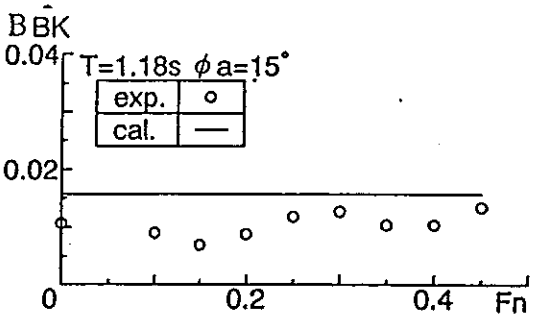

Fig.8 Effect of advance speed on bilge keel component of Ship B

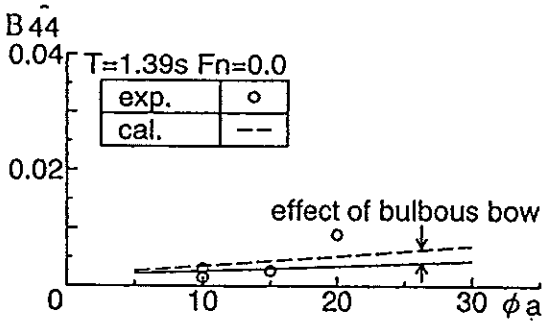

Fig.9 Effect of bulbous bow on roll damping of Ship A

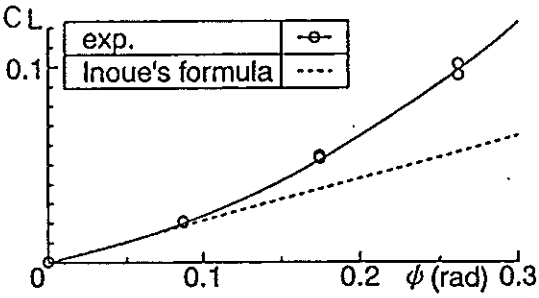

Fig.10 Lift coefficient of Ship B

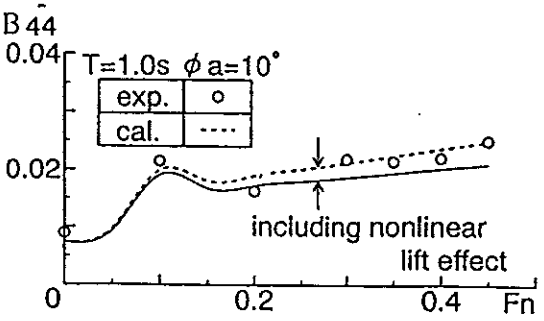

Fig.11 Roll damping coefficient of Ship A using measured lift coefficient

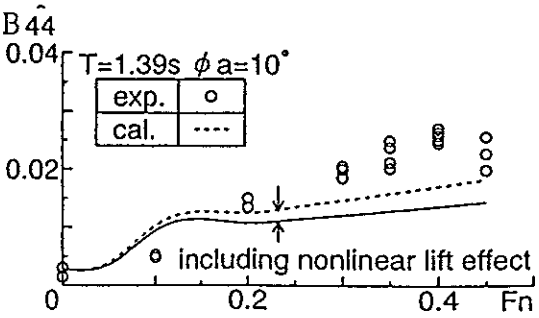

Fig.12 Roll damping coefficient of Ship A using measured lift coefficient

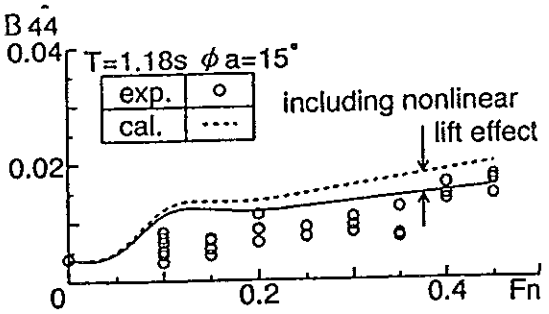

Fig.13 Roll damping coefficient of Ship B using measured lift coefficient

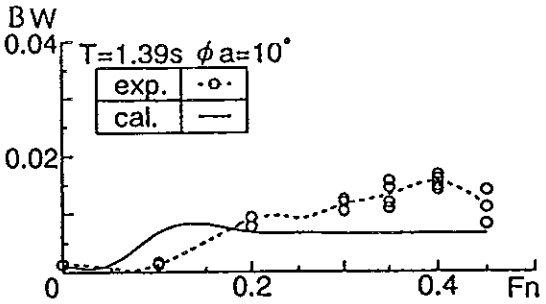

Fig.14 Effect of advance speed on wave making component of Ship A

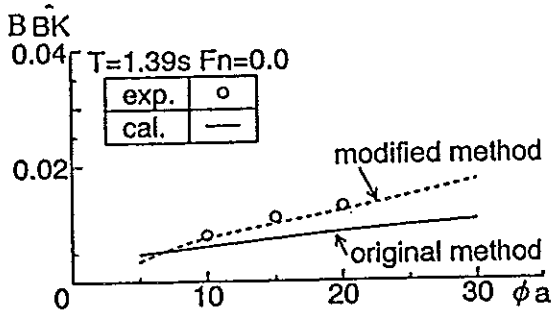

Fig.15 Effect of roll angle on bilge keel component of Ship A

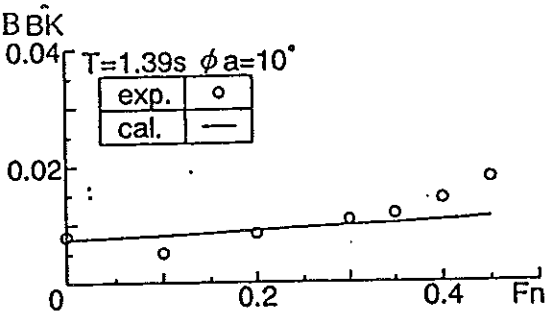

Fig.16 Effect of lift force acting on bilge keel on roll damping of Ship A

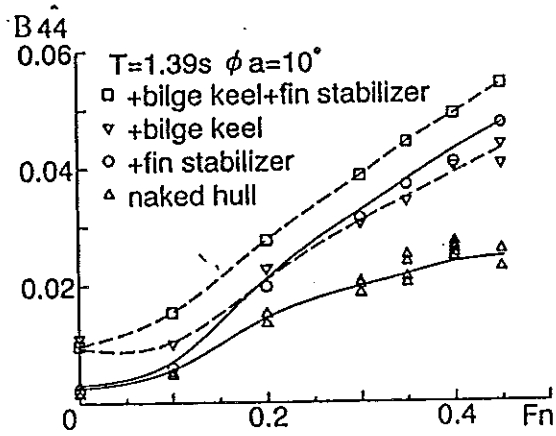

Fig.17 Effect of bilge keel roll damping due to fin stabilizer for Ship A

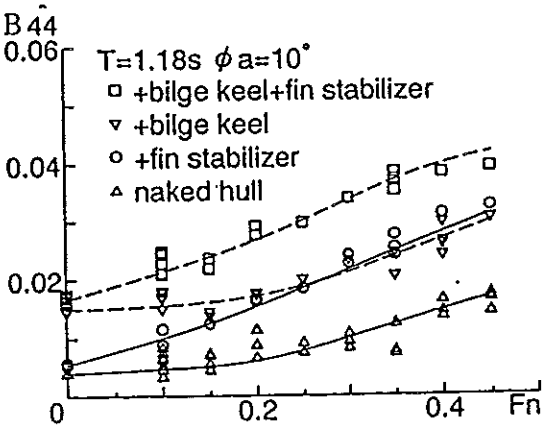

Fig.18 Effect of bilge keel on roll damping due to fin stabilizer for Ship B

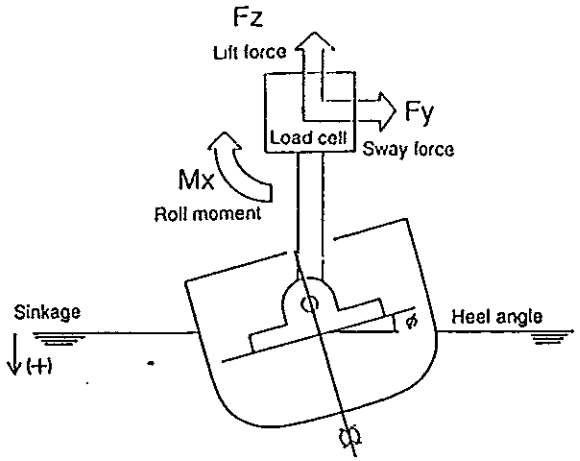

Fig.19 Schematic view of experiment

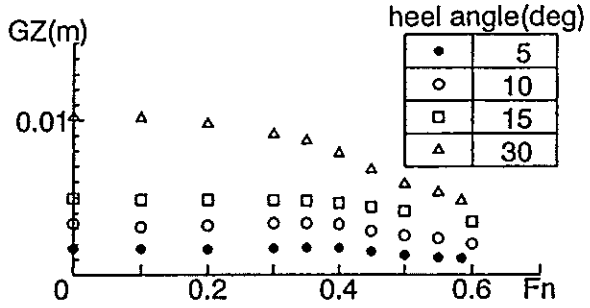

Fig.20 GZ values of Ship A obtained by a fully captive test

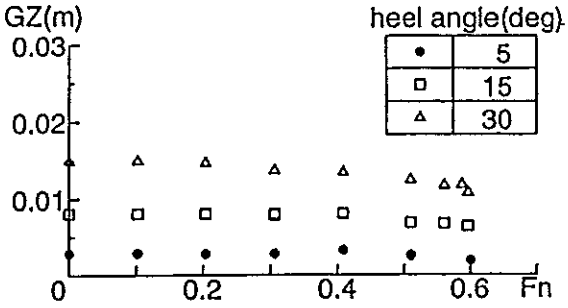

Fig.21 GZ values of Ship B obtained by a fully captive test

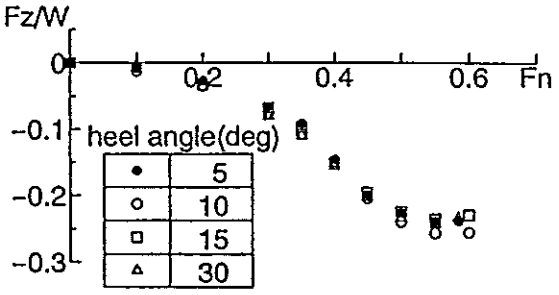

Fig.22 Lift force of Ship A obtained by a fully captive test

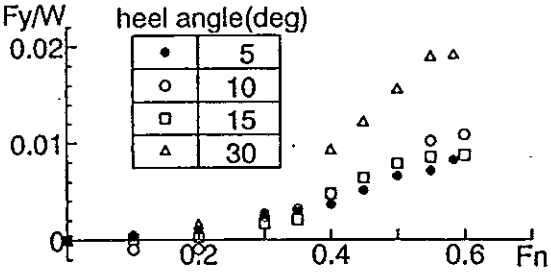

Fig.23 Transverse force acting on Ship A obtained by a fully captive test

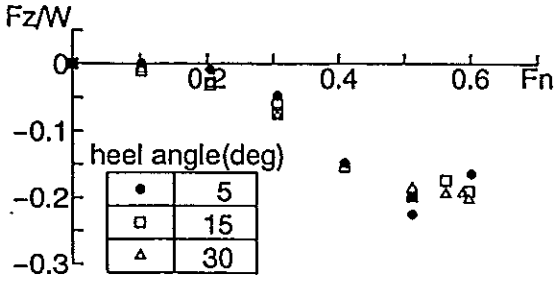

Fig.24 Lift force of Ship B obtained by a fully captive test

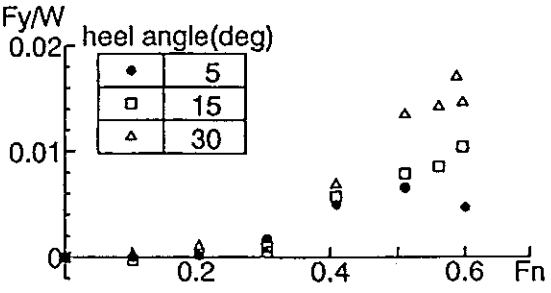

Fig.25 Transverse force acting on Ship B obtained by a fully captive test

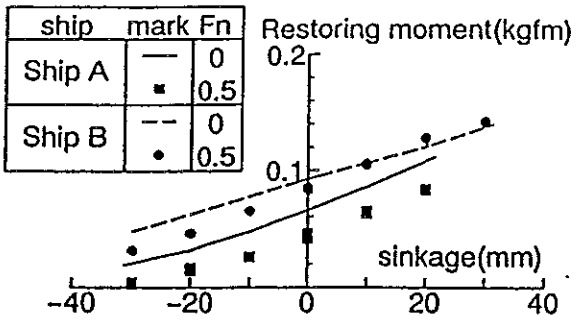

Fig.26 Restoring moment about the center of gravity of Ship A and B heel angle of 15 degree

SECRETARIAT STAB 94

GENERAL CHAIRMAN	W. A. Cleary, Jr - Adjunct Professor O/E
OCEAN ENGINEERING PROGRAM CHAIRMAN	Professor A. Zborowski, Ph.D.
CENTRAL BAPTIST CHURCH - AUDITORIUM	Dr. Gary Fagan, Pastor
SPECIAL EVENTS - AUXILIARY SERVICES	Ms. Barbara Towers
OFFICE SERVICES - DIRECTOR	Mr. William Hamilton
OFFICE SERVICES - PUBLISHING	Ms. Rosary M. Pedreira
GLEASON AUDITORIUM COORDINATOR	Mr. Gary Allen
OCEAN ENGINEERING STAFF	Ms. Janet Carey Ms. Ann Bergonzoni Ms. Juanita Fennimore Mr. Daryl Slocum
OCEAN ENGINEERING STUDENTS	Ms. Jennifer Clark Mr. Michael Callahan Mr. Damian Hite Mr. Joe Blodgett Mr. Alejandro Gutierrez Mr. Mathew Craven
SOCIETY OF NAVAL ARCHITECTS AND MARINE ENGINEERS FLORIDA TECH STUDENT SECTION	Ms. Allison Link

AND

THE FLORIDA TECH STUDENT SUPPORTING TEAM

STAB 94 COMMITTEES

INTERNATIONAL PROGRAMME

Prof. C. Kuo, University of Strathclyde, Glasgow
Prof. M. Fujino, University of Tokyo
Prof. L. Kobylinski, Tech. Univeristy of Gdansk, Poland
Prof. P. Cassella, University of Naples, Italy
Prof. P. Bogdanov, Ship Hydrodynamics Center, Varna, Bulgaria
Dr. S. Grochowalski, National Research Council, Ottawa, Canada
Prof. P. Blume, Hamburg Ship Model Basin, Germany
Prof. D. Huang, Dalien University, Dalien, China
H. Hormann, Head Marine Safety Germanischer Lloyd
H. Vermeer, Netherlands Shipping Directorate
I. Manum, Norwegian Maritime Directorate
Prof. C. Guedes Soares, Instituto Superior Tech Libson, Portugal
Dr. I. Boroday, Krilov Ship Research Inst., St. Petersburg, Russia
Dr. N. Rachmanin, Krilov Ship Research Institute, Russia
Dr. R. Ozkan, Instanbul, Turkey
Chairman - W. A. Cleary Jr., Florida Institute of Technology

COMMITTEE of the AMERICAS

Prof. B. Adee, University of Washington, Seattle, WA USA
Prof. R. Battacharyya, Annapolis, MD USA
H. P. Cojeen, USCG Headquarters, Washington, DC USA
Prof. R. G. La torre, University of New Orleans, LA USA
Dr. M. A. S. Neves, COOPE/UFRJ, Rio de Janiero, Brazil
Prof. J. R. Paulling Jr., Richmand, CA USA
Prof. N. Perez, University of Chile, Valdiva, Chile
Prof. G. L. Petrie, Webb Institute, New York, NY USA
Prof. C. Sanguinetti, University of Chile, Valdiva, Chile
R. J. Sonnenschein, MARAD, Washington, DC USA
Dr. C. Spadavecchia, Prefectura Navale, Burnos Aires, Argentina
Prof. M. Santarelli, Buenos Aires, Argenina
Dr. J. S. Spencer, ABS AMERICAS, Huston, Texas USA
Prof. R. Yagle, University of Michigan, Ann Arbor, Michigan USA